ROTATIONAL FLOW IN FLUID DYNAMICS

James D. Murray

A Thesis Submitted for the Degree of PhD
at the
University of St Andrews

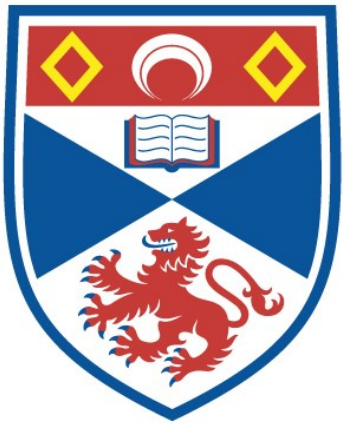

1955

ROTATIONAL FLOW IN FLUID DYNAMICS

BY

JAMES D. MURRAY, B.Sc.

A THESIS PRESENTED TO THE

UNIVERSITY OF ST. ANDREWS

FOR THE

DEGREE OF DOCTOR OF PHILOSOPHY

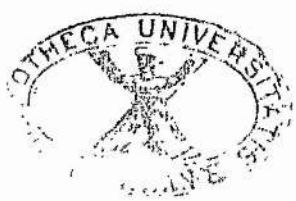

1955

ProQuest LLC.
789 East Eisenhower Parkway
P.O. Box 1346
Ann Arbor, MI 48106 – 1346

Declaration

I hereby declare that the following thesis is based on work carried out by me, that the thesis is my own composition, and that no part of it has been presented previously for a Higher Degree.

The research was carried out in the Department of Mathematics in the United College of St. Salvator and St. Leonard, University of St. Andrews, under the supervision of A.R. Mitchell, B.Sc., Ph.D., F.R.S.E..

Certificate

I hereby certify that James D. Murray, B.Sc., has spent nine terms engaged in research work under my direction, and that he has fulfilled the conditions of Ordinance 16 (St. Andrews), and is qualified to submit the accompanying thesis in application for the Degree of Doctor of Philosophy.

DIRECTOR OF RESEARCH

Personal Preface

In October, 1949, I first matriculated in the University of St. Andrews (United College of St. Salvator and St. Leonard) and obtained the degree of B.Sc. with First Class Honours in Mathematics in June, 1953.

In September, 1953, I registered as a research student. From October, 1953, until September, 1955, I held a Carnegie Trust for the Universities of Scotland Research Scholarship. In October, 1955, I was appointed Lecturer in Applied Mathematics in King's College, University of Durham.

INDEX

List of Symbols

c	velocity of sound
c_L	lift coefficient
c_p, c_v	specific heats at constant pressure, and volume respectively
$\frac{D}{Dt}$	total differential ($= \frac{\partial}{\partial t} + \underline{q}.\underline{\nabla}$ in vector form)
G	mass flow per second
h	enthalpy
k	constant in adiabatic gas law
L	lift force
ℓ	significant linear dimension
M	Mach number ($= q/c$)
N	rotational flow parameter ($=\frac{U}{\omega \ell}$, U being a significant velocity)
p	pressure
q	velocity
q_x, q_y	velocity components in x- and y- directions
q_r, q_θ	radial and transverse velocity components
q_ξ, q_η	velocity components in ξ- and η- directions
q_u, q_v	velocity components in u- and v- directions
R	gas constant ($= c_p - c_v$)
r, θ	polar coordinates
S	entropy
T	absolute temperature
U	significant velocity
u, v	parabolic coordinates
x, y	cartesian coordinates

z complex variable ($= x + iy$, $i^2 = -1$)

Γ circulation

γ ratio of specific heats ($= c_p/c_v$)

δ deflection of the stagnation stream line

$\frac{\partial (g_1, g_2)}{\partial (h_1, h_2)}$ Jacobian of g_1 and g_2 with respect to h_1 and h_2

ε eccentricity of ellipse

K specific conductivity

ξ, η elliptic coordinates

ρ density

χ $\rho^{-\frac{1}{2}}$

ψ stream function

ω vorticity

$\underline{\nabla}$ gradient vector operator ($= \underline{i} \frac{\partial}{\partial x} + \underline{j} \frac{\partial}{\partial y}$ in two-dimensional cartesian coordinates, $\underline{i}$ and $\underline{j}$ unit vectors)

∇^2 Laplacian operator ($= \frac{\partial^2}{\partial x^2} + \frac{\partial^2}{\partial y^2}$ in two-dimensional cartesian coordinates).

Introduction

Except for classical vortex motion, analytical solutions of rotational flow problems did not exist until 1943 when Tsien [16] published his paper on aerofoils in a constant shear flow. Previously, in 1937, Young and Maas [35] carried out experiments on the nature of the flow past a pitot tube in a transverse pressure gradient, and found that there was a displacement in the free stream, of the stagnation stream line. During the last few years, some controversy has arisen concerning the magnitude and direction of this displacement as measured by Young and Maas. Accordingly, it was felt that much use could be made of a theoretical study of the two-dimensional motion of flows with rotation. By obtaining the stream functions, in a closed form, for several shear flows past cylinders with various cross sections, it is hoped to establish, on a theoretical basis, the fact that there is a displacement, as mentioned above, in any rotational flow. Such solutions and methods of solutions will also help to fill the present gap in the rotational flow theory in fluid dynamics. Further, in view of the fact that analytical solutions to compressible flow problems with rotation do not seem likely in the near future, it is also decided to investigate the possibility of relaxational solutions of such problems.

References [3] to [37] constitute the bulk of the work published on rotational flow of any description, with the exception of the rotational flow present in vortex motion.

The thesis is divided into four chapters. Chapter I gives a brief resumé of the state of rotational flow theory up to 1955. Chapter II contains a study of the constant shear flow past cylinders with various cross sections.

Chapter III contains a method for obtaining the stream functions for cylinders in a variable shear flow when the latter approximates firstly to a linear vorticity distribution, and secondly to the rotational flow present in a boundary layer. Further, it illustrates the nature of the difficulties likely to be encountered in trying to obtain analytical solutions of problems where the rotation is of a more complicated nature. Finally, Chapter IV contains a relaxation solution to the two-dimensional isentropic compressible rotational flow of a gas through a channel containing a constriction. It also illustrates the complexity of the numerical work required in obtaining relaxation solutions of compressible flow problems with rotation.

J.D.M.

CHAPTER I

RESUMÉ OF ROTATIONAL FLOW THEORY

Resumé of Rotational Flow Theory

In this section, a short account of the present state of the theory of a steady, continuous, frictionless rotational fluid is given. This account is in three sections, the second and third being of primary importance for the requirements of the subsequent chapters in this thesis.

Included in the second part of the resumé are several results derived by the author from the fundamental equations.

In compiling this summary, use was made of references [1] to [37].

Basic assumptions

All the work throughout this thesis, unless otherwise stated, is based on the assumption that the fluid is

(1) continuous

(2) steady

(3) two-dimensional

(4) inviscid

(5) rotational.

I. General Rotational Flow of Ideal Gases

The study of vortex motion or rotational flow was instigated by Helmholtz [1] in 1858, and the majority of his results are still in use. An introductio and discussion of classical rotational flow is given in Lamb [2].

The general work is covered by references [3] to [15], the study being concerned with steady, non-viscous, thermally non-conducting rotational flow of gases, subject to no extraneous force fields.

Prim [12], in 1949, gives a comprehensive review of the state of rotational flow theory, concentrating on the establishment of general properties of such

flows, and the discovery of exact solutions of the governing equations. The references in his review, unless they have a particular bearing on the subject matter of this thesis, will not be reproduced in the bibliography. It should be noted that his work also includes axially symmetric and spatial flow fields, together with two-dimensional flows.

Subsequent papers discuss further exact solutions of the equations, and also steady, plane rotational Prandtl-Meyer flows. Heinrich [6] makes reference to the effect of external heat in frictionless rotational flow, and discusses the geometrical significance of vectors arising in the discourse. Sears [13] describes a linear-perturbation theory for rotational flow. Vazsonyi [15] discusses individual problems of a more practical and physical nature, and derives relations, between the vorticity, enthalpy and entropy.

II. The Rotational Flow Equations and Theoretical Solutions

The fundamental equations governing the steady, inviscid, compressible flow of a gas, with constant c_p and c_v, the specific heats at constant pressure and volume respectively, are,

Equations of Motion (Navier-Stokes)

$$q_x \frac{\partial q_x}{\partial x} + q_y \frac{\partial q_x}{\partial y} = -\frac{1}{\rho}\frac{\partial p}{\partial x}\,,$$

$$q_x \frac{\partial q_y}{\partial x} + q_y \frac{\partial q_y}{\partial y} = -\frac{1}{\rho}\frac{\partial p}{\partial y}\,, \qquad \text{----------(1)}$$

Equation of Energy

$$\rho c_p\left(q_x \frac{\partial T}{\partial x} + q_y \frac{\partial T}{\partial y}\right) - \left(q_x \frac{\partial p}{\partial x} + q_y \frac{\partial p}{\partial y}\right)$$

$$= k\nabla^2 T + \frac{\partial k}{\partial x}\frac{\partial T}{\partial x} + \frac{\partial k}{\partial y}\frac{\partial T}{\partial y}\,, \qquad \text{----------(2)}$$

Equation of Continuity

$$\frac{\partial(\rho q_x)}{\partial x} + \frac{\partial(\rho q_y)}{\partial y} = 0 \quad ,----------(3)$$

and

Equation of State

$$p = \rho R T \quad ,----------(4)$$

where x and y are the cartesian coordinates, q_x and q_y the component velocities in the x- and y- directions respectively, p the pressure, ρ the density, T the absolute temperature, K the specific conductivity, and R the gas constant. The rotation ω, is given in cartesian coordinates by

$$\omega = \frac{\partial q_y}{\partial x} - \frac{\partial q_x}{\partial y} \quad .----------(5)$$

Differentiating the first equation (1) by y, and the second by x, subtracting, and using the continuity equation, the following result

$$\omega\left(\frac{\partial q_x}{\partial x} + \frac{\partial q_y}{\partial y}\right) + q_x\frac{\partial \omega}{\partial x} + q_y\frac{\partial \omega}{\partial y} = -\frac{\partial(\rho^{-1}, p)}{\partial(x,y)} \quad ,$$

is obtained, which, after a little manipulation may be written as

$$q_x\frac{\partial(\omega\rho^{-1})}{\partial x} + q_y\frac{\partial(\omega\rho^{-1})}{\partial y} = \frac{1}{\rho}\frac{\partial(p,\rho^{-1})}{\partial(x,y)} \quad ,----(6)$$

where $\frac{\partial(p,\rho^{-1})}{\partial(x,y)}$ is the Jacobian of p and $\frac{1}{\rho}$ with respect to x and y. The corresponding result in three dimensions is easily obtained using vector methods, and may be written in vector notation as

$$(\underline{q}\cdot\underline{\nabla})(\rho^{-1}\underline{\omega}) = \rho^{-1}(\underline{\omega}\cdot\underline{\nabla})\underline{q} + \rho^{-1}\,\underline{\nabla}p \times \underline{\nabla}\rho^{-1} \quad ,-----(7)$$

where the vector operator $\underline{\nabla} \equiv \underline{i}\frac{\partial}{\partial x} + \underline{j}\frac{\partial}{\partial y} + \underline{k}\frac{\partial}{\partial z}$ ($\underline{i}$, $\underline{j}$ and $\underline{k}$ being the unit vectors in the x-, y-, and z-directions respectively), and $\underline{\omega} \equiv \underline{\nabla} \times \underline{q}$.

The continuity equation (3) permits the introduction of the stream function ψ , where the cartesian coordinate velocities q_x and q_y are given by

$$q_x = \frac{1}{\rho}\frac{\partial \psi}{\partial y} \quad , \quad q_y = -\frac{1}{\rho}\frac{\partial \psi}{\partial x} \quad . \qquad \text{---------(8)}$$

A gas is considered to be barotropic if there is a unique functional relationship between the pressure and density. For compressible flows the relationship is the adiabatic gas law

$$P/\rho^{\gamma} = k \, , \qquad \text{----------(9)}$$

where $\gamma = c_p/c_v$ is the ratio of specific heats, and k is the adiabatic gas constant.

On substitution of relation (9) in equation (2), it is seen, using equation (4), that K must be zero and equation (2) is thus an identity. On the other hand, if K is assumed to be zero, it can be easily shown that the fluid must be barotropic. Thus, the governing equations reduce to three in number, as expected, namely equations (1), (3) and (9). The temperature at any point can be obtained immediately from equation (4). It should be noted that equation (9) is the law governing isentropic flow, which is not the case in the rotational flow behind a bow shock wave, where the entropy S, varies from stream line to stream line, although the stagnation enthalpy for each stream line is the same.

When the fluid satisfies equation (9), the right hand side of equation (6) is zero, and on substitution of relations (8) inthe left hand side, equation (6) becomes, since ρ is non-zero,

$$\frac{\partial \psi}{\partial y}\frac{\partial(\omega\rho^{-1})}{\partial x} - \frac{\partial \psi}{\partial x}\frac{\partial(\omega\rho^{-1})}{\partial y} = 0 ,$$

which has a general solution of the form

$$\omega/\rho = f(\psi), \qquad \text{----------(10)}$$

where $f(\psi)$ is a general differentiable function of ψ, independent of x and y. Equation (10) shows that ω/ρ is constant along a stream line. Equations (8) and (5) become

$$\frac{\partial}{\partial x}\left(\frac{1}{\rho}\frac{\partial \psi}{\partial x}\right) + \frac{\partial}{\partial y}\left(\frac{1}{\rho}\frac{\partial \psi}{\partial y}\right) + \omega = 0. \qquad \text{------(11)}$$

One further well-known relation arising from the fundamental equations, is Bernoulli's equation, which for an adiabatic gas is

$$\frac{\gamma}{\gamma-1}\frac{p}{\rho} + \frac{1}{2}q^2 = h_s , \qquad \text{----------(12)}$$

where h is the enthalpy, the suffix s denoting stagnation conditions.

Vaszonyi [15] derives the relationship between the velocity, entropy, and stagnation enthalpy, given by

$$q\omega = T\frac{\partial S}{\partial n} - \frac{\partial h_s}{\partial n} , \qquad \text{----------(13)}$$

where $\frac{\partial}{\partial n}$ denotes differentiation normal to a stream line. Since both the entropy S, and stagnation enthalpy h_s are functions of ψ alone, and using the fact that $\frac{\partial}{\partial x} = q\rho\frac{\partial}{\partial \psi}$, it is seen from equation (13), that

$$\omega = \frac{p}{R}\frac{\partial S}{\partial \psi} - \rho\frac{\partial h_s}{\partial \psi} . \qquad \text{----------(14)}$$

It is also apparent from equation (14), that if the flow is isentropic, ω/ρ is a function of ψ, since h_s and thus $\frac{\partial h_s}{\partial \psi}$ are functions of ψ alone. In conclusion, it should be noted that rotation is present if either the entropy or the stagnation enthalpy is variable.

For convenience, two-dimensional rotational flows are now subdivided as follows, the relevant literature being included in each section;

1. Incompressible Flow with Constant Rotation

In this case, equation (10) implies that the vorticity ω is constant throughout the fluid: this result is, of course, in agreement with Helmholtz's theorem $\frac{D\omega}{Dt} = 0$, where $\frac{D}{Dt}$ denotes the total differential. The problem thus reduces to finding solutions, with specific boundary conditions, of equation (11), which in this case is a particular example of Poisson's equation,

$$\nabla^2\psi + \omega = 0 \quad , \text{----------} \quad (15)$$

where ω is a constant, and the Laplacian operator $\nabla^2 \equiv \frac{\partial^2}{\partial x^2} + \frac{\partial^2}{\partial y^2}$.

In 1943, Tsien's paper, 'Symmetrical Joukowski Airfoils in Shear Flow' [16] was published, in which he gives the first particular solution of equation (15). It is the solution for constant shear flow past a circular cylinder. Tsien defines the stream function ψ as a sum of two functions ψ_0 and ψ_1, where ψ_0 is the stream function of the undisturbed constant shear flow, and ψ_1 is the disturbance stream function, due to the presence of the cylinder. The function ψ_1 is thus a solution of Laplace's equation, which satisfies the following conditions:

(i) the disturbance velocity due to ψ_1 must vanish at points far from the body, which ensures parallel constant shear flow in the free stream;

(ii) the normal component of the disturbance velocity at the surface of the body must equal the negative of that due to ψ_0, so that the resultant normal

velocity is equal to zero.

Using this method, he obtains and illustrates the flow fields of a source and vortex in a constant shear flow, and derives the stream function for the constant shear flow past a circular cylinder. This method is modified and extended by the author in the second chapter. Although stream functions for cylinders with cross sections other than a circle can only be obtained by Tsien's method with great difficulty, he obtains formulae for the force and moment on a Joukowski aerofoil, by transforming the circle. He further, discusses circulation, strength of doublets and quadruplets, lift and moment coefficients, and aerodynamic centre.

Coombs [17] , employing complex variable theory, and James [18] , using the Poisson integral, consider aerofoils in constant shear flow, and put forward methods for obtaining the stream functions for constant shear flow past cylinders. However, except for the case of the circular cylinder, the stream functions can not be obtained in a closed form, if at all. In each case, however, without obtaining the stream functions, the resultant forces and moments are discussed fully.

References [19], [20], and [21] further discuss forces, moments and pressures on general aerofoil sections by extending the Blasius Theorem. Prakash [22] discusses the possibility of superposing parallel shear flows on sources, sinks and doublets: he concludes that the superposed flows must be irrotational, whereas in actual fact, the vorticity may be a non-zero constant, as is illustrated by Tsien [16] . In the paper by Mitchell and Murray [23] , the stream functions for constant shear flow past cylinders of varying cross sections are obtained in a closed form, particular attention being paid to positions of stagnation points and deflections of the stagnation stream lines: this work is described in detail in chapter II of this thesis.

Goldstein and Lighthill [24] use the hodograph transformation on the constant shear flow past a circular cylinder, and show that the hodograph plane is a Riemann surface of six sheets. They give some indication of the difficulti likely to be encountered in using the hodograph plane to obtain analytical solutions of flows with vorticity present.

Kramer and Stanitz [25] calculate numerically the two-dimensional incompressible constant shear flow round a 90° bend, paying particular attention to the regions of high velocity and vorticity.

Thom [26] makes an arithmetical calculation of the flow at the mouth of a Stanton pitot tube as the Reynold's number tends to zero. Although the flow is viscous, and incompressible, the initial rotation in the free stream is constant. He finds a stationary eddy under the lip of the pitot and calculates the height of the effective centre of the pitot.

In chapter IV of this thesis, a numerical solution is obtained for constant shear flow through a channel with straight parallel sides, containing a constriction. The results are given under this section.

2. Incompressible Flow with Variable Rotation

Equations (10) and (11) reduce, in this case, to solving the single partial differential equation

$$\nabla^2\psi + f(\psi) = 0 , \qquad (16)$$

with given boundary conditions. In this case the vorticity at any point is given by $\omega = f(\psi)$.

As far as the author is aware, no theoretical solutions have yet been obtained for incompressible, two-dimensional flow with variable shear. In chapter III, the particular example of $f(\psi)$ equal to $\lambda\psi$ is discussed, where λ is a real constant (positive or negative) and the analysis results in a

theorotical solution for flow with variable rotation.

Cornock [27] puts forward a method for the numerical solution of Poisson's equation using matrices, but leaves the matrices and their inverses in general form. It is seen in the numerical example in chapter IV, where $f(\psi)$ is a constant, that numerical relaxation is probably quicker than inverting the matrix. The inversion of the general matrix, or large order matrices, is extremely difficult practically, if not impossible.

3. Compressible Isentropic Flow with Rotation

The boundary conditions and equations in this section and the next, require very careful consideration, due to the non-linear nature of the partial differential equations.

Since the fluid is isentropic, the entropy S, on each stream line must have the same value, and thus $\frac{\partial S}{\partial \psi} = 0$. Also, since the fluid is rotational the stagnation enthalpy h_s must vary from stream line to stream line, and thus equation (14) reduces to

$$\omega = -\rho \frac{\partial h_s}{\partial \psi} \quad \text{----------(17)}$$

The two fundamental equations are thus

$$\frac{\partial}{\partial x}\left(\frac{1}{\rho}\frac{\partial \psi}{\partial x}\right) + \frac{\partial}{\partial y}\left(\frac{1}{\rho}\frac{\partial \psi}{\partial y}\right) - \rho \frac{\partial h_s}{\partial \psi} = 0 \text{ ,------(18)}$$

and

$$\frac{\gamma}{\gamma-1}\frac{p}{\rho} + \frac{1}{2}q^2 = h_s \text{ .----------(19)}$$

If h_s (or the stagnation speed of sound c_s), is given as a function of ψ, then a solution is defined for any ψ-distribution. It should be noted, that a simila result is obtained using equation (10), where $f(\psi)$ is defined by the original

density and vorticity. To conclude, an isentropic rotational flow can not arise from a reservoir where the pressure, density, and thus the temperature are constant.

In chapter IV, equations (18) and (19) are taken in non-dimensional form, expressed in the form of finite difference equations, and solved by simultaneous relaxation for the problem of flow through a channel with parallel sides containi a constrictio

4. Compressible Non-Isentropic Flow.

The flow, being non-isentropic, is rotational, and equation (14) gives

$$\omega = \frac{P}{R}\frac{\partial S}{\partial \psi} \quad , \qquad (20)$$

assuming in this case that the stagnation enthalpy is the same on every stream li

Equation (18) becomes

$$\frac{\partial}{\partial x}\left(\frac{1}{\rho}\frac{\partial \psi}{\partial x}\right) + \frac{\partial}{\partial y}\left(\frac{1}{\rho}\frac{\partial \psi}{\partial y}\right) + \frac{P}{R}\frac{\partial S}{\partial \psi} = 0 \quad . \qquad (21)$$

The form of the other equations is dependent on the specific problem.

Mitchell [28] employs a relaxation method of solution to evaluate the mixed subsonic and supersonic non-isentropic flow regions downstream of a bow shock wave, formed when a parallel supersonic flow impinges on a blunt nosed two-dimensional obstacle. The equations he uses are equation (21), and Bernoulli's equation for the r^{th} stream line downstream of the shock in the form

$$\left(\frac{q}{c_s}\right)^2 = \frac{2}{\gamma - 1}\left[1 - \frac{P}{\rho}\frac{(\rho_s)_r}{(P_s)_r}\right] \quad , \qquad (22)$$

where $(\rho_s)_r$, $(p_s)_r$, and c_s are the values of the stagnation density and pressure downstream of the shock, and the stagnation speed of sound, respectively. The equations connecting the pressure, density and entropy are

$$\frac{P}{\rho^\gamma} = \frac{p_s}{\rho_s^\gamma}\, e^{(S_r - S_0)/c_r} = k_r = \frac{(p_s)_r}{(\rho_s)_r^\gamma} \quad ,$$

where S_0, p_s and ρ_s are the entropy, stagnation pressure and density on all stream lines upstream of the shock and S_r, k_r and c_r the entropy, adiabatic gas constant and speed of sound respectively, on the r^{th} stream line downstream of the shock. In non-dimensional form, the flow parameter ν_r, on the r^{th} stream line appears, where $\nu_r = \frac{G}{(\rho_s)_r c_s H}$, G being the mass flow per second under free stream conditions, and H some typical length in the problem. A detailed description of the method of obtaining ν_r and $\frac{1}{R}\frac{\partial s}{\partial \psi}$ on the stream lines downstream of the shock is given, using shock wave data. Equations (21) and (22) are expressed in dimensionless form, replaced by the corresponding finite difference equations and relaxed simultaneously, the field being evaluate for a parallel stream of Mach number 1.8. The vorticity is calculated, using equation (20), everywhere in the field, and it is found that the stream line starting from the point of maximum vorticity on the shock wave, is a locus of high vorticity in the rotational field downstream of the shock wave. Mitchell further shows that the angle ϕ, between the line of constant Mach number and the stream line through a point is given by

$$\tan\phi = \frac{\left(\frac{\partial M}{\partial s}\right)_n}{\frac{M}{L}\left(1+\frac{\gamma-1}{2}M^2\right) + \omega\left(1+\frac{\gamma-1}{2}M^2\right)^{3/2}}, \qquad \text{----------(23)}$$

where ds is the elementary arc length along a stream line, L is the radius of curvature of the stream line at the point, n = constant is the family of stream lines, and M is the Mach number. Using equation (23), it is seen that on the obstacle L is infinite and ω is zero, resulting in the fact that lines of constant Mach number meet the obstacle at right angles.

The most important feature of the paper, is the adaption of relaxation technique to the evaluation of mixed subsonic and supersonic fields, changes in entropy being taken into account.

Emmons [29] puts forward a method of relaxation, applicable to subsonic regions only, which he uses to evaluate the rotational subsonic field of flow behind an arbitrarily placed shock in a hyperbolic channel.

Although not quite relvant from the point of view of this thesis, the paper by Pai [30] should be mentioned. He discusses some of the properties of the supersonic rotational flow over two-dimensional ogives. Charney [31] and Platzman [32] discuss the numerical integration of the unsteady baratropic vorticity equation, from the point of view of determining the vorticity in the atmosphere. Mitchell and McCall [33] evaluate numerically the rotational field behind a bow shock wave in axially symmetric flow, using methods similar to those described by Mitchell [28] . Although the problem is three-dimensional the relaxation solution is for all practical purposes two-dimensional.

It is not possible to examine the finite difference replacements of the compressible rotational flow equations for stability and convergence (O'Brien, Hyman, and Kaplan [34]), due to the non-linear nature of the differential equations.

III. Experimental Work in connection with Rotational Flow

Young and Maas [35] in 1936 investigated the nature of the displacement of the stagnation stream line when a pitot tube is placed in a region of transverse total-pressure gradient. The experiments were carried out by making pitot traverses behind the trailing edge of a symmetrical wing section at different distances from the trailing edge, with varying sizes of pitot, the air speed being approximately 75 ft./sec.. It should be noted that the work is of a three-dimensional nature.

The most important qualitative result arising from the investigation is the fact that the stagnation stream line is displaced to a region where the velocity is higher than that opposite the geometric centre of the face of

the pitot.

The observations related to the parts of the traverses where $\frac{d(\frac{1}{2}\rho q^2)}{dx}$ was substantially constant, x being the distance through wake, measured from some fixed point. Young and Maas found that for a range of $\frac{2D}{\rho q^2}\frac{d(\frac{1}{2}\rho q^2)}{dx}$ from 0.1 to 0.2, where D is the external diameter of the pitot, the ratio δ/d is substantially constant, where δ is the displacement of the effective centre of pressure. For a value of D_1/D of 0.6, where D_1 is the internal diameter of the pitot, the experiments gave $\delta/D = 0.16$.

The case $\frac{d(\rho q^2)}{dx}$ being constant is equivalent to a parabolic velocity distribution over the constant range. The case of a cylinder in a flow, which approximates to that with a parabolic velocity profile is discussed in chapter III.

Johannesen and Mair [36] carried out an investigation on the effect of the size of pitot tubes in a two-dimensional supersonic wake, and their experimental results show hardly any effect of the kind found by Young and Maas.

Davies [37] describes some effects of pitot size on measurements of laminar boundary layers on a flat plate and cones in a supersonic wind tunnel, and compares them with results obtained by other investigators. The results obtained by Davies conflict with those of Young and Maas. Davies found in the supersonic case that the deflection of the stagnation stream line is to a region where the velocity is lower than that opposite the pitot tube centre. The conditions of the investigation in the subsonic case were different however, the pitots Davies used being of a two-dimensional nature. Due to the small amount of data published on the pitot size effects at supersonic speeds, the results as yet seem inconclusive.

F.A. MacMillan in Cambridge, is at present carrying out experimental

work on rotational flow, but his work is as yet unpublished.

No attempt has been made in this chapter, to give a full account of rotational flow theory. The author has concentrated on the parts which are important for the requirements of this thesis, and the papers discussed in detail are those which have some direct bearing on the subsequent chapters of the thesis.

Chapter II

Flow With Constant Vorticity

Two-Dimensional Flow with Constant Shear past Cylinders with Various Cross Sections

Several authors have obtained stream functions for incompressible flow with constant shear past cylinders of different shapes in two dimensions ([16], [17], and [18]). The forces and moments have been calculated using the methods described, but except in the case of the circular cylinder, closed expressions for the stream function in the physical plane can be obtained only with great difficulty, if at all. Accordingly, in this chapter, the stream functions for constant shear flow past a variety of cylinders are obtained. From each stream function the main characteristics of the flow are determined.

The General Transformation and Circular Cylinder

For two dimensional motion, assumed to be continuous, steady, incompressibl and inviscid, the equation of continuity in rectangular cartesian coordinates is (I.3)

$$\frac{\partial (q_x)}{\partial x} + \frac{\partial (q_y)}{\partial y} = 0 ,$$

where q_x and q_y are the cartesian velocity components.

Since the flow is everywhere rotational, the potential can not be employed. The continuity equation, however, permits the introduction of the stream function ψ, where

$$q_x = \frac{\partial \psi}{\partial y} , \quad \text{and} \quad q_y = - \frac{\partial \psi}{\partial x} .$$

The vorticity, ω, is defined by

$$\omega = \frac{\partial q_y}{\partial x} - \frac{\partial q_x}{\partial y} ,$$

which on substitution for q_x and q_y gives (I.15)

$$\frac{\partial^2 \psi}{\partial x^2} + \frac{\partial^2 \psi}{\partial y^2} + \omega = 0 . \qquad \text{----------(1)}$$

The stream function ψ, must thus satisfy equation (1), and the vorticity ω, satisfies

$$\frac{D\omega}{Dt} = 0 \ , \qquad (2)$$

where $\frac{D}{Dt}$ denotes the total differential. However, since the vorticity is constant in the free stream, and the flow is incompressible, ω is constant at every point in the field. The problem reduces to finding a solution, under given boundary conditions, of equation (1), where ω is a constant.

An auxiliary stream function Ψ, which satisfies Laplace's Equation, is introduced by means of the transformation

$$\Psi = \psi + \frac{\omega}{2} \frac{Ax^2 + By^2}{A + B} \ , \qquad (3)$$

where A and B are constants. On differentiating,

$$\nabla^2 \Psi = \nabla^2 \psi + \nabla^2 \left[\frac{\omega}{2} \frac{Ax^2 + By^2}{A + B} \right]$$

$$= \nabla^2 + \omega$$

$$= 0 \ ,$$

where ∇^2 is the Laplacian operator $\frac{\partial^2}{\partial x^2} + \frac{\partial^2}{\partial y^2}$. The transformation yields $\nabla^2 \Psi = 0$ in all normal coordinate systems, which include, for example, plane polar, elliptic, and parabolic systems. Ψ represents a stream function which satisfies the conditions for irrotational flow.

For the case of flow with constant shear parallel to the x-axis

$$\omega = -\frac{\partial q_x}{\partial y} \ ,$$

which gives

$$q_x = U - \omega y \ ,$$

where U is the velocity along the x-axis, and

$$\psi = Uy - \frac{\omega}{2} y^2 \ , \qquad (4)$$

where the constant of integration is taken to be zero. From the transformation given by relation (3),

$$\Psi = Uy + \frac{\omega}{2}\,\frac{A(x^2 - y^2)}{A + B} \quad . \qquad \text{----------(5)}$$

The stream function for sheer flow past a circular cylinder derived by Tsien [1], can be obtained very quickly as follows. Equation (5) gives Ψ for parallel flow, as the imaginary part of the complex function

$Uz + \frac{A\omega}{2(A+B)}\, iz^2$, where $z = x + iy$, which according to Milne Thomson's Circle Theorem [36] is modified to $U(z + \frac{r_o^2}{z}) + \frac{A\omega i}{2(A+B)}\,(z^2 - \frac{r_o^4}{z^2})$, when a circle of radius r_o is inserted at the origin. Substituting Ψ, the imaginary part of the latter complex function, into the transformation formula, the stream function ψ, which still contains A and B, is obtained, which, in polar coordinates r and θ, is

$$\psi = Ur \sin\theta\,(1 - \frac{r_o^2}{r^2}) + \frac{A\omega}{2(A+B)}\, r^2 \cos 2\theta\,(1 - \frac{r_o^4}{r^4})$$

$$- \frac{\omega}{2(A+B)}\,(Ar^2 \cos^2\theta + Br^2 \sin^2\theta).$$

Since the cylinder $r = r_o$ is a solid boundary, ψ is constant on $r = r_o$. Thus, on $r = r_o$,

$$\psi = - \frac{\omega r_o^2}{2(A+B)}\,(A \cos^2\theta + B \sin^2\theta),$$

which varies with θ, unless A = B, under which conditions ψ would be constant and equal to $-\omega r_o^2/4$ on the circular cylinder. Thus, putting A = B, the required stream function is

$$\psi = \frac{\omega r_o^2}{4} + U \sin\theta\,(r - \frac{r_o^2}{r})$$

$$- \frac{\omega}{4}\,(2r^2 \sin^2\theta + \frac{r_o^4}{r^2} \cos 2\theta), \qquad \text{----------(6)}$$

where ψ takes the constant value zero on the cylinder, and tends to $\frac{\omega r_o^2}{4} + Uy - \frac{\omega}{2} y^2$ as $r \longrightarrow \infty$.

The transformation, which in this case reduces to $\psi = \Psi - \frac{\omega}{4} r^2$, in plane

polar coordinates, used in conjunction with Milne Thomson's Circle Theorem, constitutes a useful extension to this theorem, which permits the inclusion of constant shear flows past circular cylinders.

It should be noted, that this extension has certain limitations. Constan shear flow past cylinders of cross sections other than a circle, can not be obtained by directly transforming the region outside the circular boundary on t the region outside the boundary of the desired cross section: this is, however permissible in irrotational flow under certain conditions [38]. To illustrate the limitation of using transformations in this way for rotational flows, the case of a circle being transformed to a flat plate is used.

The transformation $z = Z + \frac{r_o^2}{Z}$ maps the region outside a circle in the Z-plane on to the region outside a straight line of length $4r_o$ lying along the x-axis in the z-plane. The complex function for rotational flow past the circular cylinder in the Ψ-field is $U(Z + \frac{r_o^2}{Z}) + \frac{i\omega}{4}(Z^2 - \frac{r_o^4}{Z^2})$, which, on using the above transformation to the z-plane, becomes $Uz + \frac{i\omega}{4} z(z^2 - 4r_o^2)^{\frac{1}{2}}$. This represents the complex function for the same free stream flow past a flat plate in the Ψ-field. However, the complex function in the physical plane is

$$Uz + \frac{i\omega}{4} z(z^2-4r_o^2)^{\frac{1}{2}} - \frac{i\omega}{4}\left[z/2 + \tfrac{1}{2}(z^2-4r_o^2)^{\frac{1}{2}}\right]\left[\bar{z}/2 + \tfrac{1}{2}(\bar{z}^2-4r_o^2)^{\frac{1}{2}}\right],$$

where $\bar{z}$ is the complex conjugate of z. The stream function ψ for the flow past a flat plate would then be the imaginary part of the latter complex function. It is easily seen that this imaginary part is not equal to $Uy - \frac{\omega}{2} y^2$, which is the true stream function for shear flow past a flat plate lying along the x-axis. Further, ψ must satisfy the condition that on the boundary it assumes a constant value. From the imaginary part of the stream function, it is easily shown that ψ is not constant along the x-axis.

However, for a given value of the constant ω, ψ equal to a constant does give a solid boundary, and the ψ thus represents the shear flow past the cylinder whose cross section is this solid boundary. The solid boundary, however, would then vary with each value of the constant taken by the vorticity ω, and this, of course, limits the practical application of the method. Although the analysi may be somewhat tedious, retention of the general A and B in the transformation may enable the true stream functions past the transformed bodies to be obtained. If a body, however, has natural coordinates, the general method, described subsequently, should, of course, be used.

General Considerations

The stream function ψ, for all flows with constant shear, must satisfy the following boundary conditions:

1. $\nabla^2\psi + \omega = 0$
2. $\psi \longrightarrow$ constant + $Uy - \frac{\omega}{2} y^2$ as $x \longrightarrow -\infty$
3. $\psi = 0$ on the given cylinder.

This constant, in condition 2., may be omitted, which would result in ψ = consta (other than zero) on the cylinder.

These three conditions do not determine a unique solution for flow with constant shear past a cylinder, since the addition of circulation about the cylinder to the stream function does not alter the satisfaction of the boundary conditions. Thus, for uniqueness, the value of the circulation must be stipulated.

If Γ is the circulation and $\underline{q}$ and $d\underline{\ell}$ are the velocity, and element of length vectors respectively, then the circulation round any closed path L is given by

$$\Gamma = \oint_L \underline{q} \cdot d\underline{\ell}$$

$$= \int_S \nabla \times \underline{q} \cdot d\underline{S} \qquad \text{(Stokes's Theorem)}$$

$$= \omega \int_S dS .$$

Thus,

$$\Gamma = \omega S, \qquad \text{----------(7)}$$

where S is the area enclosed, in the plane, by the closed path L and ω is the two-dimensional vorticity. Thus, Γ has the same value round a closed path in the field of parallel constant shear flow as in the field of constant shear flow past a cylinder. The path L can be any closed path in the field (including or excluding the cylinder). If it is taken as the cross sectional boundary of the cylinder, the result, given by equation (7), shows that the insertion of a smooth cylinder in the flow with constant shear does not alter the circulation round the path now occupied by the boundary of the cylinder. This result has been put forward, but not proved, by Tsien in a paper by Richardson [21].

In particular, the stream function for a circulation round the circular cylinder of radius r_o, is of the form $-K \log {}^{r}/_{r_o}$, where $2\pi K$ is the strength of the circulation. The addition of this term, which is included in Ψ, being a solution of Laplace's Equation, alters the position of the stagnation points in the finite field, as in the case of irrotational flow. In the following work of this chapter, however, unless otherwise stated, the circulatio will conform with the result stated by equation (7), that K is zero. This gives the circulation Γ, in a clockwise direction round the circular cylinder, as $\pi\omega r_o^2$, where, in this case, $S = \pi r_o^2$.

Examination of the Flow Field for Shear Flow past the Circular Cylinder

To ease the analysis carried out at a later stage, it is desirable to introduce non-dimensional quantities at the outset. If

$$x' = \frac{x}{h}, \; y' = \frac{y}{h}, \; q' = \frac{q}{U}, \text{ and } \psi' = \psi/G,$$

where Q is the mass flow under free stream conditions and equal to Uh, and h is some significant linear dimension in the particular problem, then equation (1) becomes

$$\nabla'^2 \psi' + \frac{\omega h}{U} = 0,$$

where $\nabla'^2 = \frac{\partial^2}{\partial x'^2} + \frac{\partial^2}{\partial y'^2}$. The non-dimensional number $\frac{U}{\omega h}$ will be denoted throughout this thesis by N, and unless otherwise stated, will be taken to be positive. This number N, a dimensionless parameter for rotational flow, appears repeatedly in the results obtained in this thesis. Equation (1), in its dimensionless form, becomes

$$\nabla'^2 \psi' + \frac{1}{N} = 0. \qquad (8)$$

The stream function for constant shear flow past a circular cylinder of radius r_o, has been derived, and is given by equation (6). Taking r_o to be the significant linear dimension, and putting $r' = r/r_o$, the stream function ψ' which is a solution of equation (8), and which satisfies the general boundary conditions 1., 2., and 3. in dimensionless form, is

$$\psi' = \frac{1}{4N} + \sin\theta \left(r' - \frac{1}{r'}\right) - \frac{1}{4N}\left(2r'^2 \sin^2\theta + \frac{1}{r'^2}\cos 2\theta\right). \qquad (9)$$

It should be noted that the flow is symmetrical about the y-axis.

The velocity q, at any point in the field, is given by

$$q^2 = q_r^2 + q_\theta^2 , \qquad (10)$$

where q_r and q_θ are the radial and transverse components of the velocity respectively. The non-dimensional poler coordinate velocities are given by

$$q'_r = \frac{1}{r'}\frac{\partial \psi'}{\partial \theta} , \quad q'_\theta = -\frac{\partial \psi'}{\partial r'} .$$

Equation (10) thus gives the velocity q', in its non-dimensional form.

In the subsequent analysis on the circular cylinder, the dash notation is dropped, but it must be remembered that non-dimensional quantities are still

being used, unless otherwise stated.

The components of velocity are thus

$$q_r = \frac{1}{r}\frac{\partial \psi}{\partial \theta} = \cos\theta\left(1 - \frac{1}{r^2}\right) - \frac{r \sin 2\theta}{2N}\left(1 - \frac{1}{r^4}\right), \qquad \text{---------(11)}$$

$$q_\theta = -\frac{\partial \psi}{\partial r} = -\sin\theta\left(1 + \frac{1}{r^2}\right) + \frac{1}{2N}\left(2r\sin^2\theta - \frac{\cos 2\theta}{r^3}\right), \qquad \text{---------(12)}$$

which on substitution in equation (10), gives the velocity at any point (r,θ). Stagnation points in the flow are given by

$$q_r = q_\theta = 0.$$

With q_r and q_θ zero, equations (11) and (12) become a set of simultaneous equations in two unknowns r and θ, the coordinates of the stagnation points. Equation (11) becomes

$$\left[N - r\sin\theta\left(1 + \frac{1}{r^2}\right)\right]\left(1 - \frac{1}{r^2}\right)\cos\theta = 0,$$

solutions of which are

I. $\sin\theta = \frac{Nr}{(r^2+1)}$,

II. $r = 1$,

III. $\cos\theta = 0$.

The values of r and θ for stagnation points are obtained when these three conditions are incorporated with equation (12), with q_θ zero. Each case is considered separately.

I. Equation (12), with q_θ zero, becomes

$$\frac{Nr}{(r^2+1)}\left(1 + \frac{1}{r^2}\right) - \frac{1}{2N}\left[\frac{2N^2r^3}{(r^2+1)^2} - \frac{1}{r^3} + \frac{2N^2}{r(r^2+1)^2}\right] = 0,$$

which reduces to

$$r^4(1 + 4N^2) + 2r^2 + 1 = 0,$$

since $r \neq 0$, the solution of which is purely imaginary. Thus, condition I results in no real values of r and θ for stagnation points.

II. When $r = 1$, (i.e. on the circular cylinder), equation (12) with q_θ zero, gives

$$\sin\theta = \frac{N}{2} \pm \frac{1}{2}\,(N^2 + 1)^{\frac{1}{2}} \,. \qquad \text{---------- (13)}$$

Thus, for any value of N, there are at least two stagnation points on the cylinder, and if N is small ($N < 3/4$), there are four. Examination of equation (13) shows that there are four values of θ_c, where the suffix c denotes the value of θ taken by the stagnation point on the cylinder, if $N < 3/4$, three if $N = 3/4$, and two, if $N > 3/4$: this corresponds at the two extremes to flow with large vorticity and small vorticity respectively. Infinite vorticity (or zero standard velocity), corresponding to zero N, gives values for θ_c of $\pi/6$, $5\pi/6$, $7\pi/6$, and $11\pi/6$. The stagnation points in the region $\pi \leqslant \theta \leqslant 2\pi$ have values of θ_c, which always satisfy $2\pi \geqslant \theta_c \geqslant \frac{11\pi}{6}$, and $\pi \leqslant \theta_c \leqslant \frac{7\pi}{6}$. As N grows larger, the two upper stagnation points move upwards until $N = 3/4$, when they coalesce at $\theta_c = \frac{\pi}{2}$. Henceforth the combined point moves off the cylinder leaving two stagnation points symmetrically placed about the y-axis on the cylinder below the x-axis ($y < 0$). The three distinct cases for stagnation points on the cylinder are shown schematically in Figure (a), where crosses denote positions of stagnation points.

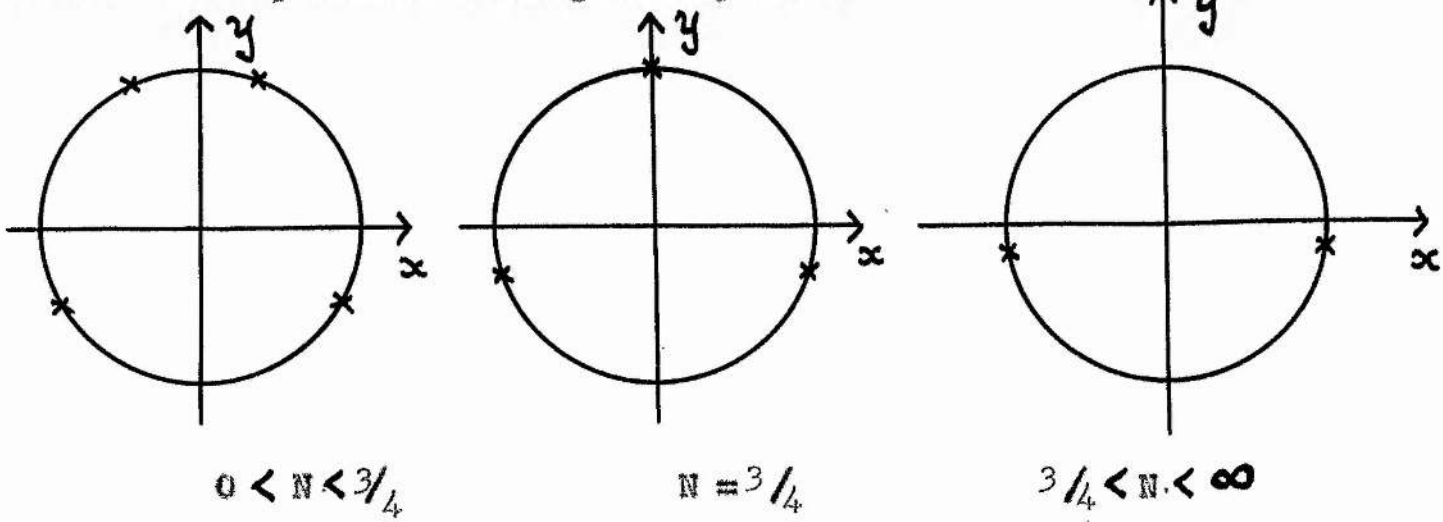

Figure (a)

The value taken by the stream function on the cylinder is zero, this being obtained by putting $r = 1$ in relation (9). As $r \to \infty$, $\psi = \frac{1}{4N} + y - \frac{y^2}{2N}$, and on putting ψ zero, two values of the non-dimension ordinate y_s are obtained, where the suffix s denotes the stagnation stream line. Thus, the stagnation stream line comes from points in the free stream, whose positions are given by the equation

$$2y_s^2 - 4Ny_s - 1 = 0.$$

The latter has solution

$$y_s = N \pm (N^2 + \tfrac{1}{2})^{\frac{1}{2}}. \qquad \text{(14)}$$

The stream line from the non-dimensional ordinate $N - (N^2 + \frac{1}{2})^{\frac{1}{2}}$, is the stagnation stream line of the lower stagnation points ($y_s < 0$), and is the stream line with the most representative total head. It is seen from the schematic free stream velocity diagram, given in Figure (b), that this stagnation stream line comes from a region of higher velocity than that opposite the diameter of the cylinder. This result is in agreement with the experimental results of Young and Maas [35], although, in their case, the transverse pressure gradient is constant, and not the vorticity. Qualitatively the direction of the displacement of the stagnation stream line is the same. Both stream lines $\psi = 0$, move on to the cylinder if $N \leq 3/4$, but only the lower if $N > 3/4$. In this case the zero ψ from $y > 0$ becomes a normal stream line containing no stagnation points.

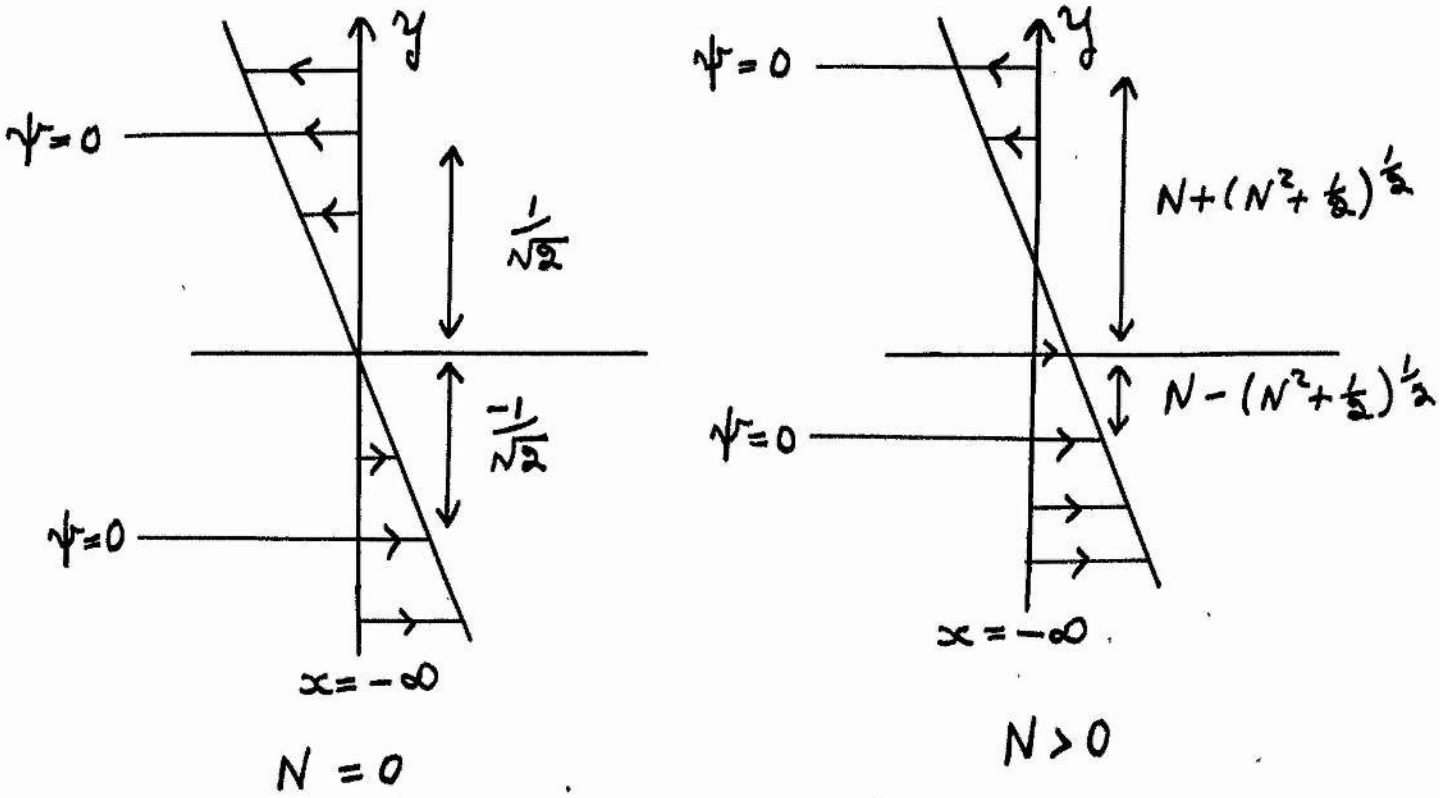

Figure (b)

Before the complete field of flow can be determined, the third condition must be considered in conjunction with equation (12), with q_θ zero.

III. The solution of

$$\cos\theta = 0,$$

is $\theta = (2n+1)\pi/2$, where n can take integral values, positive or negative, including zero. Since the expression for the stream function is of period 2π, the two cases, n zero and unity, need only be considered.

When $\theta = \frac{3\pi}{2}$, equation (12) with q_θ zero, gives

$$(1 + \frac{1}{r^2}) + \frac{1}{2N}(2r + \frac{1}{r^3}) = 0,$$

which for $N \geqslant 0$ yields only negative or imaginary values of r. Thus, there are no stagnation points on the line $\theta = \frac{3\pi}{2}$ (the y-axis for $y < 0$). On the other hand, $\theta = \frac{\pi}{2}$ gives values of r, which are solutions of

$$r^4 - Nr^3 - Nr + \tfrac{1}{2} = 0 \quad .\text{----------(15)}$$

Depending on the value of N, r is real (and positive) or imaginary. Solution of equation (15) numerically, proved quicker than the tedious manipulation required to obtain the solution theoretically. As a check to the previous case (II.), $N = 3/4$ gives $r = 1$ as the only real positive solution ($r \geq 1$) of equation (15). Any solution must naturally have a value of $r \geq 1$ for real stagnation points in the field. It can be easily shown that for $N < 3/4$, there is no real value of $r \geq 1$ satisfying equation (15), whereas for $N \geq 3/4$, there is one real positive value of $r \geq 1$.

Thus, when the two upper stagnation points ($y > 0$) on the cylinder move towards $\theta = \frac{\pi}{2}$, they coalesce at $\theta = \frac{\pi}{2}$ for $N = 3/4$, and henceforth move off the cylinder as one. The combined point moves along the y-axis towards $y = +\infty$, which is reached when N is infinite, corresponding to irrotational flow.

Bernoulli's Theorem, for incompressible flow, may be written as

$$\frac{p}{\rho} + \frac{1}{2} q^2 = H \text{ ,} \qquad \text{----------(16)}$$

where p is the pressure, ρ is the constant density, and H, the Bernoulli constant, is a constant for a given stream line.

The resultant force on the cylinder is a lift force (in y direction, Figure (c)).

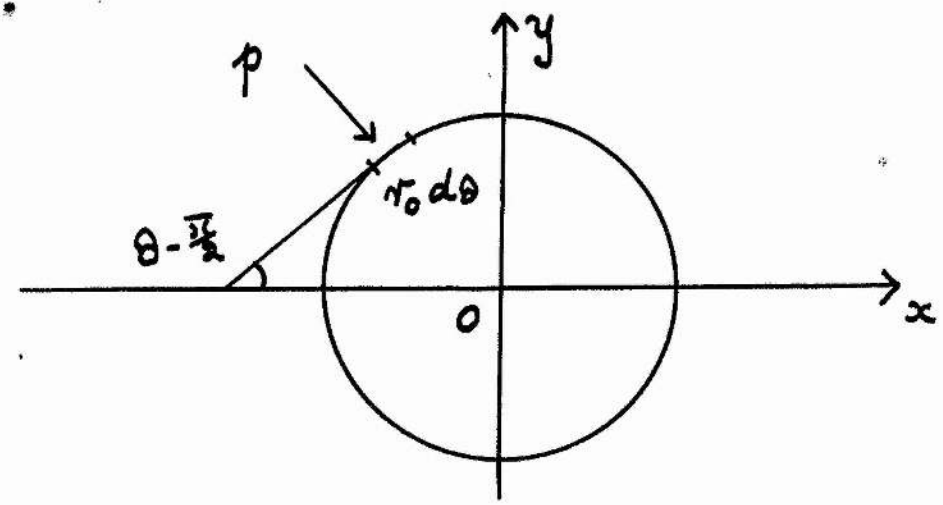

Figure (c)

This lift force L is given in dimensional form by

$$L = 2r_o \int_{-\frac{\pi}{2}}^{\pi/2} p_{r=r_o} \sin\theta \, d\theta \ ,$$

per unit length of cylinder. Using equation (16), this becomes

$$L = - r_o \rho \int_{-\frac{\pi}{2}}^{\pi/2} q^2_{r=r_o} \sin\theta \, d\theta \ , \qquad (17)$$

where $q_{r=r_o}$, the value of the velocity on the cylinder, is obtained from equat (10). On the circular cylinder, $q_{r=r_o} = (q_\theta)_{r=r_o}$, and so

$$(q_\theta)^2_{r=r_o} = 4\omega^2 r_o^{\,2} \sin^4\theta - 8Uor_o \sin^3\theta + (4U^2 - 2\omega^2 r_o^{\,2}) \sin^2\theta + 2Uor_o \sin\theta + \frac{\omega^2 r_o^{\,2}}{4} \ .$$

Thus, substituting this expression in equation (17), and evaluating the resulting integral, the lift force is found to be

$$L = 2\pi\rho r_o^{\,2} U\omega,$$

which may be written as

$$L = \tfrac{1}{2}\rho c_L (2r_o) U^2 \ , \qquad (18)$$

where the lift coefficient $c_L = {}^{2\pi}/_{N}$, with $N = {}^{U}/_{\omega r_o}$ as before.

The important geometrical quantities, in the flow are as follows:

(1) the deflection of the stagnation stream line in the free stream, given by the non-dimensional ordinate

$$y_s = N - (N^2 + \tfrac{1}{8})^{\frac{1}{2}} \ ,$$

(2) the deflection of the stagnation point ($y < 0$) on the cylinder given by the non-dimensional ordinate

$$y_c = {}^{N}/_{2} - \tfrac{1}{8} (N^2 + 1)^{\frac{1}{2}} \ ,$$

(3) and the non-dimensional deflection δ, of the stagnation stream line, given by the difference in the two expressions above, namely

$$\delta = y_s - y_c = {}^{N}/_{2} + \tfrac{1}{8}(N^2 + 1)^{\frac{1}{2}} - (N^2 + \tfrac{1}{8})^{\frac{1}{2}} \ .$$

Although the stream function for the circular cylinder can not be obtained as a particular example of the general elliptic cylinder, the above quantities, together with the lift force, are particular cases of the general results. Accordingly, graphs of these quantites are shown with the results for the elliptic cylinders in Figures (3), (5) and (6), respectively.

On giving particular values to ψ , the flow field can be described fully. Although such flows are physically improbable, the case most likely to arise in practice is the flow corresponding to $N \gg 3/4$. Accordingly, a schematic flow field for $N > 3/4$ is shown in Figure (1), the region $x \leq 0$ only, being shown, since the flow is symmetrical about the y-axis. The flow fields for other ranges of N have similar characteristics to those portrayed in Figures (4) and (7) for the elliptic cylinder.

The General Method

The general transformation, from equation (3) gives, in its dimensional form,

$$\psi = \Psi - \frac{\omega}{2} \frac{Ax^2 + By^2}{A + B} ,$$

where Ψ is a solution of Laplace's Equation. For flow with constant shear, parallel to the x-axis, Ψ is given by

$$\Psi = Uy + \frac{\omega}{2} \frac{A(x^2 - y^2)}{A + B} .$$

In the presence of a cylinder, it is convenient to write

$$\Psi = \Psi_0 + \Psi_1 ,$$

where $\Psi_0 = Uy + \frac{\omega}{2} \frac{A(x^2 - y^2)}{A + B}$, and Ψ_1 is a solution of Laplace's Equation, which tends to a constant as $x \to -\infty$. The general transformation is then

$$\psi = \Psi_0 + \Psi_1 - \frac{\omega}{2} \frac{Ax^2 + By^2}{A + B} ,$$

which results in

$$\psi = Uy - \frac{\omega}{2} y^2 + \Psi_1 . \qquad \text{(19)}$$

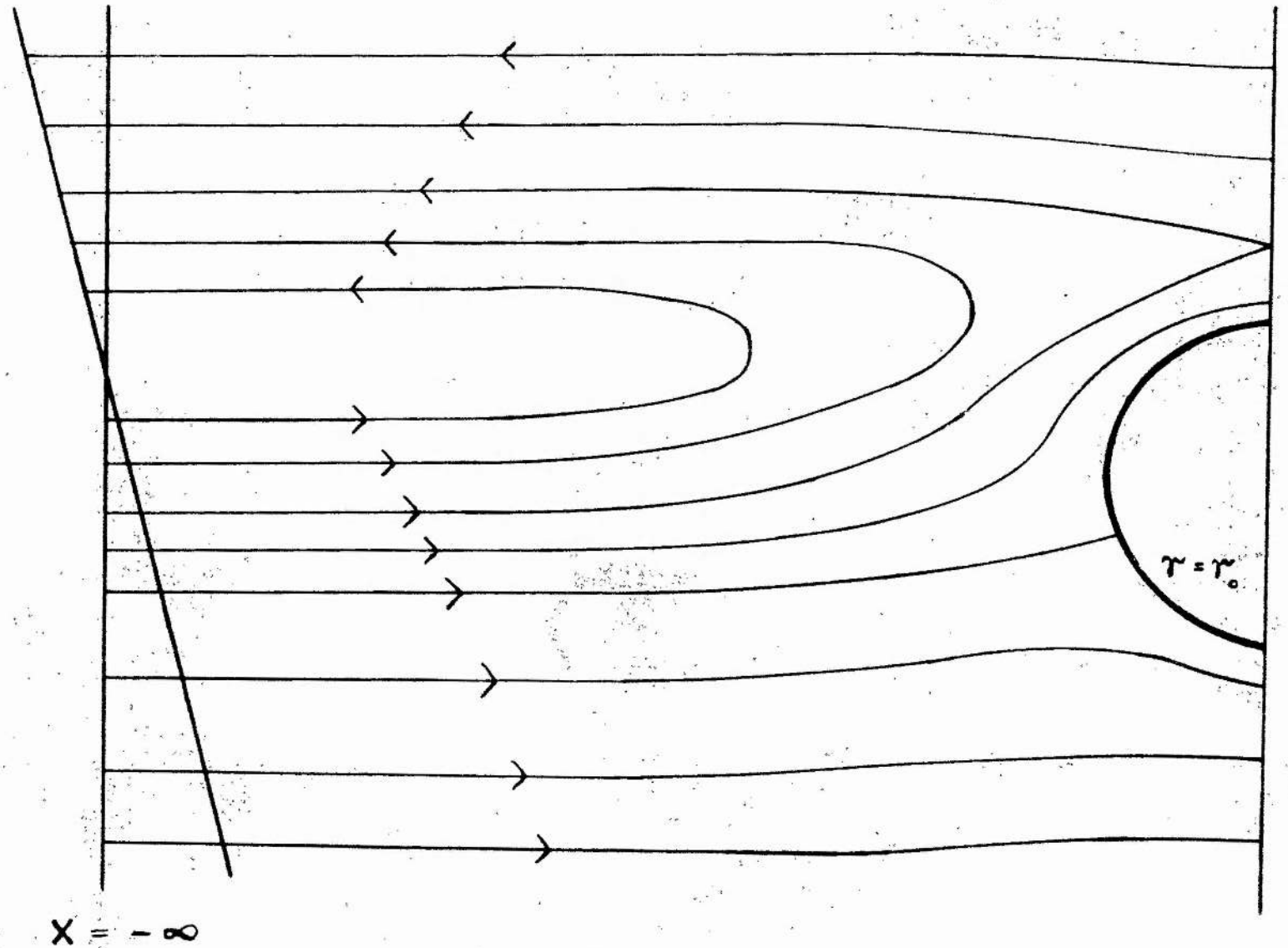

Figure (1) Illustration of the stream lines for a circle when there is a stagnation point in the field, not on the cylinder.

This result can also be obtained by taking Ψ as Uy plus a general solution of Laplace's Equation involving A and B, which tends to a constant as $x \to -\infty$. Taking the elliptic cylinder as a specific example, it can easily be shown that A must be zero, in order to satisfy the free stream boundary condition, and again equation (19) is obtained.

If a body has natural coordinates, Ψ_1 is found in its general form in terms of those coordinates, by solving Laplace's equation using the method of separation of variables. The solution must satisfy the condition that $\Psi_1 \to$ constant as $x \to -\infty$, and the general coefficients in the solution are found by Fourier Analysis, using the condition that ψ is zero on the cylinder. To illustrate this method, stream functions are obtained for the general elliptic cylinder, with minor axis parallel and perpendicular to the flow, the finite flat plate, the infinite flat plate and the parabolic cylinder. It should be noted that Tsien's method is a slight modification of the case with Ψ_1 in polar coordinates.

<u>The Elliptic Cylinder and Flat Plate.</u>

<u>Derivation of the Stream Functions.</u>

In the case of flow with constant shear past an ellipse, centred at the origin (Figure (2)), elliptic coordinates ξ, η are introduced by means of the formulae

$$x = c \cosh \xi \cos \eta \,, \qquad \text{----------(20)}$$
$$y = c \sinh \xi \sin \eta \,,$$

where c is a constant. The ellipse $\xi = \xi_0$, (major and minor axes a and b along the x- and y- axes respectively) is taken as the solid boundary, and the velocity profile as $x \to -\infty$ is given by the first two terms on the right-hand-side of equation (19), which, in elliptic coordinates, become

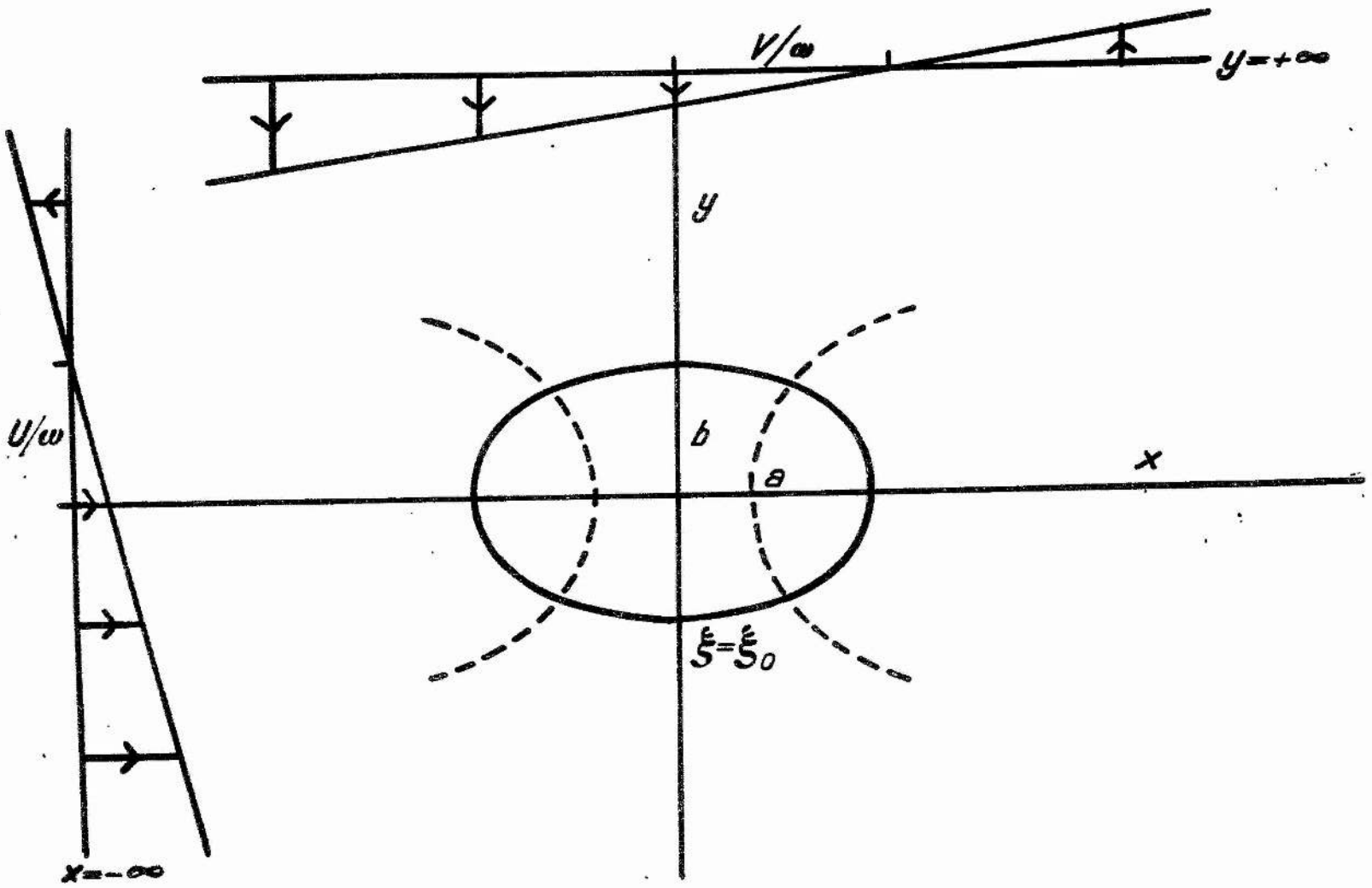

Figure (2) Illustration of rotational flow past an elliptic cylinder.

$Uc \sinh \xi \sin \eta - \frac{\omega}{2} c^2 \sinh^2 \xi \sin^2 \eta$. Laplace's Equation in elliptic coordinates with solution Ψ_1, is

$$\frac{\partial^2 \Psi_1}{\partial \xi^2} + \frac{\partial^2 \Psi_1}{\partial \eta^2} = 0 . \qquad \text{(21)}$$

Writing

$$\Psi_1 = \Xi(\xi)H(\eta) ,$$

substituting in equation (21) and solving by separation of variables, the result

$$\Psi_1 = \sum_n (a_n \cos n\eta + b_n \sin n\eta)(c_n e^{n\xi} + d_n e^{-n\xi}),$$

is obtained, where n is the separation constant, and a_n, b_n, c_n, and d_n are constants. Since the stream function (and Ψ_1) is of period 2π, n must take all the integral values, and since $\Psi_1 \longrightarrow$ constant as $\xi \to \infty$, c_n must be zero. Thus,

$$\Psi_1 = \sum_{n=0}^{\infty} (A_n \cos n\eta + B_n \sin n\eta) e^{-n\xi}, \quad (n = 0, 1, 2, \ldots) \qquad \text{(22)}$$

where A_n and B_n are constants. On substituting this value of Ψ_1 in equation (19), the stream function ψ is obtained. In order that ψ may retain the constant value zero on the ellipse $\xi = \xi_0$ $(0 \leq \eta \leq 2\pi)$, the coefficients A_n and B_n in equation (22) must satisfy the relation

$$0 = Uc \sinh \xi_0 \sin \eta - \frac{\omega}{2} c^2 \sinh^2 \xi_0 \left[\tfrac{1}{2}(1 - \cos 2\eta)\right]$$
$$+ \sum_{n=0}^{\infty} (A_n \cos n\eta + B_n \sin n\eta) e^{-n\xi_0} .$$

Equating the coefficients of $\sin n\eta$ and $\cos n\eta$, A_n and B_n are found to be

$$A_0 = \frac{\omega}{4} c^2 \sinh^2 \xi_0 , \quad A_2 = -\frac{\omega}{4} c^2 \sinh^2 \xi_0 \; e^{2\xi_0}$$

$$A_1 = A_3 = A_4 = A_5 = \ldots = 0, \quad B_1 = -Uc \sinh \xi_0 \, e^{\xi_0} ,$$

$$B_2 = B_3 = B_4 = \ldots\ldots = 0 .$$

Since $a = c \cosh \xi_o$, $b = c \sinh \xi_o$, and $c^2 = a^2 - b^2$, the non-zero constants are thus

$$A_o = \frac{\omega}{4} b^2, \quad A_2 = -\frac{\omega}{4} b^2 \left(\frac{a+b}{a-b}\right), \quad B_1 = -Ub\left(\frac{a+b}{a-b}\right)^{\frac{1}{2}},$$

leading to the required expression

$$\psi = \frac{\omega}{4} b^2 + U\left[c \sinh \xi - b\, e^{(\xi_o - \xi)}\right] \sin \eta$$
$$- \frac{\omega}{4}\left[c^2 \sinh^2 \xi + \left\{b^2 e^{2(\xi_o - \xi)} - c^2 \sinh^2 \xi\right\} \cos 2\eta\right] \text{-----(23}$$

for the stream function in the case of constant shear flow past an ellipse with its minor axis perpendicular to the stream. When ω is zero, the stream function for irrotational flow past an ellipse is obtained. The value of ψ, given by equation (23) satisfies the three necessary conditions:

1. $\nabla^2 \psi + \omega = 0$,
2. $\psi = 0$ on $\xi = \xi_o$,
3. $\psi \to \frac{\omega}{4} b^2 + Uy - \frac{\omega}{2} y^2$ as $\xi \to \infty$.

In an exactly similar manner, if the velocity profile at $y = +\infty$ is taken to be

$$\frac{\partial \psi}{\partial x} = -q_y = V - \omega x, \text{----------(24)}$$

where V is the standard velocity on the y-axis, the required stream function is

$$\psi = Vx - \frac{\omega}{2} x^2 + \sum_{n=0}^{\infty} (A_n \cos n\eta + B_n \sin n\eta) e^{-n\xi},$$

where the constants A_n and B_n are found as before. The resulting stream function ψ, for constant shear flow past an ellipse $\xi = \xi_o$, with its major axis perpendicular to the flow, is

$$\psi = \frac{\omega}{4} a^2 + V\left[c \cosh\xi - a e^{(\xi_0 - \xi)}\right]\cos\eta$$

$$- \frac{\omega}{4}\left[c^2 \cosh^2\xi - \left\{a^2 e^{2(\xi_0 - \xi)} - c^2 \cosh^2\xi\right\}\cos 2\eta\right], \qquad (25)$$

where again ψ satisfies the three necessary conditions:

1. $\nabla^2\psi + \omega = 0$,
2. $\psi = 0$ on $\xi = \xi_0$,
3. $\psi \to \frac{\omega}{4} a^2 + Vx - \frac{\omega}{2} x^2$ as $\xi \to \infty$.

In the limit, as the minor axis tends to zero, the ellipse becomes a flat plate of length 2c, and the stream function past this plate (at right angles to the stream) is given by

$$\psi = \frac{\omega}{4} c^2 + Vc \sinh\xi \cos\eta$$

$$- \frac{\omega c^2}{4}\left[\cosh^2\xi + (\sinh 2\xi - \sinh^2\xi)\cos 2\eta\right], \qquad (26)$$

which satisfies the previous three conditions with c replacing a.

It should be noted at this stage, that the stream function for the circular cylinder can not be obtained as a particular example of the elliptic cylinder, since it entails ξ being infinite.

The flow fields, represented by relations (23) and (25), as in the case of the circular cylinder, are symmetrical about the y- and x- axes respectively

The velocity q at any point is given by

$$q^2 = q_\xi^2 + q_\eta^2 , \qquad (27)$$

where the velocity components in the ξ and η directions are q_ξ and q_η where

$$q_\xi = \frac{1}{g(\xi,\eta)} \frac{\partial\psi}{\partial\eta} , \quad q_\eta = -\frac{1}{g(\xi,\eta)} \frac{\partial\psi}{\partial\xi} , \qquad (28)$$

and

$$g(\xi,\eta) = c\,(\sinh^2\xi + \sin^2\eta)^{\frac{1}{2}} .$$

In particular, stagnation points are given by

$$\frac{\partial \psi}{\partial \eta} = \frac{\partial \psi}{\partial \xi} = 0 .$$

Examination of the Flow Field.

The Elliptic Cylinder with its major axis in the Direction of the Stream.

The velocity at any point (ξ, η) can be calculated using equation (27). The positions of the stagnation points are given by solving the following two equations:

$$\frac{\partial \psi}{\partial \eta} = 0 = U\left[c \sinh \xi - b\, e^{(\xi_0 - \xi)}\right] \cos \eta + \frac{\omega}{2}\left[b^2 e^{2(\xi_0 - \xi)} - c^2 \sinh^2 \xi\right] \sin 2\eta , \qquad (29)$$

$$\frac{\partial \psi}{\partial \xi} = 0 = U\left[c \cosh \xi + b\, e^{(\xi_0 - \xi)}\right] \sin \eta - \frac{\omega}{4}\left[c^2 \sinh 2\xi - \left\{2b^2 e^{2(\xi_0 - \xi)} + c^2 \sinh 2\xi\right\} \cos 2\eta\right]. \qquad (30)$$

Equation (29) reduces to

$$\left[U - \omega\left\{c \sinh \xi + b\, e^{(\xi_0 - \xi)}\right\} \sin \eta\right]\left[c \sinh \xi - b\, e^{(\xi_0 - \xi)}\right] \cos \eta = 0$$

solutions of which are

I. $\sin \eta = U/\omega \left[c \sinh \xi + b\, e^{(\xi_0 - \xi)}\right]$,

II. $c \sinh \xi = b\, e^{(\xi_0 - \xi)}$,

III. $\cos \eta = 0$.

Again, each case is considered separately.

I. Equation (30) can be written as

$$\omega\left[b^2 e^{2(\xi_0 - \xi)} + \frac{c^2}{2} \sinh 2\xi\right] \sin^2 \eta - U\left[c \cosh \xi + b\, e^{(\xi_0 - \xi)}\right] \sin \eta - \frac{\omega b^2}{2} e^{2(\xi_0 - \xi)} = 0,$$

which, on substituting the value of $\sin \eta$ given by relation I, becomes

$$\left(\frac{U}{\omega}\right)^2\left[b^2e^{a(\xi_o-\xi)}+\frac{c^2}{2}\sinh 2\xi\right]$$

$$-\left(\frac{U}{\omega}\right)^2\left[c\cosh\xi+be^{(\xi_o-\xi)}\right]\left[c\sinh\xi+be^{(\xi_o-\xi)}\right]$$

$$-\frac{b^2}{2}e^{a(\xi_o-\xi)}\left[c\sinh\xi+be^{(\xi_o-\xi)}\right]^2=0,$$

which reduces to

$$\left[e^{(\xi_o-\xi)}\left\{c\sinh\xi+be^{(\xi_o-\xi)}\right\}\right]^2=-\frac{2(a+b)}{b}\left(\frac{U}{\omega}\right)^2,$$

the solutions of which are imaginary.

II. A solution of relation II is $\xi=\xi_o$, which on substitution in equation (30) gives values of η for stagnation points on the ellipse, where

$$\sin\eta=\tfrac{1}{2}\left(\frac{U}{\omega b}\right)\pm\tfrac{1}{2}\left[\left(\frac{U}{\omega b}\right)^2+\frac{2b}{a+b}\right]^{\frac{1}{2}}.$$

As yet, no mention of dimensionless quantities has been made, but from the form of the last equation, the typical linear dimension chosen is b, the semi-minor axis; that is the axis which tends to obstruct the flow. Thus, the formula giving the stagnation points on the cylinder is

$$\sin\eta=\frac{N}{2}\pm\tfrac{1}{2}\left(N^2+\frac{2b}{a+b}\right)^{\frac{1}{2}},\qquad\text{(31)}$$

where $N=\frac{U}{\omega b}$.

As in the case of the circular cylinder, examination of equation (31) shows that for all values of $N(\geq 0)$, there are two stagnation points in the range $\pi\leq\eta\leq 2\pi$, the value of η being given by relation (31), the negative sign being taken. The range of movement of these two points is from positions on the ellipse, the joins of which to the origin make angles $\sin^{-1}\left[\frac{b}{2(a+b)}\right]$ with the major axis, to the ends of the major axis. (Corresponding to infinit N, and irrotational flow).

The depth of either stagnation point below the x-axis ($y<0$), using equation (31) is given by the non-dimensional ordinate $y_e=\frac{y}{b}$, where

$$y_c = \frac{N}{2} - \frac{1}{2}\left(N^2 + \gamma\right)^{\frac{1}{2}}, \qquad (32)$$

y being the dimensional ordinate equal to c $\sinh \xi_0 \sin \eta$, with $\sin \eta$ given by equation (31), and $\gamma = {}^{2b}/_{a+b}$, where $0 \leq \gamma \leq 1$. The graph of the non-dimensional quantity y_c against ${}^{1}/_{N}$ for $\gamma = \frac{1}{2}$ is shown in Figure (3). It should be noted, that although the stream function for the circular cylinder cannot be obtained as a particular case of the elliptic cylinder, the formula for the depth of the stagnation points can be obtained by putting $\gamma = 1$ (a = b) in equation (32).

The number of stagnation points in the range $0 \leq \eta \leq \pi$, depends on N. From equation (31) it can easily be shown that for $0 \leq N < \frac{2a+b}{2(a+b)}$, there are two stagnation points lying on the ellipse, where η is given by equation (31) with the positive root. That is

$$\sin\eta = \frac{N}{2} + \frac{1}{2}\left(N^2 + \gamma\right)^{\frac{1}{2}}.$$

When $N = \frac{2a+b}{2(a+b)}$, the two upper points coalesce at $\eta = \frac{\pi}{2}$, and when $N > \frac{2a+b}{2(a+b)}$ this point moves off the cylinder. Thus, the nature of the stagnation points on the cylinder can be determined completely, and the various cases are shown schematically in Figure (d). The circular cylinder is again a particular case

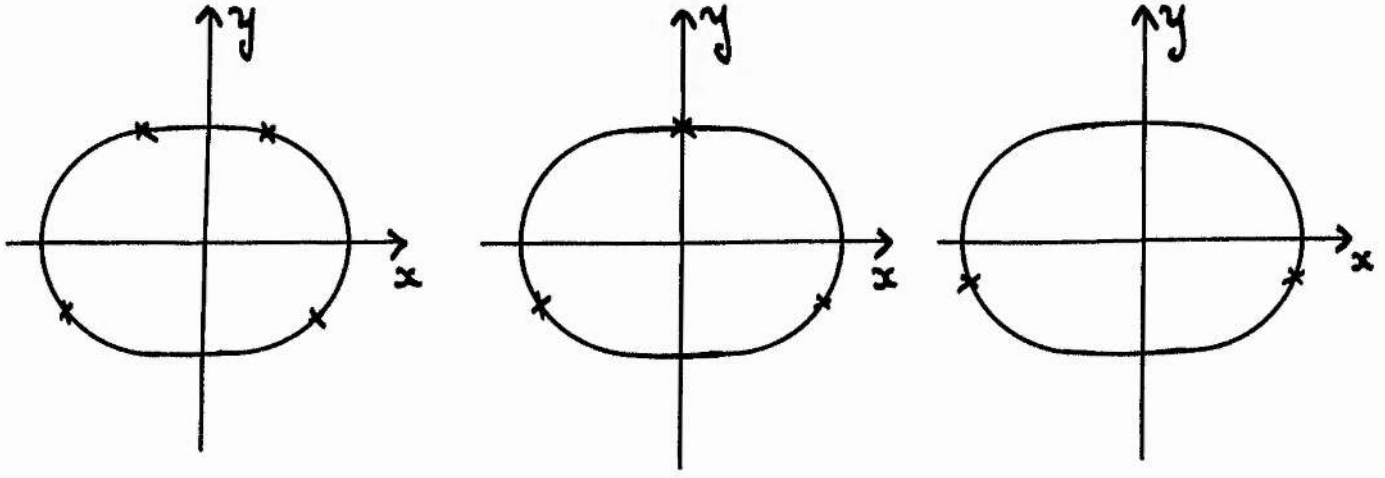

$0 < N < \frac{2a+b}{2(a+b)}$ $\qquad$ $N = \frac{2a+b}{2(a+b)}$ $\qquad$ $\frac{2a+b}{2(a+b)} < N < \infty$

Figure (d)

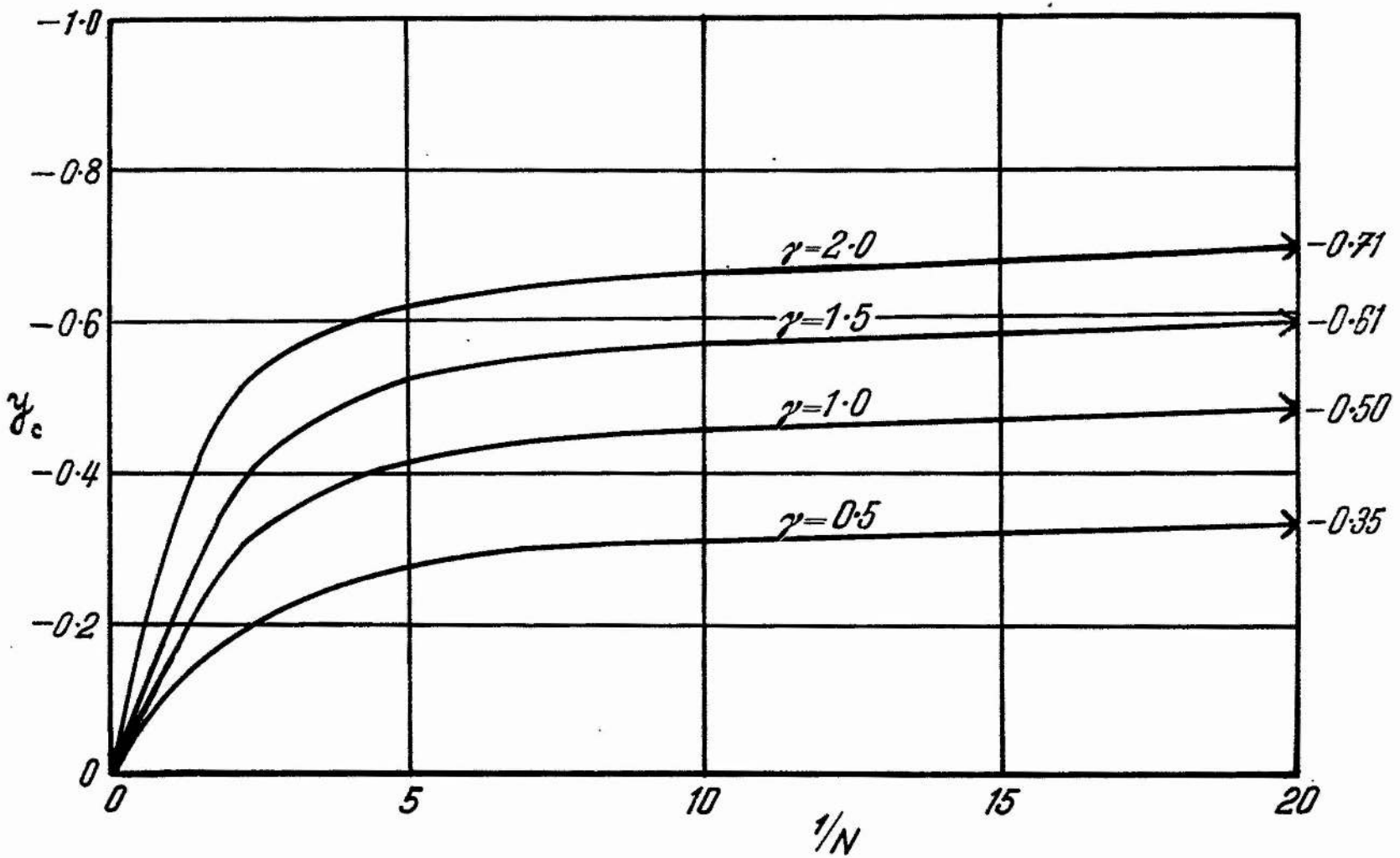

Figure (3) Variation of the position of the lower stagnation point for the circle, ellipse, and flat plate.

Finally, condition III must be considered together with equation (30).

III. The solution of

$$\cos\eta = 0,$$

is $\eta = \frac{\pi}{2}$, $\frac{3\pi}{2}$, since the field is periodic. When $\eta = \frac{3\pi}{2}$, equation (30) gives

$$\left(\frac{U}{\omega}\right)\left[c\cosh\xi + b\,e^{(\xi_0-\xi)}\right] + \frac{1}{2}\left[c^2\sinh 2\xi + b^2e^{2(\xi_0-\xi)}\right] = 0,$$

which, for $\frac{U}{\omega} \geqslant 0$, has no positive roots for ξ . When $\eta = \frac{\pi}{2}$, however,

$$\left(\frac{U}{\omega}\right)\left[c\cosh\xi + b\,e^{(\xi_0-\xi)}\right] - \frac{1}{2}\left[c^2\sinh 2\xi + b^2e^{2(\xi_0-\xi)}\right] = 0, \qquad (33)$$

which gives $\xi = \xi_0$ as a solution when $N = \frac{2a+b}{2(a+b)}$, and $\xi > \xi_0$ as a solution when $N > \frac{2a+b}{2(a+b)}$. To have any physical meaning, the solution must be positiv and greater than or equal to ξ_0.

Thus, to conclude the question of stagnation points, if $\frac{2a+b}{2(a+b)} \leqslant N \leqslant \infty$, there is one stagnation point, which lies on the y-axis ($y > 0$) and whose position is given by $b \leqslant y \leqslant \infty$, where $y = c\sinh\xi$ and $\xi \geqslant \xi_0$ is the solution of equation (33). The two upper stagnation points thus start off from positions on the ellipse, the joins of which to the origin make angles $\sin^{-1}\left[\frac{b}{a(a+b)}\right]^{\frac{1}{2}}$ with the major axis, move round the ellipse away from the major axis until they coincide at the upper end of the minor axis, whence the combined point moves off along the y-axis to infinity.

The stream function takes the constant value zero on the cylinder, and, a in the case of the circular cylinder, the non-dimensional ordinate y_s at $x = -\infty$ is given by

$$y_s = \frac{y}{b} = N \pm (N^2 + \tfrac{1}{2})^{\frac{1}{2}} ,$$

where y is the ordinate of the zero stream line at $x = -\infty$. This gives the non-dimensional ordinate of the lower zero stagnation stream line, which always moves on to the cylinder, as

$$y_s = N - (N^2 + \tfrac{1}{2})^{\frac{1}{2}} . \qquad \text{----------(34)}$$

This is the same form as that for the circular cylinder, where y_s and N have corresponding meanings. The schematic free stream flow is exactly the same as shown for the circular cylinder in Figure (b), with the appropriate change in N.

The flow field when there are two stagnation points on the cylinder is comparable to the field already shown in Figure (1), and so the field when the upper stagnation points have just coincided, is shown in Figure (4). Again, in view of the symmetry of the flow field about the y-axis, it is sufficient to illustrate the region $x \leq 0$.

Bernoulli's theorem for incompressible flow is given by equation (16).

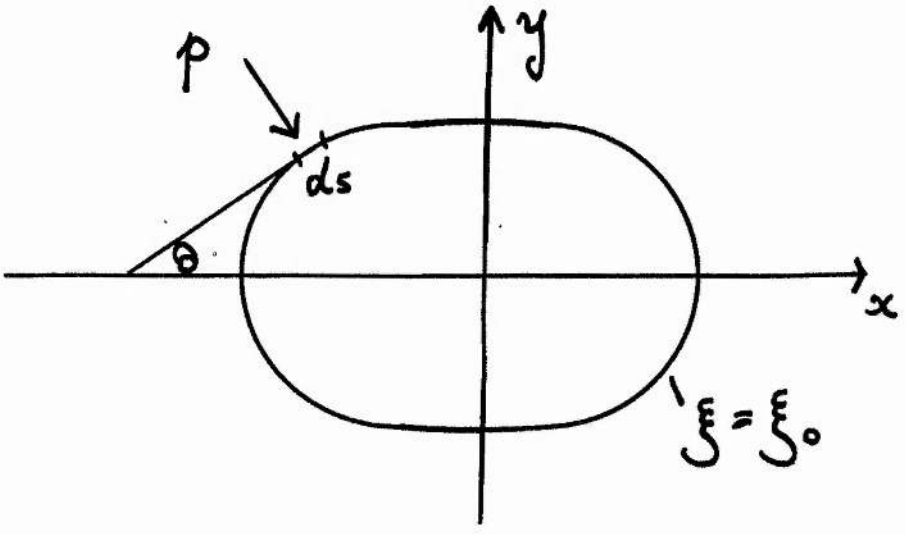

Figure (e)

Again, the resultant force is a lift force L, and its magnitude per unit length of cylinder is by

$$L = -\oint_{\xi=\xi_0} p \cos\theta \, ds , \qquad \text{[Figure (e)]}$$

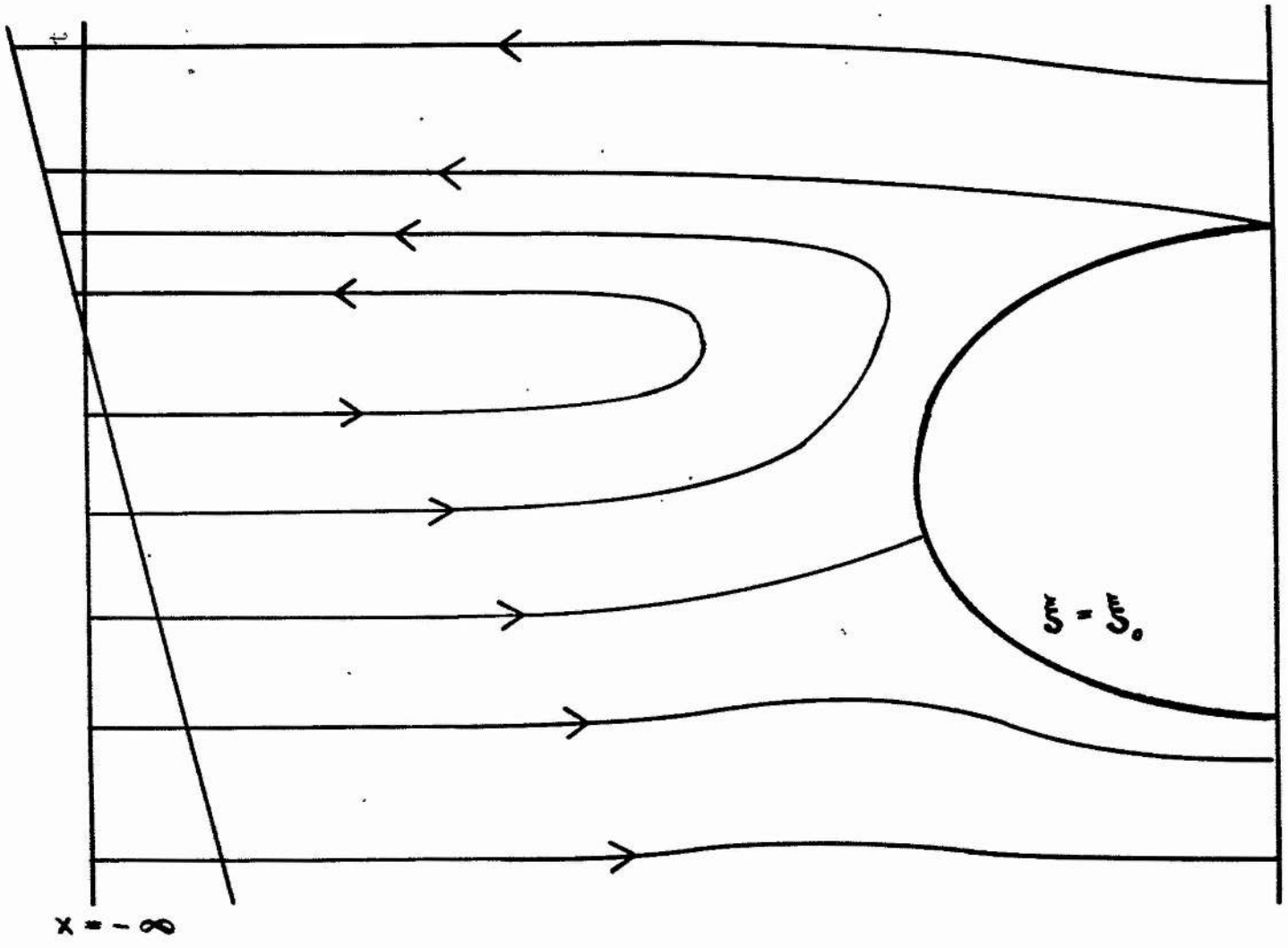

Figure (4) Illustration of the stream lines for an ellipse (minor axis perpendicular to the stream) when the upper stagnation points coincide.

where ds is the element of length on the ellipse, and θ is the angle the tangent to the ellipse at ds makes with x-axis. Thus, L becomes

$$L = -\oint p\, dx$$
$$= 2a \int_{-\frac{\pi}{2}}^{\pi/2} p \sin\eta\, d\eta \,.$$

That is, using Bernoilli's Theorem,

$$L = -a\rho \int_{-\frac{\pi}{2}}^{\pi/2} q^2_{\xi=\xi_0} \sin\eta\, d\eta \,, \qquad \text{----------(35)}$$

where $q_{\xi=\xi_0}$, the value of the velocity on the ellipse, is obtained from equation (27). Equation (35) becomes

$$L = -a\rho \int_{-\frac{\pi}{2}}^{\pi/2} \frac{\sin\eta}{[g(\xi_0,\eta)]^2} \left[\left(\frac{\partial\psi}{\partial\xi}\right)_{\xi=\xi_0}\right]^2 d\eta \,,$$

$$= -a\rho \int_{-\frac{\pi}{2}}^{\pi/2} \frac{\sin\eta}{(b^2\cos^2\eta + a^2\sin^2\eta)} \left[\left(\frac{\partial\psi}{\partial\xi}\right)_{\xi=\xi_0}\right]^2 d\eta \,,$$

where, from equation (30),

$$\left[\left(\frac{\partial\psi}{\partial\xi}\right)_{\xi=\xi_0}\right]^2 = \omega^2b^2(a+b)^2\sin^4\eta - 2U\omega b(a+b)^2\sin^3\eta$$
$$+ (a+b)\left[U^2(a+b) - \omega^2b^3\right]\sin^2\eta$$
$$+ b^2\omega U(a+b)\sin\eta + \frac{b^4\omega^2}{4} \,.$$

On substituting this expression in the last integral, the only non-zero integr are those of even power of $\sin\eta$ in the numerator. Using De Haan's Tables of Integrals [39], the following integrals are evaluated to give

$$\int_{-\frac{\pi}{2}}^{\pi/2} \frac{\sin^2\eta}{b^2\cos^2\eta + a^2\sin^2\eta}\, d\eta = \frac{\pi}{a(a+b)} ,$$

and

$$\int_{-\frac{\pi}{2}}^{\pi/2} \frac{\sin^4\eta}{b^2\cos^2\eta + a^2\sin^2\eta}\, d\eta = \frac{\pi}{(a^2-b^2)^2}\left[\frac{b^3}{a} + \frac{1}{2}(a^2 - 3b^2)\right] ,$$

which as a result,

$$L = \rho\pi k_0 b\,(a + b).$$

Introducing a lift coefficient c_L, which depends only on N, the lift force L, may be written as

$$L = \tfrac{1}{2} c_L \rho\,(a + b)U^2 , \qquad (36)$$

where $c_L = 2\pi/N$, with $N = \frac{U}{\omega b}$, as before.

The drag D, on the cylinder is, of course, zero, as can be easily checked analytically from the evaluation of the integrals involved.

To summarize, the three important quantities in the flow, excepting the lift force, are, as in the case of the circular cylinder;

(1) the deflection of the stagnation streamline in the free stream ($x = -\infty$) given by the non-dimensional ordinate $y_s = y/b$, where y is the ordinate of th zero stream line which moves on to the cylinder at the stagnation point $y < 0$ and where

$$y_s = N - (N^2 + \tfrac{1}{2})^{\frac{1}{2}} , \qquad (37)$$

(2) the deflection, or depth, of the stagnation point $y < 0$ on the cylinder, given by the non-dimensional quantity $y_c = y/b$, where in this case, y is the ordinate of the lower stagnation point on the cylinder, and

$$y_c = N/2 - \tfrac{1}{2}(N^2 + \gamma)^{\frac{1}{2}} , \qquad (38)$$

where $\gamma = {}^{2b}/_{a+b}$, and

(3) the non-dimensional deflection δ, of the stagnation stream line, given by

$$\delta = y_s - y_c = \frac{N}{2} + \frac{1}{2}\left(N^2 + \gamma\right)^{\frac{1}{2}} - \left(N^2 + 1\right)^{\frac{1}{2}} \quad , \text{----------(39)}$$

and the asymptote to the curve δ against $\frac{1}{N}$ by

$$\delta_{N \to 0} = \frac{1}{2}\left(\gamma^{\frac{1}{2}} - 2^{\frac{1}{2}}\right) \text{ .----------(40)}$$

Graphs of y_s and δ against $\frac{1}{N}$, are shown in Figures (5) and (6) respectively, y_c having been graphed in Figure (3). It should be noted, that as b, the min axis becomes smaller, the non-dimensional δ, becomes correspondingly larger. Thus, care should be taken in interpreting the graphs in Figure (6).

<u>The Elliptic Cylinder with its minor axis in the direction of the stream, and the Flat Plate at right angles to the stream</u> .

An exactly similar state of affairs exists for the ellipse whose minor axis is in the direction of the stream, and for the flat plate perpendicular to the stream direction. Starting with equations (25) and (26) and applying the general method described in the last section, corresponding formulae are derived. These are similar to the formulae of the last section, except that a and b are interchanged and V replaces U. The flat plate at right angles to the stream is obtained by setting b = 0. The flow is now symmetrical about the x-axis, and the lift force is in the x-direction (increasing x). The value of N, at which the two 'upper' stagnation points coalesce, is ${}^{a+2b}/_{2(a+b)}$, which reduces to the limiting values of ${}^{3}/_{4}$ and $\frac{1}{2}$ for the circular cylinder and flat plate respectively. Equations (36), (37), (38), (39), and (40) are applicable in the same form, with x replacing y in equatio (37), (38), (39) for the stagnation points below the y-axis ($x < 0$), and with

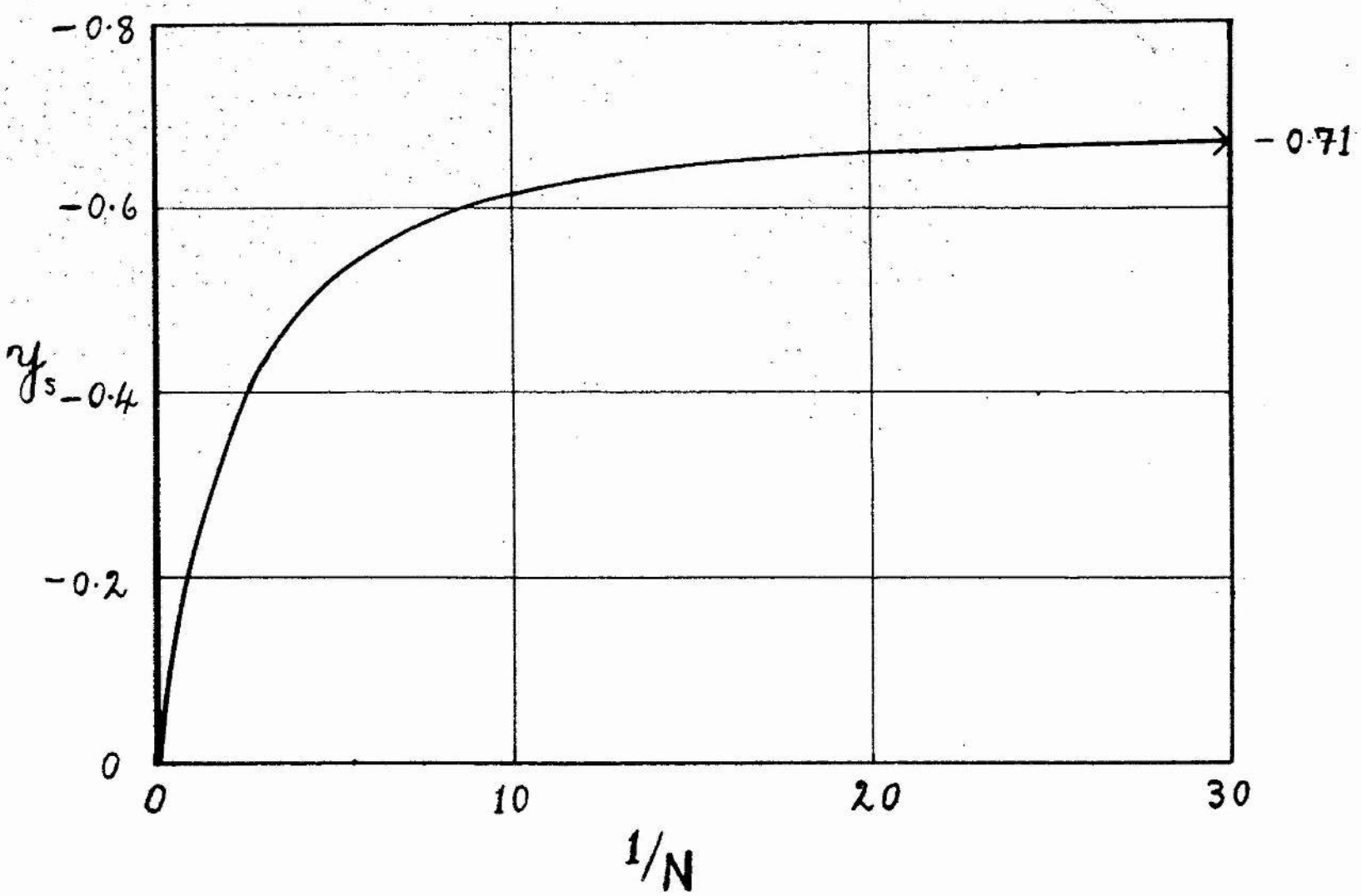

Figure (5) Deflection in the stagnation stream line in the free stream for all closed cylinders.

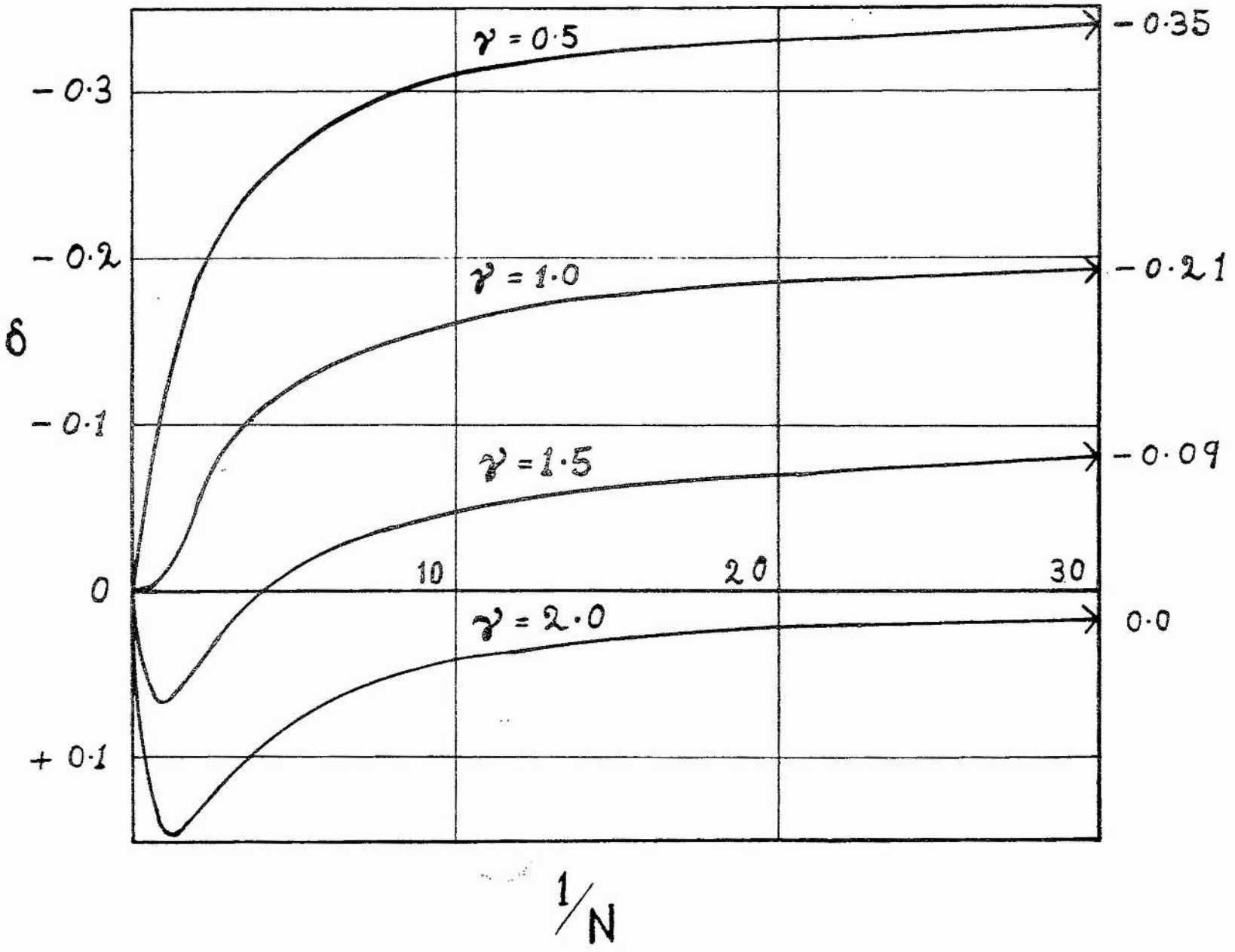

Figure (6) Deflection in the stagnation stream line for the circle, ellipse, and flat plate.

$N = \frac{V}{a\omega}$, and $\delta = x_0 - x_c$. In this case, $\gamma = 1$, $2a/a+b$ $(1 < \gamma < 2)$, and 2 for the circle, ellipse, and flat plate (length 2a), respectively. Graphs of the requisite quantities are shown in Figures (3), (5), and (6). It should be noted that y_0, y_c, δ, and N, change their significance at $\gamma = 1$ in these figures. The lift force is again given by equation (36) with $N = \frac{V}{a\omega}$. Figure (7) shows a schematic diagram of the flow past an elliptic cylinder with its minor axis in the direction of the stream, for $N < \frac{a+2b}{2(a+b)}$, and $y \geq 0$. This case has four stagnation points on the cylinder.

Conclusions for the General Elliptic Cylinder.

The formulae, derived for the general elliptic cylinder with its minor axis perpendicular to the stream are applicable, with the appropriate changes in meaning of γ, N, and the non-dimensional deflections, to all elliptic cylinders, the flat plate perpendicular to the stream, and the circular cylinder. The exceptions are the formulae for the stream function and velocity at a general point in the field for flow past a circular cylinder. This is occasioned by the fact that ξ must be infinite to obtain the circle in elliptic coordinates.

If polar coordinates are used for Ψ in the general method, the circular cylinder can, of course, be obtained: a slight modification of the method was used by Tsien to obtain the stream function for shear flow past the circular cylinder. The manipulation involved is several times that employed to obtain the same stream function at the beginning of this chapter, using Milne Thomson's Circle Theorem.

The non-dimensional parameter N, may have as its typical linear dimension any length connected with the cylinder. At first sight, c, where $c^2 = a^2 - b^2$, would appear to be a reasonable choice, but, in the case of the circle, this

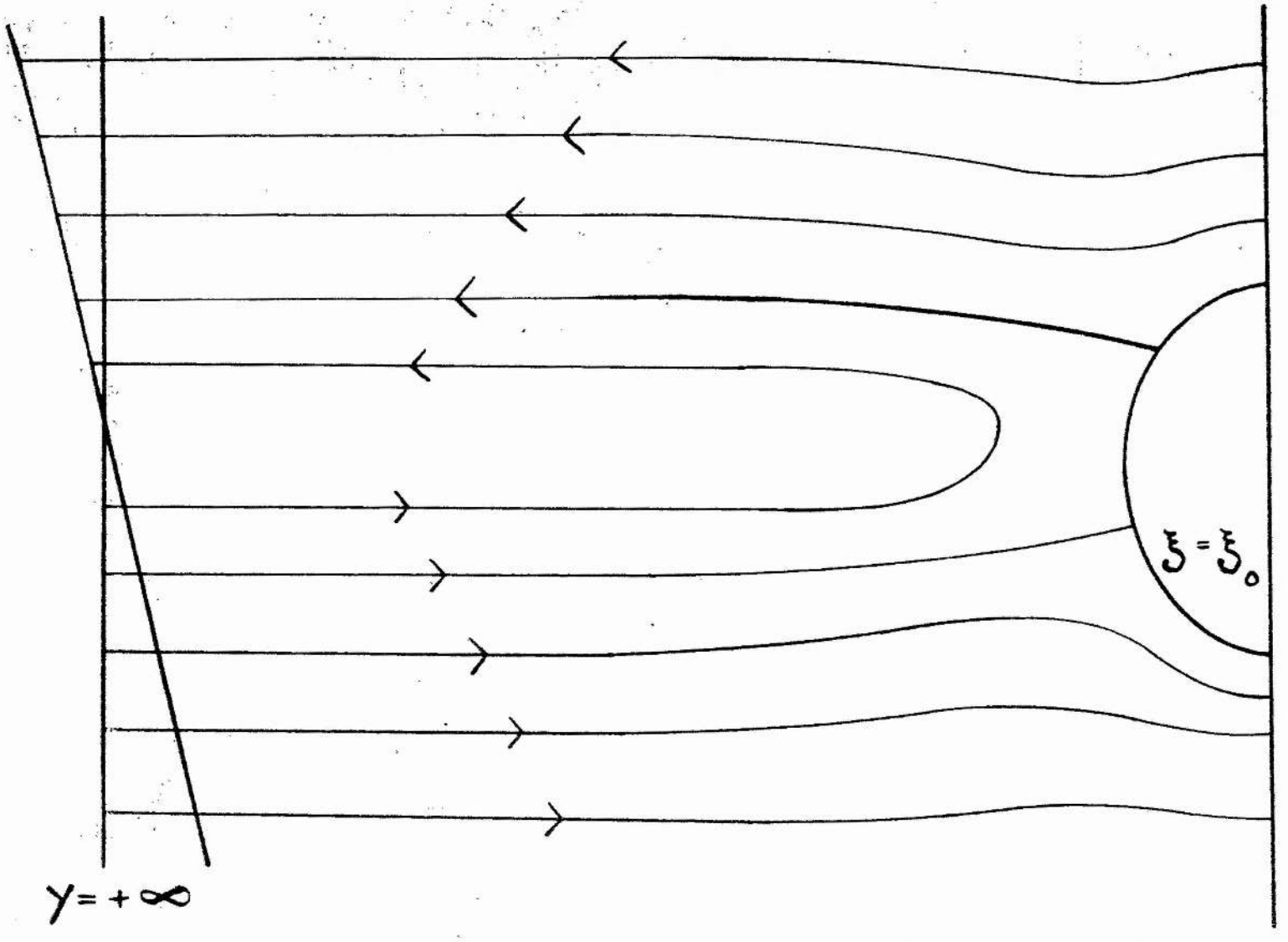

Figure (7) Illustration of the stream lines for an ellipse (minor axis in the direction of the stream) when there are four stagnation points on the cylinder.

gives N infinite. Several attempts were made to combine the major and minor axes in the typical length, but the conclusion reached was that the semi-axis at right angles to the flow direction is the most reasonable choice of typical length.

The shape of the graphs of δ against $\frac{1}{N}$, in Figure (6) shows that for some values of N, δ is positive. This means that the stagnation stream line moves down to the stagnation point, $x_0 < 0$, on the cylinder, for an elliptic cylinder with its minor axis in the direction of the stream. In all flow fields drawn, the value of N is chosen to ensure the deflection being negative, and the stagnation stream line thus moves up to the stagnation point on the cylinder. The turning value in the region of small $\frac{1}{N}$ (< 3) can be obtained analytically by solving the equation

$$\frac{\partial \delta}{\partial(1/N)} = 0 . \qquad \text{----------(41)}$$

The flow fields shown in Figures (1), (4) and (7) have characteristics which are common to all flows considered in the preceding work of this chapter.

It should be noted at this stage, that the stagnation stream line, the maximum deflection of which can be obtained from equation (40), in all cases comes from a region of higher velocity than that opposite the diameter of the cylinder.

General conclusions and summary are given at the end of this chapter.

The Parabolic Cylinder.

Derivation of the Stream Function.

Unlike the cylinders already discussed, the parabolic cylinder is not a closed shape, and consequently, the method described previously is not directly applicable. The general procedure, however, follows similar lines.

In the case of constant shear flow past a parabolic cylinder (Figure (8)), parabolic coordinates u, v are introduced by means of the formulae

$$x = u^2 - v^2 ,$$
$$y = 2uv . \qquad \text{----------(42)}$$

The parabola $v = v_0$ is taken as the solid boundary, and the velocity profile as $x \to -\infty$ is given by the first part of equation (19), that is $u = U - \omega y$. Proceeding exactly as in the case of the elliptic cylinder, Laplace's Equation in parabolic coordinates reduces to

$$\frac{\partial^2 \Psi_1}{\partial u^2} + \frac{\partial^2 \Psi_1}{\partial v^2} = 0, \qquad \text{----------(43)}$$

where Ψ_1 is defined by equation (19). Putting $\Psi_1 = F(u)\, G(v)$, substituting this in equation (43), and solving by separation of variables, a solution is obtained of the form

$$\Psi_1 = \begin{matrix}\cos \\ \sin\end{matrix} nu \; e^{\pm nv} ,$$

where n is the separation constant. In this case, however, n takes all values (continuous) from zero to infinity. This results in the general solution of the form

$$\Psi_1 = \int_0^\infty \left[a(n) \cos nu + b(n) \sin nu \right] e^{-nv}\, dn , \qquad \text{----------(44)}$$

which tends to zero as $v \to \infty$, a necessary condition on Ψ_1 from equation (19). The required stream function ψ, is obtained from equation (19) as

$$\psi = 2Uuv - 2\omega u^2 v^2 + \int_0^\infty \left[a(n) \cos nu + b(n) \sin nu \right] e^{-nv}\, dn . \qquad \text{-----(45)}$$

In order that ψ may take the constant value zero on the parabola $v = v_0$, the coefficients a(n) and b(n) must satisfy the relation

$$2\omega u^2 v_0^2 - 2Uuv_0 = \int_0^\infty \left[a(n) \cos nu + b(n) \sin nu \right] e^{-nv_0}\, dn = \int_0^\infty \left[A(n) \cos nu + B(n) \sin nu \right] dn ,$$

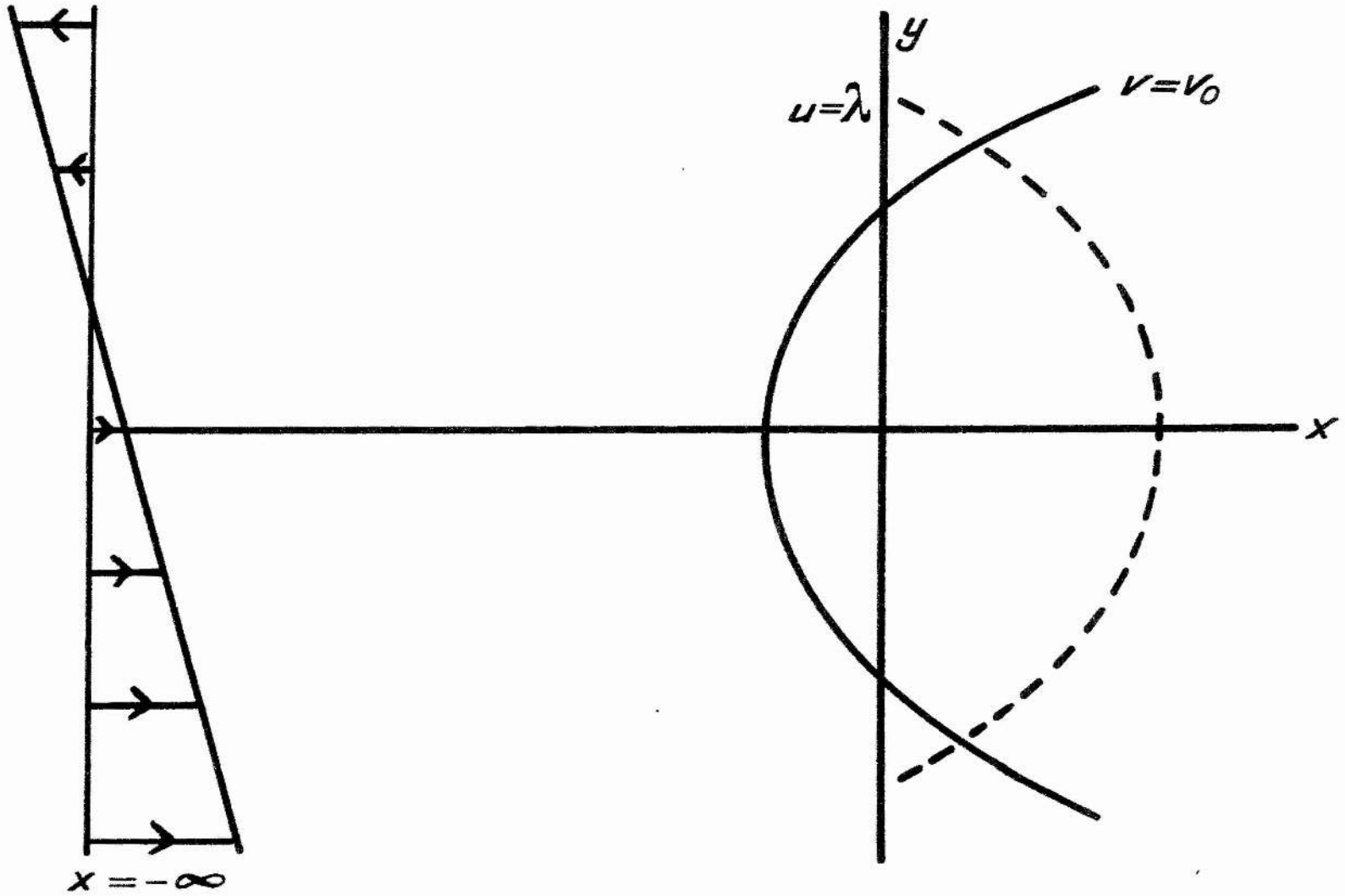

Figure (8) Illustration of rotational flow past a parabolic cylinder.

where $A(n) = a(n)e^{-nv_o}$, and $B(n) = b(n)\, e^{-nv_o}$. Using Fourier Transforms, A(n) and B(n) are determined as

$$A(n) = \frac{4}{\pi}\omega v_o^2 \int_0^\infty u^2 \cos nu\, du ,$$

$$B(n) = -\frac{4}{\pi}\, Uv_o \int_0^\infty u \sin nu\, du . \qquad \text{----------(46)}$$

From the form of A(n) and B(n) the Transforms are justified [40] . In order to keep the coefficients finite, the integration in equations (46) is restricted to a finite range λ, which can be chosen arbitrarily large. With this limitation, equations (46) can be integrated by parts to give

$$A(n) = \frac{4}{\pi}\omega v_o^2 \int_0^\lambda u^2 \cos nu\, du$$

$$= \frac{4}{\pi}\omega v_o^2 \left[\frac{1}{n}\left(\lambda^2 - \frac{2}{n^2}\right) \sin \lambda n + \frac{2\lambda}{n^2} \cos \lambda n \right] , \text{-------(47)}$$

and

$$B(n) = -\frac{4}{\pi}\, Uv_o \int_0^\lambda u \sin nu\, du$$

$$= -\frac{4}{\pi}\, Uv_o \left[\frac{1}{n^2} \sin \lambda n - \frac{\lambda}{n} \cos \lambda n \right] . \text{----------(48)}$$

Substituting these values in equation (45), the stream function ψ, becomes

$$\psi = 2Uuv - 2\omega u^2 v^2$$

$$+ \frac{4}{\pi}\omega v_o^2 \int_0^\infty \left[\frac{1}{n}\left(\lambda^2 - \frac{2}{n^2}\right) \sin \lambda n \right.$$

$$\left. + \frac{2\lambda}{n^2} \cos \lambda n \right] \cos nu\, e^{-n(v-v_o)}\, dn$$

$$- \frac{4}{\pi}\, Uv_o \int_0^\infty \left[\frac{1}{n^2} \sin \lambda n - \frac{\lambda}{n} \cos \lambda n \right] \sin nu\, e^{-n(v-v_o)}\, dn ,$$

which after a little manipulation, may be written as

$$\psi = 2\,Uxv - 2\,\omega U^2 v^2$$
$$+ \frac{2}{\pi}\,\omega v_o^2\,\lambda^2 \int_0^\infty \Big[\sin(\lambda+u)n + \sin(\lambda-u)n\Big]\, e^{-n(v-v_o)}\,\frac{dn}{n}$$
$$+ \frac{2}{\pi}\,Uv_o\lambda \int_0^\infty \Big[\sin(\lambda+u)n - \sin(\lambda-u)n\Big]\, e^{-n(v-v_o)}\,\frac{dn}{n}$$
$$- \frac{4}{\pi}\,Uv_o \int_0^\infty (\sin\lambda n \sin un)\, e^{-n(v-v_o)}\,\frac{dn}{n^2}$$
$$+ \frac{8}{\pi}\,\omega v_o^2 \int_0^\infty \Big[\frac{\lambda}{n^2}\cos\lambda n \cos un$$
$$- \frac{1}{n^3}\sin\lambda n \cos un\Big]\, e^{-n(v-v_o)}\,dn \quad .\text{----------(49)}$$

The infinite integrals in equation (49), except for the last integral, are convergent. Using De Haan's Tables of Integrals (tables 365 and 368), the convergent integrals are evaluated as follows;

$$\int_0^\infty \Big[\sin(\lambda+u)n \pm \sin(\lambda-u)n\Big]\, e^{-n(v-v_o)}\,\frac{dn}{n}$$
$$= \tan^{-1}\frac{\lambda+u}{v-v_o} \pm \tan^{-1}\frac{\lambda-u}{v-v_o} \quad ,\text{----------(50)}$$

and

$$\int_0^\infty (\sin\lambda n \sin un)\, e^{-n(v-v_o)}\,\frac{dn}{n^2} = \frac{\lambda}{2}\tan^{-1}\frac{2u(v-v_o)}{(v-v_o)^2+\lambda^2-u^2}$$
$$+ \frac{u}{2}\tan^{-1}\frac{2\lambda(v-v_o)}{(v-v_o)^2+u^2-\lambda^2} + \frac{(v-v_o)}{4}\log\frac{(v-v_o)^2+(u-\lambda)^2}{(v-v_o)^2+(u+\lambda)^2} \quad .\text{-----(51)}$$

The final integral in equation (49) consists of two integrals, each of which taken separately is divergent. Taken together, however, the integration can be carried out to give a finite answer, as follows:

Let

$$I = \int_0^\infty \left[\frac{\lambda}{n^2} \cos\lambda n \cos un - \frac{1}{n^3} \sin\lambda n \cos un \right] e^{-n(v-v_o)} dn$$

$$= I_1 + I_2 ,$$

where

$$I_1 = \int_0^\infty \left(\frac{\lambda}{n^2} \cos\lambda n \cos un\right) e^{-n(v-v_o)} dn ,$$

and

$$I_2 = - \int_0^\infty (\sin\lambda n \cos un) e^{-n(v-v_o)} \frac{dn}{n^3} .$$

Integrating I_1 and I_2 by parts, the following results are obtained:

$$I_1 = \left[- \frac{\lambda}{n} \cos\lambda n \cos un \; e^{-n(v-v_o)} \right]_0^\infty$$

$$- \lambda^2 \int_0^\infty \sin\lambda n \cos un \; e^{-n(v-v_o)} \frac{dn}{n}$$

$$- \lambda u \int_0^\infty \cos\lambda n \sin un \; e^{-n(v-v_o)} \frac{dn}{n}$$

$$- \lambda(v-v_o) \int_0^\infty \cos\lambda n \cos un \; e^{-n(v-v_o)} \frac{dn}{n} ,$$

and

$$I_2 = \left[\frac{1}{2n^2} \sin\lambda n \cos un \; e^{-n(v-v_o)} \right]_0^\infty$$

$$- \frac{\lambda}{2} \int_0^\infty \cos\lambda n \cos un \; e^{-n(v-v_o)} \frac{dn}{n^2}$$

$$+ \frac{u}{2} \int_0^\infty \sin\lambda n \sin un \; e^{-n(v-v_o)} \frac{dn}{n^2}$$

$$+ \frac{(v-v_o)}{2} \int_0^\infty \sin\lambda n \cos un \; e^{-n(v-v_o)} \frac{dn}{n^2} ,$$

$$= \left[\frac{1}{2n^2} \sin\lambda n \cos un \; e^{-n(v-v_o)} \right]_0^\infty - \frac{1}{2} I_1 +$$

$$+\frac{u}{2}\left[\frac{\lambda}{2}\tan^{-1}\frac{2u(v-v_o)}{(v-v_o)^2+\lambda^2-u^2}+\frac{u}{2}\tan^{-1}\frac{2\lambda(v-v_o)}{(v-v_o)^2+u^2-\lambda^2}\right.$$

$$\left.+\frac{(v-v_o)}{4}\log\frac{(v-v_o)^2+(u-\lambda)^2}{(v-v_o)^2+(u+\lambda)^2}\right]$$

$$+\frac{(v-v_o)}{2}\int_0^\infty \sin\lambda n\cos un\; e^{-n(v-v_o)}\frac{dn}{n^2}\ .$$

Writing the above expression in full, and integrating the last integral by parts, I becomes

$$I = I_1 + I_2$$

$$= \frac{1}{\pi}\left[\left(\frac{1}{n^3}\sin\lambda n-\frac{\lambda}{n}\cos\lambda n\right)\cos un\; e^{-n(v-v_o)}\right]_0^\infty$$

$$-\frac{\lambda^2}{2}\int_0^\infty \sin\lambda n\cos un\; e^{-n(v-v_o)}\frac{dn}{n}$$

$$-\frac{\lambda u}{2}\int_0^\infty \cos\lambda n\sin un\; e^{-n(v-v_o)}\frac{dn}{n}$$

$$-\frac{\lambda(v-v_o)}{2}\int_0^\infty \cos\lambda n\cos un\; e^{-n(v-v_o)}\frac{dn}{n}$$

$$+\frac{u}{2}\left[\frac{\lambda}{2}\tan^{-1}\frac{2u(v-v_o)}{(v-v_o)^2+\lambda^2-u^2}+\frac{u}{2}\tan^{-1}\frac{2\lambda(v-v_o)}{(v-v_o)^2+u^2-\lambda^2}\right.$$

$$\left.+\frac{(v-v_o)}{4}\log\frac{(v-v_o)^2+(u-\lambda)^2}{(v-v_o)^2+(u+\lambda)^2}\right]$$

$$+\frac{(v-v_o)}{2}\left[-\frac{1}{n}\sin\lambda n\cos un\; e^{-n(v-v_o)}\right]_0^\infty$$

$$+\frac{\lambda(v-v_o)}{2}\int_0^\infty \cos\lambda n\cos un\; e^{-n(v-v_o)}\frac{dn}{n}$$

$$-\frac{u(v-v_o)}{2}\int_0^\infty \sin\lambda n\sin un\; e^{-n(v-v_o)}\frac{dn}{n}$$

$$-\frac{(v-v_o)^2}{2}\int_0^\infty \sin\lambda n\cos un\; e^{-n(v-v_o)}\frac{dn}{n}\ .$$

Cancelling the two equal (opposite sign) divergent integrals, and carrying out the integration, using equations (50) and (51) and De Haan's Tables for

$$\int_0^\infty \sin\lambda n \sin un \; e^{-n(v-v_o)} \frac{dn}{n} = \frac{1}{4} \log \frac{(v-v_o)^2 + (u+\lambda)^2}{(v-v_o)^2 + (u-\lambda)^2} \quad , \qquad (52)$$

and

$$\int_0^\infty \sin\lambda n \cos un \; e^{-n(v-v_o)} \frac{dn}{n} = \frac{1}{2} \tan^{-1} \frac{2\lambda(v-v_o)}{(v-v_o)^2+u^2-\lambda^2} \quad , \qquad (53)$$

I becomes

$$I = \frac{1}{2}\left[\left(\frac{1}{n^2} \sin\lambda n - \frac{\lambda}{n} \cos\lambda n\right) \cos un \; e^{-n(v-v_o)} \right]_0^\infty$$

$$+ \frac{(v-v_o)}{2} \left[-\frac{1}{n} \sin\lambda n \cos un \; e^{-n(v-v_o)} \right]_0^\infty$$

$$+ \frac{1}{4} \left[u^2 - (v-v_o)^2 - \lambda^2 \right] \tan^{-1} \frac{2\lambda(v-v_o)}{(v-v_o)^2+u^2-\lambda^2}$$

$$+ \frac{u(v-v_o)}{4} \log \frac{(v-v_o)^2+(u-\lambda)^2}{(v-v_o)^2+(u+\lambda)^2} \quad .$$

Considering the terms in the square brackets, the following is obtained:

$$\frac{(v-v_o)}{2} \left[-\frac{1}{n} \sin\lambda n \cos un \; e^{-n(v-v_o)} \right]_0^\infty$$

$$= \lim_{n\to 0} \frac{(v-v_o)}{2} \left[\frac{\sin\lambda n}{n} \cos un \; e^{-n(v-v_o)} \right]$$

$$= \frac{\lambda(v-v_o)}{2} \quad ,$$

and

$$\frac{1}{2}\left[\frac{1}{n} \cos un \; e^{-n(v-v_o)} \left(\frac{\sin\lambda n}{n} - \lambda\cos\lambda n \right) \right]_0^\infty$$

$$= \lim_{n\to 0} \frac{1}{2}\left[\frac{\cos un}{n} \; 3^{-n(v-v_o)} \left(\lambda - \frac{\lambda^3 n^2}{3!} + \frac{\lambda^5 n^4}{5!} - \ldots. \right.\right.$$

$$\left.\left. - \lambda + \frac{\lambda^3 n^2}{2!} - \ldots. \right) \right]$$

$$= \lim_{n\to 0} \frac{1}{2} \left[\cos un \; e^{-n(v-v_o)} \left(\frac{1}{3} \lambda^3 n \ldots. \right) \right] =$$

$= 0$, for all values of u and $(v-v_o)$.

Thus

$$I = \frac{1}{4}\left[u^2 - (v-v_o)^2 - \lambda^2\right] \tan^{-1} \frac{2\lambda(v-v_o)}{(v-v_o)^2+u^2-\lambda^2}$$

$$+ \frac{u(v-v_o)}{4} \log \frac{(v-v_o)^2+(u-\lambda)^2}{(v-v_o)^2+(u+\lambda)^2} + \frac{\lambda(v-v_o)}{2} \quad \text{.----------(54)}$$

On substituting the values of the integrals from equations (50), (51), (52), (53) and (54), in equation (49), the stream function ψ is obtained as

$$\psi = 2Uuv - 2\omega u^2v^2$$

$$- \frac{v_o(v-v_o)}{\pi} (U - 2\omega v_o u) \log \frac{(v-v_o)^2+(u-\lambda)^2}{(v-v_o)^2+(u+\lambda)^2}$$

$$- \frac{2v_o}{\pi}\left[Uu - \omega v_o\left\{u^2 - (v-v_o)^2\right\}\right] \tan^{-1} \frac{2\lambda(v-v_o)}{(v-v_o)^2+u^2-\lambda^2}$$

$$+ \frac{4\omega v_o^2 \lambda(v-v_o)}{\pi} \quad \text{.----------(55)}$$

In equation (44), it was tacitly assumed that Ψ_1 tended to zero as v tended to infinity: this is obvious in the integrand, except at the lower limit, zero, of n. That is, it was assumed that

$$\lim_{v\to\infty} \int_0^\infty a(n) \cos nu \; e^{-nv} \, dn = 0 \; .$$

It is seen that the integral I is a part of the integral given above, using a(n) obtained from equation (47). The integrand obviously tends to zero for all n, except n zero, but from the evaluation of I, it is seen that the two divergent terms cancel, that is, the integrals and the square bracket term tend to zero for all v. Thus, the above assumption is valid, and Ψ_1 satisfies the necessary conditions. This is verified in the following check on ψ.

The value of the stream function ψ, given by equation (55), must

satisfy the three conditions:

1. $\nabla^2\psi + \omega = 0$,

2. $\psi = 0$ on $v = v_0$, provided $u < \lambda$,

3. $\psi \to Uy - \frac{\omega}{2} y^2$ as $v \to \infty$.

The verification of condition 1. is obtained by direct differentiation. Before considering 2. and 3., the function $\tan^{-1} \frac{2\lambda(v-v_0)}{(v-v_0)^2+u^2-\lambda^2}$ must be studied in detail. This is carried out in two parts, $u < \lambda$, and $u \geq \lambda$. For convenience, let

$$F(v) = \frac{2\lambda(v-v_0)}{(v-v_0)^2+u^2-\lambda^2} .$$

$u \leq \lambda$

There is no loss in generality if u is taken to be zero, and λ is given a particular value. Since v_0 is a constant, λ, for example, may be taken equal to v_0. The inverse function thus becomes

$$\tan^{-1} \frac{2v_0(v-v_0)}{(v-v_0)^2-v_0^2} = \tan^{-1} \frac{2v_0(v-v_0)}{v(v-2v_0)} = \tan^{-1} F(v),$$

where $F(v) = \frac{2v_0(v-v_0)}{v(v-2v_0)}$. On giving values to v the following table is obtained:

v	v_0	$1.5v_0$	$2v_0(-)$	$2v_0(+)$	$2.5v_0$	∞
F(v)	0	-1.33	$-\infty$	$+\infty$	+2.4	0

Thus, $\tan^{-1} F(v)$ may be graphed schematically as shown in Figure (f).

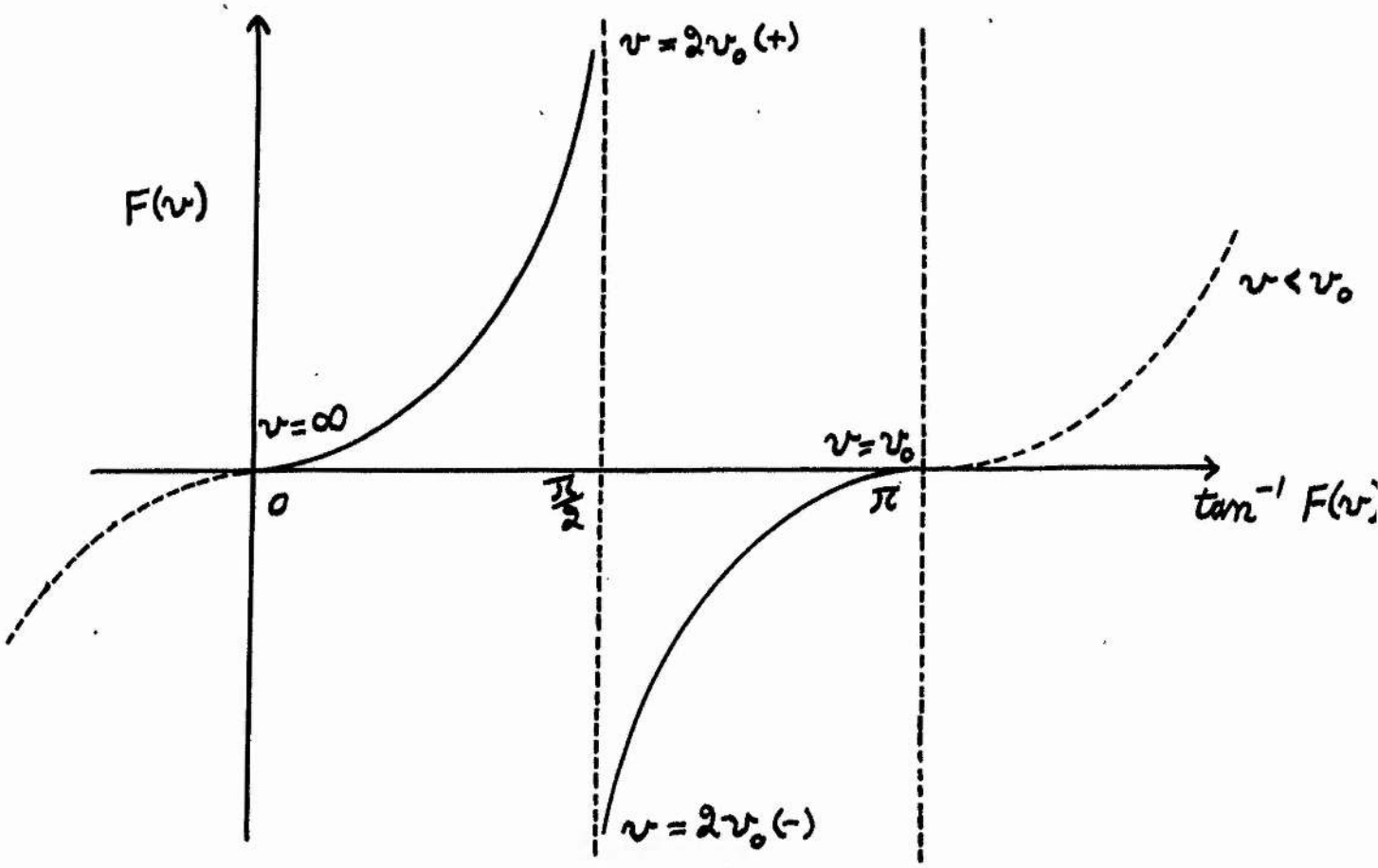

Figure (f)

The two important results for $u < \lambda$ arising from the figure, are

$$\lim_{v \to \infty} \tan^{-1} \frac{2\lambda(v-v_o)}{(v-v_o)^2 + u^2 - \lambda^2} = 0,$$

$$\lim_{v \to v_o} \tan^{-1} \frac{2\lambda(v-v_o)}{(v-v_o)^2 + u^2 - \lambda^2} = \pi . \qquad \text{----------(56)}$$

If u is not taken to be zero, then there is some value of $v > v_o$, such that F(v) is infinite. There is also a value of $v < v_o$ which makes F(v) infinite. Thus, for $u < \lambda$, $\tan^{-1} \frac{2\lambda(v-v_o)}{(v-v_o)^2+u^2-\lambda^2}$ lies in the first and second quadrants for $v > v_o$, and the third and fourth quadrants for $v < v_o$. In Figure (g) the dotted lines are the loci on which F(v) is infinite, the numbers denoting the quadrant in which $\tan^{-1} \frac{2\lambda(v-v_o)}{(v-v_o)+u^2-\lambda^2}$ lies.

$u \gtrless \lambda$

When $u = \lambda$, the point $v = v_0$ is a singularity of the field ($F(v)$ being infinite) and is the terminus of the two loci, along one of which $\tan^{-1} F(v)$ is $\frac{\pi}{2}$, and along the other $\frac{3\pi}{2}$. When $u > \lambda$, $F(v)$ is always finite. It takes the value zero on $v = v_0$, is negative for $v < v_0$, and so $\tan^{-1} F(v)$ lies in the fourth quadrant, is positive for $v > v_0$, and so $\tan^{-1} F(v)$ lies in the first quadrant. Thus, the line $v = v_0$, $u \geqslant \lambda$ is a cut in the plane, acros which $\tan^{-1} F(v)$ changes value from 0 to 2π. It may be considered as a line o singularities. Thus, as stated previously, the flow is only valid for $u < \lambda$.

These results are summarised in Figure (g), where the red lines $v = v_0$, $u > \lambda$ represent singularities in the field.

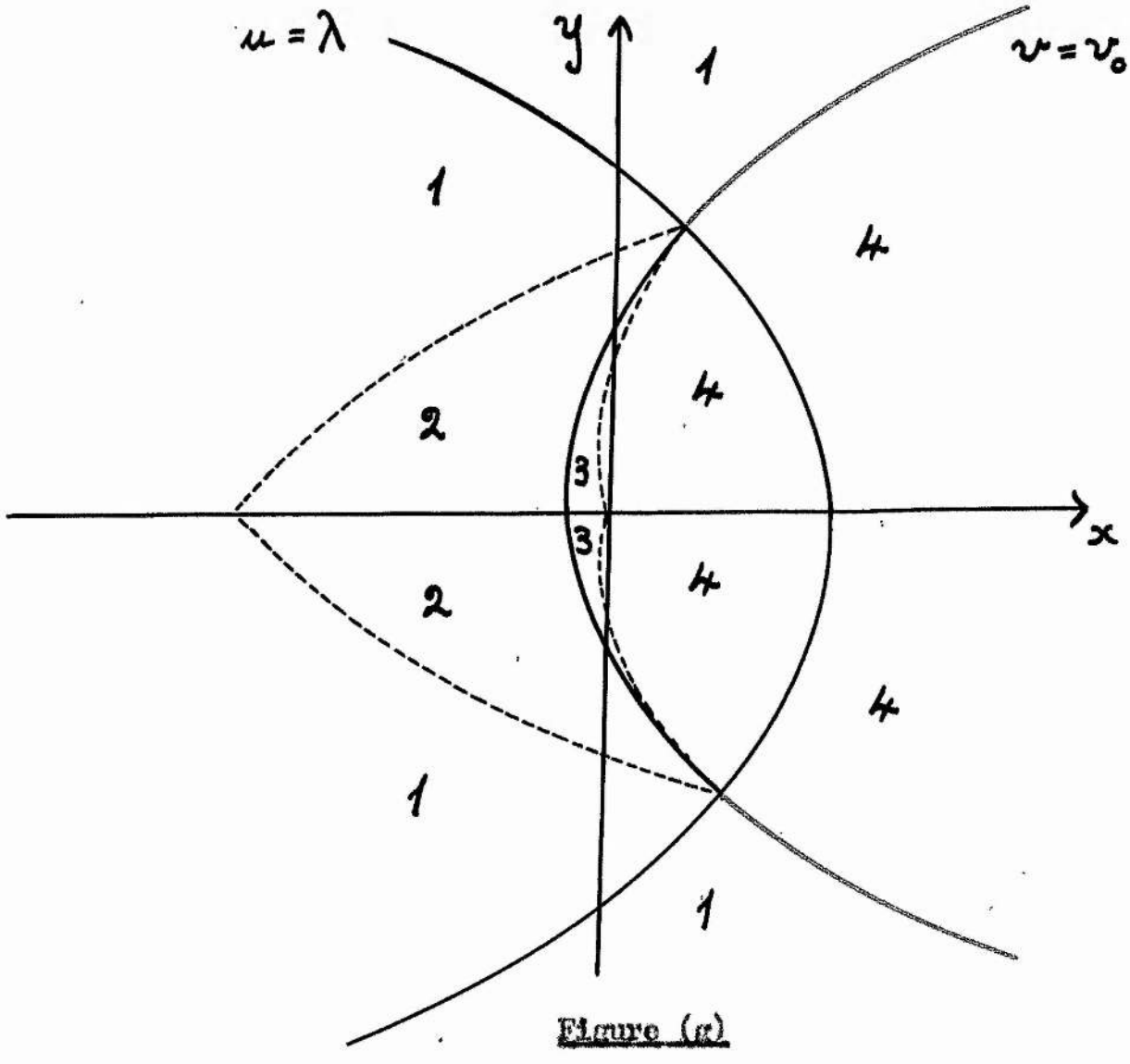

Figure (g)

Thus, using equation (56), the stream function defined by equation (55) satisfies the three requisite boundary conditions. It should be noted that in the verification of condition 3,

$$-\frac{2\omega v_o^2}{\pi}(v-v_o)^2 \tan^{-1}\frac{2\lambda(v-v_o)}{(v-v_o)^2+u^2-\lambda^2}$$

$$\rightarrow -\frac{2\omega v_o^2}{\pi}(v-v_o)^2\,\frac{2\lambda}{(v-v_o)} \qquad \left[\text{for large } (v-v_o)\right]$$

$$= -\frac{4\lambda\omega v_o^2\,(v-v_o)}{\pi} \quad ,$$

and so it cancels with the final term in relation (55).

The introduction of λ, which may be taken arbitrarily large, but not infinite, restricts the number of solutions of Laplace's Equation, which are added to the parallel flow in equation (19), and so equation (55) is an approximation to the required flow in the region $u < \lambda$.

In the case of constant shear flow past closed cylinders (finite shapes), a constant appeared in the general expression for the stream function. This general expression reduced to $\psi = 0$ on the cylinder. If ψ had taken a non-zero value on the cylinder, the flow pattern would have remained unaltered In the case of open cylinders, however, a constant does not appear in the general stream function as a result of the analysis and the stagnation stream line always comes from $y = 0$ in the free stream. If, however, $\psi = A$ (non-zer on the parabolic cylinder, then a further term of the form $\frac{A}{\pi}\tan^{-1}\frac{2\lambda(v-v_o)}{(v-v_o)^2+u^2-\lambda}$ must be added to the stream function ψ, given by equation (55); the resulting stream function still satisfies the necessary boundary conditions. The value taken by A does not appear as a result of the analysis, and it cannot be evaluated from circulation considerations, as is done in Section III of this thesis. Thus, as to its nature a tentative suggestion can only be

made. In all cases already discussed, the corresponding constant was of the form $-\frac{\omega}{4}$ ($\frac{1}{2}$ length obstructing the flow)^2, and so as a first suggestion $-\omega(\lambda v_o)^2$ can be taken. Although, in the subsequent examination, A is taken to be zero to conform with previous examples, it should be noted, that a value of $-\omega(\lambda\omega_o)^2$ for A, would yield a state of affairs in the free stream, comparabl to that in the case of constant shear flow past finite closed cylinders.

Examination of the Flow Field

Since the flow field, with the singularities already described, is extremely complicated, the state of affairs on the cylinder $v = v_o$, $u < \lambda$, will be considered, particular attention being paid to the stagnation points.

The velocity q, is given by

$$q^2 = q_u^2 + q_v^2 , \qquad (57)$$

where q_u and q_v are the component velocities in the u- and v- directions respectively, and where

$$q_u = \frac{1}{h(u,v)} \frac{\partial\psi}{\partial v} , \quad q_v = -\frac{1}{h(u,v)} \frac{\partial\psi}{\partial u} , \qquad (58)$$

with $h(u,v) = 2(u^2+v^2)^{\frac{1}{2}}$.

In particular, stagnation points are given by

$$\frac{\partial\psi}{\partial v} = \frac{\partial\psi}{\partial u} = 0 ,$$

where, from equation (55)

$$\frac{\partial\psi}{\partial u} = 2Uv - 4\omega uv^2 + \frac{2\omega v_o^2 (v-v_o)}{\pi} \log \frac{(v-v_o)^2 + (u-\lambda)^2}{(v-v_o)^2 + (u+\lambda)^2}$$

$$- \frac{2v_o}{\pi} (U-2\omega v_o u) \tan^{-1} \frac{2\lambda(v-v_o)}{(v-v_o)^2+u^2-\lambda^2}$$

$$+ \frac{4\lambda v_o(v-v_o)}{\pi} \left[\frac{U\{u^2+\lambda^2+(v-v_o)^2\} - 2\omega v_o u\lambda^2}{\{(v-v_o)^2+u^2-\lambda^2\}^2 + 4\lambda^2(v-v_o)^2} \right] , \qquad (59)$$

and

$$\frac{\partial\psi}{\partial v} = 2Uu - 4\omega u^2 v - \frac{v_o}{\pi}(U - 2\omega v_o u)\log\frac{(v-v_o)^2+(u-\lambda)^2}{(v-v_o)^2+(u+\lambda)^2}$$

$$- \frac{4\omega v_o^2}{\pi}(v-v_o)\tan^{-1}\frac{2\lambda(v-v_o)}{(v-v_o)^2+u^2-\lambda^2} + \frac{4\omega v_o^2\,\lambda}{\pi}$$

$$+ \frac{4\lambda v_o}{\pi}\left[\omega v_o\left\{(u^2+(v-v_o)^2)^2 - \lambda^2(u^2-(v-v_o)^2)\right\}\right.$$

$$\left. - Uu\left\{u^2-\lambda^2+(v-v_o)^2\right\}\right]$$
$$\left\{(v-v_o)^2+u^2-\lambda^2\right\}^2+4\lambda^2(v-v_o)^2$$

.----------(60)

On the cylinder $v = v_o$, $u < \lambda$, $\frac{\partial\psi}{\partial u} = 0$ identically (as is necessary), and $\left(\frac{\partial\psi}{\partial v}\right)_{v=v_o} = 0$ gives the following equation for stagnation points on the parabola:

$$(U-2\omega v_o u)\left[\pi u(\lambda^2-u^2)+v_o(\lambda^2-u^2)\log\frac{\lambda+u}{\lambda-u} + 2\lambda v_o u\right]$$
$$+ 2\lambda^3\omega v_o^2 = 0.$$

Introducing the typical linear dimension λ^2, the following equation gives the stagnation points on the cylinder for all v_o, λ, and N:

$$(N-2u'v_o')\left[2u'v_o' + v_o'(1-u'^2)\log\frac{1+u'}{1-u'} + \pi u'(1-u'^2)\right]$$
$$+ 2v_o'^2 = 0\,,\text{----------(61)}$$

where $N = \frac{U}{\omega\lambda^2}$, $u' = \frac{u}{\lambda}$ (< 1), and $v_o' = v_o/\lambda$.

In particular, the stagnation point, which lies on the cylinder below the x-ax (y < 0) is given by

$$(N+2u'v_o')\left[2u'v_o' + v_o'(1-u'^2)\log\frac{1+u'}{1-u'} + \pi u'(1-u'^2)\right]$$
$$- 2v_o'^2 = 0.\text{----------(62)}$$

There is one value of $u'(<1)$ satisfying equation (62) for each N in the range $0 \leq N \leq \infty$. It should be noted that the stream line to this stagnation point always comes from y = 0 in the free stream. This state of affairs was discussed in the section on the derivation of the stream function. The

stagnation point at N = 0, occupies a position on the parabola depending on v_o'. As N increases, it moves along the parabola towards the x-axis, reaching the latter at infinite N (zero vorticity). The non-dimensional depth $y_o' = {}^{y_c}/_{2\lambda v_o}$, of this stagnation point, which is also equal to the non-dimensional deflection δ', in the stagnation stream line, is given by the valu u', which is a solution of equation (62), since $\delta' = {}^{\delta}/_{2\lambda v_o} = u'$. The graph of δ' against $\frac{1}{N}$ is shown in Figure (9).

The stagnation points which lie on the cylinder above the x-axis are give by

$$(N-2u'v_o')\left[2u'v_o' + (1-u'^2)v_o' \log \frac{1+u'}{1-u'} + \pi u'(1-u'^2)\right] + 2v_o'^2 = 0 , \qquad (63)$$

The state of affairs above the x-axis ($y > 0$) is of a much more complicated nature. If $0 \leqslant N < v_o'$, there is one stagnation point on the parabola above the x-axis. When N = 0, this stagnation point and the one below the axis are symmetrically placed with respect to y = 0. As N increases, the upper point moves along the parabola away from the x-axis. Its position at $N = v_o'$ depen on v_o'. However, when $N = v_o'$, another stagnation point appears at $u' = 1$, noting in this case that $\lim_{u' \to 1} (1-u'^2) \log \frac{1+u'}{1-u'} = 0$. Thus, for $N = v_o'(+)$, there are two stagnation points above the x-axis. It is seen, that for $N \geqslant v_o'$ the situation is rather complicated, and is best illustrated by an example. When $v_o' = 1$, the stagnation point above the x-axis moves fro a position $u' = 0.39$ to $u' = 0.80$, as N goes from 0 to 1. For $N \geqslant 1$ the complication appears. For N = 1, a second stagnation point appears at $u' = 1$ and as N goes from 1 to 1.15, the original point moves from the position $u' = 0.80$ to $u' = 0.95$, whilst the new stagnation point moves from $u' = 1$ to

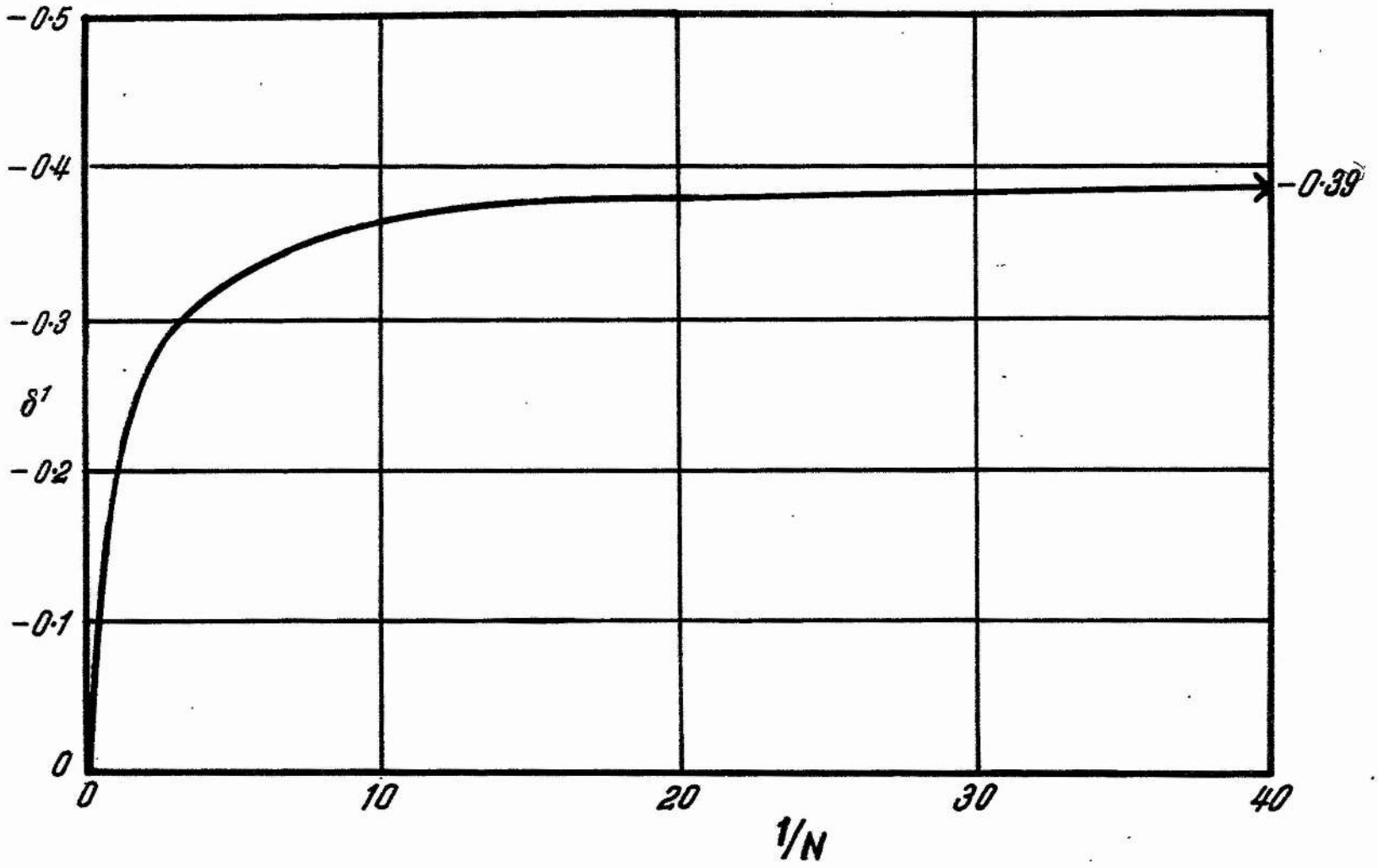

Figure (9) Variation of the position of the lower stagnation point for a parabolic cylinder.

Deflection of the stagnation stream line for a parabolic cylinder.

$u' = 0.95$. The points thus coalesce at $u' = 0.95$, and for $1.15 < N \leqslant \infty$, there are no stagnation points on the cylinder above the axis.

The flow picture for $N < v_0'$ is shown in Figure (10), where the flow for $|y| > 2\lambda v_0$ is found to be approximately plane parallel flow with constant shear the singularities above the x-axis being sources, and those below being sinks.

The results obtained on the parabolic cylinder require careful considerat in view of the presence of singular points on the cylinder at $u \geqslant \lambda$. Before attempting an assessment of the accuracy of the method, an approximation to the flow past an infinite flat plate is obtained, by the same method, and comparison made with the flow past a finite flat plate, already discussed.

The Infinite Flat Plate perpendicular to the Flow.

Proceeding in a manner exactly similar to that adopted in the case of the parabolic cylinder, (i.e. solving Laplace's Equation in cartesian coordinates for Ψ_1, and evaluating the constants by introducing λ in the Fourier Transforms), the stream function ψ, satisfying the three necessary condition is found to be

$$\psi = Uy - \frac{\omega}{2}y^2 - \frac{1}{2\pi}(U - \omega y)\log\frac{x^2+(y-\lambda)^2}{x^2+(y+\lambda)^2} - \frac{1}{\pi}\left[Uy - \frac{\omega}{2}(y^2-x^2)\right]\tan^{-1}\frac{2\lambda x}{x^2+y^2-\lambda^2} + \frac{\omega\lambda x}{\pi} \quad \text{.----------(64)}$$

This approximates to the stream function for constant shear flow past an infinite flat plate which lies along the y-axis, in the range $-\lambda < y < +\lambda$, wher λ is again an arbitrarily large finite quantity (compare Figure (8)). The analytical discussion of the functions involved in the stream function for the parabolic cylinder, the singular points, and general remarks, are all applicable to the flow given by equation (64), with only slight modification to the symbols involved. The equation giving the stagnation points on the plate ($|y| < \lambda$) is

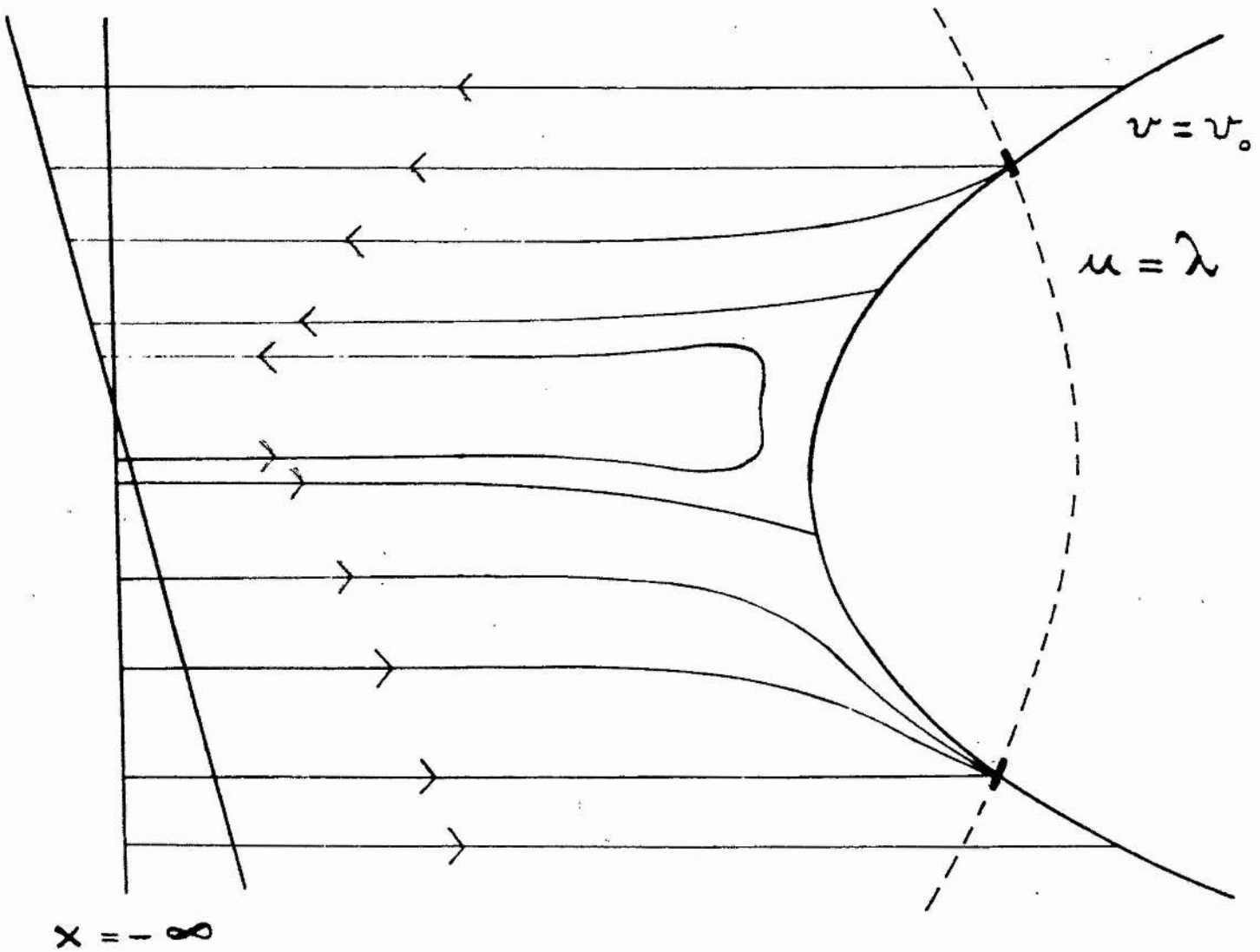

Figure (10) Illustration of the stream lines for a parabola when there are two stagnation points on the parabola.

$$(N - y')\left[2y' + (1 - y'^2)\log\frac{1 + y'}{1 - y'}\right] + 1 = 0 \quad \text{----------(65)}$$

where $N = \frac{U}{\omega\lambda}$, and $y' = \frac{y}{\lambda}$ (< 1). Again, if $0 \leqslant N \leqslant \infty$, there is one stagnation point on the plate, below the x-axis ($|y_0| < \lambda$), and a graph of this depth, which is also equal to the deflection of the stagnation stream line δ, is shown against $\frac{1}{N}$ in Figure (11), where δ' is used, being the non-dimensional deflection $\frac{\delta}{\lambda}$. In this case the typical linear dimension is λ. The state of affairs above the x-axis is comparable to that in the correspondi part of the field of the parabolic cylinder. The value of N for which the third stagnation point appears is $N = \frac{1}{3}$. The nature of the stagnation points for $N \geqslant \frac{1}{3}$ is similar to that in the case of the parabolic cylinder. The flow field for $N < \frac{1}{3}$ exhibits all the physical features shown in Figure (10).

Discussion of the results on Open Cylinders.

From a purely physical point of view, the flows on to a finite and infinite flat plate, should not differ appreciably on the plates, in the vicinity of the x-axis, for large values of N. The stream functions for these two flows have been derived, and their respective physical features studied.

The main features of the two flows are identical in the neighbourhood of the y-axis. The lower stagnation point in each case starts off at a position on the plate at $N = 0$, and as N increases, the point moves along the plate towards the axis, reaching the centre of the plate at $N = \infty$. The stagnation points in each case, are symmetrically situated on the plate at $N =$ and as N increases, the upper stagnation point moves away from the axis, leavi the finite plate at $N = \frac{1}{3}$, and the infinite plate at a value of N slightly larger than $\frac{1}{3}$. For $\frac{1}{3} < N \leqslant \infty$, the top half of the plate is free from stagnation points. However, when $\frac{1}{3} \leqslant N < \frac{1}{3} + \epsilon$, where ϵ is small quantity

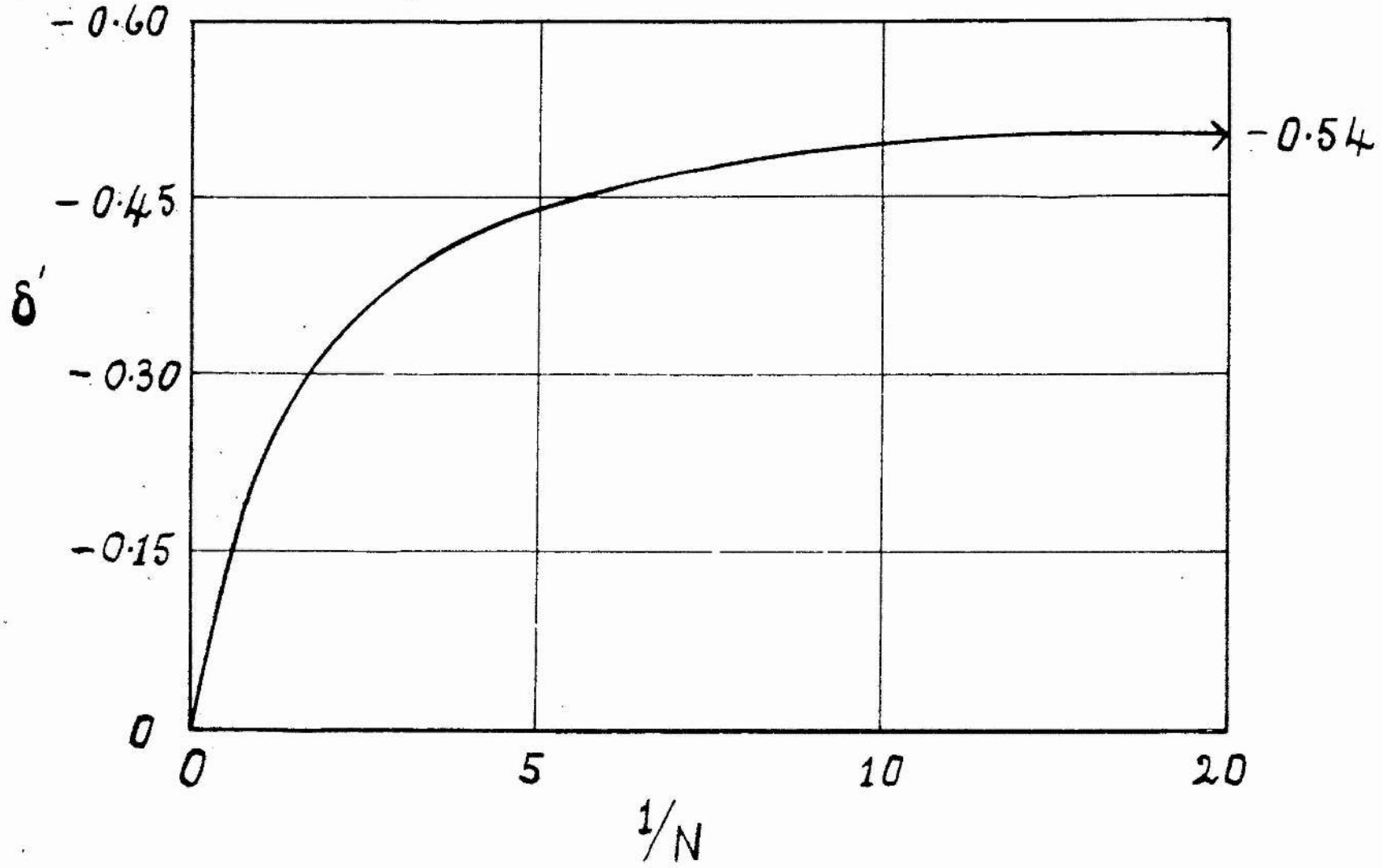

Figure (11) Variation of the position of the lower stagnation for an infinite flat plate.

Deflection of the stagnation stream line for an infinite flat plate.

($\epsilon < \frac{1}{8}$), the situation on the infinite plate differs considerably. By direct comparison of Figures (3) and (11), the deflections of the lower stagnation points are approximately equal for $\frac{1}{N} \leqslant 0.3$. The values of the velocity at identical points in the flow field are not in so close agreement. Sufficient to say that the closest correspondence occurs on the plates away from the edges, where $y = \pm \lambda$ are taken as the 'edges' in the infinite plate. Thus, the flow given by equation (64) probably contains all the principal physical features of the true flow on the plate, in the neighbourhood of the axis. The region covers a slightly larger range below the axis than above, the lower range including the lower stagnation point.

As a result of this comparison, it seems reasonable to suppose that the flow field represented by the stream function given by equation (55) will contain all the principal features of the field of flow past a finite parabolic cylinder ($v = v_o$, $0 \leqslant u < \lambda$). In addition, equation (55) can be used to give a good approximation to the flow on the surface of the parabola in the vicinity of the nose. As λ can be chosen arbitrarily large, the valid region can be extended considerably.

A summary and list of conclusions will now be given, of the results obtained in this chapter on constant shear flow.

Summary and Conclusions.

By applying a transformation to the stream function for parallel flow with constant shear, an extension to Milne Thomson's Circle Theorem is found, and the stream function for constant shear flow past a circular cylinder is obtained using this extension. Using this transformation, in conjunction with the natural coordinates of the body, the stream functions for constant shear flow past the general elliptic cylinder, including the flat plate, and

approximations to the shear flow past a parabolic cylinder and an infinite flat plate, are obtained.

Although the use of elliptic coordinates enables the flow past elliptic cylinders to be obtained, it is of no advantage in solving the problem of shear flow past one branch of a hyperbolic cylinder. The cut along the x-axis between the foci of the families of hyperbolae divides each branch of every hyperbola into two sections, each with its own value of η. For example, the branch of the hyperbola passing through the point $\frac{c}{2}$ on the x-axis has equation $\eta = \frac{\pi}{3}$ and $\eta = \frac{5\pi}{3}$ above and below the x-axis respectively. As a result, it is not possible to obtain the required stream function using the methods outlined in this section.

In applying the method to cylinders, whose boundaries are not closed and finite, certain difficulties arise. Using parabolic and cartesian coordinates, the stream functions are obtained for flows, which approximate to the shear flow past a parabolic cylinder and an infinite flat plate respectively. The separation constant in the solution of Laplace's Equation takes continuous values from zero to infinity. In order to preserve the convergence of the integrals involved, the parabolic cylinder (a directly comparable method being used for the infinite flat plate) is restricted in extent to the range $0 \leqslant u < \lambda$. The flow pattern obtained is artificial in that the points $u = \lambda$ (and $u > \lambda$) on the cylinder are singular points in the flow, being either sources or sinks. As a result, the stream function obtained gives an accurate representation of constant shear flow past a parabolic cylinder only in the vicinity of the nose, which can be extended by taking λ sufficiently large.

The main features of the shear fields are determined, particular

attention being paid to the location of the stagnation points, and to the lift force, in the case of finite closed cylinders. It should be noted that the deflection of the stagnation stream line in the free stream is in a direction towards a region of higher velocity than that opposite the diameter of the cylinder.

A feature of this study, is the repeated appearance of the non-dimensional number $N = \frac{U}{\omega h}$, where U and h are a typical velocity and length in the field respectively, and ω is the vorticity. This number appears as the only non-dimensional parameter in the formulae for the deflections of the stream lines and in the lift coefficient c_L. It also plays an important role in constant rotational flow through a channel with straight parallel sides, where it is easily shown that a necessary condition for no back flow is $N \geq \frac{1}{2}$, where U is the undisturbed velocity along the centre line and h is the breadth of the channel. In fact N seems to have an importance in rotational flow comparable to the Reynold's number in viscous flow.

In conclusion, it is not suggested that elliptic and parabolic coordinates (with polars and cartesians) exhaust the possible cross sections for which constant shear flow stream functions can be obtained. These coordinate systems do, however, serve to illustrate the methods described in this chapter.

Chapter III

Flow With Variable Vorticity

Two-Dimensional Flow with Variable Shear past Cylinders with Various Cross Sections

It was stated in Chapter I that, as far as the author is aware, no theoretical solutions are available for incompressible variable shear flow past cylinders in two dimensions. Accordingly, in this chapter, a method is outlined for obtaining the stream functions for variable shear flow past two-dimensional cylinders for a vorticity distribution in the free stream which approximates to a linear shear distribution. The particular examples chosen, are the flows past circular and elliptic cylinders. A similar method is also obtlined when the free stream has a sine velocity distribution. By considering a sufficiently small circular cylinder suitably situated in this velocity distribution, an approximation is obtained to the flow past a small circular cylinder in the boundary layer. From the stream functions obtained, the main characteristics of the flows are determined.

The Fundamental Equations and Transformation for the Linear Shear Approximation

The stream function ψ, for the steady, rotational two-dimensional flow of an incompressible inviscid fluid, satisfies the equation (I.15)

$$\nabla^2\psi + \omega = 0 , \qquad \text{----------(1)}$$

where the Laplacian operator $\nabla^2 = \frac{\partial^2}{\partial x^2} + \frac{\partial^2}{\partial y^2}$, and ω, the vorticity, given by (I.5)

$$\omega = \frac{\partial q_y}{\partial x} - \frac{\partial q_x}{\partial y} ,$$

satisfies the equation (I.10)

$$\frac{\omega}{\rho} = f(\psi),$$

where ρ is the density, which in this case is constant, and q_x and q_y are the x- and y- cartesian velocity components respectively. The latter equation in this incompressible flow becomes

$$\omega = f(\psi)$$

from which it should be noted, that the vorticity is constant along a stream line. Substitution of this last equation in equation (1) results in the single fundamental equation (I.16)

$$\nabla^2\psi + f(\psi) = 0.$$

Throughout this chapter, $f(\psi)$ is taken to be equal to $\lambda\psi$, where λ is either positive or negative. The problem where $f(\psi)$ is general is either extremely difficult or impossible. From dimensional consideration, λ is of the form $\pm 1/\ell^2$, where ℓ is a typical linear dimension of the flow. Thus, equation (1) finally becomes

$$\nabla^2\psi \pm \psi/\ell^2 = 0 \quad . \text{----------} \quad (2)$$

This particular choice of $f(\psi)$ is made to suit the required vorticity distribution near $x = -\infty$. The two cases possible from equation (2) are considered separately, one giving rise to the approximate linear shear case, the other to the sine velocity distribution case.

The particular form of equation (2) used for the approximation to the linear shear flow is

$$\nabla^2\psi = \psi/\ell^2 \quad . \text{----------} \quad (3)$$

A ψ-distribution consistent with equation (3) is given by

$$\psi = a\, e^{y/\ell} + b\, e^{-y/\ell} \quad , \text{----------} \quad (4)$$

where a and b are arbitrary, real constants, resulting, in this case, in the vorticity distribution

$$\omega = -a/\ell^2\, e^{y/\ell} - b/\ell^2\, e^{-y/\ell} \quad , \text{----------} \quad (5)$$

and on integrating equation (5) (or differentiating equation (4)) the velocity q, is given by

$$q = q_x = a/\ell\, e^{y/\ell} - b/\ell\, e^{-y/\ell} \quad . \text{----------} \quad (6)$$

Now, introducing the stream function Ψ, by the transformation

$$\psi = ae^{y/\ell} + be^{-y/\ell} + \Psi, \qquad (7)$$

it is easily seen from equation (3) that

$$\nabla^2 \Psi = \Psi/\ell^2 . \qquad (8)$$

Thus, if the free stream flow is given by equation (4), which is flow parallel to the x-axis, the necessary condition on Ψ, is that it tends to zero as $x \longrightarrow \pm\infty$.

To summarise, the stream function ψ, as given by equation (7), where satisfies equation (8), must satisfy the following boundary conditions:

(i) $\nabla^2 \psi = \psi/\ell^2$,

(ii) $\psi \longrightarrow ae^{y/\ell} + be^{-y/\ell}$ as $x \longrightarrow -\infty$,

(iii) ψ = constant c, on the cylinder.

As is seen later, these conditions are not sufficient to give a unique solution to the problem unless the constant value c is known, thus, one further condition is necessary, and this is discussed subsequently. Before proceeding with the general method, however, the free stream distribution near $x = -\infty$ is discussed in detail.

<u>The Distribution at Infinity</u>

In this section, free stream conditions are discussed, and so the following results in the section hold only near $x = -\infty$.

If the constants a and b are chosen properly, the distribution of vorticity given by equation (5) becomes an approximation to a linear distribution.

A linear vorticity distribution in the free stream is given by

$$\omega = \omega_0 (1 - y/k\ell), \qquad (9)$$

where ω_0 is a constant vorticity, and k is any number other than zero. It should be noted that k is not in general, integral. In the following analysis

it is assumed to be always positive. Because $q_y = 0$ in parallel flow, integration of equation (9) gives rise to the velocity distribution

$$\frac{\partial \psi}{\partial y} = q_x = U - \omega_o y + \frac{\omega_o}{2k\ell} y^2 \quad , \text{----------(10)}$$

which is a parabolic distribution, where U is some constant velocity. The stream function, if required, can be obtained by integrating equation (10). Equations (9) and (10) give the ideal linear shear free stream flow, and the purpose of this section is to make equations (5) and (6) represent as closely as possible the flow conditions represented by equations (9) and (10) respectively. In these equations there are three variable parameters ω_o, U, and $k\ell$, thus leading to a triple infinity of possible flow cases. There are several methods of choosing a and b to make equations (5) and (6) represent approximately a linear shear distribution. The following two methods seem very reasonable to the author.

1. In any specific problem, the cylinder is situated on the x-axis, and so the region of primary importance in the free stream is that region near the x-axis, that is, the region where y is small. Thus, comparing equations (5) and (9) for small y, it is seen that

$$\frac{a+b}{\ell^2} = -\omega_o \quad , \quad \text{and} \quad \frac{a-b}{\ell^2} = \frac{\omega_o}{k} \quad ,$$

which give

$$\frac{a}{\ell^2} = \frac{\omega_o}{2}\left(\frac{1}{k} - 1\right) \quad , \text{ and } \frac{b}{\ell^2} = -\frac{\omega_o}{2}\left(\frac{1}{k} + 1\right).$$

Thus equation (5) becomes

$$\omega = \omega_o \left(\cosh y/\ell - 1/k \sinh y/\ell\right) , \text{----------(11)}$$

where, as before, k has an unrestricted finite range, excepting the value zero One condition still to be applied, is that $\omega = -\psi/\ell^2$, which implies that th constant of integration on integrating equation (11) is zero, giving the

velocity profile as

$$q = q_x = -\omega_o \ell \sinh y/\ell + \frac{\omega_o \ell}{k} \cosh y/\ell \ , \qquad (12)$$

where the condition $U = \frac{\omega_o \ell}{k}$ must hold if $q_x = U$ on $y = 0$. This velocity profile is of a hyperbolic cosine form, except for $k = 1$, where a pure exponential is obtained. Equations (9) and (11) are similar to the first order in y, equations (10) and (12) being similar to the second order if the condition $U = \frac{\omega_o \ell}{k}$ holds. With these conditions the stream functions are similar to the third order. It should also be noted that the tangents to the two velocity curves on the x-axis are the same. One further correspondence, is that for small values of k, the minimum velocities for the distributions given by equations (10) and (12) are approximately similar, for the same value of y, namely $y = k\ell$ (from equation (9)). In the latter it is assumed that k^2 and higher powers are negligible. There are now only two parameters in the distributions given by equations (11) and (12), since there is a relation connecting U, ω_o, k and ℓ, namely $U = \frac{\omega_o \ell}{k}$. Introducing the non-dimensional parameter $N = U/\omega_o \ell$, as before, equation (12) becomes

$$q = q_x = -\frac{U}{N} \sinh y/\ell + U \cosh y/\ell \ , \qquad (13)$$

since $N = 1/k$. For completeness, integration of equation (13) gives

$$\psi = -\frac{U\ell}{N} \cosh y/\ell + U\ell \sinh y/\ell \ , \qquad (14)$$

the constant of integration being necessarily zero. Now, from equation (10), it is seen that the minimum velocity, at $y = k\ell$, is given by

$$(q_x)_{min.} = U - \tfrac{1}{2} \omega_o k \ell \ .$$

This minimum value for the velocity must be greater than zero for no back flow to occur, which results in the condition

$$N > k/2$$

It is seen, that in the approximate case, where the necessary condition

$N = 1/k$ applies, the above relation becomes $k^2 < 2$, or $N^2 > \frac{1}{2}$ for no back flow to exist in the corresponding linear case. Figure (1) illustrates the two velocity profiles given by equations (10) and (13) in non-dimensional form, for $N = 1/k = \frac{1}{2}$.

If the free stream flow were considered alone, it would, of course, be more convenient to take $k\ell = R$, say, taking R as the typical linear dimension, the condition for no back flow becoming again $N > \frac{1}{2}$ as mentioned in chapter I and derived in chapter IV. However, in view of the subsequent work, the general form, already discussed, is maintained. This argument also applies to the second method of comparison.

To summarise the first method of comparison therefore, taking the values of a and b given previously, it is seen that $N = 1/k$, that in the region $-4k\ell < y < +4k\ell$ (approximately) the vorticity profiles are the same to the first order, the velocity distributions to the second order, and the ψ-distribution to the third order, that the tangents to the velocity profiles are the same for $y = 0$, and finally, that for small k, the minimum velocities have the same value at the same value of y, namely $y = k\ell$. Of course, the smaller the value of k, the more accurate is the comparison, particularly near the x-axis. To maintain a velocity profile of a hyperbolic cosine form k must be less than unity. Far from the axis, however, the method is invalid, since the comparison was based on the assumption of small y.

The stream function given by equation (4) becomes

$$\psi = \omega_0 \ell^2 \left[\tfrac{1}{2}\left(\tfrac{1}{k} - 1\right) e^{y/\ell} - \tfrac{1}{2}\left(\tfrac{1}{k} + 1\right) e^{-y/\ell} \right]$$

$$= U\ell \, \frac{1}{N} \left[\tfrac{1}{2}(N - 1) e^{y/\ell} - \tfrac{1}{2}(N + 1) e^{-y/\ell} \right],$$

which, on introducing the non-dimensional quantities

$$\psi' = \psi/Ul \ , \ y' = y/l \ , \ a' = a/Ul = \tfrac{1}{2}(1 - \tfrac{1}{N}), \ b' = b/Ul = \tfrac{-1}{2}(1 + \tfrac{1}{N}) \ ,$$

becomes

$$\psi' = \sinh y' - \tfrac{1}{N} \cosh y' \ , \qquad \text{----------(15)}$$

which gives

$$q' = q/U = \cosh y' - \tfrac{1}{N} \sinh y' \ ,$$

and $$\omega' = \omega/\omega_o = -\frac{1}{\omega_o} \psi/l^2 = -N\psi' = -N \sinh y' + \cosh y'$$

The linear vorticity distribution may be written as

$$\omega' = 1 - y'/k \ ,$$

and the velocity distribution as

$$q' = 1 - y'/N + y'^2/2kN \ ,$$

where in the latter two equations k and N are independent unless comparison is made with the approximate distribution. Thus, equation (15) completely determines the free stream flow, except for the static pressure which appears in Bernoulli's equation, where ψ' depends on the single parameter N. Figure (1) illustrates the two velocity distributions, which are probably the most important functions from a physical point of view, where k, as in the approximate case, is taken equal to $1/N$ in the linear case, the dashes having been dropped in the figure although dimensionless quantities are used.

2. Although a close correspondence is required near the x-axis, it may be argued that an overall picture of the two profiles should be similar over a range on both sides of the x-axis. Accordingly the following less direct alternative method is outlined.

The procedure, as before, is to make equations (5) and (6) correspond as closely as possible to equations (9) and (10) respectively, in the

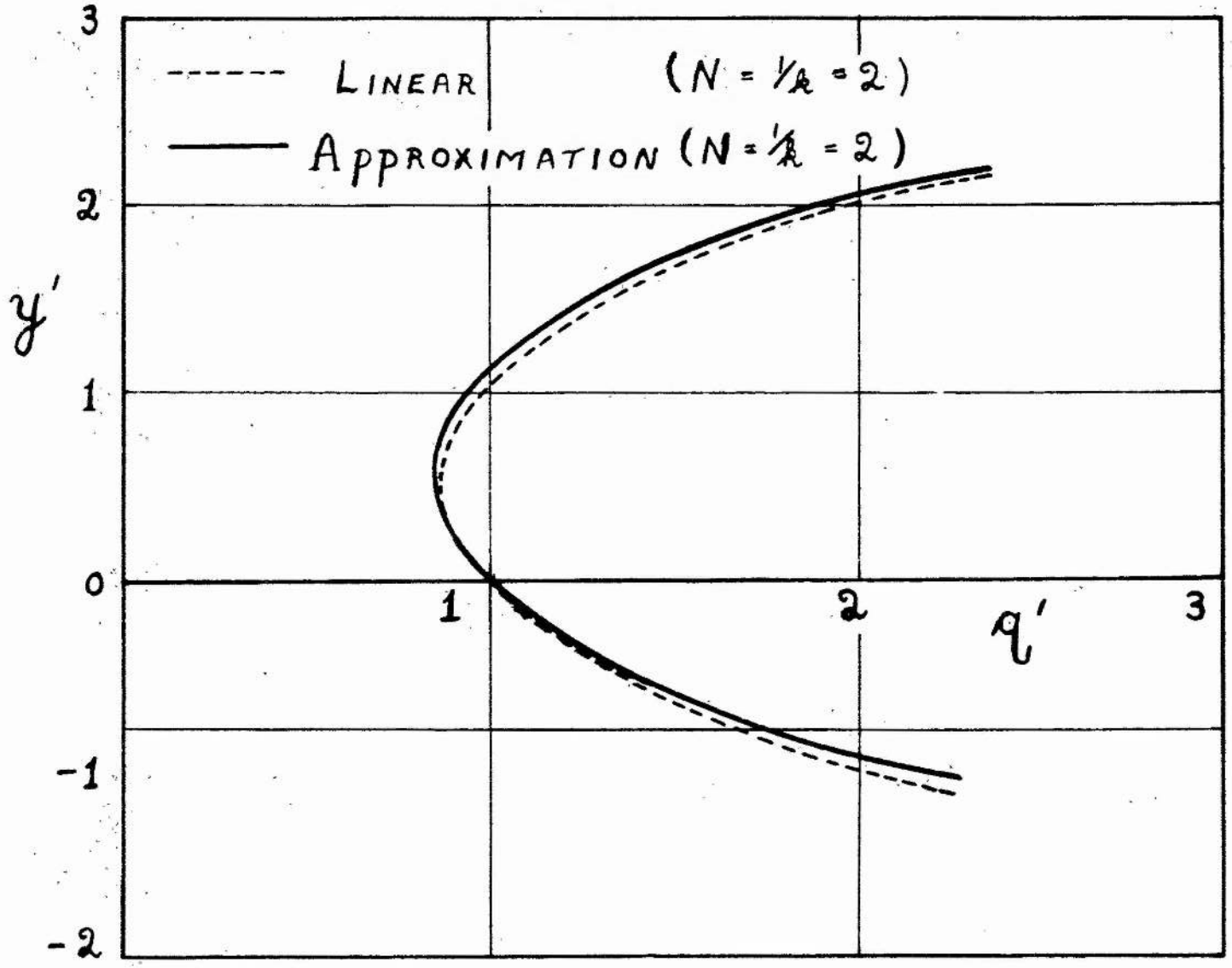

Figure (I) Velocity distribution near $x = -\infty$ (Method 1.).

neighbourhood of the x-axis. This is done by imposing the conditions given below on equations (5) and (6).

(i) $q = q_x$ is a minimum at $y = k\ell$ (implies $\omega = 0$ at $y = k\ell$), and

(ii) $q = q_x = U$ at $y = 0$.

These conditions result in the values for a and b of

$$a = \frac{U\ell}{1 + e^{2k}} \quad , \quad \text{and} \quad b = -\frac{U\ell e^{2k}}{1 + e^{2k}} \quad .$$

Thus, the distributions given by equations (4), (5) and (6) become

$$\psi = \frac{U\ell}{\cosh k} \sinh (y/\ell - k),$$

$$q = q_x = \frac{U}{\cosh k} \cosh (y/\ell - k),$$

and

$$\omega = -\frac{U/\ell}{\cosh k} \sinh (y/\ell - k) .$$

Introducing the same non-dimensional quantities given before, these equations may be written as

$$\psi' = \frac{1}{\cosh k} \sinh (y' - k), \qquad \text{----------(16)}$$

$$q' = \frac{1}{\cosh k} \cosh (y' - k),$$

and

$$\omega' = -\frac{N}{\cosh k} \sinh (y' - k).$$

In this case k has an unrestricted range of values, whilst the number N as shown in method 1, must satisfy the inequality $N > k/2$. With this basis, the method of fitting is now a trial and error method. For each k, there is a value of N which makes the vorticity distribution derived from equation (16) most closely represent the dimensionless form of the linear vorticity distribution in the vicinity of the x-axis. A schematic diagram of the vorticity profiles at $x = -\infty$ with the conditions imposed is shown in

Figure (a), the condition given by equation (17) being incorporated .

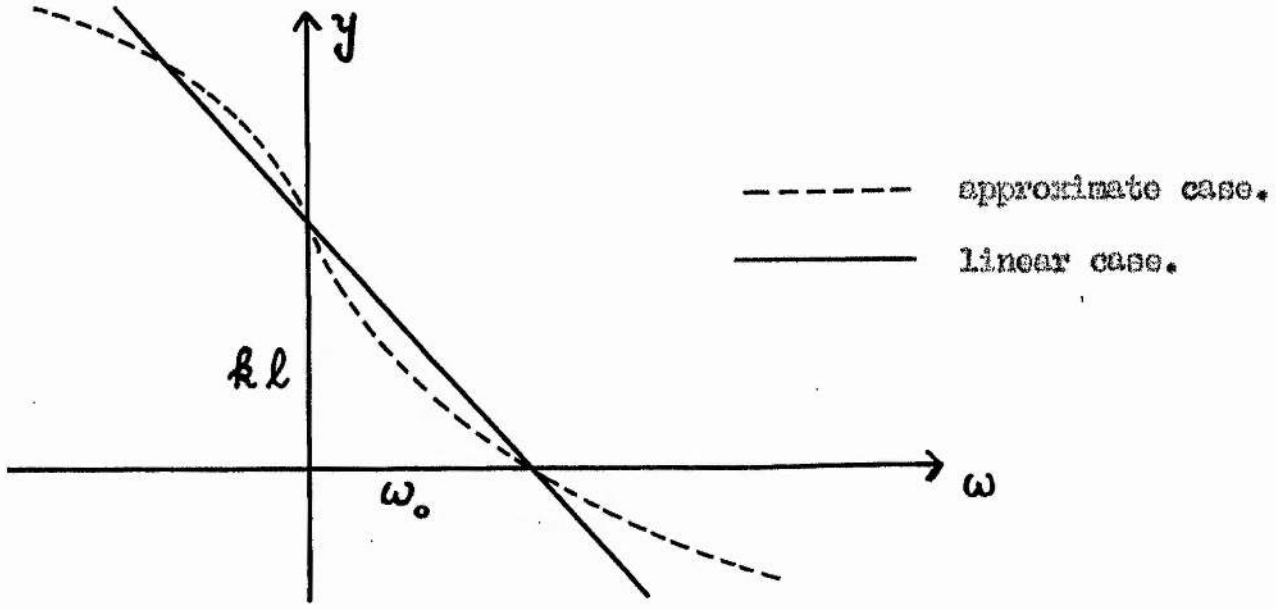

Figure (a)

For example, when k = 1, it is found by trial and error that the value is N = 1.2. The corresponding parabolic and hyperbolic cosine velocity distributions in this case are illustrated in Figure (2). In fact, when k = 1, there is a small range of values of N around N = 1.2, where the velocity distributions near the x-axis for each N are in close agreement. It should be noted, that the value of k is not necessarily small, as in method 1.

A more precise, though less accurate method of connecting k and N for best fit, is to impose an additional condition on the vorticity distribution obtained from equation (16). For example, if $\omega = \omega_0$ at y = 0, then k and N must satisfy the relationship

$$1/N = \tanh k. \qquad \text{----------(17)}$$

So, out of the multiple infinity of possible combinations of shear distribution and typical length l , those satisfying equation (17) will approximate most nearly to linear shear flow conditions in the vicinity of the axis near

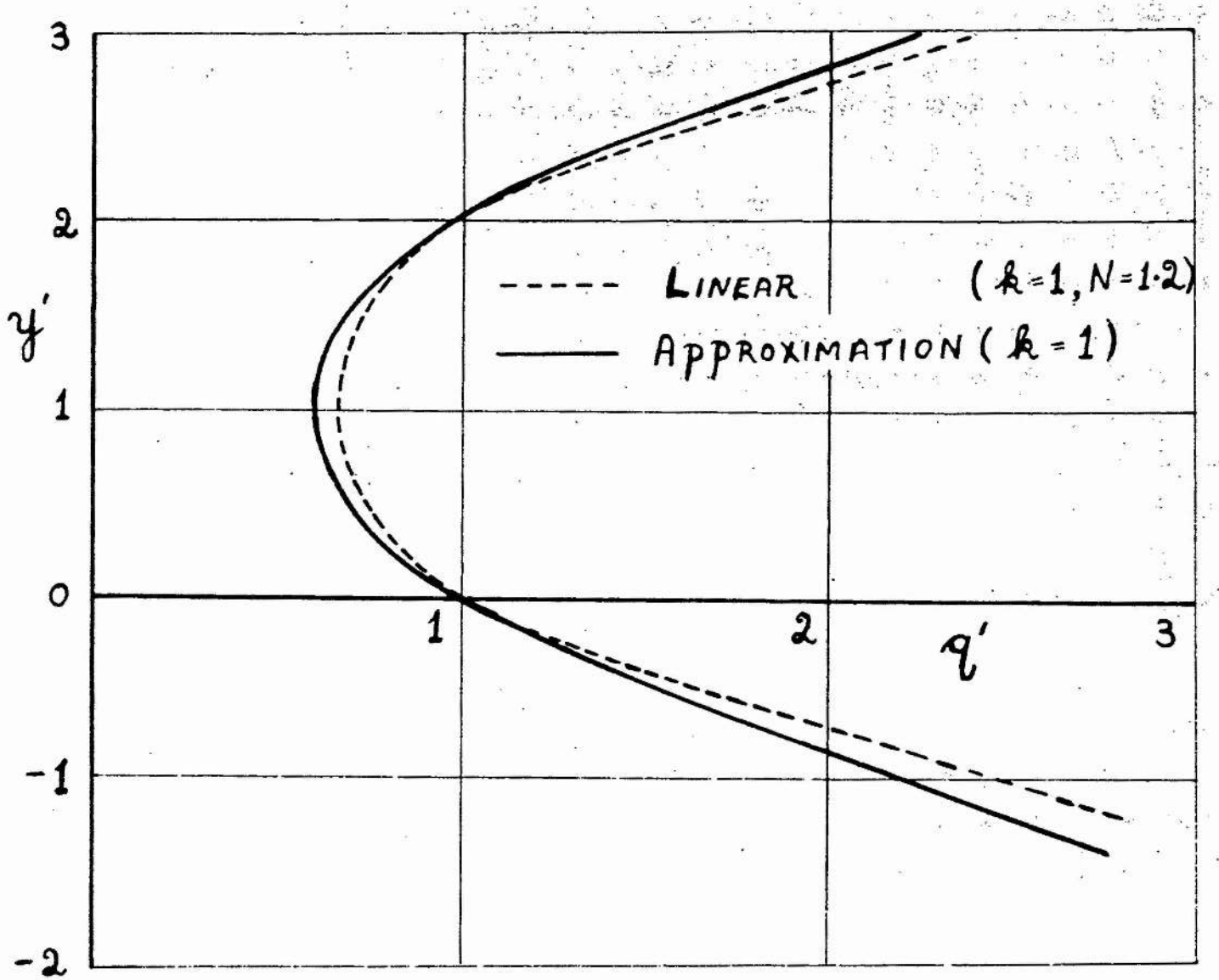

Figure (2) Velocity distribution near $x = -\infty$ (Method 2.).

$x = -\infty$. Figure (a) illustrates the vorticity profiles with this further condition.

Finally, although there is no special merit in choosing a and b to make the shear distribution approximately linear in the vicinity of the axis near $x = -\infty$, it is felt that this distribution constitutes a useful model of variable shear flow.

The general method for obtaining the stream function for a cylinder in this approximately linear shear flow is now put forward, a and b being retained to give a more general result.

The General Method

The single partial differential equation (3) governs the flow, and together with appropriate boundary conditions a unique solution is defined. The stream function ψ, must satisfy the following conditions:

(i) $\nabla^2\psi = \psi/\ell^2$,

(ii) $\psi \longrightarrow a\, e^{y/\ell} + b\, e^{-y/\ell}$ as $x \longrightarrow -\infty$, and

(iii) $= $ constant c, on the given cylinder situated at the origin.

As mentioned previously, the solution is not uniquely defined unless a specific value is given to the constant c, thus there is a single infinity of solutions satisfying (i), (ii) and (iii). The further condition required to obtain a value for c is discussed subsequently in this section.

A solution, involving c, is now obtained by making use of the general transformation, given by equation (7), resulting in a solution for Ψ which satisfies equation (8) and which tends to zero as $x \longrightarrow -\infty$. Although equation (8) can be solved generally in cartesian coordinates, it is more convenient to express it in polar coordinates r and θ, and to solve by separation of variables. Equation (8) in polar coordinates is given by

$$\frac{\partial^2\Psi}{\partial r^2} + \frac{1}{r}\frac{\partial\Psi}{\partial r} + \frac{1}{r^2}\frac{\partial^2\Psi}{\partial\theta^2} - \Psi/\ell^2 = 0 . \qquad (18)$$

Multiplying through by ℓ^2 and writing $r' = r/\ell$, equation (18) becomes dimensionless in the independent variables. Assuming a solution to exist of the form

$$\Psi = R(r').\ \Theta(\theta) ,$$

and substituting in equation (18) the following result is obtained

$$\frac{r'^2}{R}\frac{d^2R}{dr'^2} + \frac{r'}{R}\frac{dR}{dr'} - r'^2 = -\frac{1}{\Theta}\frac{d^2\Theta}{d\theta^2} = \pm m^2 ,$$

where $\pm m^2$ is the separation constant. In fact, $+ m^2$ must be taken, where m is an integer, since the stream function is necessarily periodic in θ, of period 2π. The latter equation results in the two equations

$$\frac{d^2\Theta}{d\theta^2} + m^2\Theta = 0,$$

and

$$\frac{d^2R}{dr'^2} + \frac{1}{r'}\frac{dR}{dr'} - \left(1 + \frac{m^2}{r'^2}\right)R = 0.$$

This last equation is Bessel's differential equation of order m, with imaginary independent variable, solutions of which are $I_m(r')$ and $K_m(r')$, the modified Bessel functions of the first and second kind respectively. (See for example Watson's 'Treatise on Bessel Functions [41]). Thus, a general solution to equation (18) may be written in the form

$$\Psi = \sum_m (A_m \cos m\theta + B_m \sin m\theta)(C_m I_m(r') + D_m K_m(r')),$$

where A_m, B_m, C_m, and D_m are constants. However, as is seen from the asymptotic expansion of $I_m(r')$ for large r' (see [41]), $I_m(r') \not\to 0$ as $r' \to \infty$, whereas $K_m(r') \to 0$ as $r' \to \infty$. Thus, to satisfy the necessary condition on Ψ at infinity the solution becomes

$$\Psi = \sum_m (a_m \cos m\theta + b_m \sin m\theta)\, K_m(r') , \qquad (19)$$

where $C_m = 0$ and $a_m = A_m D_m$ and $b_m = B_m D_m$ are constants. On substituting

Ψ , given by equation (19), in equation (7), the stream function ψ is obtained as

$$\psi = a\, e^{y'} + b\, e^{-y'} + \sum_m (a_m \cos m\theta + b_m \sin m\theta)\, K_m(r'). \text{----------(20)}$$

ψ , given by equation (20) satisfies the conditions (i) and (ii) since it is a solution of equation (3), and $K_m(r') \longrightarrow 0$ as $r' \longrightarrow \infty$ (or $x \longrightarrow -\infty$). If the cylinder, whose equation can be written in the form $r' = \chi(\theta)$, where $\chi($ is in each case a known function of θ, is situated at the origin, the third condition is incorporated to give the following equation

$$c = a\, e^{\chi(\theta)} \sin\theta + b\, e^{-\chi(\theta)} \sin\theta$$

$$+ \sum_m (a_m \cos m\theta + b_m \sin m\theta)\, K_m\,(\chi(\theta)), \text{----------(21)}$$

since $x' = r' \cos\theta$ and $y' = r' \sin\theta$. The terms $\frac{+}{e}\chi(\theta) \sin\theta$ and $K_m\,(\chi(\theta))$ are expressed in the form of Fourier series, and on substitution in equation (21) the coefficients a_m and b_m are obtained in terms of known quantities and c, by equating coefficients. One analytical difficulty, which is best discussed in the individual cases, is that $K_m(\chi(\theta))$ is in general an infinite Fourier series and this results in equations for a_m and b_m which may or may not give solutions. Thus, unless $\chi(\theta)$ is a simple function, difficulties may be encountered. A specific example, however, is more instructive and the flow past an elliptic cylinder will be discussed subsequently, where $\chi(\theta)$ is not a constant. The difficulties which arise are treated in detail.

The question of the non-uniqueness of the solution to the extent of the constant c, appears for all shapes of cylinder, and is therefore discussed in this section. Unlike the constant shear problems, this constant c is not defined numerically (in terms of dimensions of the flow) by the analysis, and

one further condition must therefore be imposed on the flow in order to obtain a value for c. The velocity profile given by equation (6) defines the free stream flow completely except for the value of the stagnation pressure p_o, which does not assist in obtaining a value for c, as is easily seen from Bernoulli's equation (I.12). Now, in practice, it is very probable that there is a unique solution to the physical problem, that is, that there is one, and only one stream line which moves on to the cylinder. The exact location of this stream line will depend on the free stream conditions and the dimensions of the cylinder.

In order to obtain a unique value for c, the circulation Γ is now considered. Writing

$$\Gamma = \Gamma_0 + \Gamma_1 ,$$

where Γ_0 and Γ_1 are the circulation without the cylinder and the extra circulation due to the presence of the cylinder respectively, where the contour is the perimeter of the cylinder. This is directly comparable to the case in chapter II. As can be easily checked from any of the stream functions subsequently derived, the theorem stating that $\Gamma_1 = 0$, as in the constant shear case, does not in general hold for a variable shear flow, when c is general. It seems feasible, however, that an assumption stating that $\Gamma_1 = 0$ in the variable shear case is not outwith the possibility provided the contour L, round which the circulation is measured, is the perimeter of the cylinder. This assumption implies that the introduction of a cylinder into an inviscid incompressible rotational fluid does not alter the circulation round the path L, which coincides with the perimeter of the cylinder. From the form of the stream function given by equation (20), it is seen that the contribution to the circulation Γ, namely Γ_1, which arises from Ψ must be zero. Thus,

if the vector $\underline{Q}$ defines the contribution to the velocity from the 'disturbance' stream function Ψ, and $\underline{ds}$ is the vector of elementary length on the cylinder then the following result must hold:

$$\Gamma_1 = \oint_L \underline{Q} \cdot \underline{ds} = 0, \qquad \text{----------(22)}$$

where L is the path coinciding with the cylinder perimeter, whose equation is given by $r' = \chi(\theta)$, and in polar coordinates $(ds)^2 = (dr)^2 + (rd\theta)^2$. Now, several, if not all, of a_m and b_m involve c and equation (22) in any specific example gives one further condition on the constant coefficients, which is sufficient to provide a definite value for the constant c. It should be noted at this stage, that this circulation condition is not absent in the constant shear case, since the circulation Γ_1 was always assumed to be zero. Although the theorem states that $\Gamma_1 = 0$, a circulation could be added, its value being given as a further boundary condition.

Thus to summarise, the stream function ψ must satisfy four conditions, (i), (ii) and (iii) given previously, and the new condition (iv). The last condition states that the disturbance stream function Ψ gives rise to no further circulation, that is, Γ_1 must be zero. With conditions (i), (ii) and (iii), it should be noted that with c arbitrary, there is a single infinity of solutions to the problem. In the symmetrical case when $k = 0$ in, say equation (16), it is obvious from a physical point of view that c must be zero, that is, the stagnation stream line coincides with the x-axis and is undeflected; analytically, however, any value of $c \neq 0$ gives a valid solution satisfying (i), (ii) and (iii).

The general features of the flows past the various cylinders can be calculated from the stream functions obtained by the method described above. The lift force on the cylinder per unit length can be obtained. It does

in fact vary with the change in circulation round the cylinder. Rather than discuss the general method further at this stage, it is more instructive to study particular shapes of cylinder in a shear flow of the type discussed abov

The Circular Cylinder

A circular cylinder of radius r_o, is introduced at the origin in the field of flow given by equation (4). The typical linear dimension ℓ in this case is r_o, the radius of the cylinder. For the sake of completeness, a and are retained in their general form, and may be replaced at any stage by the values obtained in either method 1. or 2.

In this case the cylinder is given by $r' = r/r_o = 1$, which gives $\chi(\theta) =$ Equation (21) thus becomes

$$c = a\, e^{\sin\theta} + b\, e^{-\sin\theta} + \sum_{m=0}^{\infty} (a_m \cos m\theta + b_m \sin m\theta) K_m(1) \quad \text{.--------(23)}$$

Using integrals given by 'Integral Tafel', [42] or directly from the British Association Mathematical Tables of Bessel Functions, [43], the Fourier expansi of $e^{\pm \sin\theta}$ is given by

$$e^{\pm \sin\theta} = I_o(1) + 2 \sum_{m=1}^{\infty} (-1)^m I_{2m}(1) \cos 2m\theta \pm 2 \sum_{m=0}^{\infty} (-1)^m I_{2m+1}(1) \sin (2m+1)\theta \,.$$

These expansions are substituted in equation (23) and coefficients equated to give

$$a_o = \left[c - (a+b) I_o(1)\right] \frac{1}{K_o(1)} \,,$$

$$a_{2m} = -2(a+b)(-1)^m \frac{I_{2m}(1)}{K_{2m}(1)} \,, \quad b_{2m} = 0 \,,$$

$$b_{2m+1} = -2(a-b)(-1)^m \frac{I_{2m+1}(1)}{K_{2m+1}(1)} \,, \quad a_{2m+1} = 0 \,,$$

which on substitution in equation (20) give the stream function as

$$\psi = ae^{y'} + be^{-y'} + \left[c - (a+b)I_0(1) \right] \frac{K_0(r')}{K_0(1)}$$

$$- 2(a+b) \sum_{m=1}^{\infty} (-1)^m \frac{I_{2m}(1)}{K_{2m}(1)} K_{2m}(r') \cos 2m\theta$$

$$+ 2(a-b) \sum_{m=0}^{\infty} (-1)^m \frac{I_{2m+1}(1)}{K_{2m+1}(1)} K_{2m+1}(r') \sin (2m+1)\theta \quad .\text{--------(24)}$$

It should be noted at this stage, that the field of flow is symmetrical about the y-axis: this is irrespective of the value of c. The stream function given by equation (24) satisfies the conditions (i), (ii) and (iii), defined in the last section, for all values of c. If k = 0 in equation (16), then, $a = -b = \frac{1}{2}$. From physical considerations, the flow is symmetrical about the x-axis and so c = 0. This state of affairs is shown in Figure (b), where the stagnation streamline is the x-axis and the perimeter of the cylinder

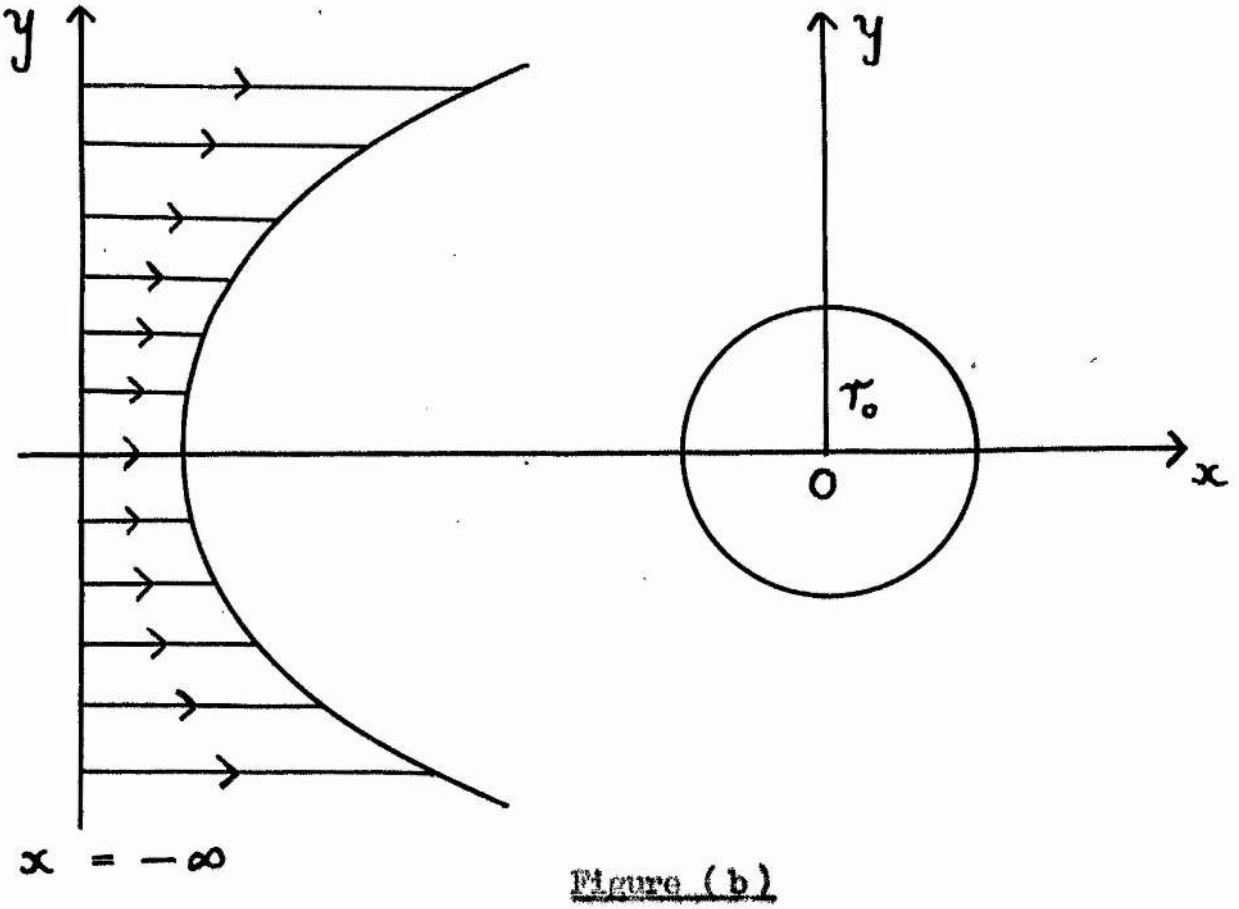

Figure (b)

In general, the constant c must be found from equation (22) as follows.

The velocity components in polar coordinates are

$$q_r = \frac{1}{r}\frac{\partial \psi}{\partial \theta} \quad \text{and} \quad q_\theta = -\frac{\partial \psi}{\partial r} \ .$$

Round the perimeter L, of the circular cylinder, $q_r = 0$, and accordingly the circulation Γ, in an anti-clockwise direction, is given by

$$\Gamma = \oint_L (q_\theta)_{r=r_o} r_o \, d\theta = \Gamma_o + \Gamma_1 ,$$

where Γ_o and Γ_1 are as defined in the preceding section. Using equation (24), it is seen that

$$\Gamma_o = -\int_o^{2\pi} (a\, e^{a\sin\theta} - b\, e^{-a\sin\theta}) \sin\theta \, d\theta$$

$$= -2\pi (a + b) I_1(1), \qquad \text{----------(25)}$$

and together with equation (22)

$$\Gamma_1 = -2\pi \frac{K_o'(1)}{K_o(1)} \left[c - (a + b) I_o(1) \right] = 0,$$

where $K_o'(1) = \left[\frac{dK_o(r')}{dr'}\right]_{r'=1}$, which leads to the result

$$c = (a + b) I_o(1). \qquad \text{----------(26)}$$

It is easily seen from equations (4) and (5) that for no back flow b must alway be negative, and numerically greater than a. As a result c, given by equation (26), is always negative. The stagnation stream line is $\psi = c$, and thus the non-dimensional deflection $y_s' = y_s/r_o$, of the stagnation stream line in the fr stream near $x = -\infty$ is, from equation (4), given as a solution of

$$a\, e^{2y_s'} - (a + b) I_o(1)\, e^{y_s'} + b = 0,$$

which, since the exponential is always positive, results in

$$y_s' = \log_e \left[\frac{\left\{ [(a+b) I_o(1)]^2 - 4ab \right\}^{\frac{1}{2}} + (a+b) I_o(1)}{2a} \right] . \text{------(27}$$

One important result arising from equation (27) is that for all $k > 0$ the stagnation stream line always comes from below the x-axis, $y'_s < 0$, which is, of course, a region of higher velocity than that opposite the centre of the cylinder. This is a comparable result to that obtained in chapter II.

Substituting relation (26) in equation (24), the stream function is obtained for any a and b. If a or b is zero, a negative or positive exponential velocity distribution respectively is obtained. It is also found that when a and b are both positive, there is a flow comparable to the constant vorticity case (that is, regions in the free stream exist where the flow is in the opposite direction) and the state of affairs from the point of view of the stagnation points is qualitatively similar.

Taking the particular values of a and b given by method 2., the stream function in dimensionless form becomes

$$\psi' = \frac{\sinh (y' - k)}{\cosh k} + 2 \tanh k \sum_{m=1}^{\infty} (-1)^m \frac{I_{2m}(1)}{K_{2m}(1)} K_{2m}(r') \cos 2m\theta + 2 \sum_{m=0}^{\infty} (-1)^{m+1} \frac{I_{2m+1}(1)}{K_{2m+1}(1)} K_{2m+1}(r') \sin(2m+1)\theta \quad , \text{------(28)}$$

where $\psi' = \psi / Ur_o$, and k if required may be related to N by equation (17). From equation (25) the circulation Γ_o is given by

$$\Gamma_o = 2\pi \, Ur_o \tanh k \; I_1 (1) . \text{----------(29)}$$

The velocity at any point is given by

$$q'^2 = (q/U)^2 = (q'_{r'})^2 + (q'_\theta)^2 \quad ,$$

where q_r and q_θ are as defined previously. In particular, the velocity on the cylinder, where $q_r = 0$, is given by

$$(q'_\theta)_{r'=1} = -\left[\frac{\sin\theta \cosh(\sin\theta - k)}{\cosh k} + 2\tanh k \sum_{m=1}^{\infty}(-1)^m \frac{I_{2m}(1)}{K_{2m}(1)} K'_{2m}(1)\cos 2m\theta + 2\sum_{m=0}^{\infty}(-1)^{m+1} \frac{I_{2m+1}(1)}{K_{2m+1}(1)} K'_{2m+1}(1)\sin(2m+1)\theta\right], \quad \text{------(30)}$$

where $K'_{2m}(1) = \left[\frac{dK_{2m}(r')}{d\,r'}\right]_{r'=1}$ and $K'_{2m+1}(1) = \left[\frac{dK_{2m+1}(r')}{d\,r'}\right]_{r'=1}$.

Putting $\gamma_m(r') = -\frac{I_m(1)}{K_m(1)} K'_m(r')$, Table (1) illustrates how rapidly the series converge in equation (30), where $r' = 1$; in cases where $r' > 1$, the series converge even more rapidly.

m	1	2	3	4	5	6
$\gamma_m(1)$	.961	.322	.071	.011	.0014	.00014

Table (1).

Stagnation points on the cylinder are given by $(q'_\theta)_{r'=1} = 0$, and in view of the values of $\gamma_m(1)$ given in Table (1), a reasonable approximation is given

$$\tanh k\,(1 + 4\gamma_2(1))\sin^2\theta - (1 + 2\gamma_1(1))\sin\theta - 2\gamma_2(1)\tanh k = 0$$

where it should be noted that $k = 0$ gives $\theta = 0, \pi$, and the solution for $k > 0$ is given by

$$\sin\theta = \frac{1}{2\tanh k\,(1+\gamma_2(1))}\left[(1 + 2\gamma_1(1)) - \left\{(1+2\gamma_1(1))^2 + 8\gamma_2(1)\tanh^2 k\,(1+4\gamma_2(1))\right\}^{\frac{1}{2}}\right]. \quad \text{-----(31)}$$

This gives stagnation points symmetrically placed about the y-axis, lying in th third and fourth quadrants of the circle. More accurate solutions are obtaine directly from expression (30), when it is equated to zero. The deflection y_c, the stagnation points on the cylinder is given in non-dimensional form by $y'_c = y_c$ $= \sin\theta$, where $\sin\theta$ is given by equation (31). The stagnation stream line ψ which, from equation (26) is $\psi_s = - Ur_o I_o(1) \tanh k$, starts in the free strea near $x = -\infty$ at the position y'_s, given by equation (27), which in this case reduces to

$$y'_s = k - \sinh^{-1}\left[I_o(1) \sinh k \right] . \qquad (32)$$

This value of y'_s is the deflection of the stagnation stream line in the free stream near $x = -\infty$. The deflection in the stagnation stream line is given by δ, the difference in the two deflections y_s and y_c, which in non-dimensional form is given by

$$\delta' = \delta/r_o = y'_s - y'_c \ , \qquad (33)$$

where y'_s and y'_c are given by equations (32) and (31) respectively. Relations (31) and (32), and consequently (33), can easily be obtained for general a and b from equation (24), with $c = (a+b)I_o(1)$. Using equations (31), (32) and (33 graphs of the various quantities are drawn, and are illustrated in Figures (3), (4) and (5) respectively, for varying values of k. If relation (17) is used in conjunction with the results in Figures (3), (4) and (5), the various deflections are obtained in terms of N, where it should be remembered that the maximum value of k/N is unity. As mentioned before, however, a trial and erro method is in the end more accurate for the best value of N for a given k. If the distribution from method 1. is used, $1/N$ and k are identical and the approximation is good for small k only. Figure (6) illustrates the flow past the circular cylinder. The region $x \leqslant 0$ only is shown, since the flow is symmetrical about the y-axis.

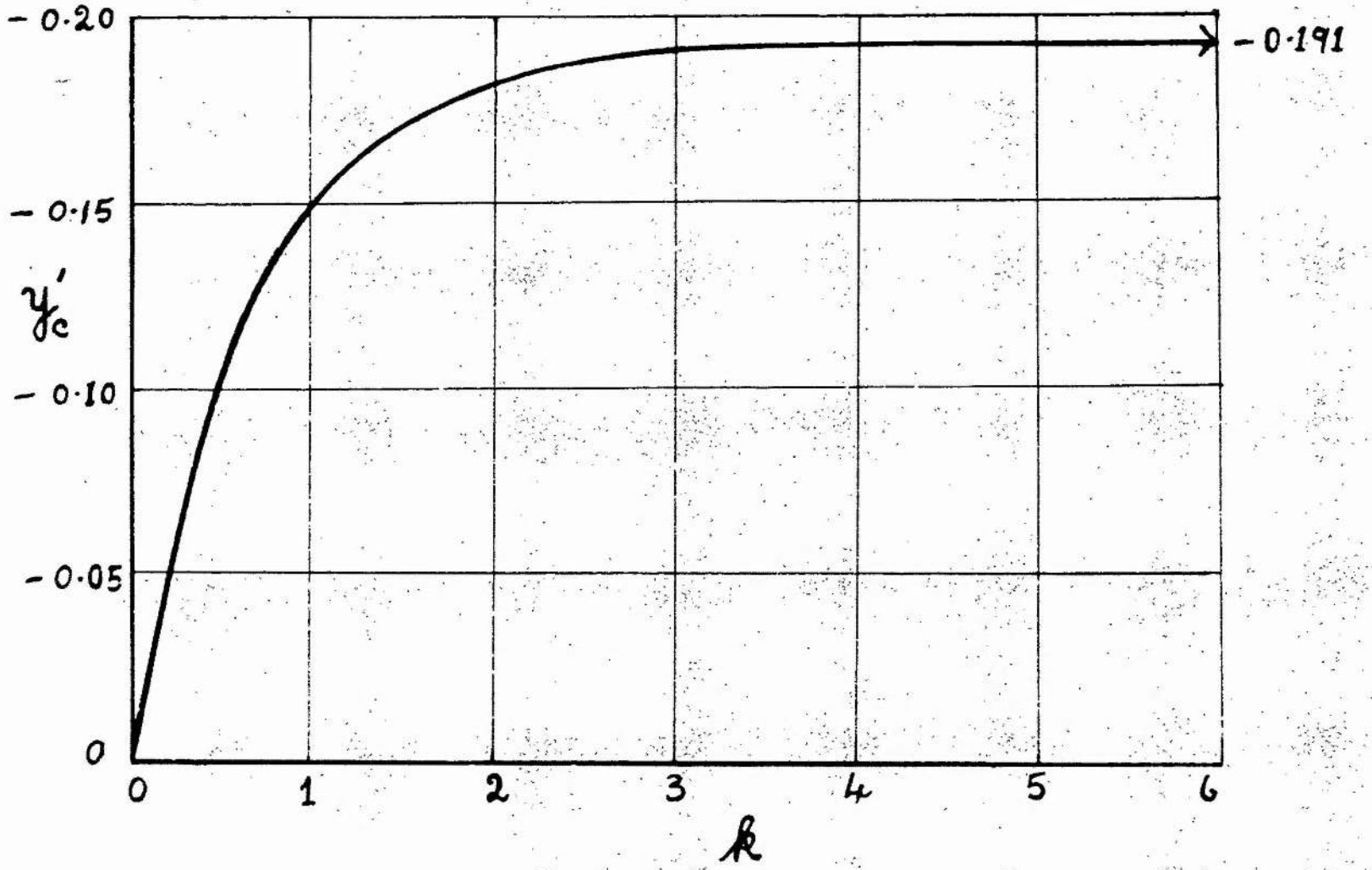

Figure (3) Variation of the position of the stagnation point on the circular cylinder (Method 2.).

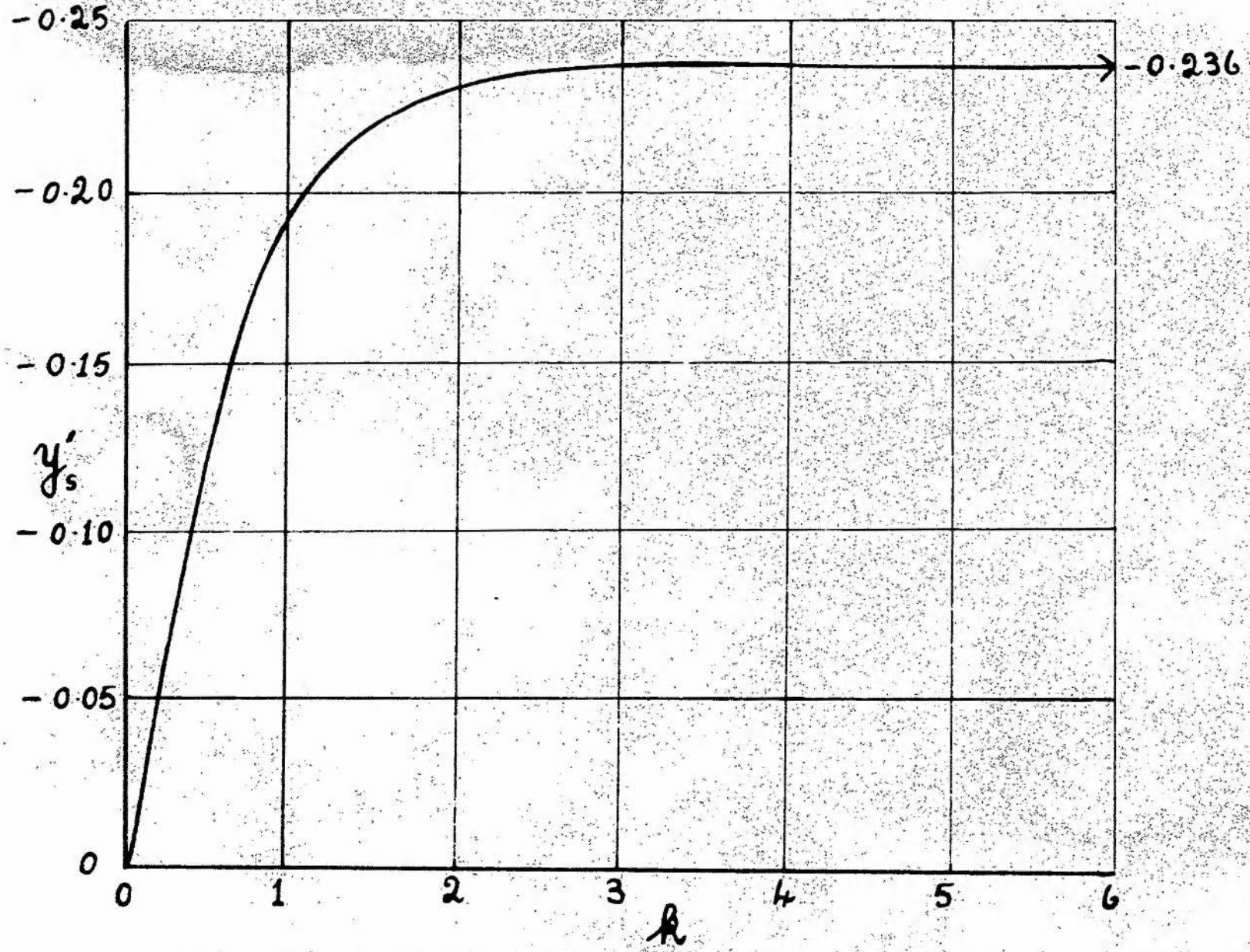

Figure (4) Deflection in the stagnation stream line in the free stream for the circular cylinder (Method 2.).

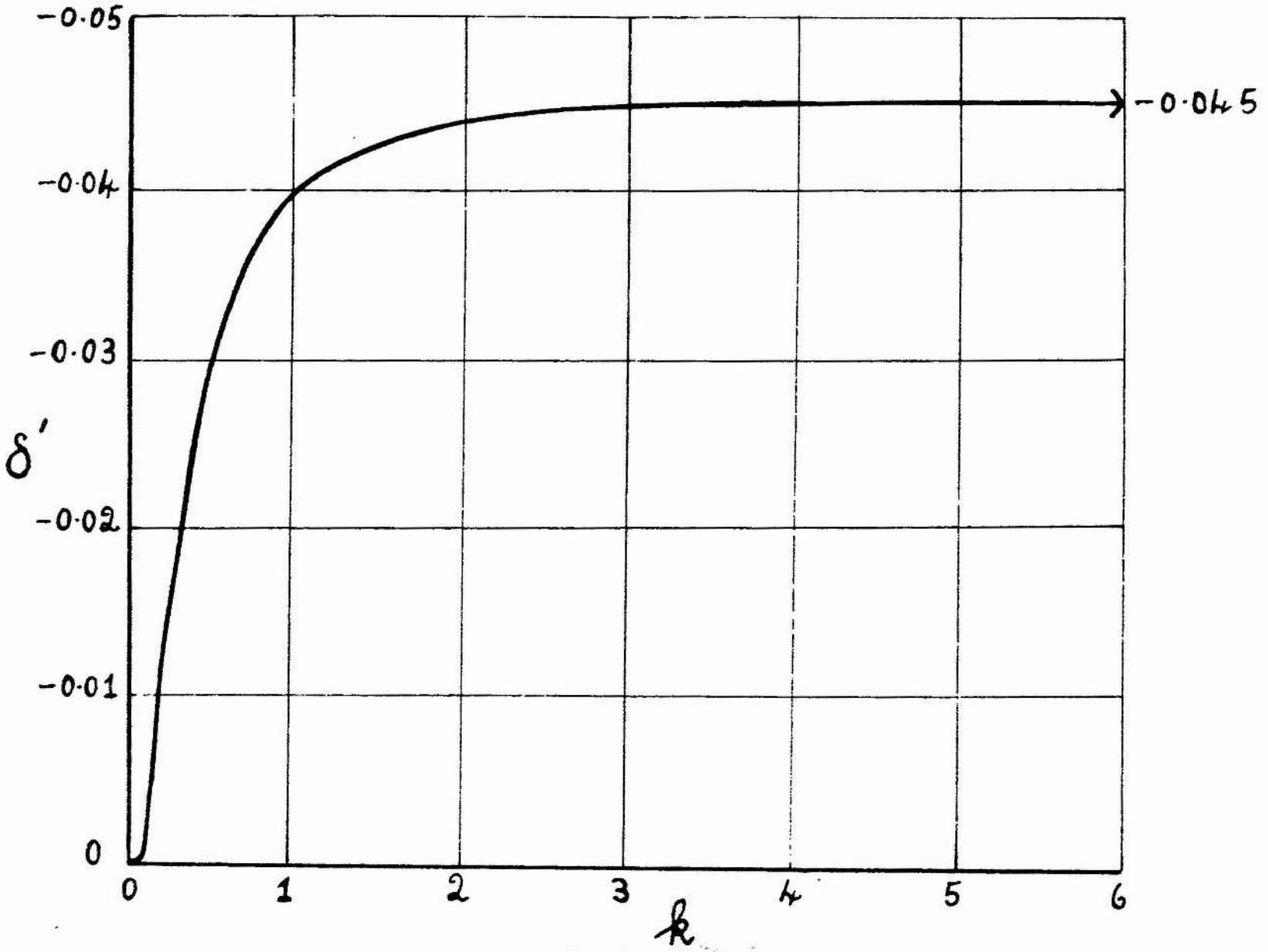

Figure (5) Deflection in the stagnation stream line for the circular cylinder (Method 2.).

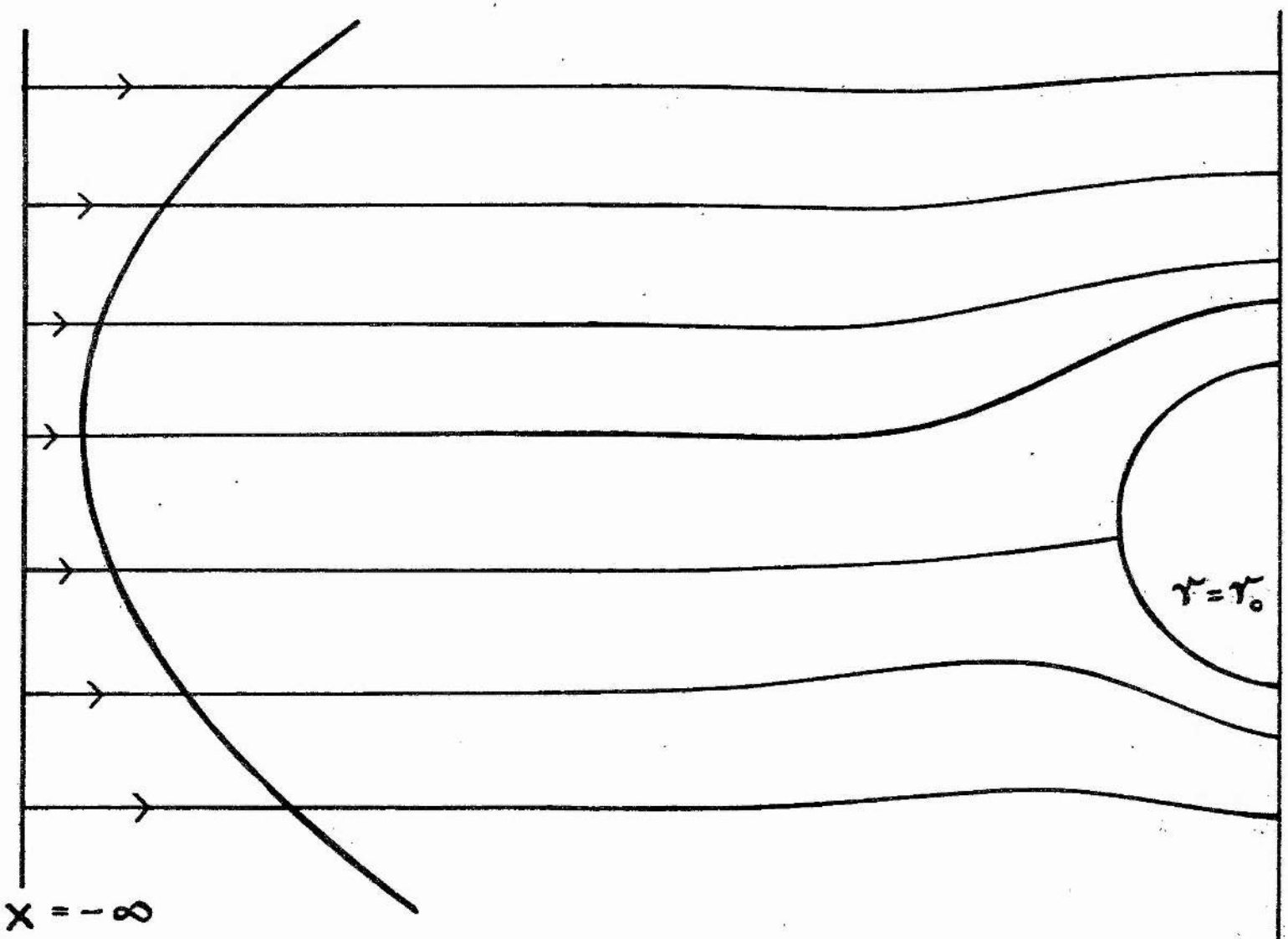

Figure (6) Illustration of the stream lines for a circular cylinder in a flow with approximately a linear shear distribution.

For the purposes of this thesis, only the case of the circular cylinder in a variable shear flow has been fully evaluated, other examples being derived with general a and b only. Accordingly a short discussion of the results on the circular cylinder will now be given.

Discussion of the Results for the Circular Cylinder

One important qualitative result arising from the general solution, is that for all values of k, positive and negative, the stagnation stream line comes from a region of higher velocity than the free stream velocity directly in line with the cylinder centre. This result is illustrated in Figure (4), and is in agreement with the conclusions given in chapter II for the case of constant shear flow. The non-dimensional parameter N again appears together with a parameter k, which is introduced by the comparison of the free stream flow with the linear shear model. General conclusions are given at the end of the chapter.

It is, however, propitious at this stage to give some tentative quantitative comparison with the experimental results of Young and Maas [35] and Davies [37], described briefly in chapter I. The displacement measured experimentally by these authors is the same as that denoted by y_s' throughout this thesis. Taking the radius of the pitot tube as the typical linear dimensi Young and Maas found that the deflection of the stagnation stream line comparab to y_s' was substantially constant over a range of readings, and was in fact, equ to 0.36. From a study of the requisite paper [35] it appears that for the experimental range considered, the results are based on a very restricted range of small values of $1/N$. The maximum deflections in the theoretical cases, which in the variable shear flow is 0.24 (Figure (4)) and in the constant shear flow is 0.71 (Figure (5), chapter II), can not be compared with the experimental results. For $1/N = 0.3$, which is probably near the upper limit of the restrict

range covered by the experiments of Young and Maas, the theoretical value for the displacement of the stagnation stream line in the variable shear case is approximately 0.05, and in the constant shear case 0.07. This apparent inconsistency in the actual numerical values is perhaps significant. In chapter I, it was mentioned that Davies [37] obtained results, which showed very small, or zero, displacements for low speed flow, to which this incompressible flow is comparable. In the experiments, he used tubes of a two-dimensional nature, which compares with the two-dimensional nature of the work in this thesis, whereas Young and Maas used tubes of a three-dimensional type. Thus, it is possible that the large displacements obtained by Young and Maas are due primarily to the three-dimensional nature of the flow. Thus, in the case of pitot tubes in a rotational flow, comparatively large displacements are to be expected in three-dimensional flow, and very much smaller displacements in two-dimensional flow. This possibility that the deflection is essentially a three-dimensional effect is of major importance.

To illustrate the general methods given previously, the case of an elliptic cylinder in a variable shear flow is considered.

The Elliptic Cylinder with its Major Axis in the Direction of Flow

An ellipse in polar coordinates r and θ, is given by

$$r = \frac{p}{1 + e \cos \theta} \quad , \qquad (34)$$

where p and e are the semi-latus rectum and the eccentricity respectively. An ellipse with its equation given by equation (34) is situated as shown in Figure (c), one of the foci being situated at the origin.

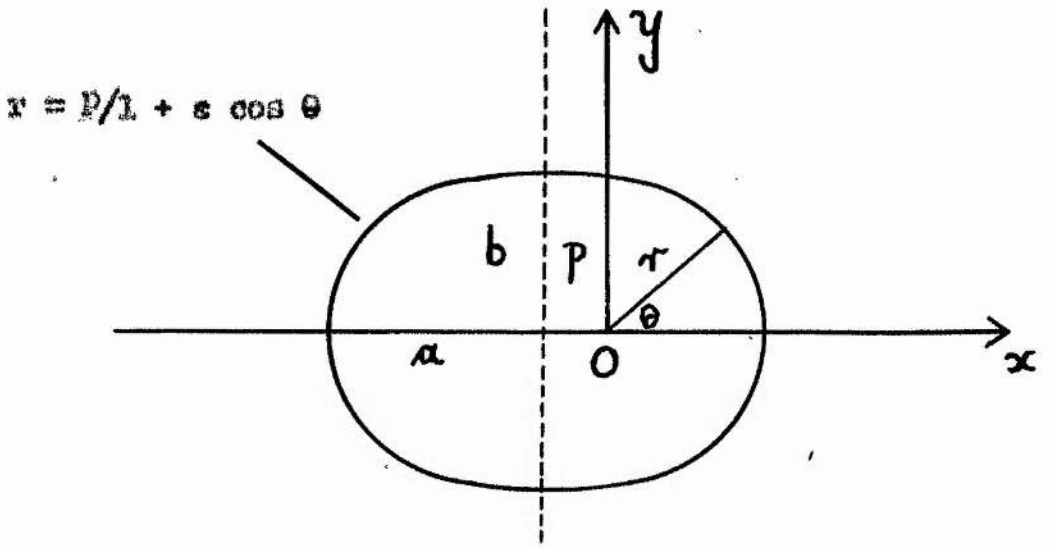

Figure (c)

The length p, may take any value, whilst the eccentricity e, for an ellipse must satisfy $0 < e < 1$, the limiting cases of $e = 0$ and 1 being a circle and a parabola respectively. The equation of this ellipse in cartesian coordinate where a and b are the semi-major and -minor axes respectively, is given by

$$\frac{(x + ae)^2}{a^2} + \frac{y^2}{b^2} = 1 .$$

When $x = 0$, $y = p$, which gives

$$a = \frac{p}{(1 - e^2)} \qquad \text{and} \quad b = \frac{p}{(1 - e^2)^{\frac{1}{2}}} . \qquad \text{----------(35)}$$

It is more convenient here to take p as the linear dimension and in the final results for deflections to multiply by the factor $p/b = (1 - e^2)^{\frac{1}{2}}$. Thus, in dimensionless form, equation (34) becomes

$$r' = r/p = \frac{1}{1 + e \cos \theta} = \chi(\theta) ,$$

which defines $\chi(\theta)$ for the elliptic cylinder situated as shown in Figure (c). With this value of $\chi(\theta)$, equation (21) becomes

$$\chi = a\, e^{\sin\theta/1 + \varepsilon\cos\theta} + b\, e^{-\sin\theta/1 + \varepsilon\cos\theta} + \sum_{m=0}^{\infty} (a_m \cos m\theta + b_m \sin m\theta) K_m \left(\frac{1}{1 + \varepsilon\cos\theta}\right) . \qquad (36)$$

It should be mentioned at this stage that one condition imposed on $\chi(\theta)$ in its general form is that $\chi(\theta)\sin\theta$ must be free from any singularities in the field. The $\chi(\theta)$ defined for the elliptic cylinder satisfies this condition only if $\varepsilon < 1$, and so the parabolic cylinder is excluded from the final results. As may be seen, most of subsequent analysis is valid if and only if $\varepsilon < 1$.

As mentioned previously, when $\chi(\theta)$ is not a constant certain difficulties arise, several of which are already apparent from equation (36). For example, Fourier expansions have to be obtained for the exponentials $e^{\pm \sin\theta/1 + \varepsilon\cos\theta}$ and for the Bessel Function $K_m \left(\frac{1}{1 + \varepsilon\cos\theta}\right)$ whose argument is a function of θ and ε. The difficulties are considered separately as follows:

1. The Fourier Expansion of $e^{\pm \sin\theta/1 + \varepsilon\cos\theta}$

The straightforward method of obtaining the coefficients in the full-range Fourier expansion of the function, is to evaluate integrals of the form

$$\frac{1}{\pi}\int_{-\pi}^{\pi} e^{\pm \frac{\sin\theta}{1+\varepsilon\cos\theta}} \begin{Bmatrix} \sin \\ \cos \end{Bmatrix} m\theta \, d\theta .$$

The evaluation of these integrals is very difficult analytically, and the following method is used.

The expansion of the exponential function is given by

$$e^{\pm \frac{\sin\theta}{1+\varepsilon\cos\theta}} = 1 + \sum_{r=1}^{\infty} \frac{(\pm 1)^r}{r!} \left(\frac{\sin\theta}{1+\varepsilon\cos\theta}\right)^r , \qquad (37)$$

and each term in the summation is expressed as a Fourier series. The latter series are summed over r, to give a final Fourier expansion for the required

function. The expansion of each individual term is carried out in two parts.

(1) Consider $1/(1 + \varepsilon \cos\theta)^r$, where r takes all values from 1 to ∞ . Irrespective of whether r is odd or even, $1/(1 + \varepsilon \cos\theta)^r$ is an even function of θ, and can thus be expanded as a half-range cosine series, which may be written as

$$\frac{1}{(1 + \varepsilon \cos\theta)^r} = \tfrac{1}{2} a_{r,o} + \sum_{n=1}^{\infty} a_{r,n} \cos n\theta \ , \qquad \text{----------(38)}$$

where $a_{r,n}$ is given, for all n and r, by

$$a_{r,n} = \tfrac{2}{\pi} \int_0^{\pi} \frac{\cos n\theta}{(1 + \varepsilon \cos\theta)^r} \, d\theta \quad .$$

Using Integral Tafel [42] , a value for this integral can be obtained in terms of a, where a is defined by the relation

$$\varepsilon = -\frac{2a}{1+a^2} \ ,$$

which gives

$$a = -\frac{1}{\varepsilon} \pm \left(\frac{1}{\varepsilon^2} - 1 \right)^{\frac{1}{2}} .$$

Since $\varepsilon < 1$, $|a| > 1$, or $|a| < 1$ according to whether the negative or positive sign is taken with the square root in the last equation. Thus, taking the positive root,

$$a = -\frac{1}{\varepsilon} + \left(\frac{1}{\varepsilon^2} - 1 \right)^{\frac{1}{2}} \ , \qquad \text{----------(39)}$$

giving a negative, and $|a| < 1$. The integral for $a_{r,n}$ is obtained as (Table 332. (31))

$$a_{r,n} = \tfrac{2}{\pi} \int_0^{\pi} \frac{\cos n \, d\theta}{(1 + \varepsilon \cos\theta)^r}$$

$$= \frac{2(1+a^2)^r \, a^{2r+n-2}}{(1-a^2)^{2r-1}} \sum_{\nu=0}^{r-1} \binom{r+n-1}{\nu} \binom{2r-\nu-2}{r-1} \left(\frac{1-a^2}{a^2} \right)^{\nu} , \qquad \text{----(40)}$$

where in general

$$\binom{p}{q} = \frac{\Gamma(p+1)}{\Gamma(q+1)\,\Gamma(p-q+1)} = \frac{p!}{q!(p-q)!} \qquad (p \geqslant q),$$

where Γ denotes the Gamma function, which for integral values of the argument may be written in factorial form as shown, since in equation (40) the numbers corresponding to p and q are integral. The expression involving the Gamma functions for integral arguments is similar to the expression for the binomial coefficients ${}^{p}C_{q}$. Thus, equation (38) gives the required Fourier expansion for $1/(1 + \varepsilon \cos\theta)^{r}$, for all r, where the $a_{r,n}$ are given by equation (40).

(ii) Consider now, the expression $\left(\sin\theta/1 + \varepsilon \cos\theta\right)^{r}$. This function is an odd or even function of θ, depending on whether r is an odd or an even integ respectively. The expansion as a Fourier series is carried out in two parts. If r is an even integer the expression gives a half-range cosine series, and if r is an odd integer, the expression gives a half-range sine series.

r even.

The function is an even function, so let

$$\left(\frac{\sin\theta}{1 + \varepsilon \cos\theta}\right)^{r} = \tfrac{1}{2} A_{r,0} + \sum_{m=1}^{\infty} A_{r,m} \cos m\theta \,, \qquad (41)$$

$$= \sin^{r}\theta \sum_{n=0}^{\infty} a_{r,n} \cos n\theta \,,$$

from equation (38), with $a_{r,n}$ given by equation (40), where the term n = 0 in the last summation must be multiplied by $\frac{1}{2}$ to conform with equation (38). By definition, the coefficients $A_{r,m}$ are given by

$$A_{r,m} = \tfrac{2}{\pi} \int_{0}^{\pi} \frac{\sin^{r}\theta}{(1+\varepsilon\cos\theta)^{r}} \cos m\theta \, d\theta$$

$$= \tfrac{2}{\pi} \int_{0}^{\pi} \left(\sin^{r}\theta \sum_{n=0}^{\infty} a_{r,n} \cos n\theta\right) \cos m\theta \, d\theta$$

$$= \tfrac{2}{\pi} \sum_{n=0}^{\infty} a_{r,n} \int_{0}^{\pi} \sin^{r}\theta \cos n\theta \cos m\theta \, d\theta \,,$$

where the interchange of the integration and summation is valid, since the integral is finite, and the summation absolutely convergent. Now, the last relation may be written in the form

$$A_{r,m} = \frac{1}{\pi}\sum_{n=0}^{\infty} a_{r,n}\int_0^{\pi} \sin^r\theta\,\cos(m+n)\theta\,d\theta + \frac{1}{\pi}\sum_{n=0}^{m} a_{r,n}\int_0^{\pi} \sin^r\theta\,\cos(m-n)\theta\,d\theta + \frac{1}{\pi}\sum_{n=m+1}^{\infty} a_{r,n}\int_0^{\pi} \sin^r\theta\,\cos(n-m)\theta\,d\theta\ .$$

Using Integral Tagel [42] (332, (12)), these integrals are given as follows:

$$\frac{1}{\pi}\int_0^{\pi} \sin^r\theta\,\cos(m+n)\theta\,d\theta$$

$$= \begin{cases} 0 & \text{for } (m+n) \text{ odd,} \\ 0 & \text{for } r < (m+n),\ (m+n) \text{ even,} \\ \dfrac{(-1)^{\frac{m+n}{2}}}{2^r}\binom{r}{\frac{r-m-n}{2}} & \text{for } r \geqslant (m+n),\ m+n \text{ even,} \end{cases}$$

$$\frac{1}{\pi}\int_0^{\pi} \sin^r\theta\,\cos(m-n)\theta\,d\theta$$

$$= \begin{cases} 0 & \text{for } (m-n) \text{ odd,} \\ 0 & \text{for } r < (m-n),\ (m-n) \text{ even,} \\ \dfrac{(-1)^{\frac{m-n}{2}}}{2^r}\binom{r}{\frac{r-m+n}{2}} & \text{for } r \geqslant (m-n),\ (m-n) \text{ even,} \end{cases}$$

and

$$\frac{1}{\pi}\int_0^{\pi} \sin^r\theta\,\cos(n-m)\theta\,d\theta$$

$$= \begin{cases} 0 & \text{for } (n-m) \text{ odd,} \\ 0 & \text{for } r < (n-m),\ (n-m) \text{ even,} \\ \dfrac{(-1)^{\frac{n-m}{2}}}{2^r}\binom{r}{\frac{r-n+m}{2}} & \text{for } r \geqslant (n-m),\ (n-m) \text{ even.} \end{cases}$$

On substituting these values in the relation for $A_{r,m}$, equation (41) gives the required Fourier Expansion as a cosine series for r an even integer. In this expansion, $A_{r,m}(m \geqslant 0)$ is given by

$$\begin{aligned}
A_{r,m} &= \sum_{n=0}^{\infty} a_{r,n} \frac{(-1)^{\frac{m+n}{2}}}{2^r} \binom{r}{\frac{r-m-n}{2}} && r \geqslant m+n \\
&= 0 && r < m+n \\
&+ \sum_{n=1}^{m} a_{r,n} \frac{(-1)^{\frac{m-n}{2}}}{2^r} \binom{r}{\frac{r-m+n}{2}} && r \geqslant m-n \\
&+ 0 && r < m-n \\
&+ \sum_{n=m+1}^{\infty} a_{r,n} \frac{(-1)^{\frac{n-m}{2}}}{2^r} \binom{r}{\frac{r-n+m}{2}} && r \geqslant n-m \\
&+ 0 && r < n-m \text{ ,} \qquad \text{--------(42)}
\end{aligned}$$

where the term $n = 0$ has been multiplied by $\frac{1}{2}$ to conform with equation (38). It must be remembered that r, $m+n$, and $m-n$ are all <u>even</u> integers, and that $a_{r,n}$ for all $n \geqslant 0$ is given by equation (40).

<u>r odd</u>.

The function is in this case an odd function, so let

$$\left(\frac{\sin\theta}{1+\epsilon\cos\theta}\right)^r = \sum_{m=1}^{\infty} B_{r,m} \sin m\theta \text{ ,} \qquad \text{----------(43)}$$

$$= \sin^r\theta \sum_{n=0}^{\infty} a_{r,n} \cos n\theta \text{ ,}$$

from equation (38), where $a_{r,n}$ is given by equation (40) and $a_{r,o}$ in the latter summation is multiplied by $\frac{1}{2}$ to conform with equation (38) as before. The coefficients $B_{r,m}$ are given by

$$B_{r,m} = 2/\pi \int_0^\pi \frac{\sin^r\theta}{(1+\epsilon\cos\theta)^r} \sin m\theta \, d\theta$$

$$= 2/\pi \int_0^\pi \left(\sin^r\theta \sum_{n=0}^{\infty} a_{r,n} \cos n\theta \right) \sin m\theta \, d\theta$$

$$= 2/\pi \sum_{n=0}^{\infty} a_{r,n} \int_0^\pi \sin^r\theta \cos n\theta \sin m\theta \, d\theta ,$$

the interchange of integration and summation again being valid. As before,

$$B_{r,m} = \frac{1}{\pi} \sum_{n=0}^{\infty} a_{r,n} \int_0^\pi \sin^r\theta \sin(m+n)\theta \, d\theta$$

$$+ \frac{1}{\pi} \sum_{n=0}^{m-1} a_{r,n} \int_0^\pi \sin^r\theta \sin(m-n)\theta \, d\theta$$

$$- \frac{1}{\pi} \sum_{n=m+1}^{\infty} a_{r,n} \int_0^\pi \sin^r\theta \sin(n-m)\theta \, d\theta ,$$

the term n=m being, of course, zero. Using Integral Tafel (332.(11)), the values of the integrals are given by

$$\frac{1}{\pi} \int_0^\pi \sin^r\theta \sin(n+m)\theta \, d\theta$$

$$= \begin{cases} 0 & \text{for } (m+n) \text{ even,} \\ 0 & \text{for } r<(m+n),\ (m+n) \text{ odd,} \\ \dfrac{(-1)^{\frac{m+n-1}{2}}}{2^r} \binom{r}{\frac{r-m-n}{2}} & \text{for } r\geqslant(m+n),\ (m+n) \text{ odd,} \end{cases}$$

$$\frac{1}{\pi}\int_0^{\pi} \sin^r\theta \sin(m-n)\theta \, d\theta$$

$$= \begin{cases} 0 & \text{for } (m-n) \text{ even,} \\ 0 & \text{for } r < (m-n),\ (m-n) \text{ odd,} \\ \dfrac{(-1)^{\frac{m-n-1}{2}}}{2^r}\binom{r}{\frac{r-m+n}{2}} & \text{for } r \geqslant (m-n),\ (m-n) \text{ odd,} \end{cases}$$

and

$$\frac{1}{\pi}\int_0^{\pi} \sin^r\theta \sin(n-m)\theta \, d\theta$$

$$= \begin{cases} 0 & \text{for } (n-m) \text{ even,} \\ 0 & \text{for } r < (n-m),\ (n-m) \text{ odd,} \\ \dfrac{(-1)^{\frac{n-m-1}{2}}}{2^r}\binom{r}{\frac{r-n+m}{2}} & \text{for } r \geqslant (n-m),\ (n-m) \text{ odd.} \end{cases}$$

Thus, when r is an odd integer, equation (43) gives the Fourier expansion of $\sin^r\theta/(1+s\cos\theta)^r$ as a sine series, where the coefficients $B_{r,m}$ for all m are given by

$$\begin{aligned} B_{r,m} &= \sum_{n=0}^{\infty} a_{r,n} \frac{(-1)^{\frac{m+n-1}{2}}}{2^r}\binom{r}{\frac{r-m-n}{2}} && r \geqslant m+n \\ &= 0 && r < m+n \\ &+ \sum_{n=1}^{m-1} a_{r,n} \frac{(-1)^{\frac{m-n-1}{2}}}{2^r}\binom{r}{\frac{r-m+n}{2}} && r \geqslant m-n \\ &+ 0 && r < m-n \\ &- \sum_{n=m+1}^{\infty} a_{r,n} \frac{(-1)^{\frac{n-m-1}{2}}}{2^r}\binom{r}{\frac{r-n+m}{2}} && r \geqslant n-m \\ &- 0 && r < n-m \text{ ,} \end{aligned} \qquad \text{----------(44)}$$

where the $a_{r,n}$ for $n = 0$ are multiplied by $\frac{1}{2}$ to conform with equation (38).

This time r, m + n, and m - n are all odd integers, and the $a_{r,n}$ for all $n \geqslant 0$ are given by equation (40).

Using these expansions from (i) and (ii), the required Fourier series, using equation (37), is thus given by

$$\frac{\pm \sin\theta}{e(1+e\cos\theta)} = 1 + \tfrac{1}{2}\sum_{r=1}^{\infty} \frac{A_{2r,0}}{(2r)!} + \sum_{r=1}^{\infty}\sum_{m=1}^{\infty} \frac{A_{2r,m}}{(2r)!} \cos m\theta \pm \sum_{r=0}^{\infty}\sum_{m=1}^{\infty} \frac{B_{2r+1,m}}{(2r+1)!} \sin m\theta \,, \qquad (45)$$

where $A_{r,m}$ and $B_{r,m}$ are given by equations (42) and (44) respectively for all $m \geqslant 0$, with the $a_{r,n}$ in these expressions given by equation (40). To conform with equation (41), $A_{r,0}$ is multiplied by $\frac{1}{2}$. It should be remembered that the expansion given by equation (45) is only valid for $0 \leqslant e < 1$, since the integrals have discontinuities when $e = 1$. Although the general expression given by equation (45) appears rather complicated, the calculation is in fact comparatively easy. The convergence of each series is dependent on e, small e corresponding to rapid convergence. For completeness and reference, Table (2) illustrates the $a_{r,n}$, for several values of r, obtained from equation(40), remembering that a and e are related by equation (39).

r	$a_{r,n}$
1	$2\ \frac{a^n(1+a^2)}{(1-a^2)}$
2	$2\ \frac{a^n(1+a^2)^2}{(1-a^2)^2}\left[\left(\frac{1+a^2}{1-a^2}\right)+n\right]$
3	$2\ \frac{a^{n+4}(1+a^2)^3}{(1-a^2)^5}\left[6/a^2+\left(\frac{1-a^2}{a^2}\right)^2+\frac{3n}{2}\left(\frac{1-a^4}{a^2}\right)+\frac{n^2}{2}\left(\frac{1-a^2}{a^2}\right)^2\right]$
4	$2\ \frac{a^{n+6}(1+a^2)^4}{(1-a^2)^7}\left[(1+15/a^2+9/a^4+1/a^6)+n/6\,(49+11/a^2)\left(\frac{1-a^2}{a^2}\right)^2+n^2\left(\frac{1-a^2}{a^2}\right)^2\left(\frac{1+a^2}{a^2}\right)+\frac{n^3}{6}\left(\frac{1-a^2}{a^2}\right)^3\right]$

Table (2)

General expressions for $B_{r,m}$ and $A_{r,m}$ are shown in Tables (3) and (4) respectively, with $a_{r,n}$ from Table (2).

r	1	3
$B_{r,1}$	$\frac{1}{8}(2a_{1,0}-a_{1,2})$	$1/8\ (6a_{3,0}-4a_{3,2}+a_{3,4})$
$B_{r,2}$	$\frac{1}{8}(a_{1,1}-a_{1,3})$	$1/8\ (2a_{3,1}-3a_{3,3}+a_{3,5})$
$B_{r,3}$	$\frac{1}{8}(a_{1,2}-a_{1,4})$	$-1/8(2a_{3,0}-3a_{3,2}+3a_{3,4}-a_{3,6})$
$B_{r,m}$	$\frac{1}{8}(a_{1,m-1}-a_{1,m+1})$ $m \geqslant 2$	$-1/8(a_{3,m-3}-3a_{3,m-1}+3a_{3,m+1}-a_{3,m+3})$ $m \geqslant 4$

Table (3)

r	2	4
$A_{r,0}$	$\frac{1}{4}(2a_{2,0} - a_{2,2})$	$\frac{1}{16}(6a_{4,0} - 4a_{4,2} + a_{4,4})$
$A_{r,1}$	$\frac{1}{4}(a_{2,1} - a_{2,3})$	$\frac{1}{16}(2a_{4,1} - 3a_{4,3} + a_{4,5})$
$A_{r,2}$	$-\frac{1}{4}(2a_{2,0} - 2a_{2,2} + a_{2,4})$	$-\frac{1}{16}(8a_{4,0} - 7a_{4,2} + 4a_{4,4} - a_{4,6})$
$A_{r,3}$	$-\frac{1}{4}(a_{2,1} - 2a_{2,3} + a_{2,5})$	$-\frac{1}{16}(3a_{4,1} - 6a_{4,3} + 4a_{4,5} - a_{4,7})$
$A_{r,4}$	$-\frac{1}{4}(a_{2,2} - 2a_{2,4} + a_{2,6})$	$\frac{1}{16}(2a_{4,0} - 4a_{4,2} + 6a_{4,4} - 4a_{4,6} + a_{4,8})$
$A_{r,m}$	$-\frac{1}{4}(a_{2,m-2} - 2a_{2,m} + a_{2,m+2})$ $m \geqslant 3$	$\frac{1}{16}(a_{4,m-4} - 4a_{4,m-2} + 6a_{4,m} - 4a_{4,m+2} + a_{4,m+4})$ $m \geqslant 5$

Table (4)

To give an illustration of the size of these quantities, Table (5) shows values for $a_{r,n}$, $A_{r,m}$ and $B_{r,m}$ for $\epsilon = 0.25$, which from equation (39) gives $a = -0.12$

r	$a_{r,0}$	$a_{r,1}$	$a_{r,2}$	$a_{r,3}$	$a_{r,4}$	$a_{r,5}$	$a_{r,6}$
1	1.0328	-.2623	.0333	-.0041	.0006	-.0001	~ 0
2	1.1018	-.5508	.1042	-.0172	.0032	-.0004	$<.0001$
3	1.2111	-.8807	.2197	-.0451	.0101	-.0008	.0001
4	1.3759	-1.2974	.3938	-.0983	.0216	-.0044	.0008

r	$A_{r,0}$	$A_{r,1}$	$A_{r,2}$	r	$B_{r,1}$	$B_{r,2}$
2	.5249	-.1334	-.4996	1	1.016	-.1291
4	.4189	-.144	-.521	3	0.80	-.2034

Table (5). ($\epsilon = 0.25$).

These values give the following approximation, with $m \ll 4$, to the exponential function when $\epsilon = 0.25$:

$$e^{\frac{\sin\theta}{1+0.25\cos\theta}} = 1.2799 - 0.0727\cos\theta - 0.2715\cos2\theta + 0.0732\cos3\theta - 0.0088\cos4\theta \ldots + 1.1494\sin\theta - 0.163\sin2\theta - 0.021\sin3\theta + \ldots .$$

As is seen from this example, the coefficients drop rapidly in value, which in this case ensures rapid convergence. The case $\epsilon = 0$, is, of course, a particular example of the general formula given by equation (45), and for comparison, the two series for $e^{\sin\theta}$ are shown, where the subscripts A and B denote the series obtained from the section on the circular cylinder, and equation (45) respectively,

$$e^{\sin\theta}_{A} = 1.266 - 0.2715\cos\theta + 0.00547\cos 4\theta \ldots + 1.1303\sin\theta - 0.04434\sin 3\theta + \ldots$$

and

$$e^{\sin\theta}_{B} = 1.2656 - 0.2709\cos 2\theta + 0.00521\cos 4\theta \ldots + 1.1300\sin\theta - 0.04427\sin 3\theta + \ldots .$$

For most practical purposes, the above expressions give the same result.

2. The Bessel Function $K_m\left(\frac{1}{1+\epsilon\cos\theta}\right)$ as a Cosine Series

The fact that $K_m\left(\frac{1}{1+\epsilon\cos\theta}\right)$ is a function of θ, prevents the direct equating of coefficients as in the case of the circular cylinder. However, since the argument of the function is itself an even function, θ only appearing in the form $\cos\theta$, $K_m\left(\frac{1}{1+\epsilon\cos\theta}\right)$ may be expressed as a cosine series. Thus, writing

$$K_m\left(\frac{1}{1+\epsilon\cos\theta}\right) = \lambda_{m,0} + \lambda_{m,1}\cos\theta + \ldots = \sum_{\nu=0}^{\infty}\lambda_{m,\nu}\cos\nu\theta \quad ,-------(46$$

the problem is to find values for the $\lambda_{m,\nu}$, which depend on ϵ and, of course,

on m. Now θ lies in the range $-\pi \leqslant \theta < \pi$, which thus gives the limits for the argument as $\frac{1}{1-\varepsilon}$ and $\frac{1}{1+\varepsilon}$. It should be mentioned at this stage, that for very small values of ε, say $\varepsilon < 0.1$, a reasonable approximation is given by $K_m(1)$, and the previous method is directly applicable for obtaining the constants in the stream function. This approximation, however, should only be used for small values of m, the discrepancy from the true value becoming larger with increasing m.

The more terms that are taken in the expression given by equation (46), the more accurate is the approximation to the true function. However, in view of the subsequent analysis, the smaller the number of terms taken the easier is the subsequent evaluation for the stream function. Since the argument lies in a restricted range, the possibility of obtaining a reasonable approximation by terminating the series at $\nu = 1$, and amending the theoretical values for $\lambda_{m,0}$ and $\lambda_{m,1}$ by trial and error, is considered.

Using the 'Treatise on Bessel Functions' by Gray and Mathews [44] the following expansion as a series of cosines is given for $K_m(R)$;

$$K_m(R) = \left(\frac{2R}{ab}\right)^m \prod(m-1) \sum_{p=0}^{\infty} (m+p) C_p^m(\cos\theta)\, K_{m+p}(b)\, I_{m+p}(a) \quad , \text{----------} (47)$$

where $R^2 = a^2 + b^2 - 2ab\cos\theta$, $m \neq 0$, $|a| < |b|$. $\prod$ is the product sign ar $C_p^m(\cos\theta)$ is defined by

$$C_p^m(\mu) = \frac{\prod(m+p-1)}{\prod(m-1)} \frac{(2\mu)^p}{p!} \left[1 - \frac{p(p-1)}{1!(m+p-1)} \frac{1}{(2\mu)^2} + \frac{p(p-1)(p-2)(p-3)}{2!(m+p-1)(m+p-2)} \frac{1}{(2\mu)^4} \cdots \right],$$

from which $C_0^m(\mu) = 1$ and $C_1^m(\mu) = 2m\mu$. The particular case $m = 0$, which is not covered by equation (47) is given by

$$K_o(R) = I_o(a)K_o(b) + 2\sum_{p=1}^{\infty} K_p(b)I_p(a)\cos p\theta \ , \qquad \text{----------(48)}$$

where again $|a| < |b|$. Comparing these formulae with the Bessel function in question, it is seen that

$$R^{-2} = \left(\frac{1}{1 + e\cos\theta}\right)^2 \doteq \tfrac{1}{2}a_{2,0} + a_{2,1}\cos\theta \ ,$$

to a first approximation from equation (38), where $a_{2,0}$ and $a_{2,1}$ are given by equation (40). This first approximation gives reasonably good results if $e \ll 0.5$, the smaller the value of e, the better the approximation. With this last relation, and remembering that $|a| < |b|$, comparison with R^{-2} in equation (4 gives

$$a^2 + b^2 = \tfrac{1}{2}a_{2,0} \quad \text{and} \quad 2ab = -a_{2,1} \ ,$$

which leads to

$$a = \tfrac{1}{2}\left[(\tfrac{1}{2}a_{2,0} - a_{2,1})^{\frac{1}{2}} - (\tfrac{1}{2}a_{2,0} + a_{2,1})^{\frac{1}{2}}\right] \ ,$$

and

$$b = \tfrac{1}{2}\left[(\tfrac{1}{2}a_{2,0} - a_{2,1})^{\frac{1}{2}} + (\tfrac{1}{2}a_{2,0} + a_{2,1})^{\frac{1}{2}}\right] \ . \qquad \text{---------(49)}$$

Now, a and b must necessarily be real, which gives a condition on $a_{2,0}$ and $a_{2,1}$ which in turn imposes a condition on e in the approximation for equation (46). From Table (2), noting that the a is not that given by equation (49), but by equation (39),

$$\tfrac{1}{2}a_{2,0} = \left(\frac{1 + a^2}{1 - a^2}\right)^3 \ , \text{ and } a_{2,1} = \frac{4a(1 + a^2)^2}{(1 - a^2)^3} \ .$$

Since a in these expressions is negative, the condition for a and b in equation (49) to be real is thus

$$\left|\left(\frac{1 + a^2}{1 - a^2}\right)^3\right| > \left|\frac{4a(1 + a^2)^2}{(1 - a^2)^3}\right| \ ,$$

which reduces to

$$1 + |a|^2 - 4|a| > 0 ,$$

that is

$$(|a| - 2 - \sqrt{3})(|a| - 2 + \sqrt{3}) > 0.$$

Now, since $|a| < 1$ from equation (37) and tends to 1 as ε tends to 1, this last inequality gives $|a| < 2 - \sqrt{3}$, and since a in equation (37) is negative, this reduces to the condition that

$$a > \sqrt{3} - 2 = a_{\varepsilon = 0.5} .$$

The convergence of the series given by equation (47), is dependent on $|a|$ being less than $|b|$, and although, over the range taken by the argument, the limiting case of $\varepsilon = 0.5$ could be considered, the approximation involving only $\lambda_{m,0}$ and $\lambda_{m,1}$ would have to be amended considerably. Actually, approximations over the restricted range $0.5 < \varepsilon < 1$ can be obtained using equation (47) where the amended $\lambda_{m,0}$ and $\lambda_{m,1}$ with suitable changes in a and b form the basis for a trial and error method. Now, in equation (47) R appears in the form R^m, and so further use must be made of equation (38), and in particular, if $m = 1$,

$$R = \frac{1}{1 + \varepsilon \cos\theta} = \tfrac{1}{2}a_{1,0} + a_{1,1} \cos\theta .$$

Substituting the required quantities in equation (47), multiplying out and collecting terms, approximate expressions for $\lambda_{m,\nu}$ are obtained for the particular cases $m = 0, 1$ and 2 and $\nu = 0$ and 1. These values for $\lambda_{m,\nu}$ are shown in Table (6) where a and b are given by equations (49), and the $a_{r,n}$ by equation (40). Terms for $\nu > 1$ are similarly obtained from equations (45) and (49).

m	$\lambda_{m,0}$
0	$I_0(a)K_0(b)$
1	$\frac{2}{ab}\left[a_{1,0}\, I_1(a)K_1(b) + 2a_{1,1}\, I_2(a)K_2(b)\right]$
2	$\left(\frac{2}{ab}\right)^2\left[2a_{2,0}\, I_2(a)K_2(b) + 6a_{2,1}\, I_3(a)K_3(b)\right]$
m	$\lambda_{m,1}$
0	$2I_1(a)K_1(b)$
1	$\frac{2}{ab}\left[a_{1,1}\, I_1(a)K_1(b) + 4a_{1,0}\, I_2(a)K_2(b)\right]$
2	$\left(\frac{2}{ab}\right)^2\left[12a_{2,0}\, I_3(a)K_3(b) + 2a_{2,1} I_2(a)K_2(b)\right]$

Table (6)

As an illustration of the order of magnitude of these coefficients and of the difference between the theoretical values of $\lambda_{m,0}$ and $\lambda_{m,1}$ and the values actually used to give a good approximation when only two terms in the series are retained, the cases m = 0, 1 and 2 are considered. In the numerical example, $\epsilon = 0.25$ as before, and thus

$$K_m\left(\frac{1}{1 + 0.25\cos\theta}\right) = \lambda_{m,0} + \lambda_{m,1}\cos\theta .$$

Table (7) shows $\lambda_{m,0}$ and $\lambda_{m,1}$ for m = 0, 1, and 2, where the first figures are the theoretical values using Table (6), and the second figures are the values obtained by trial and error amendment (where necessary) of the theoretical figures to give a better approximation over the range $0 \leqslant \theta \leqslant 2\pi$.

It should be noted, that the special case $\epsilon = 0$ reduces, of course, to the required condition $\lambda_{m,0} = K_m(1)$ and $\lambda_{m,\nu} = 0$ for $\nu > 0$.

m	$\lambda_{m,0}$	$\lambda_{m,1}$
0	.4227 / .4227	.1603 / .1603
1	.5665 / .5978	.1174 / .2424
2	.7701 / 1.7101	.7004 / .8954

Table (7)

Figures (7), (8) and (9) illustrate the graphs of $K_m\left(\frac{1}{1+.25\cos\theta}\right)$ against θ for m = 0, 1 and 2 respectively. In each figure the exact curve is drawn from $K_m\left(\frac{1}{1+.25\cos\theta}\right)$, for comparison with the theoretical curve using the value obtained from Table (6), and with the final approximation obtained by trial and error alteration of the theoretical values, (second figures). As is seen from the graphs, the theoretical values give a good approximation for m = 0, the departure from the exact curve becoming greater as m increases. Also, the smaller the value of ϵ, the better is the initial theoretical approximation for each m. It should be noted, that $K_m\left(\frac{1}{1+\epsilon\cos\theta}\right)$ and its approximation are of period 2π, for all $1 > \epsilon > 0$.

To summarise, $K_m\left(\frac{1}{1+\epsilon\cos\theta}\right)$ can be obtained as a cosine series of the form given by equation (46), where the $\lambda_{m,\nu}$ are obtained from equation (47) and (48) with the condition that $\epsilon < 0.5$. When the series is terminated at $\nu = 1$, the theoretical values of $\lambda_{m,0}$ and $\lambda_{m,1}$ must be amended by trial and error. The accuracy of the initial approximation depends on ϵ, the smaller the value of ϵ, the better the initial approximation. The condition $\epsilon < 0.5$ is not

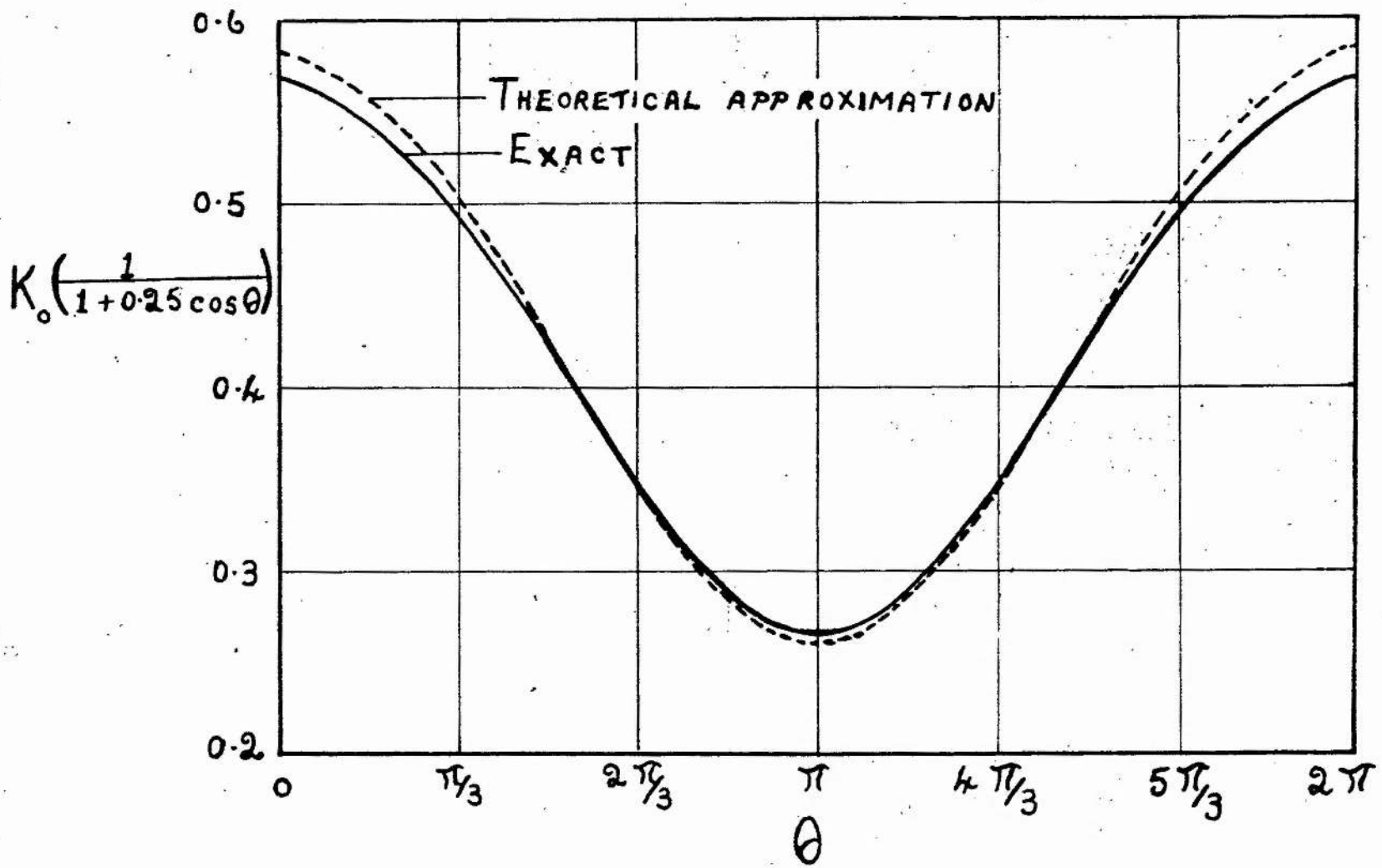

Figure (7) Illustration of the approximation to $K_o\left(\frac{1}{1+\varepsilon\cos\theta}\right)$ by a series replacement. ($\varepsilon = 0.25$).

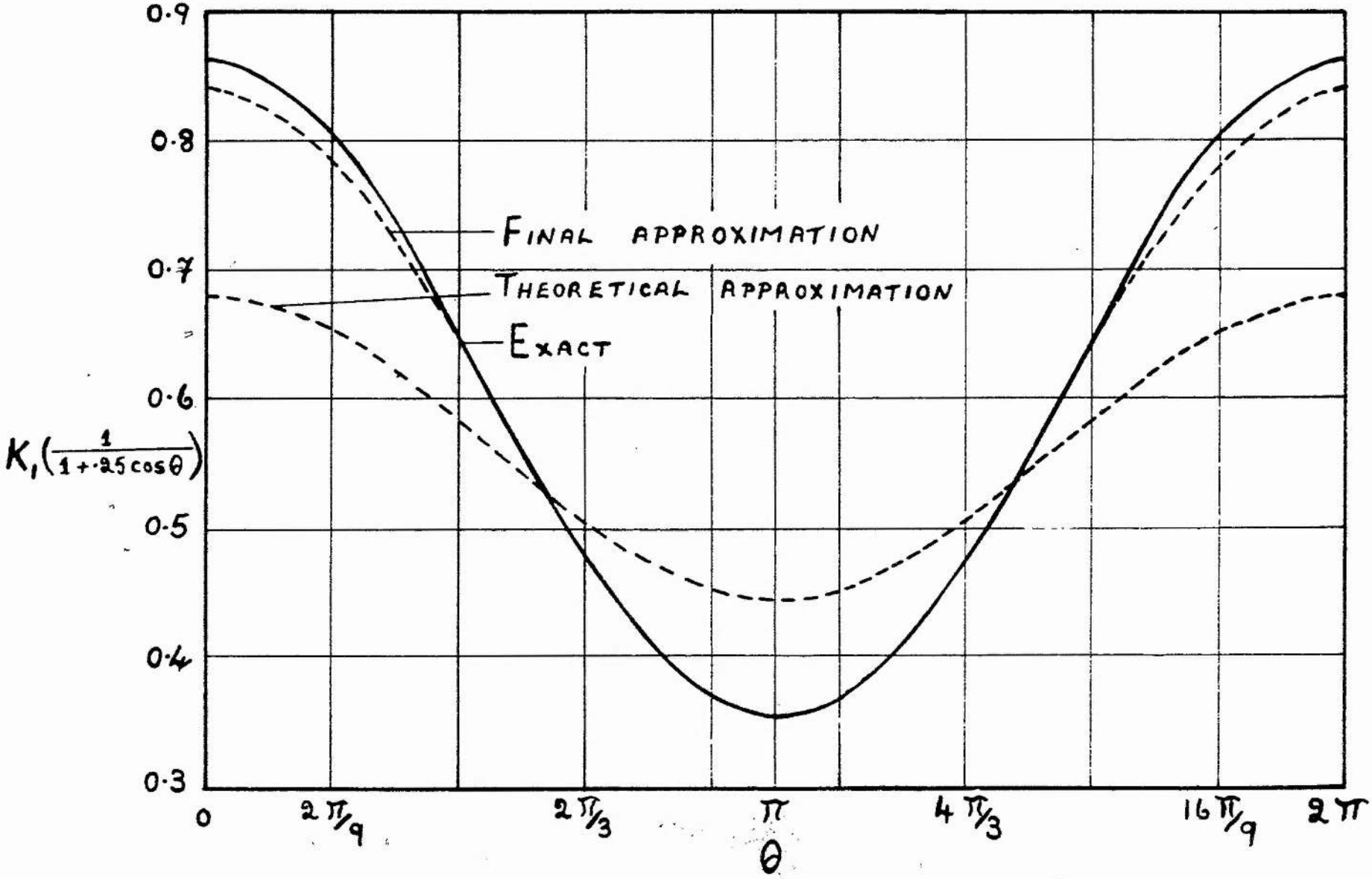

Figure (8) Illustration of the approximation to $K_1\left(\frac{1}{1+\varepsilon\cos\theta}\right)$ by a series replacement. ($\varepsilon = 0.25$).

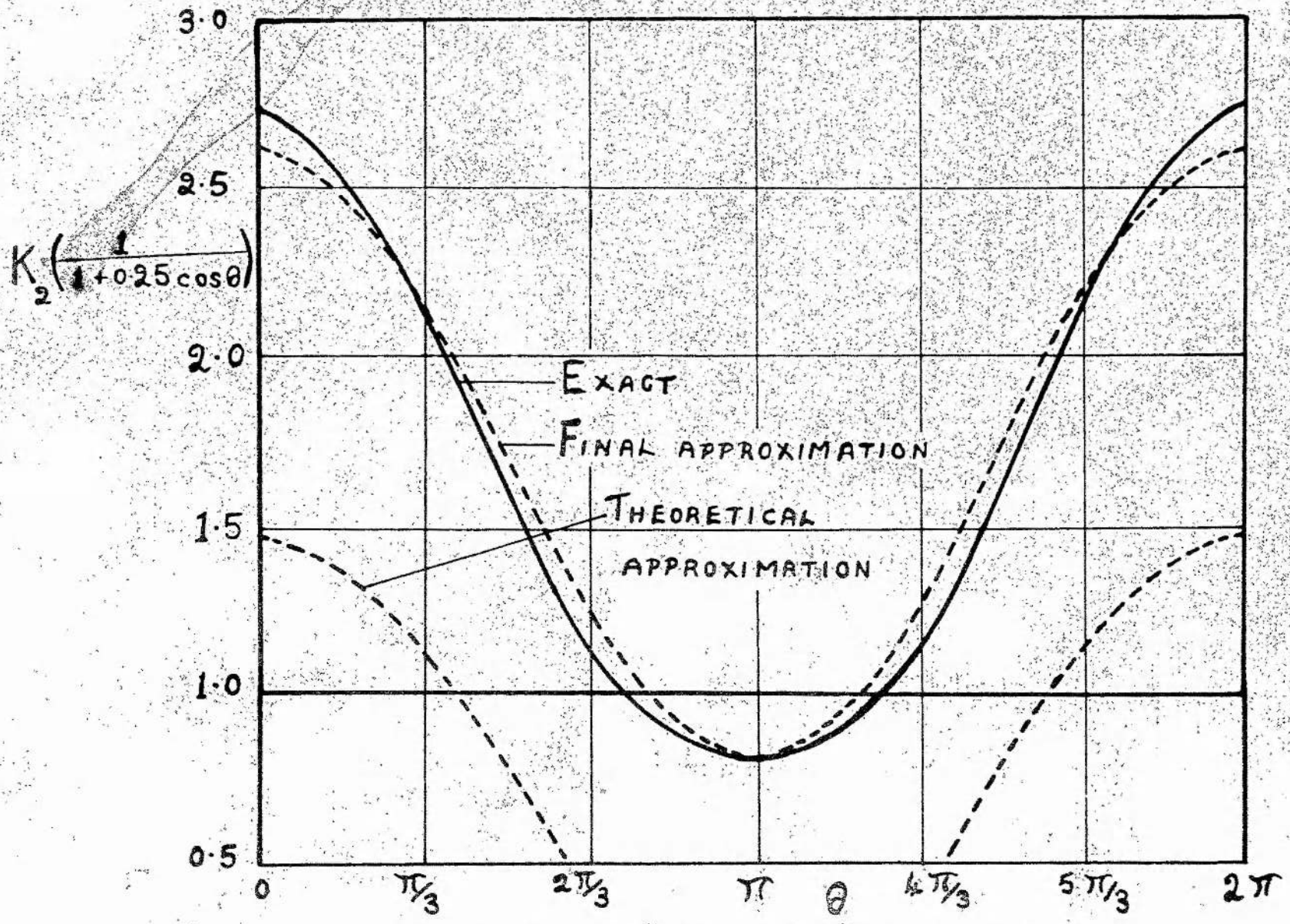

Figure (9) Illustration of the approximation to $K_2\left(\frac{1}{1+\varepsilon\cos\theta}\right)$

absolutely necessary, since approximations can easily be obtained by trial and error for values of e lying in the range $1 > e \geq 0.5$. If further terms $\lambda_{m,\nu}(\nu > 1)$ are included in the approximation to $K_m\left(\frac{1}{1 + e\cos\theta}\right)$, a more accurate representation is obtained, with a proportional increase in labour. It is sufficient, however, for the purposes of illustrating the method, to assume that the series given by equation (46) terminates at $\nu = 1$, and so

$$K_m\left(\frac{1}{1 + e\cos\theta}\right) \doteq \lambda_{m,0} + \lambda_{m,1}\cos\theta \quad \text{----------(50)}$$

where the $\lambda_{m,0}$ and $\lambda_{m,1}$ are the values which give the best approximation to the function for a given e. The case $e = 0$ is merely a particular example with $\lambda_{m,\nu} = 0$ for $\nu \geq 1$.

To return to the evaluation of the constants a_m and b_m in equation (36), making use of the expressions given by equations (45) and (50), equation (36) becomes

$$\begin{aligned} c = (a + b) &+ \frac{(a + b)}{2}\sum_{r=1}^{\infty}\frac{A_{2r,0}}{(2r)!} \\ &+ (a + b)\sum_{r=1}^{\infty}\sum_{m=1}^{\infty}\frac{A_{2r,m}}{(2r)!}\cos m\theta \\ &+ (a - b)\sum_{r=0}^{\infty}\sum_{m=1}^{\infty}\frac{B_{2r+1,m}}{(2r+1)!}\sin m\theta \\ &+ \sum_{k=0}^{\infty}(a_k\cos k\theta + b_k\sin k\theta)(\lambda_{k,0} + \lambda_{k,1}\cos\theta), \quad \text{------(51)} \end{aligned}$$

where the final summation is now taken over k, to avoid confusion with the three other summations which are taken over r and m. For convenience, the notation X_m and Y_m is now introduced by writing equation (51) in the form

$$\begin{aligned} c = &\sum_{m=0}^{\infty}X_m\cos m\theta + \sum_{m=1}^{\infty}Y_m\sin m\theta \\ &+ \sum_{k=0}^{\infty}(a_k\cos m\theta + b_k\sin m\theta)(\lambda_{k,0} + \lambda_{k,1}\cos\theta), \quad \text{-----(5} \end{aligned}$$

which gives

$$X_0 = (a + b) + \frac{(a + b)}{2}\sum_{r=1}^{\infty} \frac{A_{2r,0}}{(2r)!} \quad , X_m = (a + b)\sum_{r=1}^{\infty} \frac{A_{2r,m}}{(2r)!} \quad , (m > 0) ,$$

and

$$Y_m = (a - b) \sum_{r=0}^{\infty} \frac{B_{2r+1,m}}{(2r+1)!} \quad .$$

Equating the coefficients of cos mθ and sin mθ a set of equations is obtained whose solution gives expressions for a_k and b_k. However, in this case, equating the coefficients does not give direct values for a_k and b_k, but yields a set of equations, which must be solved, to give the required values. Thus, equating the coefficients of cos mθ, the following equations are obtained, the left hand sides being the coefficients of cos mθ from the k-series:

$$\begin{aligned}
\lambda_{0,0}\, a_0 + \tfrac{1}{2}\lambda_{1,1}\, a_1 &= c - X_0 \\
\lambda_{0,1}\, a_0 + \lambda_{1,0}\, a_1 + \tfrac{1}{2}\lambda_{2,1}\, a_2 &= -X_1 \\
\tfrac{1}{2}\lambda_{1,1}\, a_1 + \lambda_{2,0}\, a_2 + \tfrac{1}{2}\lambda_{3,1}\, a_3 &= -X_2 \\
\tfrac{1}{2}\lambda_{2,1}\, a_2 + \lambda_{3,0}\, a_3 + \tfrac{1}{2}\lambda_{4,1}\, a_4 &= -X_3 \\
\text{-------------------------} &= \text{--------} \\
\tfrac{1}{2}\lambda_{m-1,1}\, a_{m-1} + \lambda_{m,0}\, a_m + \tfrac{1}{2}\lambda_{m+1,1}\, a_{m+1} &= -X_m \qquad (m \geqslant 2) \\
\text{-------------------------} &= \text{--------} \quad . \text{------(5}
\end{aligned}$$

Assuming, for the purposes of the following discussion, that c is known, (it is in fact subsequently given by equation (60)), it is seen that the system of equations (53), if terminated at a given value of m, contains (m + 1) unknowns although there are only m equations. Thus, unless the number of equations is infinite there is not a unique solution to the set of equations (53). Ther are at least two methods of approach which give solutions and these are now discussed separately as follows:

(1) The Least Squares Method. From a practical point of view, the X_m-series terminates at a given value of m, say s, and it is assumed that $X_{m>s} \doteq 0$. It is also feasible to assume that the a_k drop rapidly in value since the k-series must, of course, converge. The question arises as to the point at which to terminate the k-series. If the two terminated series have to be equal for all θ, then with the X_m-series terminated at m = s, the k-series must be terminated at k = s - 1, which implies that $a_{k>s-1} \doteq 0$, since k = s gives a term in $\cos(s+1)\theta$. With this method of comparison of the two series a system of (s + 1) linear equations in s unknowns is obtained, and the method of least squares can be used to get a solution. Assuming the set of (s + 1) equations to be exact, and all of equal weight, a solution approximating to all the (s + 1) equations is given as follows:

If the matrices

$$X = \begin{bmatrix} c - X_0 \\ -X_1 \\ -X_2 \\ \vdots \\ -X_s \end{bmatrix}, \qquad A = \begin{bmatrix} a_0 \\ a_1 \\ a_2 \\ \vdots \\ a_{s-1} \end{bmatrix},$$

and $\Lambda \equiv$ the (s + 1) X s matrix of the coefficients of $a_0, a_1 \ldots\ldots a_{s-1}$, then the system of equations may be written in the form

$$\Lambda A = X ,$$

noting that Λ is not a square matrix. The least squares solution is given directly by

$$A = (\Lambda'\Lambda)^{-1}\Lambda' X ,$$

where a dash denotes the transpose of a matrix and -1 denotes the inverse.

<u>(ii) The Iterative Method.</u> In actual fact, the equations are not all of equal weight and accuracy, and an iterative process is perhaps more appropriate. The method is to terminate the X_m-series as before and from equations (53) express $a_{r>0}$ in terms of a_0, the known X's, and e. Finally, values are assigned to a_0 which make the two terminated series correspond exactly for several values of θ between 0 and 2π. Thus, from equations (53),

$$a_1 = \frac{2}{\lambda_{1,1}}\left[e - X_0 - \lambda_{0,0}\, a_0\right],$$

$$a_2 = \frac{2}{\lambda_{2,1}}\left[-X_1 - \lambda_{0,1}\, a_0 - \frac{2\lambda_{1,0}}{\lambda_{1,1}}\left(e - X_0 - \lambda_{0,0}\, a_0\right)\right],$$

$$- ,$$

are substituted in the k-series, a_0 chosen to make the two series equal for $\theta = \theta_0, \theta_1, \ldots$ and the a_0 averaged over the above values of θ. Thus $a_1, a_2, \ldots$ are obtained as the best values for these values of θ. In practice, the values of θ are chosen to give equally placed points round the perimeter of the ellipse as shown in Figure (d).

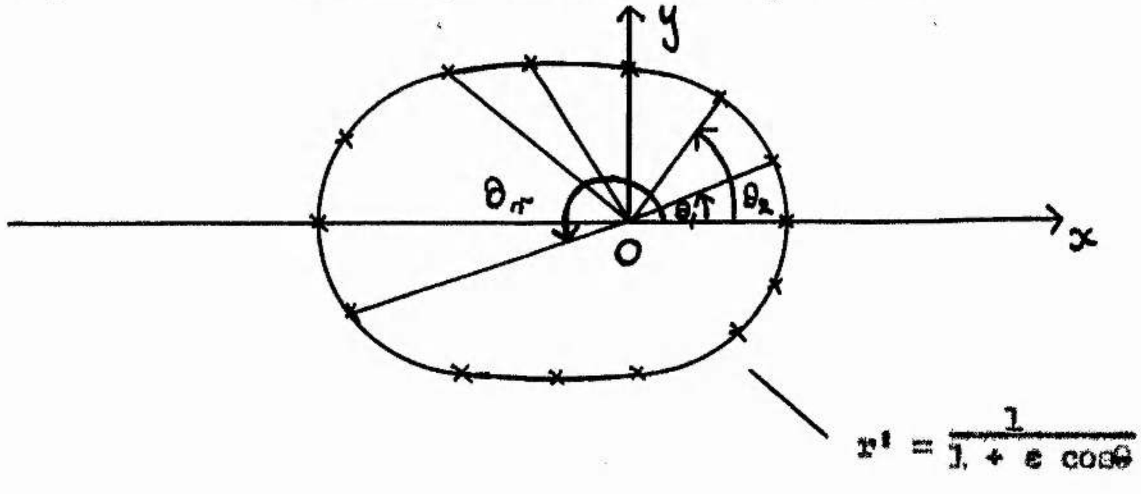

Figure (d)

As an illustration of the method, when the X_m-series is terminated at m = 3, and thus the k-series at k = 2, the two series equated are

$$(e - X_0) - X_1\cos\theta - X_2\cos 2\theta - X_3\cos 3\theta ,$$

and

$$a_0(\lambda_{0,0} + \lambda_{0,1}\cos\theta) + \frac{2}{\lambda_{1,1}}(c - X_0 - \lambda_{0,0}a_0)(\lambda_{1,0} + \lambda_{1,1}\cos\theta)\cos\theta$$
$$+ \frac{2}{\lambda_{2,1}}\left[-X_1 - \lambda_{0,1}a_0 - \frac{2\lambda_{1,0}}{\lambda_{1,1}}(c - X_0 - \lambda_{0,0}a_0)\right](\lambda_{2,0} + \lambda_{2,1}\cos\theta)\cos 2\theta \; .$$

Thus, when c is known, method (ii) gives a better practical method for obtainin the constants a_k.

In a similar manner, equating the coefficients in the Y_m-series and the k-series and using this iterative process, the b_k are obtained. These can be evaluated immediately, since c does not appear in the set of equations, which for completeness, is given as follows:

$$\begin{aligned}
&\lambda_{1,0}\,b_1 + \tfrac{1}{2}\lambda_{2,1}\,b_2 &&= -Y_1\\
&\tfrac{1}{2}\lambda_{1,1}\,b_1 + \lambda_{2,0}\,b_2 + \tfrac{1}{2}\lambda_{3,1}\,b_3 &&= -Y_2\\
&\qquad\tfrac{1}{2}\lambda_{2,1}\,b_2 + \lambda_{3,0}\,b_3 + \tfrac{1}{2}\lambda_{4,1}\,b_4 &&= -Y_3\\
&- - - - - - - - - - - - - - - - &&= - - -\\
&\tfrac{1}{2}\lambda_{m-1,1}\,b_{m-1} + \lambda_{m,0}\,b_m + \tfrac{1}{2}\lambda_{m+1,1}\,b_{m+1} &&= -Y_m\\
&- - - - - - - - - - - - - - - - &&= - - - \qquad (54)
\end{aligned}$$

Once again, values are given to b_1 at the various values of θ, as shown in Figure (d).

Thus, except for the value of c, which can be found, the constants a_k and b_k can be calculated from the data given by equation (36) with the appropriate series replacements. It should be noted at this stage, that further terms in equation (46) can be included, making the method more accurate, but, of course, more complicated.

Assuming then, that the a_k and b_k are evaluated by one of the

previous methods, the stream function from equation (20) is

$$\psi = ae^{r' \sin\theta} + be^{-r' \sin\theta} + \sum_{k=0}^{\infty} (a_k \cos k\theta + b_k \sin k\theta) K_k(r') ,$$

where c is given subsequently by equation (60). The components of velocity are given by

$$q_r = \frac{1}{pr'} \frac{\partial \psi}{\partial \theta} , \quad \text{and} \quad q_\theta = -\frac{1}{p} \frac{\partial \psi}{\partial r'} ,$$

and the velocity at any point, by

$$q^2 = q_r^2 + q_\theta^2 .$$

As in the case of the circular cylinder, the evaluation of c is obtained from the calculation of the circulation and use of equation (22). However, unlike the circular cylinder, the velocity on the elliptic cylinder is not q_θ but must be obtained by considering $q_\perp$ and $q_\parallel$, the velocities perpendicular and parallel to the boundary of the elliptic cylinder as illustrated in Figure (e).

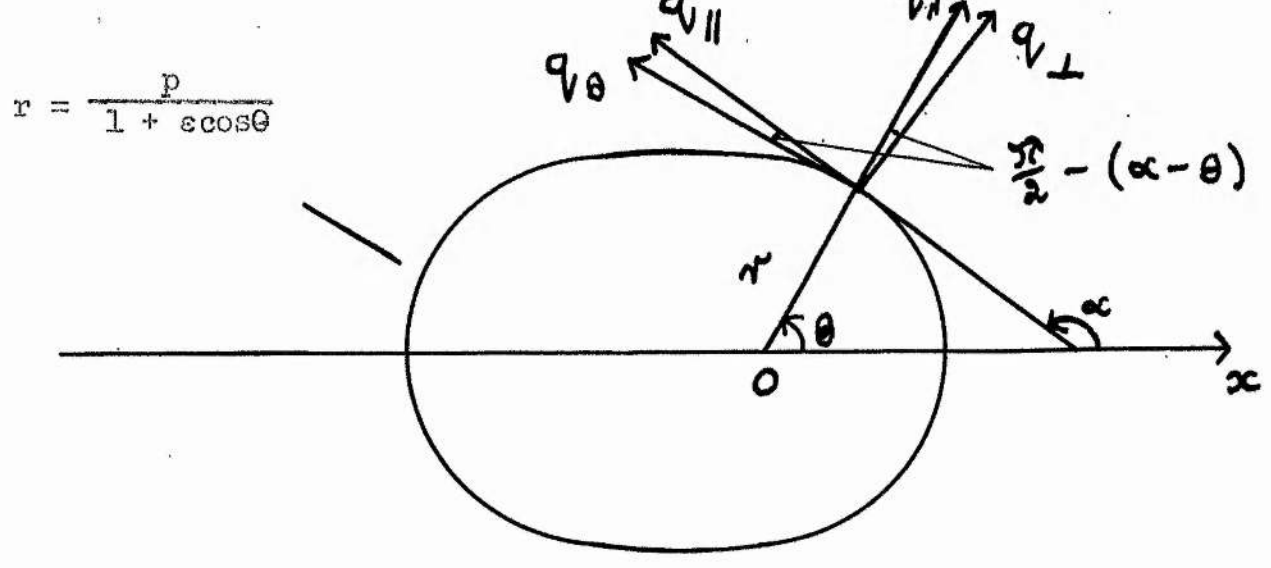

Figure (e)

The ellipse in cartesian coordinates is given by

$$x^2(1 - \varepsilon^2) + y^2 + 2\varepsilon p x - p^2 = 0,$$

from which

$$\frac{dy}{dx} = \tan\alpha = -\left[\frac{x(1 - \varepsilon^2) + \varepsilon p}{y}\right],$$

$$= -\left(\frac{\cos\theta + \varepsilon}{\sin\theta}\right),$$

giving, with α as shown in Figure (c),

$$\sin\alpha = \frac{\cos\theta + \varepsilon}{(1 + \varepsilon^2 + 2\varepsilon\cos\theta)^{\frac{1}{2}}}, \text{ and } \cos\alpha = -\frac{\sin\theta}{(1 + \varepsilon^2 + 2\varepsilon\cos\theta)^{\frac{1}{2}}}.$$

Resolving the velocity components perpendicular and parallel to the tangent at the point,

$$q_\perp = \left[q_r \sin(\alpha - \theta) - q_\theta \cos(\alpha - \theta)\right]_{r' = \frac{1}{1+\varepsilon\cos\theta}},$$

and

$$q_{\parallel} = \left[q_r \cos(\alpha - \theta) + q_\theta \sin(\alpha - \theta)\right]_{r' = \frac{1}{1+\varepsilon\cos\theta}},$$

which, on substitution of the above expressions for $\sin\alpha$ and $\cos\alpha$, become

$$q_\perp = \frac{1}{(1+\varepsilon^2+2\varepsilon\cos\theta)^{\frac{1}{2}}}\left[q_r (1+\varepsilon\cos\theta) - \varepsilon\sin\theta\, q_\theta\right]_{r' = \frac{1}{1+\varepsilon\cos\theta}},$$

and

$$q_{\parallel} = \frac{1}{(1+\varepsilon^2+2\varepsilon\cos\theta)^{\frac{1}{2}}}\left[q_r \varepsilon\sin\theta + (1+\varepsilon\cos\theta) q_\theta\right]_{r' = \frac{1}{1+\varepsilon\cos\theta}} \quad \text{-----(}$$

It is now shown that $q_\perp = 0$, as is necessary from physical considerations.

$$(1+\varepsilon^2+2\varepsilon\cos\theta)^{\frac{1}{2}} q_\perp = (1+\varepsilon\cos\theta)\left[\frac{1}{pr'}\frac{\partial\psi}{\partial\theta}\right]_{r' = \frac{1}{1+\varepsilon\cos\theta}}$$

$$+ \varepsilon\sin\theta\left[\frac{1}{p}\frac{\partial\psi}{\partial r'}\right]_{r' = \frac{1}{1+\varepsilon\cos\theta}}$$

$$= \frac{(1+\varepsilon\cos\theta)}{p}\left[a\cos\theta\, e^{\frac{\sin\theta}{1+\varepsilon\cos\theta}} - b\cos\theta\, e^{-\frac{\sin\theta}{1+\varepsilon\cos\theta}}\right.$$

$$\left. + (1+\varepsilon\cos\theta)\sum_{k=0}^{\infty}(-ka_k\sin k\theta + kb_k\cos k\theta)K_k\left(\frac{1}{1+\varepsilon\cos\theta}\right)\right] +$$

$$\frac{\varepsilon\sin\theta}{p}\left[a\sin\theta\, e^{\frac{\sin\theta}{1+\varepsilon\cos\theta}} - b\sin\theta\, e^{-\frac{\sin\theta}{1+\varepsilon\cos\theta}}\right.$$

$$\left. + \sum_{k=0}^{\infty}(a_k\cos k\theta + b_k\sin k\theta)\left\{\frac{d}{dr'}K_k(r')\right\}_{r'=\frac{1}{1+\varepsilon\cos\theta}}\right]$$

$$= \frac{(1+\varepsilon\cos\theta)^2}{p}\left[\frac{a(\cos\theta+\varepsilon)}{(1+\varepsilon\cos\theta)^2}\, e^{\frac{\sin\theta}{1+\varepsilon\cos\theta}} - \frac{b(\cos\theta+\varepsilon)}{(1+\varepsilon\cos\theta)^2}\, e^{-\frac{\sin\theta}{(1+\varepsilon\cos\theta)}}\right.$$

$$+ \sum_{k=0}^{\infty}K_k\left(\frac{1}{1+\varepsilon\cos\theta}\right)\frac{d}{d\theta}(a_k\cos k\theta + b_k\sin k\theta)$$

$$\left. + \frac{\varepsilon\sin\theta}{(1+\varepsilon\cos\theta)^2}\sum_{k=0}^{\infty}(a_k\cos k\theta + b_k\sin k\theta)\left\{\frac{d}{dr'}K_k(r')\right\}_{r'=\frac{1}{1+\varepsilon\cos\theta}}\right]$$

$$= \frac{(1+\varepsilon\cos\theta)^2}{p}\frac{d}{d\theta}\left[a\, e^{\frac{\sin\theta}{1+\varepsilon\cos\theta}} + b\, e^{-\frac{\sin\theta}{1+\varepsilon\cos\theta}}\right.$$

$$\left. + \sum_{k=0}^{\infty}(a_k\cos k\theta + b_k\sin k\theta)K_k\left(\frac{1}{1+\varepsilon\cos\theta}\right)\right]$$

$$= \frac{(1+\varepsilon\cos\theta)^2}{p}\frac{d}{d\theta}\left[c\right] = 0,$$

from equation (36), and where

$$\frac{d}{dr'}K_k(r') = -\frac{k}{r'}K_k(r') - K_{k-1}(r').$$

Thus, if $\varepsilon < 1$, $q_\perp = 0$.

Equation (55) defines $q_{\parallel}$, which gives the velocity onthe cylinder, and in particular, stagnation points as solutions of $q_{\parallel} = 0$. Also, the circulati round the perimeter of the ellipse is given by

$$\Gamma = \Gamma_0 + \Gamma_1 = \oint_L q_{\parallel}\, d\ell \quad , \text{----------(56)}$$

where L is the perimeter of the ellipse $r = \frac{p}{1+\epsilon\cos\theta}$, and $(d\ell)^2 = (dr)^2+(rd\theta$

From equation (55), $q_{\parallel}$ is given by

$$q_{\parallel} = \frac{1}{p(1+\epsilon^2+2\epsilon\cos\theta)^{\frac{1}{2}}} \Bigg[-a\sin\theta\, e^{\frac{\epsilon\sin\theta}{1+\epsilon\cos\theta}} + b\sin\theta\, e^{-\frac{\epsilon\sin\theta}{1+\epsilon\cos\theta}}$$

$$+ \epsilon\sin\theta\,(1+\epsilon\cos\theta)\sum_{k=0}^{\infty}(-ka_k\sin k\theta + kb_k\cos k\theta)(\lambda_{k,0} + \lambda_{k,1}\cos\theta)$$

$$+ (1+\epsilon\cos\theta)\sum_{k=0}^{\infty}(a_k\cos k\theta + b_k\sin k\theta)\Big\{k(1+\epsilon\cos\theta)(\lambda_{k,0} + \lambda_{k,1}\cos\theta)$$

$$+(\lambda_{k-1,0} + \lambda_{k-1,1}\cos\theta)\Big\}\Bigg] \quad ,\text{----(}$$

where the approximation to $K_k\left(\frac{1}{1+\epsilon\cos\theta}\right)$ given by equation (50) is taken, since the velocity is that on the cylinder, and the a_k and b_k are chosen to satisfy equation (52) with these approximations. From the form of equation (57) it is easily seen that the first two terms give the circulation Γ_0, the remainder giving the contribution Γ_1 to the circulation Γ. Now, since $q_{\parallel}$ is a function of θ, $(d\ell)^2$ must be written in the form

$$(d\ell)^2 = (dr)^2 + r^2(d\theta)^2$$

$$= \frac{p^2\epsilon^2\sin^2\theta}{(1+\epsilon\cos\theta)^4}\,(d\theta)^2 + \frac{p^2}{(1+\epsilon\cos\theta)^2}\,(d\theta)^2 \quad ,$$

which gives

$$d\ell = \frac{p(1+\epsilon^2+2\epsilon\cos\theta)^{\frac{1}{2}}}{(1+\epsilon\cos\theta)}\,d\theta \quad .$$

On substitution in equation (56) of the required part of $q_{\parallel}$ as given by equation (57), and the value of $d\ell$ as given by the last equation, Γ_1 becomes

$$\Gamma_1 = \int_{-\pi}^{\pi}\Bigg[\epsilon\sin\theta\sum_{k=0}^{\infty}(-ka_k\sin k\theta + kb_k\cos k\theta)(\lambda_{k,0} + \lambda_{k,1}\cos\theta) +$$

$$+ \sum_{k=0}^{\infty} \{a_k \cos k\theta + b_k \sin k\theta) \left\{ k(1+\varepsilon \cos\theta)(\lambda_{k,0} + \lambda_{k,1} \cos\theta) + (\lambda_{k-1,0} + \lambda_{k-1,1} \cos\theta) \right\} \Bigg] d\theta \quad . \text{----------(58)}$$

Now

$$\int_{-\pi}^{\pi} \sin r\theta \cos s\theta \, d\theta = 0, \text{ for all } r \text{ and } s, \text{ and}$$

$$\int_{-\pi}^{\pi} \begin{Bmatrix} \cos \\ \sin \end{Bmatrix} r\theta \quad \begin{Bmatrix} \cos \\ \sin \end{Bmatrix} s\theta \, d\theta = \begin{cases} 0 \text{ for } r \neq s, \\ \pi \text{ for } r = s, \end{cases}$$

from which it is easily seen that all terms in equation (58) involving b_k are zero, and from the latter integral the only non-zero a_k- terms are those involving a_1 and a_2. Thus, integrating equation (58), Γ_1 may be written as

$$\Gamma_1 = -\varepsilon\pi (\lambda_{1,0} a_1 + \lambda_{2,1} a_2) + \pi \left[2\lambda_{1,0} a_0 + a_1(\lambda_{0,1} + \varepsilon\lambda_{1,0} + \lambda_{1,1}) + \varepsilon\lambda_{2,1} a_2 \right],$$

which leads to

$$\Gamma_1 = \pi \left[2\lambda_{1,0} a_0 + (\lambda_{0,1} + \lambda_{1,1}) a_1 \right] \quad . \text{----------(59)}$$

Now, to return to the iterative method (ii) for obtaining the a_k, a_1 is obtained in terms of c and a_0 and on substitution in equation (59), Γ_1 becomes

$$\Gamma_1 = \pi \left[2\lambda_{1,0} a_0 + \frac{2(\lambda_{0,1} + \lambda_{1,1})}{\lambda_{1,1}} (c - X_0 - \lambda_{0,0} a_0) \right].$$

Equation (22), which states that $\Gamma_1 = 0$, yields a relation between c and a_0, which from the last expression for Γ_1 becomes

$$c = X_0 + \left[\lambda_{0,0} - \frac{\lambda_{1,0} \lambda_{1,1}}{(\lambda_{0,1} + \lambda_{1,1})} \right] a_0 \quad . \text{----------(60)}$$

It should be noted, that the case $\varepsilon = 0$, from equation (59), yields the necessary result $a_0 = 0$ for Γ_1 to satisfy equation (22), which is the result

obtained in the section on the circular cylinder. It was mentioned in the section on the iterative method for obtaining the a_k, that c would be obtained i terms of a_0. The result is given by equation (60). Thus, equation (60), in conjunction with equations (53) give values for the a_k in terms of the known quantities X_m, Y_m, $\lambda_{k,0}$ and $\lambda_{k,1}$.

To summarise, equation (53), with c replaced by the value given above, and equation (54) give values for the constants a_k and b_k in equation (20). The sets of equations, given by (53) and (54) are solved preferably by the iterative method (ii). With these values, ψ, from equation (20), satisfies the boundary conditions ((i), (ii), (iii) and (iv)) and represents the stream function for variable shear flow past an elliptic cylinder, the equation of the latter being $r = \frac{p}{1+\varepsilon\cos\theta}$. The circulation Γ_0, which is again proportional to the lift force, can be calculated from equation (56), where $q_{//}$ is given by equation (57), the first two terms only being required for Γ_0. The velocity at any point is given by $q^2 = (q_\theta)^2 + (q_r)^2$, where q_r and q_θ are as defined previously. Stagnation points are given by $q = 0$ and in particular, on the cylinder by $q_{//} = 0$, where $q_{//}$ is given by equation (57). With c given by equation (60), the deflection of the stagnation stream line y_s, in the free stre near $x = -\infty$, can be obtained from a comparable equation to equation (27).

One general remark on the iterative method for obtaining the constants in the stream function, is that if an insufficient number of points are taken on the ellipse, in the comparison of the two series, the condition that $\psi = c$ on the ellipse may not be strictly accurate. The stagnation point at the leading edge, that is in the neighbourhood of $\theta = \pi$, is of more importance than that at the trailing edge. Consequently it may be argued that the series should be compared, and made to correspond as closely as possible in the region $\theta = \pi \pm \frac{\pi}{3}$ say, which would make $\psi = c$ on a curve which closely follows the perimeter of

the elliptic cylinder in that region. If this were carried out, however, it is highly probable that the remainder of the curve, given by $\psi = c$, would diverge considerably from the ellipse. Figure (f) illustrates this point, the dashed line giving a schematic representation of what this curve $\psi = c$ might look like in practice, if the comparison were made over a small restricted region round the leading edge.

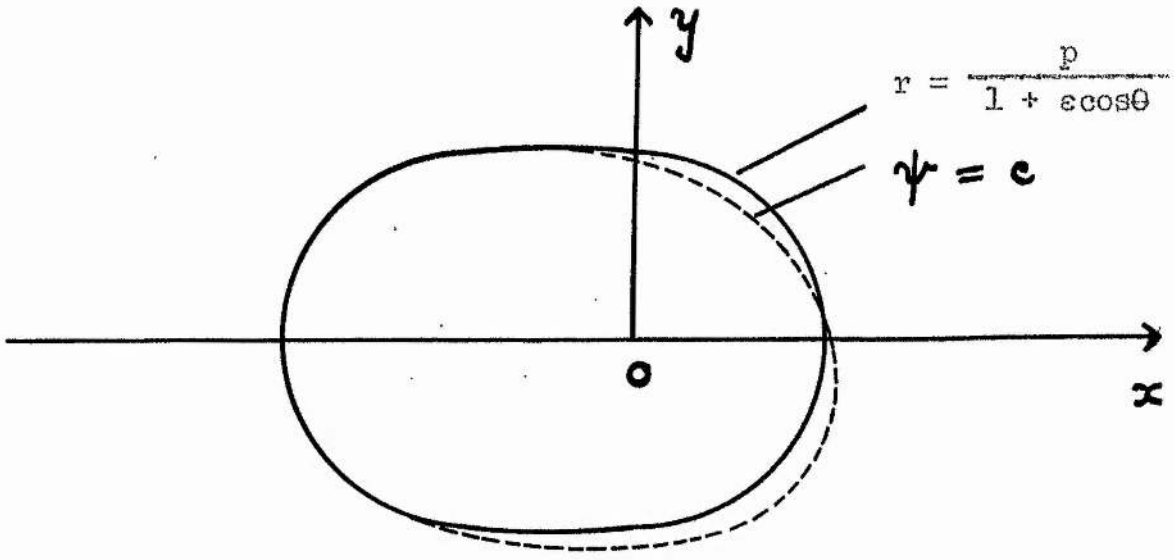

Figure (f)

Thus, emphasis is laid on the fact that the points of comparison must be numerous, and they must be distributed symmetrically round the perimeter of the elliptic cylinder.

It should be noted at this stage that in general the flow is not symmetric about a line lying along the minor axis. This is due to the form of the Fourier expansions in the analysis. The asymmetry, however, is not particularl marked. In the case discussed in the next section, however, the flow is symmetrical, due to the symmetry of the various functions about the line of the major axis.

The accuracy of the final solution is enhanced if more terms are taken in the expansion for $K_m\left(\frac{1}{1+\epsilon\cos\theta}\right)$ given by equation (46). Similarly, if the iterative process is extended to include a_k and b_k of higher order, the final solution is again, nearer the true solution. In the evaluation, it is recommended that for an ϵ in the region of $\epsilon = 0.25$, a value of $k \geqslant 4$ (where k is dependent on ϵ) is used in the equations for a_k and b_k, since small variations in a_0 change the positions of the stagnation points considerably.

Quantities, such as the deflections of the stagnation stream line and stagnation points, can be expressed in non-dimensional form with b the semi-minor axis, as the typical linear dimension. For comparison with the results obtained in chapter II, these non-dimensional quantities must be multiplied by $p/b = (1 - \epsilon^2)^{\frac{1}{2}}$.

It must be remembered in the work of this section, that the circular cylinder is the special case $\epsilon = 0$. However, some care should be exercised in putting $\epsilon = 0$ in final results. In general $\epsilon = 0$ in a formula reduces it to the circular cylinder case from a <u>numerical</u> point of view. The author has in fact evaluated the position of the stagnation points for the case $\epsilon = 0$, and the results are comparable with the previous circular cylinder results, differing only slightly in the third place of decimals, which may be reasonably attributed to inaccuracies in the numerical working.

<u>The Elliptic Cylinder with its Minor Axis in the Direction of Flow</u>

Flow, of the type given by equation (4), past an elliptic cylinder with its minor axis in the direction of the stream, can be obtained very quickly by taking the cylinder as that given by equation (34) and illustrated by Figure (c). This time the flow comes from $y = +\infty$ and it is not sufficient to replace y by x in equation (4), since the y-axis does not coincide with the minor axis, and so is not a line of symmetry of the ellipse. Accordingly the free stream distributi

given by equation (4), must be amended, the actual change being a translation of the y-axis. The distance along the x-axis between the origin and centre of the ellipse is given by as, where a and e are again the semi-major axis and eccentricity respectively. From equation (35), $as = p^*/(1-e^2) = x_0$, say. Thus, with x_0 so defined, and with the typical linear dimension again p, the flow comparable to equation (4) is given by

$$\psi = a\, e^{(x' + x_0')} + b\, e^{-(x' + x_0')} ,$$

where $x' = x/p$, and $x_0' = x_0/p$. Thus, on a line lying along the minor axis, that is $x' = - x_0'$, a value for ψ of (a + b) is given as before. Figure (10) illustrates the problem. The free stream near $y = + \infty$ may be represented by

$$\psi = A\, e^{x'} + B\, e^{-x'} , \qquad \text{----------(61)}$$

where $A = a\, e^{x_0'}$, and $B = b\, e^{-x_0'}$. Thus, in the comparison with the linear vorticity distribution, given by the appropriate function of x (see either method 1. or 2. in the section on the distribution at infinity), A and B are used in place of a and b and results similar to those in the last section are obtained. The subsequent analysis is not reproduced in detail, since a direct parallel can be drawn with the methods given in the last section. The major results are given with the minimum of analysis, and points of difference are pointed out as they occur.

As before, $\chi(\theta) = \frac{1}{1+e\cos\theta}$, and with slight amendment, the comparable equation to equation (21) is

$$c = A\, e^{\cos\theta/1+e\cos\theta} + B\, e^{-\cos\theta/1+e\cos\theta} + \sum_{k=0}^{\infty} (a_k \cos k\theta + b_k \sin k\theta) K_k \left(\frac{1}{1+e\cos\theta}\right) , \qquad \text{----------(62)}$$

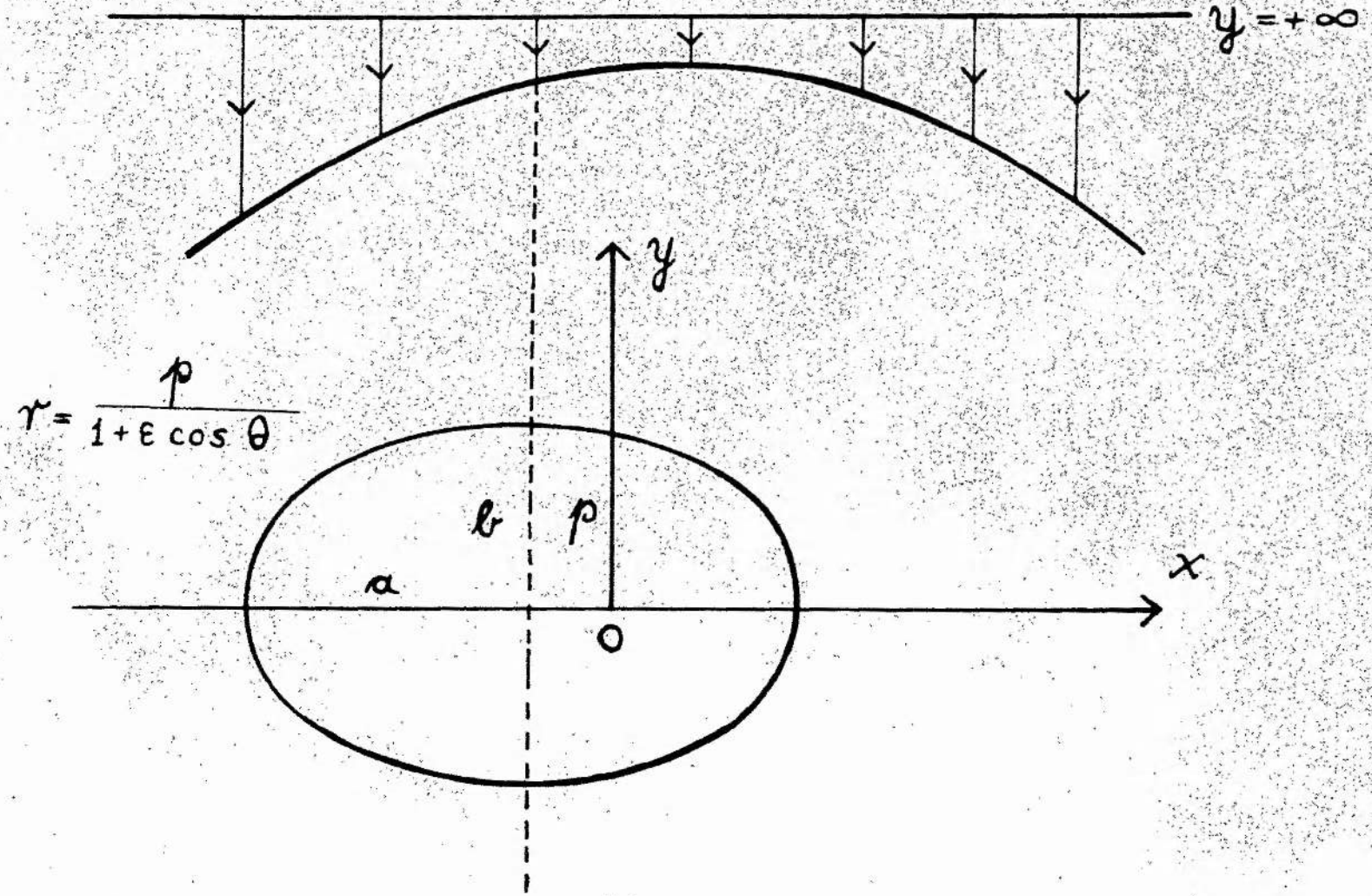

Figure (10) Illustration of the rotational flow past an elliptic cylinder.

where c is the constant taken by ψ on the cylinder and which, as before, will be evaluated from circulation considerations. The stream function ψ must satisfy the four boundary conditions given in the general method, with the exception that ψ is given by equation (61) as $y \to +\infty$. The same procedure as in the last section is now carried out.

1. The Fourier Expansion of $e^{\pm \cos\theta/1+\varepsilon\cos\theta}$.

The function can be expanded as

$$e^{\pm \frac{\cos\theta}{1+\varepsilon\cos\theta}} = 1 + \sum_{r=1}^{\infty} \frac{(\pm 1)^r}{r!} \left(\frac{\cos\theta}{1+\varepsilon\cos\theta}\right)^r \quad \text{----------(63)}$$

As before, each term $(\frac{\cos\theta}{1+\varepsilon\cos\theta})^r$ is expanded as a Fourier series and equation (38) is used, where the $a_{r,n}$ are given by equation (40) with a as a function of ε from equation (39). Now, $(\frac{\cos\theta}{1+\varepsilon\cos\theta})^r$ is an even function of θ for all values of r and the comparable equation to equation (41) is a half-range cosine series,

$$\left(\frac{\cos\theta}{1+\varepsilon\cos\theta}\right)^r = \tfrac{1}{2} A_{r,0} + \sum_{m=1}^{\infty} A_{r,m} \cos m\theta \,, \quad \text{----------(64)}$$

$$= \cos^r\theta \left[\tfrac{1}{2} a_{r,0} + \sum_{n=1}^{\infty} a_{r,n} \cos n\theta \right],$$

using equation (38). Following an exactly similar procedure as before, except that equation (64) holds for all integral values of r, from 1 to ∞, the constants $A_{r,m}$ are given by

$$A_{r,m} = \frac{2}{\pi} \int_0^{\pi} \frac{\cos^r\theta}{(1+\varepsilon\cos\theta)^r} \cos m\theta \, d\theta \,,$$

$$= \frac{2}{\pi} \int_0^{\pi} \cos^r\theta \left[\tfrac{1}{2} a_{r,0} + \sum_{n=1}^{\infty} a_{r,n} \cos n\theta \right] \cos m\theta \, d\theta \,,$$

$$= \frac{1}{\pi} \int_0^{\pi} \cos^r\theta \left[a_{r,0} \cos m\theta \right] d\theta \; +$$

$$+ \frac{2}{\pi} \sum_{n=1}^{\infty} a_{r,n} \int_0^{\pi} \cos^r\theta \cos n\theta \cos m\theta \, d\theta \ ,$$

$$= \frac{1}{\pi} \sum_{n=0}^{\infty} a_{r,n} \int_0^{\pi} \cos^r\theta \cos(m + n)\theta \, d\theta$$

$$+ \frac{1}{\pi} \sum_{n=1}^{m} a_{r,n} \int_0^{\pi} \cos^r\theta \cos(m - n)\theta \, d\theta$$

$$+ \frac{1}{\pi} \sum_{n=m+1}^{\infty} a_{r,n} \int_0^{\pi} \cos^r\theta \cos(n - m)\theta \, d\theta \ .$$

Using Integral Tafel 42 (332.(14)) these integrals are evaluated to give

$$A_{r,m} = \sum_{n=0}^{\infty} a_{r,n} \frac{1}{2^r} \binom{r}{\frac{r-n-m}{2}} \qquad r \geqslant m + n$$

$$= 0 \qquad r < m + n$$

$$+ \sum_{n=1}^{m} a_{r,n} \frac{1}{2^r} \binom{r}{\frac{r-m+n}{2}} \qquad r \geqslant m - n$$

$$+ 0 \qquad r < m - n$$

$$+ \sum_{n=m+1}^{\infty} a_{r,n} \frac{1}{2^r} \binom{r}{\frac{r-n+m}{2}} \qquad r \geqslant n - m$$

$$+ 0 \qquad r < n - m \ , \qquad \text{----------(65)}$$

where $r \pm (n \pm m)$ are all even integers (i.e. r and $(n \pm m)$ are both odd or both even integers). Thus, the Fourier expansion from equation (63), using equation (64), is

$$e^{\pm \frac{\cos\theta}{1+\varepsilon\cos\theta}} = 1 + \frac{1}{2} \sum_{r=1}^{\infty} \frac{(\pm 1)^r}{r!} A_{r,0} + \sum_{r=1}^{\infty} \sum_{m=1}^{\infty} \frac{(\pm 1)^r}{r!} A_{r,m} \cos m\theta \ , \qquad \text{----------(66)}$$

where $A_{r,m}$ for all r and m is given by equation (65).

2. The Bessel Function $K_m\left(\frac{1}{1+\varepsilon\cos\theta}\right)$ as a Cosine Series

The expansion is similar to that given by equation (46) and the values of $\lambda_{m,\gamma}$ are again given by Table (6). The complete section, and in particular equation (50) is applicable directly in this case. However, it is seen from Figures (7), (8) and (9), that regions of poor comparison occur around $\theta = 0$ and 2π. These regions may reach the minor axis, where $\theta = \cos^{-1}\varepsilon$. In this case, therefore, great care must be taken to ensure a good comparison in the region around this latter point, departing slightly, if necessary, from the exact curve near $\theta = \pi$.

Equation (62) now becomes

$$c = (A + B) + \frac{(A+B)}{2}\sum_{r=1}^{\infty}\frac{A_{2r,0}}{(2r)!} + \frac{(A-B)}{2}\sum_{r=0}^{\infty}\frac{A_{2r+1,0}}{(2r+1)!}$$
$$+ (A + B)\sum_{r=1}^{\infty}\sum_{m=1}^{\infty}\frac{A_{2r,m}}{(2r)!}\cos m\theta$$
$$+ (A - B)\sum_{r=0}^{\infty}\sum_{m=1}^{\infty}\frac{A_{2r+1,m}}{(2r+1)!}\cos m\theta$$
$$+ \sum_{k=0}^{\infty}(a_k\cos k\theta + b_k\sin k\theta)(\lambda_{k,0} + \lambda_{k,1}\cos\theta)\ .$$

Introducing the notation X_m, where

$$X_0 = (A + B) + \frac{(A+B)}{2}\sum_{r=1}^{\infty}\frac{A_{2r,0}}{(2r)!} + \frac{(A-B)}{2}\sum_{r=0}^{\infty}\frac{A_{2r+1,0}}{(2r+1)!}\ ,$$

and

$$X_m = (A + B)\sum_{r=1}^{\infty}\frac{A_{2r,m}}{(2r)!} + (A - B)\sum_{r=0}^{\infty}\frac{A_{2r+1,m}}{(2r+1)!}\ ,\quad m > 0$$

the last equation becomes

$$c = \sum_{m=0}^{\infty} X_m\cos m\theta$$
$$+ \sum_{k=0}^{\infty}(a_k\cos k\theta + b_k\sin k\theta)(\lambda_{k,0} + \lambda_{k,1}\cos\theta).\text{----------(67)}$$

Comparing the coefficients of sin kθ, it is seen immediately that $b_k = 0$ for all k. Comparing the coefficients of cos kθ, a set of equations similar to equations (53) is obtained, where the various quantities now have different meanings. For example, X_m is now as above, and a_k is a function of A and B. Either method described in the last section for solving the equations can be used, although the iterative method (2) is preferable. Again, the constant c must be obtained from circulation considerations using equation (22), and on substitution in equations (53) the required solutions for the a_k are obtained.

The stream function ψ, from a comparable equation to equation (20), is given by

$$\psi = a\, e^{\frac{\varepsilon}{1-\varepsilon^2}}\, e^{r' \cos\theta} + b\, e^{-\frac{\varepsilon}{1-\varepsilon^2}}\, e^{-r' \cos\theta}$$

$$+ \sum_{k=0}^{\infty} a_k \cos k\theta\, K_k(r'), \qquad \text{----------(68)}$$

where a and b are values which make equation (61) most nearly represent a linear vorticity distribution. They are in fact given by equations (11) or (15), and a_k is obtained from the set of equations similar to equations (53). c is again given by equation (60) where the quantities involved have the corresponding meanings. The velocity components and velocity at any point are given respectively by

$$q_r = \frac{1}{pr'} \frac{\partial \psi}{\partial \theta}, \quad q_\theta = -\frac{1}{p} \frac{\partial \psi}{\partial r'}, \text{ and } q^2 = q_r^2 + q_\theta^2, \qquad \text{--------(69)}$$

and the velocities on the cylinder by $q_\perp$ and $q_\parallel$, which, as before, are given by equation (55). In an exactly similar manner, it can be shown that $q_\perp = 0$ and that $q_\parallel$ is given by

$$q_\parallel = \frac{1}{p(1+\varepsilon^2 + 2\varepsilon\cos\theta)^{\frac{1}{2}}} \Big[-a\, e^{\left(\frac{\varepsilon}{1-\varepsilon^2}\right)} e^{\frac{\cos\theta}{1+\varepsilon\cos\theta}} (\varepsilon + \cos\theta)$$

$$+ b\, e^{-\left(\frac{\varepsilon}{1-\varepsilon^2}\right)} e^{-\frac{\cos\theta}{1+\varepsilon\cos\theta}} (\varepsilon + \cos\theta) -$$

$$- \epsilon \sin\theta \,(1 + \epsilon\cos\theta)\sum_{k=0}^{\infty} k a_k \sin k\theta \,(\lambda_{k,0} + \lambda_{k,1}\cos\theta)$$

$$+ (1 + \epsilon\cos\theta)\sum_{k=0}^{\infty} a_k \cos k\theta \left\{ k(1 + \epsilon\cos\theta)(\lambda_{k,0} + \lambda_{k,1}\cos\theta) \right.$$

$$\left. + (\lambda_{k-1,0} + \lambda_{k-1,1}\cos\theta)\right\}\Bigg] \quad \text{.----------(70)}$$

In particular, stagnation points on the cylinder are given as solutions of $q_{\parallel} =$ From equation (70) the contribution to the circulation Γ, namely Γ_1 is given by

$$\Gamma_1 = \int_{-\pi}^{\pi} \Bigg[- \epsilon \sin\theta \sum_{k=0}^{\infty} k a_k \sin k\theta (\lambda_{k,0} + \lambda_{k,1}\cos\theta)$$

$$+ \sum_{k=0}^{\infty} a_k \cos k\theta \left\{ k(1 + \epsilon\cos\theta)(\lambda_{k,0} + \lambda_{k,1}\cos\theta) \right.$$

$$\left. + (\lambda_{k-1,0} + \lambda_{k-1,1}\cos\theta)\right\}\Bigg] d\theta \quad ,$$

which on integration gives the same result as that given by equation (59), where the quantities have corresponding meanings. The expression for c is given by equation (60), where the X_m are given by equation (67).

Thus, to summarise, remembering the appropriate changes in a, b and X_m, the stream function ψ, given by equation (68) satisfies the four boundary conditions,

(i) $\nabla^2\psi = \psi/p^2$,

(ii) $\psi \longrightarrow Ae^{x'} + Be^{-x'}$ as $y \longrightarrow +\infty$,

(iii) $\psi = c$ on the elliptic cylinder, and

(iv) $\Gamma_1 = 0$.

The constants a_k are evaluated from equations (53), with c replaced by the relation given by equation (60), the iterative method of solution being preferal The velocity at any point can be calculated from equation (69) and in particula

on the cylinder by equation (70). Stagnation points on the cylinder are given by the solutions of $q_{\parallel} = 0$. The circulation Γ_o, which is also proportional to the lift force, can be evaluated by integration of the required terms, and is the same as that for the cylinder with its major axis in the direction of flow, A and B replacing a and b respectively. Again, the various deflections can be expressed in non-dimensional form with a the semi-major axis as the typical linear dimension and the respective quantities multiplied by $D_{\frac{1}{2}} = (1 - \epsilon^2)$.

One major difference in the two flows, is that this time a symmetrical flow about the x-axis is obtained. This can easily be seen, from the stream function given by equation (68), which is a function of r and the cosines of multiple angles.

The general remarks, made at the conclusion of the preceding section, apply also to this flow past the cylinder with its minor axis in the direction of flow. Once again, the special case of the circular cylinder, given by $\epsilon = 0$, can be evaluated.

A large part of the analysis, and some of the final results have not been reproduced in this section on the flow past the elliptic cylinder with its minor axis in the direction of flow, since the method, following the short discussion on the free stream distribution near $y = +\infty$, is similar, in almost all respects, to that given in the preceding section. If desired, any particular part can be expanded by making direct reference to the corresponding part in the case of flow past the elliptic cylinder with its major axis in the direction of flow.

The Fundamental Equation and Transformation for the Approximation to the Flow in a Boundary Layer

The fundamental equation used, is that given by equation (2) with λ positiv namely

$$\nabla^2\psi + \psi/\ell^2 = 0 \quad , \qquad (71)$$

the derivation of which is given at the beginning of this chapter. The procedu follows comparable lines to that given in the case of the linear shear approximation.

A ψ-distribution consistent with equation (71) is

$$\psi = a \cos y/\ell + b \sin y/\ell \quad , \qquad (72)$$

where, as before, a and b are arbitrary real constants. This results in a velocity distribution

$$q = q_x = -\frac{a}{\ell} \sin \frac{y}{\ell} + \frac{b}{\ell} \cos \frac{y}{\ell} \quad , \qquad (73)$$

and a vorticity distribution

$$\omega = \frac{a}{\ell^2} \cos \frac{y}{\ell} + \frac{b}{\ell^2} \sin \frac{y}{\ell} \quad ,$$

from which it follows that $\omega = \psi/\ell^2$. Introducing the stream function Ψ, by the transformation

$$\psi = a \cos y/\ell + b \sin y/\ell + \Psi \quad , \qquad (74)$$

it is easily seen that Ψ must satisfy the partial differential equation

$$\nabla^2\Psi + \Psi/\ell^2 = 0 \quad . \qquad (75)$$

Again, if the free stream near $x = -\infty$ is given by equation (72), one necessa condition on Ψ , from equation (74), is that it must tend to zero as x tends t $-\infty$. With a cylinder at the origin, the stream function ψ, for flow past this cylinder must satisfy the following conditions:

(1) $\nabla^2\psi + \psi/\ell^2 = 0$,

(ii) $\psi \longrightarrow a \cos y/\ell + b \sin y/\ell$, as $x \to -\infty$, and

(iii) ψ = constant c, on the cylinder.

These three conditions are not sufficient to give a unique solution to the problem and again, the circulation must be taken into consideration.

Following the same procedure as in the case of the linear shear approximation, the free stream distribution near $x = -\infty$ is discussed in detail.

The Distribution at Infinity

The results in this section, being derived from free stream conditions, onl hold near $x = -\infty$. Equation (72) gives a general distribution for a variabl shear flow, and with a suitable choice of the constants a and b an approximation can be obtained to the flow in a boundary layer.

One approximation to the velocity profile of the flow in a boundary layer, is given by

$$q = q_x = U \sin \frac{\pi}{2} y/\delta \quad , \qquad (76)$$

where $0 \leq y \leq \delta$, δ being the thickness of the boundary layer, U the free stream velocity outside the boundary layer, and the line y = 0 being the solid boundary The form of the velocity profile in a boundary layer is of course due to the viscosity of the fluid. For the purposes of this section the actual velocity profile is used as a model, although the viscosity of the fluid is neglected. The flow given by equation (76) is illustrated in Figure (g).

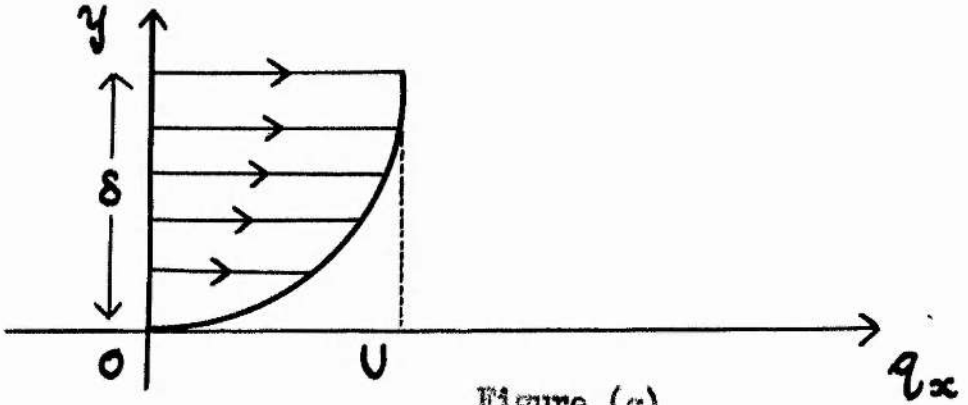

Figure (g)

Equation (76) gives the ideal flow in the range $0 \leqslant y \leqslant \delta$, and the purpose of this section is to obtain values of a and b which make the velocity profile give by equation (73) represent as closely as possible the profile given by equation (76). This can be done exactly for values of y in the range $0 \leqslant y \leqslant \delta$. However, before obtaining expressions for a and b some general points are discussed.

Equation (76) gives the velocity profile for flow along a flat plate $y = 0$, when $0 \leqslant y \leqslant \delta$, where the velocity for $y > \delta$ is given by $q_x = U$ and $q_y = 0$. The problem is to find the nature of the flow past a small cylinder situated in this flow, when the centre of the cylinder lies in the region $0 < y < \delta$. Davies [37] states that for pitot tubes in a boundary layer, the radius of the pitot should be less than one tenth of the thickness δ, of the boundary layer. In the subsequent discussion the pitot tube is replaced by a cylinder with close cross section and the above restriction on the cylinder size is observed.

In the theoretical study of flow past cylinders, the cylinder is for convenience always placed with its centre on the x-axis. In order to obtain different positions of the cylinder relative to the flow in the range $0 < y < \delta$, the flow is represented by

$$q = q_x = U \sin \frac{\pi}{2} \frac{1}{\delta} (y + y_o) , \qquad (77)$$

where y_o is a variable parameter. This velocity profile where $0 \leqslant y + y_o \leqslant \delta$, is illustrated in Figure (h).

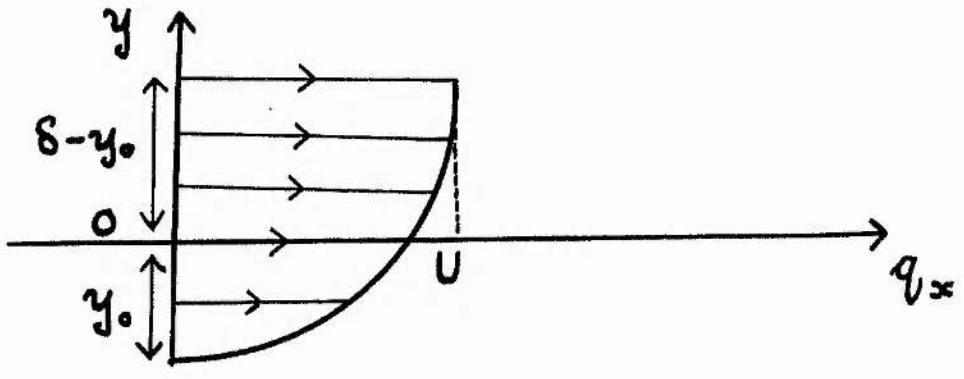

Figure (h)

Thus, the ideal state of affairs is to have a solid boundary parallel to the x-axis through the point $y = -y_o$ along which the velocity is zero, a velocity profile for $(y + y_o) \leqslant \delta$ given by equation (77), and the velocity equal to U for $(y + y_o) > \delta$. In this flow the cylinder is placed at the origin and varying conditions are obtained by altering y_o.

Equations (73) and (77) must now be compared to obtain expressions for a and b. To be consistent with the linear shear case, a change of notation is desirable from δ to kh, where h is some typical length in the body, and k is a real number. Taking the typical linear dimension ℓ as $\frac{2kh}{\pi}$, non-dimensional lengths $y' = \frac{\pi y}{2kh}$ and $y'_o = \frac{\pi y_o}{2kh}$ are obtained, and equation (77) becomes

$$q_x = U \sin (y' + y'_o) \qquad \text{----------(78)}$$

$$= U \sin y' \cos y'_o + U \cos y' \sin y'_o \ .$$

Comparing equations (73) and (78), where ℓ in equation (73) is equal to $\frac{2kh}{\pi}$, it is seen that

$$a = -U \frac{2kh}{\pi} \cos y'_o \ , \text{ and } b = U \frac{2kh}{\pi} \sin y'_o \ , \qquad \text{---------(79)}$$

and so equation (72) for the free stream ψ becomes

$$\psi = -\frac{U2kh}{\pi} \cos y'_o \cos y' + \frac{U2kh}{\pi} \sin y'_o \sin y' \ ,$$

$$= -\frac{U2kh}{\pi} \cos (y' + y'_o) \ . \qquad \text{----------(80)}$$

Unfortunately, the velocity profile obtained from equation (80) can not be restricted to the range $0 \leqslant (y' + y'_o) \leqslant \pi/2$, but covers the full range of y'. A section of the profile is illustrated in Figure (i).

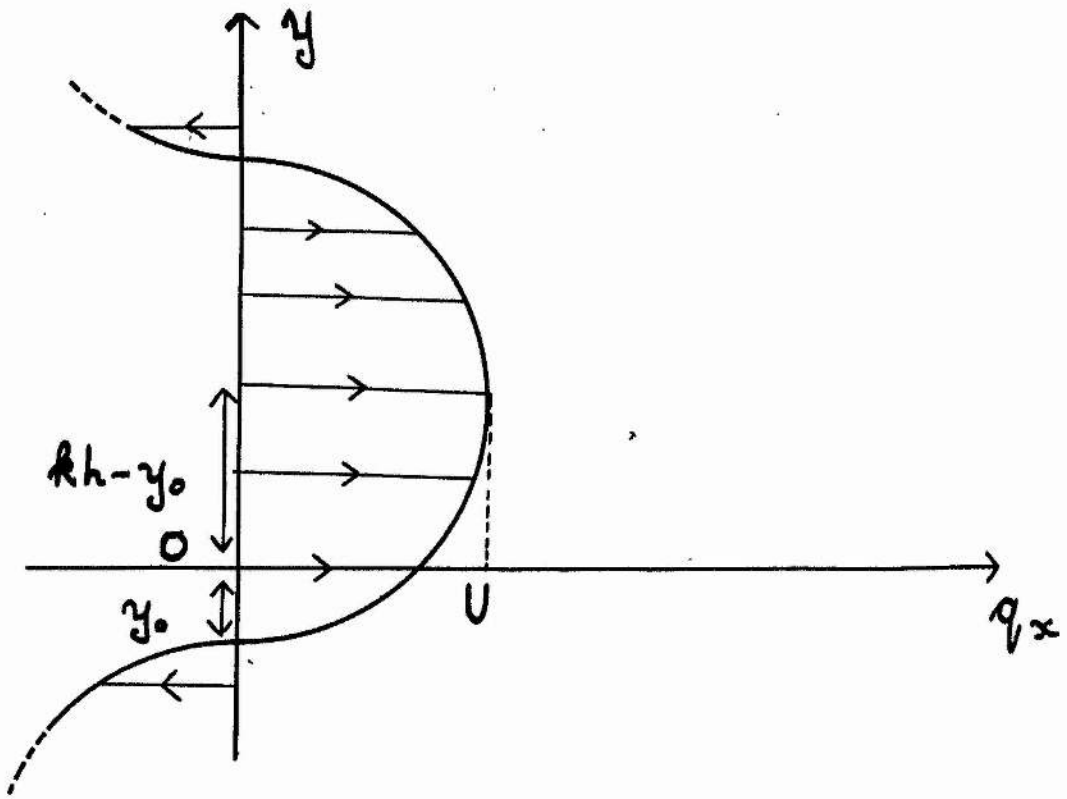

Figure (1)

To summarise, a solution with general a and b can be obtained for a variable shear flow. With the values of a and b given by equation (79), however, an approximation to the flow in a boundary layer can be obtained with certain restrictions which will be discussed subsequently. The free stream distributions may be given in non-dimensional form as

$$\left.\begin{aligned} \psi' &= \frac{\psi}{U\frac{2kh}{\pi}} = -\cos(y' + y_0') \\ q' &= {}^{q}/_{U} = \sin(y' + y_0') \\ \omega' &= {}^{\omega}/_{\omega_0} = -N\cos(y' + y_0') \end{aligned}\right\} \qquad (81)$$

and

where $N = {}^{U}/_{\omega_0}\left(\frac{2kh}{\pi}\right)$.

The general method for obtaining the stream functions for a cylinder in a flow of this type is given in the next section with a and b general.

The General Method

The field of flow past a cylinder, where the free stream flow near $x = -\infty$ is given by equation (72), or more particularly by equation (80), wi in general differ markedly from the field of flow when the cylinder is situate in a two-dimensional boundary layer. However, it is assumed in this section that the radius, or comparable length of the cylinder is less than 0.1δ, and that the cylinder is situated in a region where no back flow occurs. The principle features of the flow in the neighbourhood of the cylinder will be qualitatively the same as those in the ideal boundary layer case. Also, the quantitative deflections of the stagnation stream line will be comparable in the two cases.

The stream function ψ must satisfy the necessary conditions (i), (ii) and (iii) already stated, and a solution, which involves the constant c is obtained as before by solving equation (75) for Ψ, using polar coordinates, with the proviso that $\Psi \longrightarrow 0$ as $r \longrightarrow \infty$. Equation (75) in polar coordinates is

$$\frac{\partial^2 \Psi}{\partial r^2} + \frac{1}{r}\frac{\partial \Psi}{\partial r} + \frac{1}{r^2}\frac{\partial^2 \Psi}{\partial \theta^2} + \Psi/\ell^2 = 0 \quad \text{----------(82)}$$

Multiplying both sides of this equation by ℓ^2, and writing $r' = r/\ell$, the equation can be solved by separation of variables. Assuming a solution to exist of the form

$$\Psi = R(r')\,\Theta(\theta),$$

substitution in equation (82) gives the following equations:

$$\frac{r'^2}{R}\frac{d^2R}{dr'^2} + \frac{r'}{R}\frac{dR}{dr'} + r'^2 = -\frac{1}{\Theta}\frac{d^2\Theta}{d\theta^2} = \pm m^2 .$$

From the periodic nature of the stream function with respect to θ, the results

$$\frac{d^2\Theta}{d\theta^2} + m^2\Theta = 0 ,$$

and

$$\frac{d^2R}{dr'^2} + \frac{1}{r'}\frac{dR}{dr'} + \left(1 - \frac{m^2}{r'^2}\right) R = 0,$$

are obtained, the latter being Bessel's differential equation of order m, solutions of which are $J_m(r')$ and $Y_m(r')$, the Bessel functions of the first and second kind respectively, as given in Watson's 'Treatise on Bessel Functions' [41] . (The analysis in this section, with sufficient care, could be derived from the previous work with the variable r' replaced by ir', but for the purpose of a general theory, it is derived independently) . Thus, a general solution of equation (82) may be given as

$$\Psi = \sum_m (A_m \cos m\theta + B_m \sin m\theta)(C_m J_m(r') + D_m Y_m(r')) \quad ,---------(83)$$

where A_m, B_m, C_m and D_m are constants. Ψ , as given by equation (83), satisfies the condition that $\Psi \to 0$ as $r \to \infty$, since $J_m(r') \longrightarrow 0$ and $Y_m(r') \longrightarrow 0$ as $r \longrightarrow \infty$. Substitution of Ψ in the transformation given by equation (74), results in a stream function ψ , of the form

$$\psi = a \cos y' + b \sin y' + \sum_m (A_m \cos m\theta + B_m \sin m\theta)(C_m J_m(r') + D_m Y_m(r')) \quad .-------(84)$$

ψ , given by equation (84), satisfies conditions (i) and (ii), and condition (iii) gives

$$c = a \cos(\chi(\theta) \sin\theta) + b \sin(\chi(\theta) \sin\theta) + \sum_m (A_m \cos m\theta + B_m \sin m\theta)\left[C_m J_m(\chi(\theta)) + D_m Y_m(\chi(\theta))\right] .----------(85)$$

where the equation of the cylinder's cross section is $r' = \chi(\theta)$. As yet, th method is parallel to that given in the previous section, except that C_m and D_m are still included in the summation. However, inthe comparison of the coefficients of the sine and cosine terms, relations are obtained which imply

that J_m and Y_m are linearly dependent, which is impossible. Thus, either C_m or D_m is zero, and on comparison with the case of the linear shear approximation, it is assumed that $C_m = 0$: in the case of the circular cylinder this is actually proved, as is shown in the following section. With this modification, equations (84) and (85) become respectively

$$\psi = a \cos y' + b \sin y' + \sum_m (a_m \cos m\theta + b_m \sin m\theta) Y_m(r'), \qquad (86)$$

and

$$c = a \cos(\chi(\theta) \sin\theta) + b \sin(\chi(\theta) \sin\theta) + \sum_m (a_m \cos m\theta + b_m \sin m\theta)\, Y_m(\chi(\theta)) \qquad (87)$$

From these last two equations, further discussion on the general method is unnecessary, since a direct parallel can be drawn with the previous case for the approximation to a linear shear flow. The discourse on the circulation may be transferred also, resulting in the fourth condition on the flow, namely $\Gamma_1 = 0$. Further discussion in the general case is omitted for the sake of brevity and flows past specific cylinders are now considered.

The Circular Cylinder

A circular cylinder of radius r_o is introduced at the origin of the field of flow, the free stream conditions being given by equation (72). The typical linear dimension is r_o. In the following analysis, general a and b are retained, the specific values given by equation (79) being substituted in the final results, or at any intermediate stage if desired. The problem is illustrated in Figure (11).

The circular cylinder has equation $r = r_o$, or in non-dimensional form $r' = \frac{\pi}{2k} \frac{r}{r_o} = \frac{1}{k} \frac{\pi}{2} = K$, say, and so for the circular cylinder $\chi(\theta) =$ constant. The restriction on K is discussed subsequently.

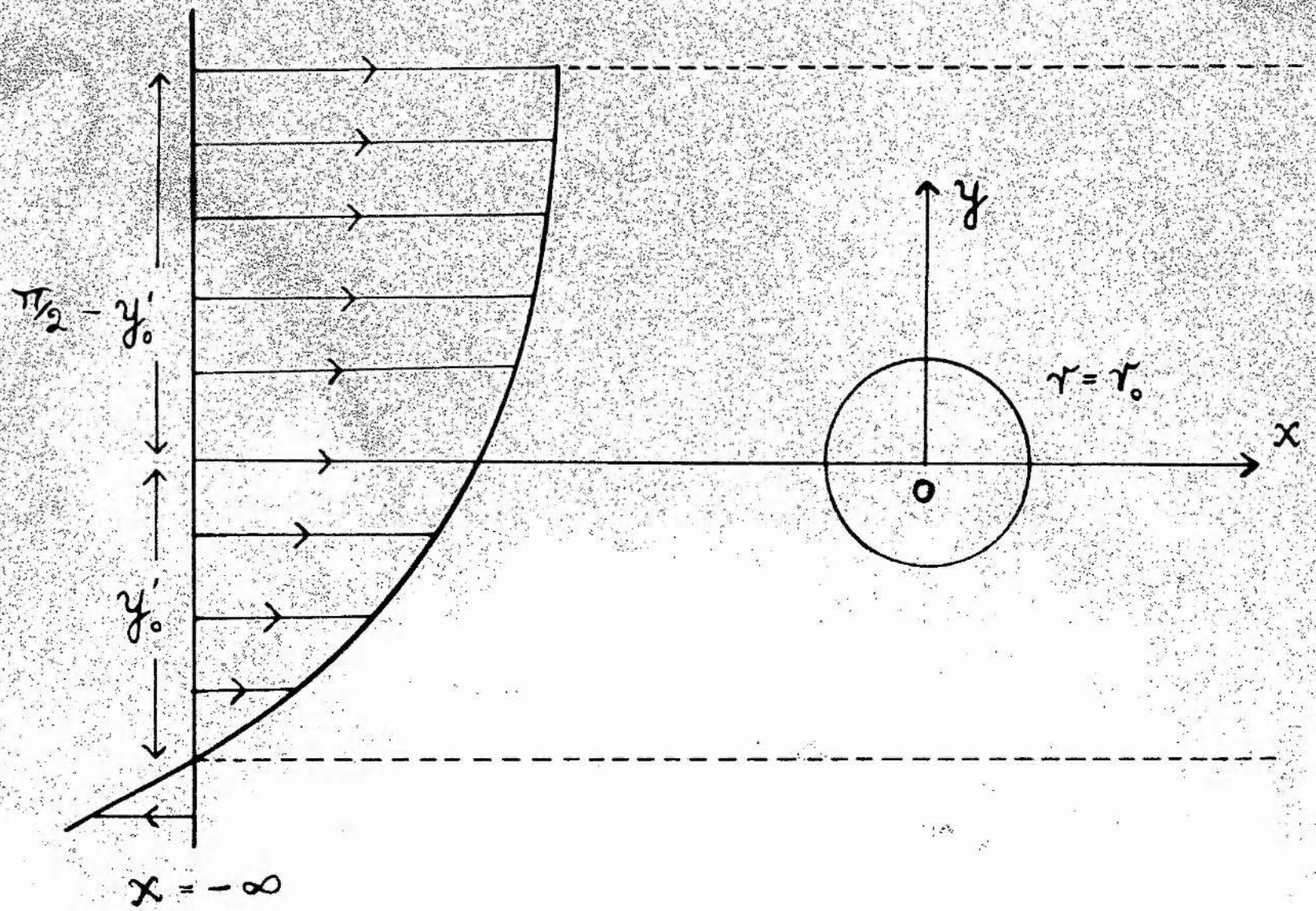

Figure (11) Illustration of rotational flow (boundary layer) past a circular cylinder.

To illustrate, and justify the assumption that $C_m = 0$, equation (85) is considered instead of equation (87), and in the case of the circular cylinder becomes

$$c = a \cos(K \sin\theta) + b \sin(K \sin\theta) + \sum_{m=0}^{\infty} (A_m \cos m\theta + B_m \sin m\theta)(C_m J_m(K) + D_m Y_m(K)). \quad \text{----------(88)}$$

Following the general method, the Fourier expansions are obtained for $\begin{matrix}\cos\\ \sin\end{matrix}$ (K sin θ) and in fact, from the 'Treatise on Bessel Functions' by Gray and Mathews [44] or from direct integration using Integral Tafel [42], are given by

$$\cos(K \sin\theta) = J_0(K) + 2 \sum_{m=1}^{\infty} J_{2m}(K) \cos 2m\theta \quad \text{----------(89)}$$

and

$$\sin(K \sin\theta) = 2 \sum_{m=0}^{\infty} J_{2m+1}(K) \sin(2m+1)\theta \ .$$

Substituting these series in equation (88), and equating the coefficients of t sine and cosine terms, it is seen that $A_{2m+1} = 0 = B_{2m}$, unless $C_{2m+1} = C_{2m+1} = D_{2m+1} = D_{2m} = 0$, which is trivial. Considering the coefficients of $\sin(2m+1)\theta$,

$$-2b\, J_{2m+1}(K) = B_{2m+1} \left[C_{2m+1} J_{2m+1}(K) + D_{2m+1} Y_{2m+1}(K) \right],$$

which implies that $J_{2m+1}(K)$ and $Y_{2m+1}(K)$ are linearly related, which is impossible, and so one of C_{2m+1} and D_{2m+1} is zero, since $B_{2m+1} \neq 0$. If $D_m = 0$ for all m, equation (88) becomes an identity, and so $C_m = 0$. Thus, equation (88), (or from equation (87)) becomes

$$c = a\, J_0(K) + 2a \sum_{m=1}^{\infty} J_{2m}(K) \cos 2m\theta \quad +$$

$$+ 2b \sum_{m=0}^{\infty} J_{2m+1}(K) \sin (2m+1)\theta$$

$$+ \sum_{m=0}^{\infty} (a_m \cos m\theta + b_m \sin m\theta) Y_m(K),$$

which gives

$$a_{2m+1} = 0 = b_{2m} \, , \quad a_0 = \left[c - aJ_0(K) \right] \frac{1}{Y_0(K)} \, ,$$

$$a_{2m} = -2a \, \frac{J_{2m}(K)}{Y_{2m}(K)} \qquad m > 0 \, ,$$

$$b_{2m+1} = -2b \, \frac{J_{2m+1}(K)}{Y_{2m+1}(K)} \qquad m \geqslant 0 \, ,$$

resulting in the stream function ψ, which from equation (86) is now

$$\psi = a \cos y' + b \sin y' + \left[c - aJ_0(K) \right] \frac{Y_0(r')}{Y_0(K)}$$

$$-2a \sum_{m=1}^{\infty} \frac{J_{2m}(K)}{Y_{2m}(K)} \, Y_{2m}(r') \cos 2m\theta$$

$$-2b \sum_{m=0}^{\infty} \frac{J_{2m+1}(K)}{Y_{2m+1}(K)} \, Y_{2m+1}(r') \sin (2m+1)\theta \, . \qquad \text{----------(90)}$$

It should be noted that the flow field is again symmetric about the y-axis, irrespective of the value of c. The velocity at any point is given by

$$q^2 = q_\theta^2 + q_r^2 \, , \qquad \text{----------(91)}$$

where q_θ and q_r, the velocity components, are as defined previously. The velocity on the cylinder is given by $(q_\theta)_{r=r_0}$ since $(q_r)_{r=r_0} = 0$ on the cylinder, and in particular stagnation points on the cylinder are given by solutions of $(q_\theta)_{r=r_0} = 0$. The circulation Γ, is given by

$$\Gamma = \Gamma_0 + \Gamma_1 = \int_0^{2\pi} r_0 \, (q_\theta)_{r=r_0} \, d\theta \, .$$

Using equation (90), it is easily shown that

$$\Gamma_0 = 2\pi\, aK J_1(K), \qquad (92)$$

and

$$\Gamma_1 = 2\pi K \frac{Y_0'(K)}{Y_0(K)} \left[c - aJ_0(K) \right],$$

where $Y_0'(K) = \left[\frac{d}{dr'} Y_0(r')\right]_{r'=K}$. This latter equation, using relation (22), gives

$$c = a J_0(K). \qquad (93)$$

The stagnation stream line is $\psi = c$, and the non-dimensional deflection $y_s' = y_s/\frac{2kr_0}{\pi}$ of the stagnation stream line in the free stream near $x = -\infty$ is given by the appropriate solution of

$$a \cos y_s' + b \sin y_s' = a J_0(K). \qquad (94)$$

Thus, equation (93) in conjunction with equation (90) gives a stream function ψ, which satisfies the four necessary conditions, namely

(i) $\nabla^2\psi + \psi/\ell^2 = 0$, where $\ell = \frac{2kr_0}{\pi}$,

(ii) $\psi \longrightarrow a \cos y' + b \sin y'$ as $x \longrightarrow -\infty$,

(iii) $\psi = c$ on the cylinder $r = r_0$, and

(iv) $\Gamma_1 = 0$.

Taking the particular values of a and b given by equation (79), and writing $\psi' = \psi/U\frac{2kr_0}{\pi}$, the non-dimensional stream function ψ' from equation (90), with c given by equation (93), becomes

$$\psi' = -\cos(y' + y_0') + 2\cos y_0' \sum_{m=1}^{\infty} \frac{J_{2m}(K)}{Y_{2m}(K)} Y_{2m}(r') \cos 2m\theta - 2\sin y_0' \sum_{m=0}^{\infty} \frac{J_{2m+1}(K)}{Y_{2m+1}(K)} Y_{2m+1}(r') \sin(2m+1)\theta. \qquad (95)$$

From equation (92), the circulation is given by

$$\Gamma = \Gamma_o = -2\pi U r_o' \cos y_o' J_1(K), \qquad (96)$$

from which it follows that the lift force, which is proportional to Γ_o, is negative in sign, and thus tends to pull the cylinder in the negative y-direction. The deflection of the stagnation stream line in the free stream near $x = -\infty$ is, from equation (94), given by

$$y_s' = \cos^{-1}\left[J_o(K)\cos y_o'\right] - y_o' \quad . \qquad (97)$$

If the deflection is required with r_o as the non-dimensionalising length, y_s' as given by equation (97) must be divided by K. Now, since $J_o(K) < 1$ for all $K > 0$, equation (97) shows that $y_s' > 0$, which again implies that the stagnation stream line comes from a region of higher velocity than that opposite the diameter of the cylinder. With values of K in the restricted range given subsequently, Figure (12) illustrates the deflection in the form y_s/r_o, which is, of course, y_s'/K, for values of y_o' in the range $0 \leqslant y_o' \leqslant \frac{\pi}{2}$. The velocity at any point can be obtained from equation (91), and in particular, the velocity on the cylinder is given by $(q_\theta)_{r=r_o}$ with stagnation points given by the values of θ satisfying the equation $(q_\theta)_{r=r_o} = 0$, which in this case is

$$\begin{aligned} &\sin\theta \sin(K\sin\theta + y_o') \\ &+ 2\cos y_o' \sum_{m=1}^{\infty} \frac{J_{2m}(K)}{Y_{2m}(K)} Y_{2m}'(K) \cos 2m\theta \\ &- 2\sin y_o' \sum_{m=0}^{\infty} \frac{J_{2m+1}(K)}{Y_{2m+1}(K)} Y_{2m+1}'(K) \sin(2m+1)\theta = 0 \quad , \end{aligned} \qquad (98)$$

where

$$Y_m'(K) = \left[\frac{d}{dr'} Y_m(r')\right]_{r'=K} \quad .$$

Now, the boundary layer thickness δ is equal to kr_o, so with a cylinder satisfying the condition $r_o < 0.1\delta$, the number k must be greater than 10, which

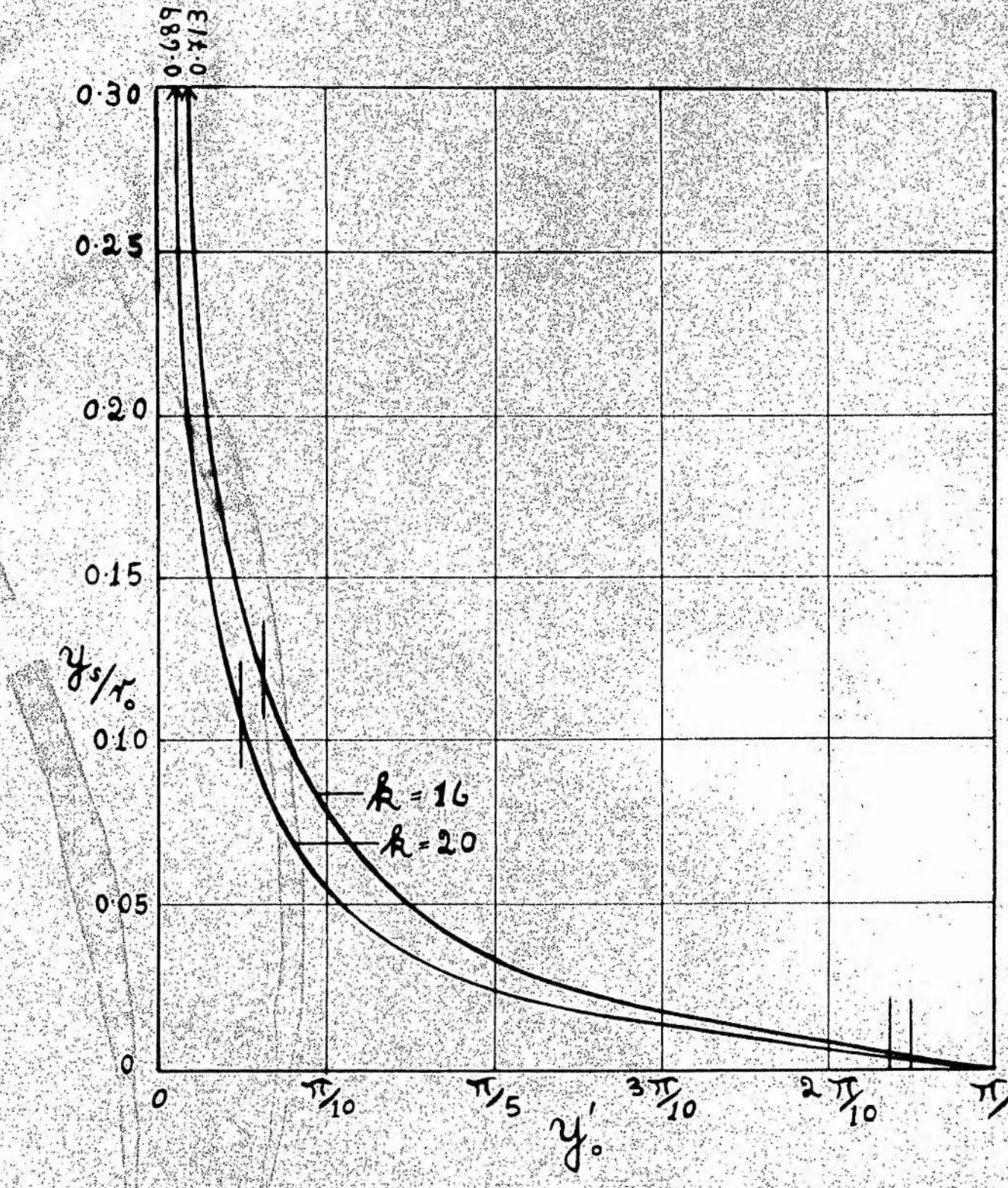

Figure (12) Deflection in the stagnation stream line in the free stream for the circular cylinder.

gives the condition on K as $K = \frac{\pi}{2}\frac{1}{k} < 0.1\,\frac{\pi}{2} \doteq 0.1571$. With this maximum value of 0.1571 for K, the series in equations (95) and (98) converge extremely rapidly, and values of $m \leqslant 2$ in the first series and $m \leqslant 1$ in the second are probably sufficient for all practical purposes, particularly in equation (98).

The restricted range for y_o, within which the flow may be assumed similar to that in a boundary layer, may be estimated by assuming that, for values of y_o' in the range, the flow past the cylinder is not affected by the difference in the velocity profiles for $(y' + y_o') > \frac{\pi}{2}$ and $(y' + y_o') \leqslant 0$. (cf. figures (h) and (i)). This is, in fact, reasonable if the radius in the form of K satisfies $K < \frac{\pi}{20}$, and if y_o' lies in the range

$$2K \leqslant y_o' \leqslant \frac{\pi}{2} - 2K \,. \qquad (99)$$

The deflection y_s'/K, for values of y_o' in this range is given by the curves in Figure (12) between the two lines with ordinates 2K and $\frac{\pi}{2} - 2K$.

The state of affairs from the point of view of stagnation points on the cylinder is of a more complicated nature than in the case of the linear shear approximation. Putting $f(\theta)$ equal to the left-hand-side of equation (98), it can be easily shown, that for K and y_o' in the restricted range given by equation (99),

$$f(0) < 0, \quad f(\pi/2) > 0, \quad f(\pi) < 0,$$

which implies that there are always two stagnation points on the cylinder in the range $0 < \theta < \pi$. Further, depending on the value y_o' there may be one or two stagnations points in the range $\pi < \theta < 2\pi$. This final result, of course, is not entirely unexpected, since the back flow is comparable to that in the constant shear case in chapter II. With y_o' in the range given by relation (99), there are only two stagnation points on the cylinder, and those lie in the range $0 < \theta < \pi$. However, a limiting value for y_o', which may be denoted by $(y_o')_c$, can easily be found, for which the two stagnation points in the range

$\pi < \theta < 2\pi$ coalesce at the point $\theta = {}^{3\pi}/_{2}$, prior to moving off the cylinder along the y-axis. This limiting value is given in terms of K by

$$(y_o')_c = \tan^{-1}\left[\frac{2\sum_{m=1}^{\infty}(-1)^m \frac{J_{2m}(K)}{Y_{2m}(K)} Y'_{2m}(K) + \sin K}{2\sum_{m=0}^{\infty}(-1)^{m+1} \frac{J_{2m+1}(K)}{Y_{2m+1}(K)} Y'_{2m+1}(K) + \cos K}\right] \text{----------(100)}$$

Thus, there are four, three and two stagnation points on the cylinder for $y_o' < (y_o')_c$, $y_o' = (y_o')_c$ and $y_o' > (y_o')_c$ respectively. The important case from the point of view of representing the flow over the cylinder in a boundary layer, is the case where $(y_o') > (y_o')_c$. Figure (13) illustrates the flow field for the case $y_o' = {}^{\pi}/_{4}$, when there are only two stagnation points on the cylinder, the region $x \leqslant 0$ only being shown, since the flow field is symmetrical about the y-axis. It should perhaps be mentioned at this stage, that the third stagnation point, which is always in the flow and on the line $\theta = {}^{3\pi}/_{2}$, is at a distance from the origin which is always greater than y_o', as is illustrated in the figure.

Denoting the solution of equation (98) in the $0 < \theta < \pi$ range by θ_c, the deflection, y_c, of the stagnation point on the cylinder from the x-axis, is given by $y_c = r_o \sin \theta_c$, or, in non-dimensional form, with $\frac{2\pi r_o}{\pi}$ as the typical linear dimension, by

$$y_c' = {}^{y_c}/_{\frac{2\pi r_o}{\pi}} = K \sin \theta_c \,. \text{----------(101)}$$

The actual deflection of the stagnation stream line in non-dimensional form, $\delta' = {}^{\delta}/_{\frac{2\pi r_o}{\pi}}$, is given by

$$\delta' = y_s' - y_c' \,, \text{----------(102)}$$

where y_s' is given by equation (97). It should be mentioned, that for y_o' in the

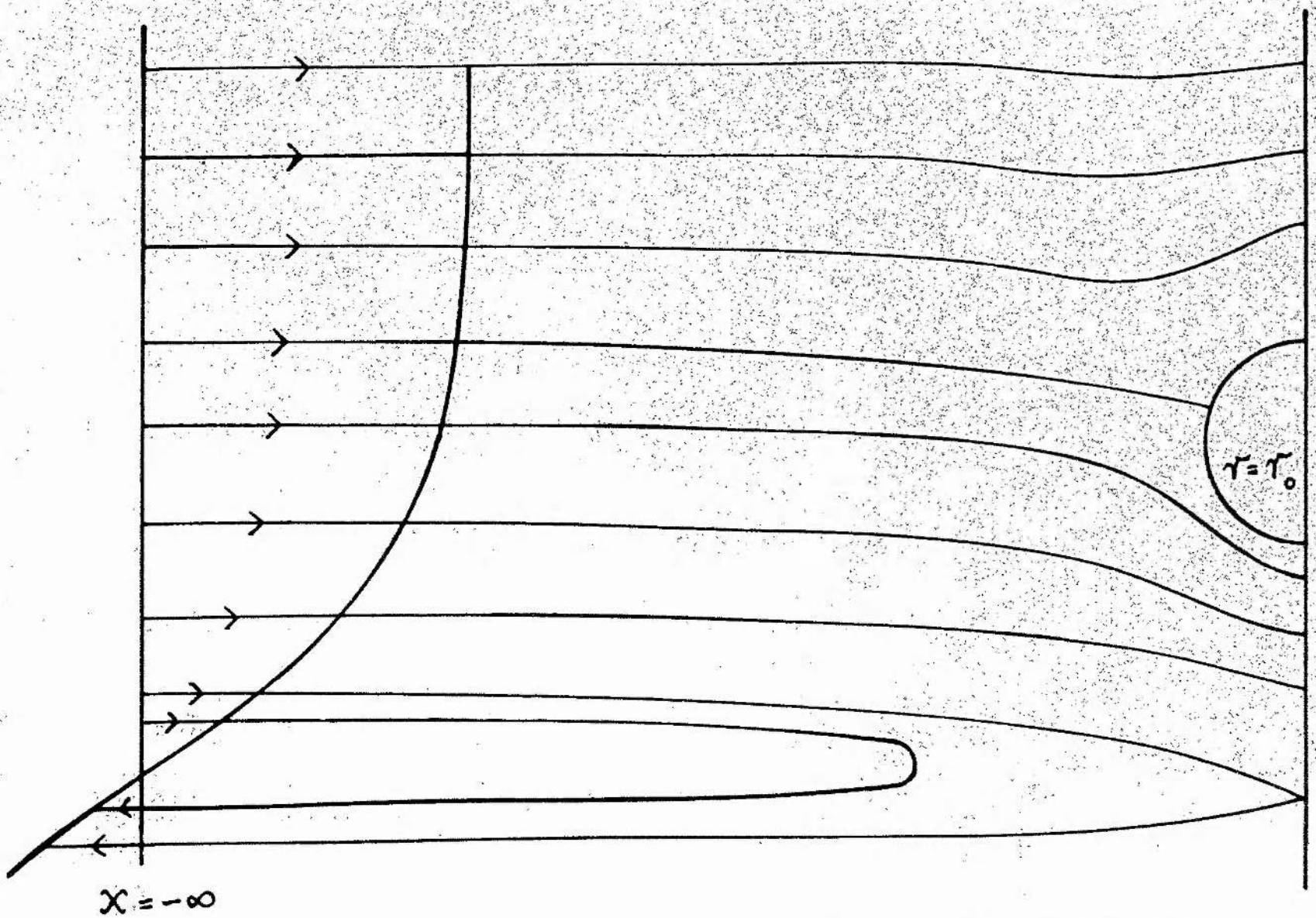

Figure (13) Illustration of the stream lines for a circular cylinder in a rotational flow approximating to that in a boundary layer.

range given by relation (99), δ' is always positive. To obtain y_c' and δ' in terms of y_c/r_o and δ/r_o, the quantities in equations (101) and (102) must be divided by K.

The profile distortion Δ is defined as the deviation of the stream line $\psi = 0$, which has free stream velocity U, measured along the y-axis through the centre of the cylinder. It is given in non-dimensional form by

$$\Delta' = \frac{\Delta}{\frac{2kr_o}{\pi}} = \left(x'_{\theta = \frac{\pi}{2}}\right)_{\psi = 0} - \left(\frac{\pi}{2} - y_o'\right) ,$$

which gives

$$\frac{\Delta}{kr_o} = \frac{2}{\pi}\left[\left(x'_{\theta = \frac{\pi}{2}}\right)_{\psi = 0} + y_o' - \frac{\pi}{2}\right]. \qquad (103)$$

Figure (14) illustrates the variation of Δ/kr_o with y_o/kr_o, for various values of k. The sections of the curves for y_o' in the range given by relation (99) are those to the left of the small segments of lines, on the actual curves, parallel to the Δ/kr_o-axis. The dashed parts of the curves are for $0 \leqslant \frac{\pi}{2} - y_o' \leqslant K$, which are included for completeness.

Again, numerical results are only obtained for the case of a circular cylinder in a variable shear flow of the type approximating to that in a boundary layer, and given by equation (80). Accordingly a short discussion of the results obtained is given at this stage.

Discussion of the Results on the Circular Cylinder

The phenomenon of the stagnation stream line coming from a region of higher velocity than that opposite the centre of the cylinder is again in evidence, and is illustrated quantitatively in Figure (12) and qualitatively in Figure (13). Also, the non-dimensional parameter $N = \frac{U}{\omega_o l}$, again appears in the vorticity distributi

Although too much stress must not be laid on the fact that the flow derived

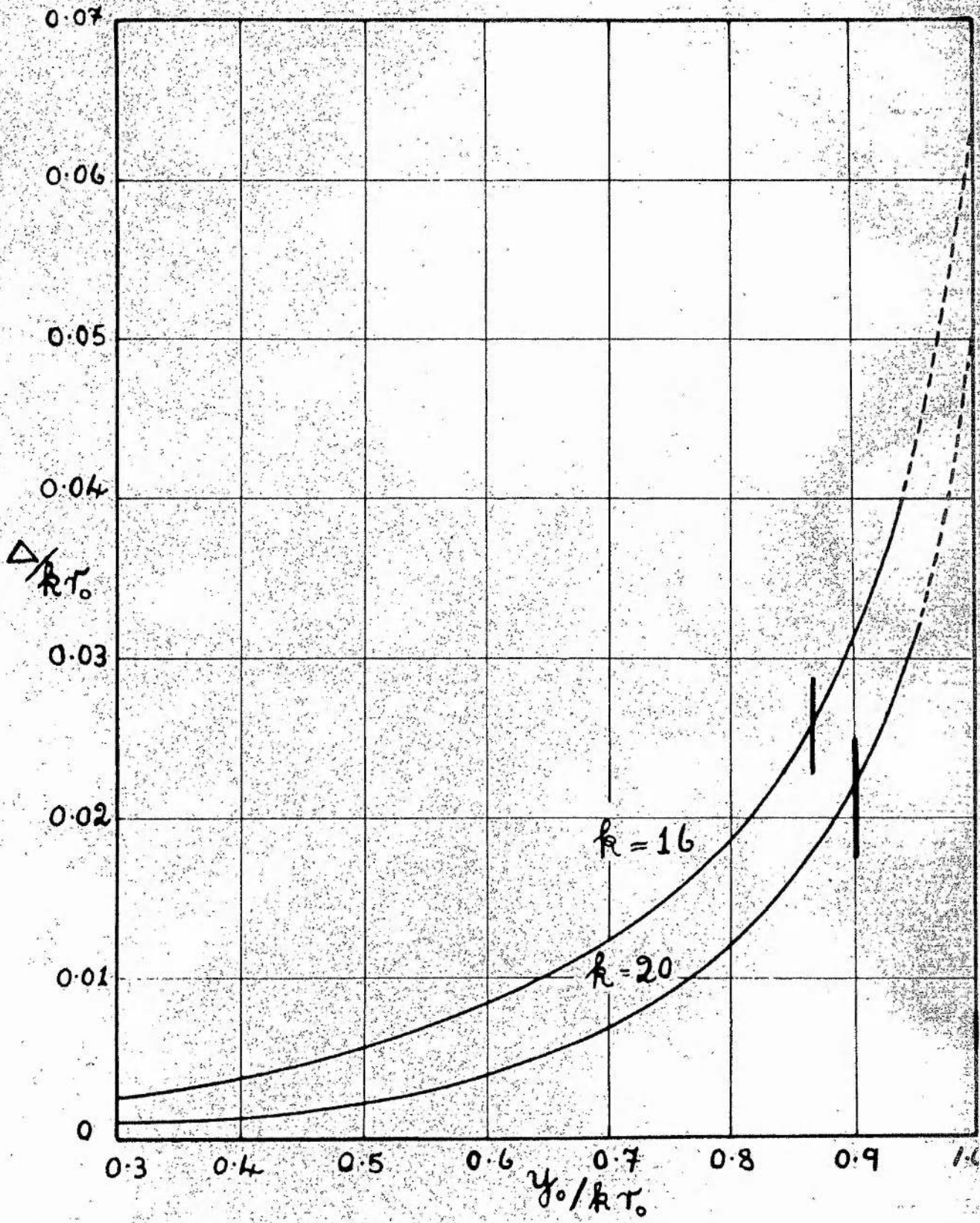

Figure (14) Illustration of the distortion in the stream line having velocity U in the free stream.

in the last section is comparable to that past the same cylinder with a boundary layer free stream velocity profile, the qualitative results obtained, especially in the range $4K < y_0' < \frac{\pi}{2} - 2K$, are probably in reasonably close agreement particularly for cylinders of small radius of say $K < \frac{\pi}{40}$, that is $r_0 < \frac{1}{20}\delta$. In fact the flows are similar over a band stretching from $x = -\infty$ to $x = +\infty$ enclosing the immediate neighbourhood of the cylinder. It can only be hoped that the back flows do not appreciably affect the flow characteristics in the neighbourhood of the cylinder. It must also be emphasized that viscosity is absent from all considerations.

Further to the discussion on the circular cylinder in a flow approximating to a linear shear distribution, the results illustrated in Figure (12) tend to substantiate the conjecture that the large displacements of the stagnation streamlines obtained from experiment are due to the three-dimensional nature of the flow. In fact for cylinders in the upper half of the 'boundary layer' the deflection is less than 0.05.

To illustrate further the general method a short discourse on the elliptic cylinder in a flow of the type given by equation (72) is now given.

The Elliptic Cylinder

Only a bare outline of the method is given at this stage, since the method of procedure is similar to that given in the case of the linear shear approximation.

An elliptic cylinder, whose equation is given by (34), is introduced at the origin and the problem illustrated by Figure (c). The flow can be obtained using the general method. Taking the typical length as b, the semi-minor axis, the equation in non-dimensional form becomes

$$r' = \frac{r}{\frac{2kb}{\pi}} = \frac{p/b \, \frac{\pi}{2k}}{1 + e\cos\theta} = \frac{(1-e^2)^{\frac{1}{2}} \, \frac{\pi}{2k}}{1 + e\cos\theta} = \chi(\theta) \ ,$$

which on putting $K = (1-e^2)^{\frac{1}{2}} \frac{\pi}{2k}$, defines $\chi(\theta)$. In the case of the elliptic cylinder with its major axis in the direction of flow, the required equation for evaluating the constants in the stream function is equation (87), which, with the value of $\chi(\theta)$ defined above, becomes

$$c = a\cos\left(\frac{K\sin\theta}{1 + e\cos\theta}\right) + b\sin\left(\frac{K\sin\theta}{1 + e\cos\theta}\right)$$

$$+ \sum_{m=0}^{\infty} (a_m \cos m\theta + b_m \sin m\theta) \, Y_m\left(\frac{K}{1 + e\cos\theta}\right) \ , \qquad (104)$$

where a and b in this equation are the constants in equation (72), and must not be confused with the semi-major and minor axes of the ellipse. The expansion of $Y_m\left(\frac{K}{1 + e\cos\theta}\right)$ as a cosine series is comparable to that given for $K_m\left(\frac{1}{1 + e\cos\theta}\right)$ and the general remarks on that expansion are applicable in this case with slight modification. The Fourier series of $\frac{\cos}{\sin}\left(\frac{K\sin\theta}{1 + e\cos\theta}\right)$ are obtained in a similar manner to the exponential function in the previous case. Each term in the expansion of the two functions is expressed as a Fourier series, i.e. each term in the two series given by

$$\cos\left(\frac{K\sin\theta}{1 + e\cos\theta}\right) = \sum_{r=0}^{\infty} \frac{(-1)^r K^{2r}}{(2r)!} \left(\frac{\sin\theta}{1 + e\cos\theta}\right)^{2r} \ ,$$

$$\text{and} \quad \sin\left(\frac{K\sin\theta}{1 + e\cos\theta}\right) = \sum_{r=0}^{\infty} \frac{(-1)^r K^{2r+1}}{(2r+1)!} \left(\frac{\sin\theta}{1 + e\cos\theta}\right)^{2r+1} \ .$$

The method, as stated, is the same as described previously and equations (38), (39), (40), (41), (42), (43), and (44) are applicable directly.

Thus, with the appropriate minor modifications, to the previous method

involving the elliptic cylinder, the stream function ψ , for flow of the type given by equation (72) past an elliptic cylinder, with its major axis in the direction of flow, can be obtained, and is given by equation (86). The coefficients a_m and b_m are evaluated as in the case of the linear shear flow past the same cylinder.

For an approximation to the boundary layer flow, the restrictions on K, defined above, and y_o' are the same as those for the circular cylinder, where s must, of course, be less than unity to keep $\chi(\theta)$ free from singularities. The velocity at any point can be obtained from equation (91), and in particular on the cylinder using equations (55), with only slight change in meaning and notation.

The stream function for the flow past the elliptic cylinder with its minor axis in the direction of flow can also be obtained following the method given in the case of the linear shear approximation. Care must be taken, however, in defining the restricted range for the quantity x_o', and K, as defined by $(1-e^a)\frac{\pi}{2k}$, must satisfy the same condition as before.

Thus, stream functions for elliptic cylinders in a flow of the type given by equation (72) can be obtained. The qualitative results are similar to those given in the case of the circular cylinder, whilst quantitative results, although involving much laborious calculation, can be easily obtained. Finall remarks of a general nature concerning the linear shear flow case are applicabl once more, with only slight modification.

Summary and Conclusions

The application of a transformation to the stream function for a free stream variable shear flow, enables the stream function to be obtained for flo past a cylinder situated in a variable shear flow. Over a range of two body diameters on either side of the axis, the free stream flow approximates to

the flow arising from a linear vorticity distribution. A general method is derived, for flow past any cylinder whose equation can be expressed in polar coordinates in the form $r' = \chi(\theta)$. The flow past a circular cylinder is considered, and the main physical features evaluated in some detail. In cases other than the circular cylinder, certain difficulties arise, which, although not unsurmountable require rather complicated analysis, as illustrated in the case of the elliptic cylinder.

The principle physical features of the shear flows are determined, particular attention being given to the deflections of stagnation points and stagnation streamlines. In each case, it is found that the deflection of the stagnation stream line in the free stream is in a direction towards a region of higher velocity than that opposite the centre of the cylinder.

Using a comparable method, a transformation is applied to the stream function for a free stream flow with a sine velocity profile and the stream function is obtained for the flow past a cylinder. If the cylinder is suffic small and reasonably situated, an approximation is obtained to the flow in a boundary layer past the cylinder. The particular case of the circular cylinder in this flow is studied, and detailed numerical results obtained. Particular attention is given to the various deflections of the stagnation points and stream lines. The method for obtaining the stream functions for the flow past the elliptic cylinder with major and minor axes in the direction of flow respectively is briefly described. No calculations were made, since the method is comparable to that for the linear shear flow past the same cylinders. Due to the rather complicated nature of the free stream distribution of flow, the range of variation of position of the cylinder in this velocity profile is somewhat limited for favourable comparison with the actual flow in a boundary layer. General limits are given for this range in

terms of the diameter of the cylinder in each specific example. In each case, the stagnation stream line comes from a region of higher velocity in the free stream than that opposite the centre of the cylinder. It must be emphasized, however, so that too close a parallel will not be drawn between this flow and that in a boundary layer, that throughout this work there is a complete absence of viscosity.

One feature of the analysis in this chapter is the necessity for a condition on the flow, involving circulation considerations. Without this condition a single infinity of solutions is obtained. Now, it is highly probable that there is only one solution to the problem in practice. Accordingly a condition stating the constancy of the circulation round a path coinciding with the perimeter of the cylinder is not unreasonable, since although not used specifically, this condition is also in evidence in constant shear flow. (Chapter II).

As in chapter II, the non-dimensional number N, appears repeatedly, and plays a major role in the final results. Although it is not the only parameter in the flow, it is still of primary importance.

An important conclusion from the work in this chapter and in chapter II is the fact that the large displacements of the stagnation stream lines in the free stream obtained from experiment are probably due to the three-dimensional nature of the experiments. This conjecture would explain the large discrepancy between the theoretical values obtained in this thesis and by Davies [37] and the three-dimensional experimental results of Young and Maas [35].

In conclusion, elliptic cylinders do not exhaust the possible cross sections for which the stream functions can be obtained using the general

methods derived in this chapter. They do, however, illustrate the difficulties involved in obtaining the stream functions for variable shear flows past cylinders whose cross sections are not circular. Further, the work in this chapter illustrates the difficulties which may be expected to arise in attempting to derive analytically stream functions for cylinders in two-dimensional variable shear flows of a more complicated nature, either compressible or incompressible. Accordingly, after several unsuccessful attempts to derive analytically the stream functions for two-dimensional compressible shear flows, it was decided to employ finite difference and relaxation methods. These methods are illustrated in the next chapter.

Chapter IV

Application of Relaxation Methods to Rotational Flow Problems

Application of Relaxation Method to Rotational Flow Problems

Relaxation methods in two dimensions were developed by A. Thom (Method of Squares) and R.V. Southwell , in order to solve certain partial differential equations arising in physics, engineering and fluid dynamics. These methods have been used extensively in the solution of equations governing flows without rotation. However, when rotation is present, the application has been somewhat limited as mentioned in chapter I. References [25] , [26], [28], [29], [31], [32] and [33], comprise the majority of papers on finite difference and relaxation methods applied to flows with rotation present.

As far as the author is aware, no solution has yet been obtained for the two-dimensional inviscid, compressible, isentropic rotational flow of a fluid through a channel with a constriction present. Accordingly, in this chapter, a relaxation solution is obtained for compressible, isentropic, rotational flow at low Mach number through a two-dimensional channel with straight parallel sides containing a discontinuous constriction: the channel is illustrated in Figure (a). A solution is also obtained for incompressible flow with constant rotation through the same channel.

From the diagrams of stream lines, constant velocity lines and constant vorticity lines, obtained from the solutions, certain tentative suggestions are made as to the nature of the physical features in the flow of a real fluid through the channel.

The method evolved in this chapter is also applicable to channels with shapes other than the one shown in Figure (a). The method, however, is only valid for flows where the velocity is everywhere subsonic, except for small

locally supersonic regions.

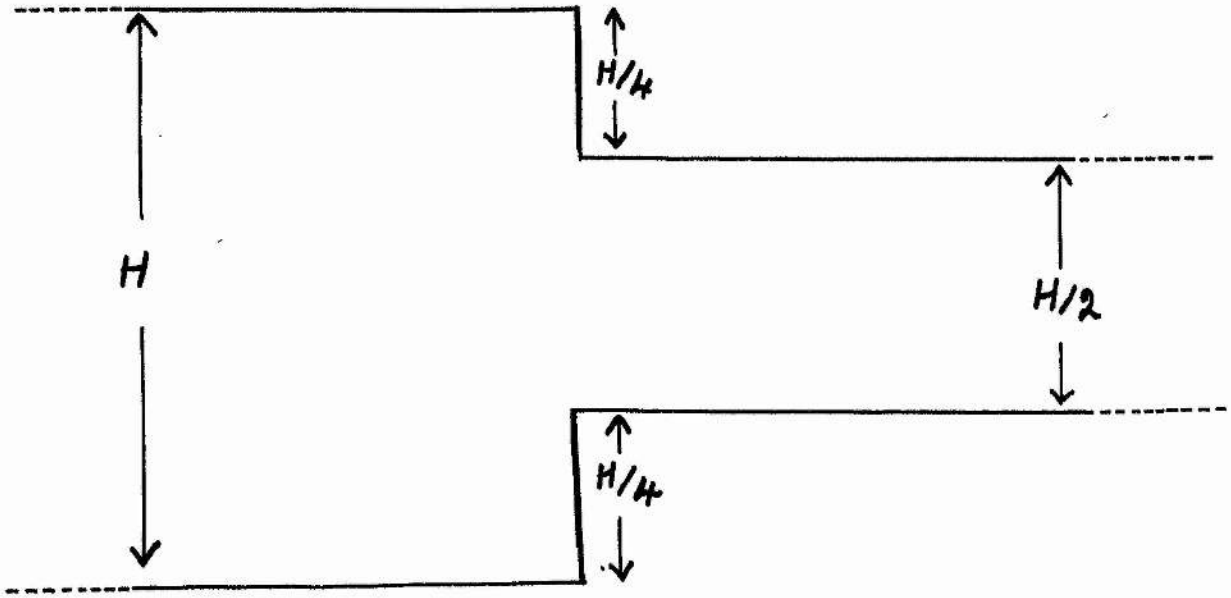

Figure (e).

Problem I

Two-Dimensional Incompressible Flow with Constant Rotation through a Channel

The Fundamental Equations and Boundary Conditions.

The channel is illustrated in Figure (a), and the region over which the equations are relaxed is from a station, upstream of the constriction, where free stream conditions (parallel flow) exist, to a station downstream, where the flow is again assumed to be parallel.

From the definition of the vorticity ω (I.5), and the introduction of the stream function ψ (I.3), the single equation governing the flow is (I.15)

$$\frac{\partial^2 \psi}{\partial x^2} + \frac{\partial^2 \psi}{\partial y^2} + \omega = 0, \qquad (1)$$

where the vorticity ω is constant across the entrance and so is constant throughout the flow (I.10), and x and y are the rectangular cartesian coordinates. The partial differential equation (1) is of elliptic type (Poisson's equation), and for a unique solution to exist, conditions must be given on a closed boundary. In the incompressible case, the boundary conditions are straightforward, consisting of the assumption of parallel flow a distance, say $2H$, upstream and downstream of the constriction. This results in

$$-q_y = \frac{\partial \psi}{\partial x} = 0,$$

at these stations, where q_x and q_y are the component velocities. Thus, from equation (1), the free stream ψ is obtained by integration and assigning values to the two constants of integration. This stream function

ψ , together with ω give a complete description of the parallel flow upstream of the constriction. Finally, in the downstream undisturbed flow ψ, q, and ω, which remains constant throughout, are obtained in a similar manner, and so ψ is defined round a boundary enclosing the field of flow.

So far, no mention has been made of the direction of flow through the channel. In fact the numerical calculation covers both cases. For convenience of description, however, the flow is assumed to be from the wide to the narrow section of the channel.

In the undisturbed parallel flow upstream and downstream of the constriction, the following conditions hold for ψ :

$$\frac{\partial \psi}{\partial x} = 0 \quad , \quad \frac{\partial^2 \psi}{\partial y^2} = -\omega \quad ,$$

which give

$$\psi = A + B y - \frac{\omega}{2} y^2 \quad , \quad q = q_x = \frac{\partial \psi}{\partial y} = B - \omega y \quad .$$

Introducing G, the mass flow through the channel per second, and letting

$$\psi = 0 \quad \text{when } y = 0,$$

and

$$\psi = G \quad \text{when } y = H,$$

the upstream free stream conditions become

$$\psi = (G + \tfrac{\omega}{2} H^2) y/H - \tfrac{\omega}{2} y^2 \quad ,$$

and ----------(2)

$$q = (G/H + \tfrac{\omega}{2} H) - \omega y \quad ,$$

respectively. Downstream of the constriction, since ψ remains constant on the channel walls, the conditions are

$$\psi = 0 \quad \text{when } y = H/4$$

and

$$\psi = G \quad \text{when } y = 3H/4 \quad ,$$

which result in the downstream free stream conditions

$$\psi = -\left(\tfrac{1}{2}G + \frac{3}{32}\omega H^2\right) + \left(2G + \frac{\omega}{2}H^2\right)\frac{y}{H} - \frac{\omega}{2}y^2 \,, \qquad \text{----------(3)}$$

and

$$q = \left(2\frac{G}{H} + \frac{\omega}{2}H\right) - \omega y \,,$$

respectively. Thus, with $\psi = 0$ and G on the walls, initial free stream conditions (2) and final free stream conditions (3), a unique solution is defined in the channel.

Introduction of Non-Dimensional Quantities.

To facilitate the calculations made at a later stage, it is desirable to introduce non-dimensional quantities. If

$$\psi' = \psi/G \,,\ q' = q/U \,,\ x' = x/H \,,\ y' = y/H \,,$$

where G (of dimensions velocity × length, since the density, being constant, may be taken as unity) as mentioned before, is the mass flow through the channel, U is a typical velocity (the velocity at the centre of the channel in the undisturbed flow upstream of the constriction) and H is the width of the channel, then equation (1) becomes

$$\nabla'^2\psi' + \frac{1}{N} = 0 \,,$$

where $\nabla'^2 = \dfrac{\partial^2}{\partial x'^2} + \dfrac{\partial^2}{\partial y'^2}$, and the non-dimensional parameter $N = \dfrac{U}{\omega H}$.

For convenience, the dashes are dropped, although in the following work it must be remembered that non-dimensional quantities are being used. Accordingly the governing equation becomes

$$\nabla^2\psi + \frac{1}{N} = 0 \,, \qquad \text{----------(4)}$$

with initial (upstream) conditions

$$\psi = \left(1 + \frac{1}{2N}\right)y - \frac{1}{2N}y^2 \,,$$

and

$$q = \left(1 + \frac{1}{2N}\right) - y/N \qquad \text{----------(5)}$$

and final (downstream) conditions

$$\psi = -\left(\tfrac{1}{3} + \frac{3}{32}\,\frac{1}{N}\right) + \left(2 + \frac{1}{2N}\right) y - \frac{1}{2N}\, y^2 ,$$

and ----------(6)

$$q = \left(2 + \frac{1}{2N}\right) - y/N ,$$

from which it is easily checked that $\psi = 0$ and 1 on the lower and upper walls respectively.

Once the stream function has been specified on the walls, the only parameter remaining is N. The value of N (> 0 for positive vorticity, < 0 for negative vorticity) is not entirely arbitrary if normal flow conditions are to prevail in the free stream. Thus, the condition for no back flow in the free stream, upstream of the constriction, is that the velocity q, given by equation (5) is greater than zero at all points $0 \leqslant y \leqslant 1$. This results in the inequality $1 - \frac{1}{2N} > 0$, which leads to the condition

$$N > \tfrac{1}{2} ,$$

which implies small vorticity. In conclusion, a given N ($> \frac{1}{2}$) defines the stream function round the closed boundary. If the vorticity is negative the condition becomes $|N| > \frac{1}{2}$.

In the following, equation (4) is replaced by a finite difference approximation, which is solved by relaxation methods.

Finite Difference Approximation to the Fundamental Equation and Method of Solu

The field is covered by a square network of the type shown in Figure (b).

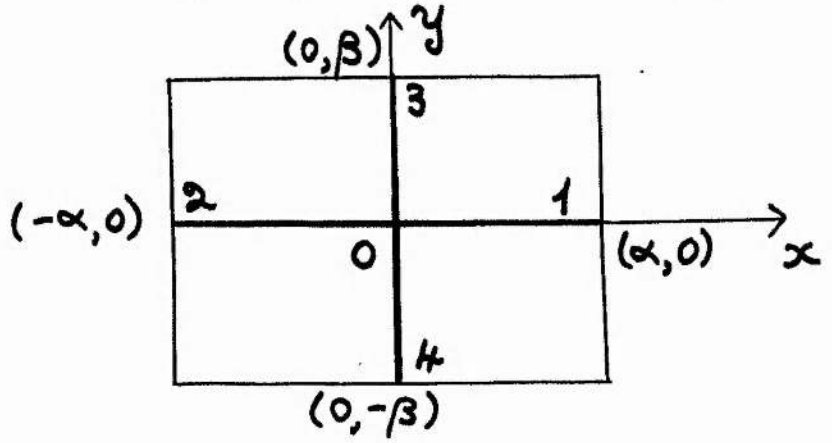

Figure (b)

The non-dimensional increments in the x- and y- directions are α and β. Figure (1) shows how such a network as illustrated in Figure (b) covers the required field of flow, leaving no irregular stars.

Using Taylor's theorem, the stream function $\psi(x,y)$ can be expanded at the nodes 1, 2, 3 and 4, as follows:

$$\psi_1 = \psi_0 + \alpha\left(\frac{\partial\psi}{\partial x}\right)_0 + \frac{\alpha^2}{2!}\left(\frac{\partial^2\psi}{\partial x^2}\right)_0 + \cdots$$

$$\psi_2 = \psi_0 - \alpha\left(\frac{\partial\psi}{\partial x}\right)_0 + \frac{\alpha^2}{2!}\left(\frac{\partial^2\psi}{\partial x^2}\right)_0 - \cdots$$

$$\psi_3 = \psi_0 + \beta\left(\frac{\partial\psi}{\partial y}\right)_0 + \frac{\beta^2}{2!}\left(\frac{\partial^2\psi}{\partial y^2}\right)_0 + \cdots$$

$$\psi_4 = \psi_0 - \beta\left(\frac{\partial\psi}{\partial y}\right)_0 + \frac{\beta^2}{2!}\left(\frac{\partial^2\psi}{\partial y^2}\right)_0 - \cdots$$

Summing these equations, and neglecting terms of the fourth order and higher in α and β, it is found that

$$\left(\frac{\partial^2\psi}{\partial x^2} + \frac{\partial^2\psi}{\partial y^2}\right)_0 = \frac{\psi_1+\psi_2-2\psi_0}{\alpha^2} + \frac{\psi_3+\psi_4-2\psi_0}{\beta^2}\ .$$

Using this last relation the approximate finite difference equation corresponding to equation (4) is

$$\frac{1}{\alpha^2}\sum_{r=1,2}(\psi_r-\psi_0) + \frac{1}{\beta^2}\sum_{r=3,4}(\psi_r-\psi_0) + \frac{1}{N} = 0\ . \qquad \text{----------(7)}$$

In effect, the problem reduces to solving a set of n equations in n unknowns, where n is the number of nodes within the boundary. The n equations are in fact equation (7) written out for each internal node. Introducing the matrix

$$\Psi = \begin{bmatrix}\psi_1\\ \vdots\\ \psi_n\end{bmatrix},$$

the n equations may be written as

$$A\Psi = B,$$

where the n × n matrix A is known, and involves the known coefficients of $\psi_1, \ldots\ldots, \psi_n$, and the matrix B involves $\frac{1}{N}$ and known boundary values of ψ. The solution is then given by

$$\Psi = A^{-1} D,$$

where A^{-1} is the non-singular inverse of the matrix A, the values of ψ being read off immediately from the matrix equation. However, as will be shown in the numerical example given subsequently, the inversion is extremely difficult even in a problem with a small number of nodes. Thus, a method of relaxation described briefly below, is used.

A value of ψ is assigned to each internal node, and the residue R_o, obtained from equation (7), is given by

$$R_o \equiv \frac{1}{\alpha^2} \sum_{r=1,2} (\psi_r - \psi_o) + \frac{1}{\beta^2} \sum_{r=2,3} (\psi_r - \psi_o) + \frac{1}{N} = 0 \quad \text{----------(8)}$$

The values of ψ are altered until R_o is approximately zero at each internal node, the largest permissible value of R_o being determined by the accuracy requ in the solution. The original mesh lengths can then be halved or quartered, and the same procedure carried out. If required, particular regions of the field can be studied in greater detail. The complete procedure is carried out until the required degree of accuracy is obtained. Figure (1) illustrated the problem with the initial mesh lengths.

The velocity at any point in the field can be obtained from

$$q^2 = \left(\frac{\partial \psi}{\partial x}\right)^2 + \left(\frac{\partial \psi}{\partial y}\right)^2,$$

after replacing $\frac{\partial \psi}{\partial x}$ and $\frac{\partial \psi}{\partial y}$ by finite difference approximations obtained from the Taylor expansions given at the beginning of this section. From the relations, neglecting terms of the second order and higher, in α and β,

$$\left(\frac{\partial \psi}{\partial x}\right)_o = \frac{1}{\alpha} (\psi_1 - \psi_0), \quad \left(\frac{\partial \psi}{\partial x}\right)_o = \frac{1}{\alpha} (\psi_2 - \psi_0)$$

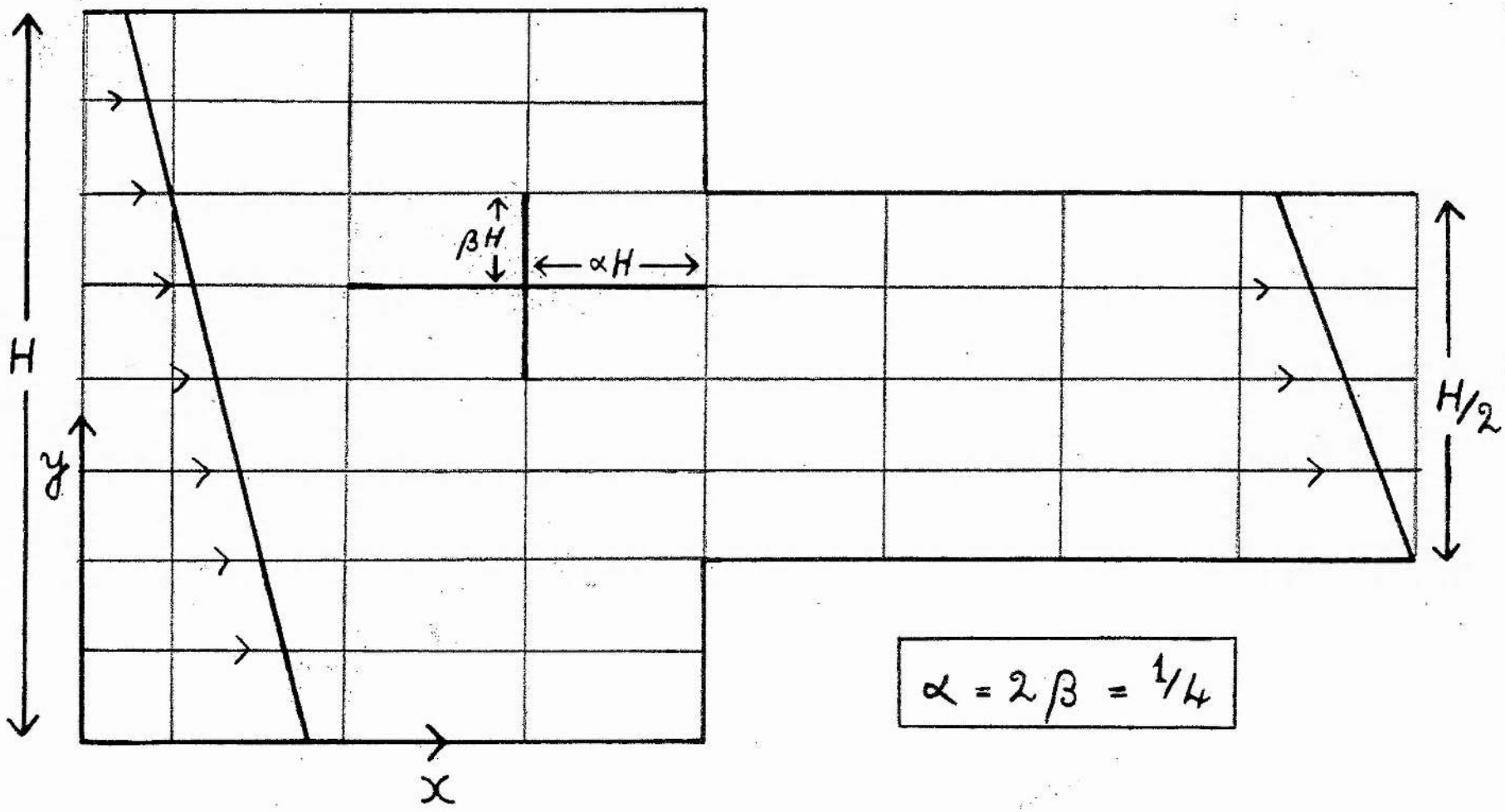

Figure (1) Illustration of the incompressible constant shear flow problem.

$$\left(\frac{\partial \psi}{\partial y}\right)_0 = \frac{1}{\beta}(\psi_3 - \psi_0) \quad , \quad \left(\frac{\partial \psi}{\partial y}\right)_0 = -\frac{1}{\beta}(\psi_4 - \psi_0) \quad .$$

On squaring and averaging the two values for each derivative squared, the approximate finite difference relation for the velocity at a regular star (i.e. a node not on the channel walls) is given by

$$q^2 = \frac{1}{2}\left[\frac{1}{\alpha^2}\sum_{r=1,2}(\psi_r - \psi_0)^2 + \frac{1}{\beta^2}\sum_{r=3,4}(\psi_r - \psi_0)^2\right] \quad .\text{-------(9)}$$

The same result can also be obtained by replacing the right-hand-side of

$$\left(\frac{\partial \psi}{\partial x}\right)^2 + \left(\frac{\partial \psi}{\partial y}\right)^2 = \frac{1}{2}\nabla^2(\psi^2) - \psi\nabla^2\psi$$

by the requisite finite difference approximation. Depending on the position of the node on the channel walls, either $\frac{\partial \psi}{\partial x}$ or $\frac{\partial \psi}{\partial y}$ is zero and the following method is adopted. A 3 point formula is used in the approximation as shown in Figure (c), where

$$\frac{\partial \psi}{\partial y} \neq 0.$$

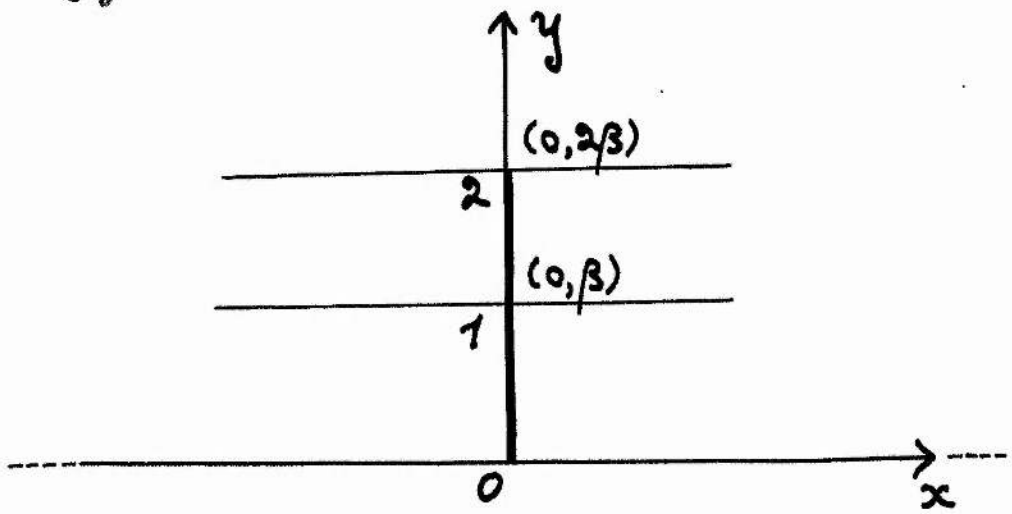

Figure (c)

Now $$\psi_1 = \psi_0 + \beta\left(\frac{\partial \psi}{\partial y}\right)_0 + \frac{\beta^2}{2!}\left(\frac{\partial^2 \psi}{\partial y^2}\right)_0 + \cdots\cdots$$

$$\psi_2 = \psi_0 + 2\beta \left(\frac{\partial \psi}{\partial y}\right)_0 + \frac{(2\beta)^2}{2!} \left(\frac{\partial^2 \psi}{\partial y^2}\right)_0 + \cdots\cdots$$

leading to

$$q^2 = \left(\frac{\partial \psi}{\partial y}\right)^2 = \frac{1}{4\beta^2} \left[3\psi_0 - 4\psi_1 + \psi_2\right]^2 .$$

At the constriction on the walls, where $\frac{\partial \psi}{\partial x} \neq 0$, the approximation

$$q^2 = \left(\frac{\partial \psi}{\partial x}\right)^2 = \frac{1}{4\beta^2} \left[3\psi_0 - 4\psi_1 + \psi_2\right]^2$$

is similarly obtained, using Figure (d).

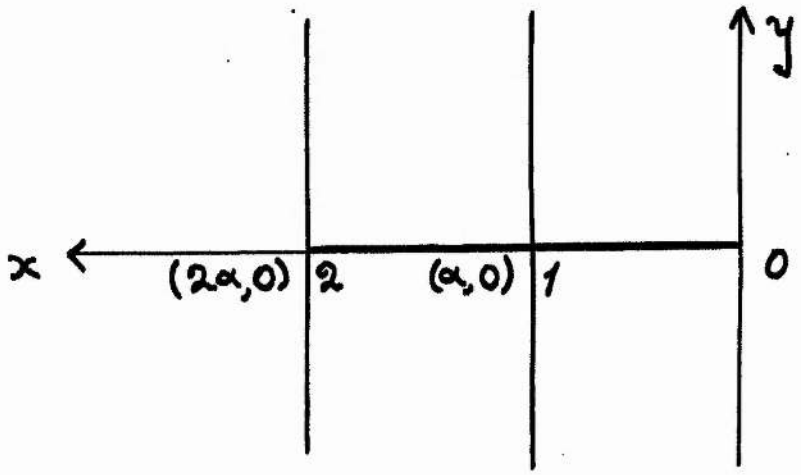

Figure (d)

Numerical Example

The problem evaluated has N = 1, equations (5) and (6) giving the initial and final free stream conditions respectively.

For completeness, the matrix form of equation (7) for twenty-three internal nodes, the unknowns being numbered from top to bottom, left to right, is shown in Figure (2). The form of the matrix A, is seen to be of diagonal type, $\psi_{(k)}$ denoting the known quantities on the boundary, ψ_k the unknown values within the boundary, N being left general, and with $\alpha = 2\beta = \frac{1}{4}$.

The inversion of the matrix A is extremely difficult and complicated numerically

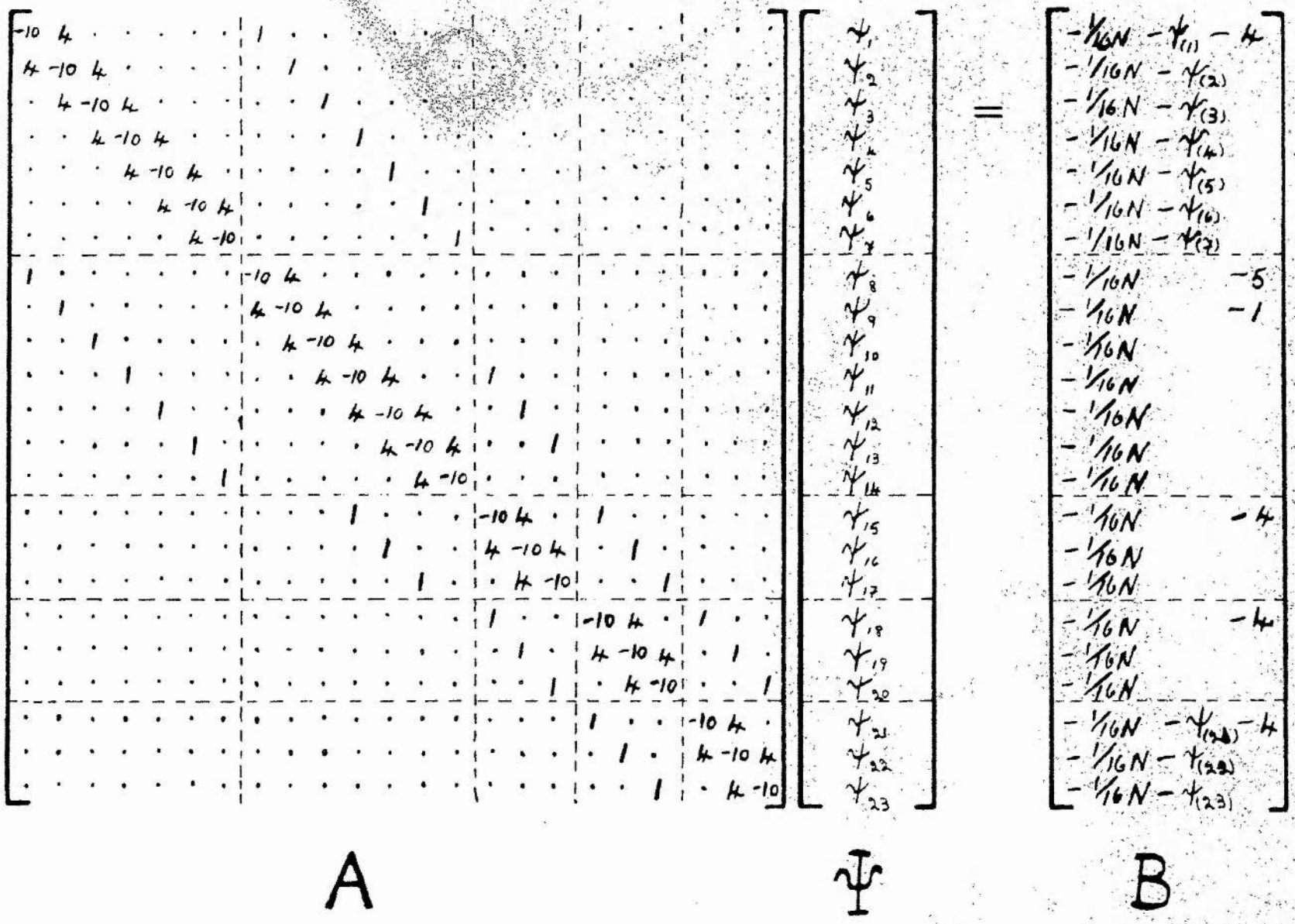

Figure (2) The matrix equation for the incompressible constant shear flow problem.

Accordingly, relaxation is employed at all stages.

The initial relaxation solution is obtained with a mesh length of $\alpha = 2\beta =$ (i.e. the x-mesh length is one quarter of the channel width) and free stream conditions are assumed to exist at a distance 1.5 H upstream of the constrictio Relaxation is carried out with values of ψ, taken to the third place of decimals, until the residue at each node is $\leqslant 0.005$. The mesh lengths, α and β, are then halved, and the same procedure carried out. The whole process is repeated until the required degree of accuracy is obtained. Figures (3) and (4) show the stream lines, with the initial and final velocity profiles, and the lines of constant velocity, respectively, for this particular problem.

Since relaxation is a purely numerical process, no distinction is made between flow from left to right in the channel, and vice-versa. Thus, Figures (3) and (4) also represent the flow field for the incompressible constant shear flow from the narrow to the wider section of the channel, the arrows in the profiles being merely reversed.

When the flow is <u>into</u> the narrow section of the channel, the central stream line in the undisturbed flow downstream of the constriction comes from a region of <u>higher</u> velocity in the undisturbed flow upstream of the constriction, than that opposite the centre of the channel, the non-dimensional deflection being -0.09. When the flow is <u>out of</u> the narrow section the corresponding central stream line comes from a region of <u>lower</u> velocity, the deflection being + 0.05. From Figure (4), it is seen that there are two regions of very low velocity in the outer corners of the constriction, as is expected from a physical point of view. It is also seen that there is a general overall displacement of regions of high velocity towards the lower

channel wall, as is also expected since the vorticity is everywhere constant, and the largest velocity is initially nearest the lower wall.

One further point arising from the analysis is the fact that the rotation present in the flow must be reasonably small in order to prevent back flow occurring in the channel, the condition on the shear parameter N, being $N > \frac{1}{8}$.

In problem II, compressibility is introduced, and a comparison is made with the incompressible case. Thus the effects due to compressibility on the shear flow through a channel containing a constriction are illustrated.

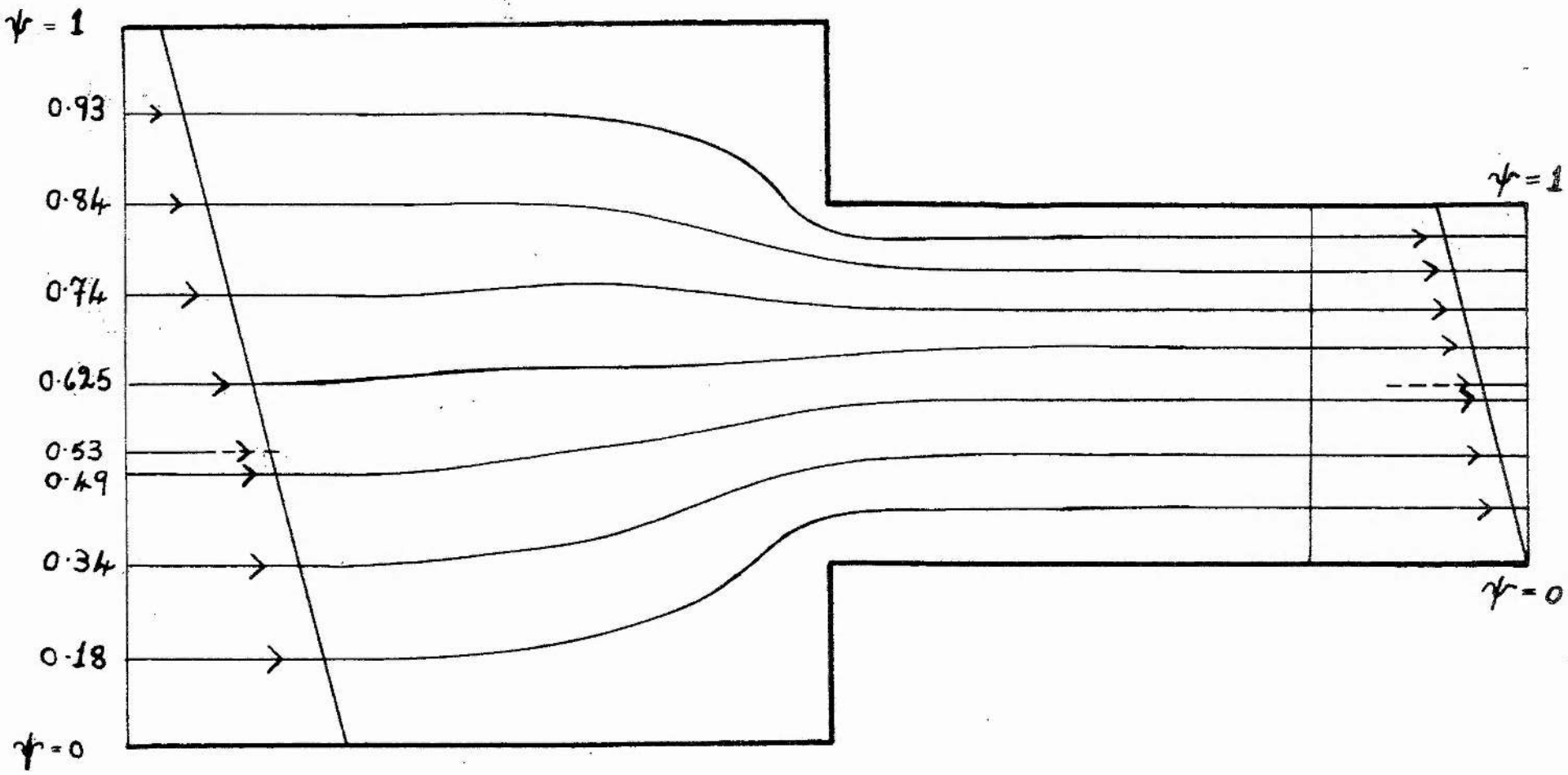

Figure (3) Illustration of the stream lines for the incompressible constant shear problem.

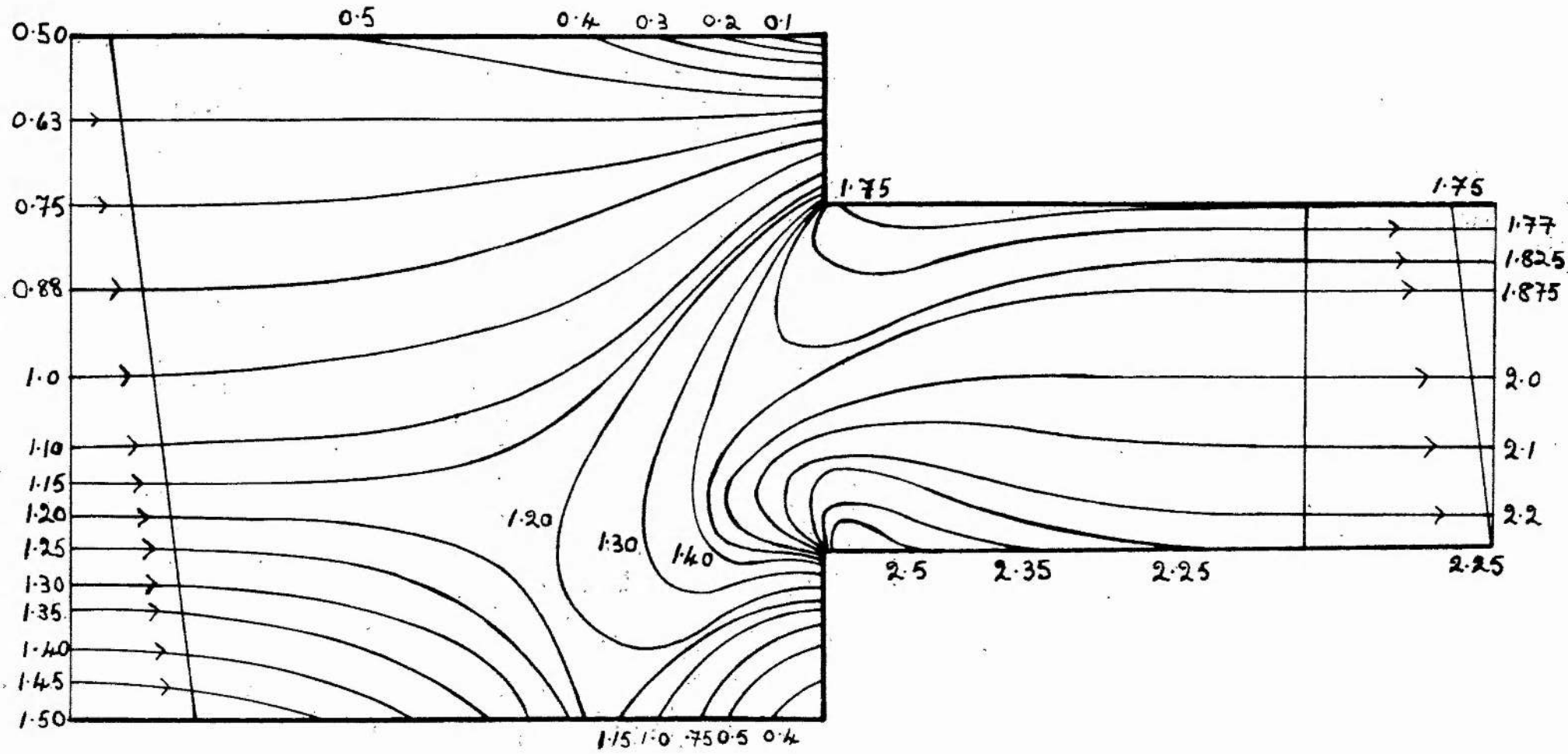

Figure (4) Constant velocity lines for the incompressible constant shear flow.

Problem II

Two-Dimensional Compressible Isentropic Rotational Flow through a Channel

The Fundamental Equations and Boundary Conditions.

In the two-dimensional steady motion of an isentropic rotational inviscid compressible fluid through a channel containing a constriction, as illustrated in Figure (a), the stream function ψ, and the stagnation enthalpy h_s, from the definition of vorticity, must satisfy (I.16)

$$\frac{\partial}{\partial x}\left(\frac{1}{\rho}\frac{\partial \psi}{\partial x}\right)+\frac{\partial}{\partial y}\left(\frac{1}{\rho}\frac{\partial \psi}{\partial y}\right)-\rho\frac{\partial h_s}{\partial \psi}=0 \quad . \qquad (10)$$

Bernoulli's equation for this flow, the fluid satisfying the adiabatic gas law, is given by (I.19),

$$\frac{\gamma}{\gamma-1}\frac{p}{\rho}+\frac{1}{2}q^2=h_s \quad , \qquad (11)$$

where p, ρ and q are the pressure, density and velocity respectively, (γ is the ratio of specific heats), and where the velocity is given by (I.8),

$$q^2=q_x^2+q_y^2=\left(\frac{1}{\rho}\frac{\partial \psi}{\partial y}\right)^2+\left(-\frac{1}{\rho}\frac{\partial \psi}{\partial x}\right)^2 \quad ,$$

where q_x and q_y are the component velocities.

It should be noted that in the free stream, where the flow is parallel, there is no pressure gradient across the channel: the density must also be constant across the channel since the adiabatic gas law $p/\rho^\gamma = k$ holds throughout the flow.

One further relation connection h_s, q, and the vorticity ω, in the free stream is (I.13)

$$\frac{\partial h_s}{\partial y}=-\omega q \quad , \qquad (12)$$

since y is, in this case, normal to the stream line.

Equation (10), which is a non-linear partial differential equation, must be solved simultaneously with equation (11). As to the nature of the boundary conditions, necessary for a unique solution, there is still some doubt in the general case, but in this particular problem the necessary conditions are more straightforward. In the free stream, if the vorticity ω is given (or h_s as a function of ψ), the stream function ψ is obtained from equation (10) by integrating and assigning values to the two arbitrary constants which appear, and since the density is constant, h_s follows from equation (11). In the case where the flow is into the constriction, the undisturbed flow downstream of the constriction satisfies the condition $\frac{\partial \psi}{\partial x} = 0$, since the flow at this station is assumed parallel, and, since h_s is constant along a stream line, a complete set of data can be obtained. Thus, in this problem, if $\frac{\partial \psi}{\partial x} = 0$ and ψ are given as the upstream conditions, and $\frac{\partial \psi}{\partial x} = 0$ is the downstream condition, a solution is defined in the required region of the channel containi the constriction.

In the undisturbed flow upstream of the constriction, the vorticity ω is constant across the channel and equal to ω_o, and, since the flow is parallel, and $q = q_x$,

$$\frac{\partial q_x}{\partial y} = -\omega_o \ ,$$

which gives

$$q_x = U - \omega_o y \ , \qquad \text{(13)}$$

where the velocity is U on the lower channel wall. Since the density $\rho = \rho_o$ is constant, and $q_x = \frac{1}{\rho_o} \frac{\partial \psi}{\partial y}$, integration gives

$$\psi = \rho_o U y - \tfrac{1}{2} \rho_o \omega_o y^2 \ , \qquad \text{(14)}$$

where the constant of integration is zero, since $\psi = 0$ when $y = 0$. From

equation (12), the stagnation enthalpy h_s, is given by

$$h_s = A - \omega_o U y + \frac{\omega_o^2}{2} y^2 \ ,$$

where A is the constant of integration, which is not arbitrary. Equation (11) must be satisfied by h_s, q, and ρ_o, where $p_o = k\rho_o^{\gamma}$, k being the adiabatic gas constant, and so the result

$$\frac{\gamma}{\gamma-1} k \rho_o^{\gamma-1} + \tfrac{1}{2}(U - \omega_o y)^2 = A - \omega_o U y + \frac{\omega_o^2}{2} y^2 \ ,$$

is obtained, from which

$$A = \frac{\gamma}{\gamma-1} k\rho_o^{\gamma-1} + \tfrac{1}{2} U^2 \ .$$

Thus, h_s as a function of ψ is given by

$$h_s = \left[\frac{\gamma}{\gamma-1} k\rho_o^{\gamma-1} + \tfrac{1}{2} U^2\right] - \frac{\omega_o}{\rho_o}\psi \ . \qquad (15)$$

This function of ψ remains as it is given by equation (15), since h_s is constan along a stream line. Thus, the upstream boundary conditions are given complet by relations (13) and (14), equation (15) being a subsequent result.

In the undisturbed flow downstream of the constriction, $\frac{\partial \psi}{\partial x} = 0$, and the density is again necessarily constant, equal to ρ_1 say. From equation (10

$$\frac{\partial}{\partial y}\left(\frac{1}{\rho_1}\frac{\partial \psi}{\partial y}\right) = \rho_1 \frac{\partial h_s}{\partial \psi} \ ,$$

from which

$$\psi = B + Cy - \tfrac{1}{2}\left(\frac{\omega_o}{\rho_o}\right)\rho_1^2 y^2 \ ,$$

where B and C are the constants of integration. The flow being continuous, gives the following two necessary conditions on ψ ,

$$\psi = 0 \text{ when } y = H/4 \ ,$$

$$\psi = \rho_o UH - \tfrac{1}{2}\rho_o \omega_o H^2 \text{ when } y = 3H/4 \ ,$$

where H is the width of the channel upstream of the constriction, and so

$$\psi = \left(\tfrac{1}{4} \rho_0 \omega_0 H^2 - \tfrac{1}{2} \rho_0 U H - \frac{3}{32} \frac{\omega_0}{\rho_0} \rho_1^2 H^2 \right)$$

$$+ \left(\tfrac{1}{2} \frac{\omega_0}{\rho_0} \rho_1^2 H + 2\rho_0 U - \rho_0 \omega_0 H \right) y - \tfrac{1}{8} \frac{\omega_0}{\rho_0} \rho_1^2 y^2 \quad , \text{----------(16)}$$

and the velocity

$$q = q_x = \frac{1}{\rho_1} \frac{\partial \psi}{\partial y} = \left(\tfrac{1}{2} \frac{\omega_0}{\rho_0} \rho_1 H + 2 \frac{\rho_0 U}{\rho_1} - \frac{\rho_0 \omega_0}{\rho_1} H \right) - \frac{\omega_0}{\rho_0} \rho_1 y \text{ .-------(17)}$$

As yet, ρ_1 is undetermined, but q given by equation (17) and h_s given by equation (15) must satisfy equation (11), which resultsin an equation involvin ρ_1 and the known constants ω_0, U, H and ρ_0, one solution of which is the requi value of ρ_1.

Alternatively, starting with equation (11), and obtaining the velocity, and stream function by integration and using the conditions on ψ, equations (16) and (17) are again obtained. In certain problems, it may be that this second procedure is quicker.

In conclusion, equations (13), (14), (16) and (17) completely determine the boundary conditions round a closed curve and are sufficient to ensure a solution for equations (10) and (11) within the required region.

Introduction of Non-Dimensional Quantities.

It is desirable to introduce dimensionless quantities at this stage, to facilitate the calculations made at a later stage.

If the basic quantites are taken as p_0, ρ_0, H and c_0, the values in the undisturbed flow upstream of the constriction, then $c_0^2 = \frac{\gamma p_0}{\rho_0}$, and $T_0 = \frac{1}{R} \frac{p_0}{\rho_0}$, where R is the gas constant. Further, introducing $G = \rho_0 c_0 H$, an

$$\psi' = \psi/G \ , \ q' = q/c_0 \ , \ \omega' = \omega/\omega_0 \ , \ h_s' = h_s/c_0^2 \ ,$$

$$p' = p/p_0, \ \rho' = \rho/\rho_0 \ , \ x' = x/H \ , \ y' = y/H$$

are substituted in equations (10) and (11) they become

$$\frac{\partial}{\partial x'}\left(\frac{1}{\rho'}\frac{\partial \psi'}{\partial x'}\right)+\frac{\partial}{\partial y'}\left(\frac{1}{\rho'}\frac{\partial \psi'}{\partial y'}\right)-\rho'\frac{\partial h_s'}{\partial \psi'}=0,$$

and

$$\frac{1}{\gamma-1}\frac{p'}{\rho'}+\tfrac{1}{2}q'^2=h_s'\ .$$

It should be noted that q' is not the local Mach number. Dropping the dashes, although it must be remembered that dimensionless quantities are being used, the problem may be given as follows:

the governing equations are

$$\frac{\partial}{\partial x}\left(\frac{1}{\rho}\frac{\partial \psi}{\partial x}\right)+\frac{\partial}{\partial y}\left(\frac{1}{\rho}\frac{\partial \psi}{\partial y}\right)-\rho\frac{\partial h_s}{\partial \psi}=0,\qquad\text{(18)}$$

and

$$\frac{1}{\gamma-1}\rho^{\gamma-1}+\tfrac{1}{2}q^2=h_s\ ,\qquad\text{(19)}$$

with initial condition

$$\psi=Uy-\frac{\omega_0}{2}y^2\ ,\qquad\text{(20)}$$

which leads to

$$q=q_x=U-\omega_0 y\ ,\qquad\text{(21)}$$

and final condition

$$\psi=\left(\tfrac{1}{4}\omega_0-\tfrac{1}{2}U-\frac{3}{32}\omega_0\rho_1^2\right)+\left(\tfrac{1}{8}\omega_0\rho_1^2+2U-\omega_0\right)y-\tfrac{1}{2}\omega_0\rho_1^2y^2\ ,\qquad\text{(22)}$$

which leads to

$$q=q_x=\left(\tfrac{1}{2}\omega_0\rho_1+\frac{2U}{\rho_1}-\frac{\omega_0}{\rho_1}\right)-\omega_0\rho_1 y\ .\qquad\text{(23)}$$

Now, ψ takes the required values on the channel walls for all ρ_1, and so to obtain a specific value for ρ_1, use is made of equation (19), which must be satisfied by the velocity given by equation (23), and by h_s, written in its dimensionless form. On substitution, the result

$$\frac{1}{\gamma-1}\,\rho_1^{\gamma-1} + \frac{1}{\gamma}\left[\left(\tfrac{1}{2}\omega_0\rho_1 + \frac{2U}{\rho_1} - \frac{\omega_0}{\rho_1}\right) - \omega_0\rho_1\, y\right]^2$$

$$= \left(\frac{1}{\gamma-1} + \tfrac{1}{2}U^2\right) - \omega_0\psi\,,$$

is obtained, where ψ is given by equation (22). This last equation reduces to an equation in ρ_1 as follows:

$$\frac{1}{16}\,\omega_0^{\,2}\rho_1^{\,4} + \frac{2}{\gamma-1}\,\rho_1^{\gamma+1} + \left(U\omega_0 - \tfrac{1}{2}\omega_0^{\,2} - U^2 - \frac{2}{\gamma-1}\right)\rho_1^{\,2}$$

$$+ (2U - \omega_0)^2 = 0, \qquad \text{----------(24)}$$

which gives ρ_1 as a function of U, ω_0 and γ. Generally there are two solutions for ρ_1 0, where the larger value is taken in subsonic flow, and the smaller, in the supersonic case.

To sum up, with ψ prescribed in the undisturbed flow upstream of the constriction, $\psi = 0$ on the lower wall, and ψ = the mass flow parameter on the upper wall, the stagnation enthalpy h_s given as a function of ψ, and with parallel flow conditions assumed to exist a suitable distance (approximately 2 upstream and downstream of the constriction, a solution is defined in the required rggion. The latter effectively stretches from $x = -\infty$ to $x = +\infty$, where the constriction is taken as $x = 0$. In a problem of this type, $h_s(\psi)$ defines the vorticity everywhere in the field from the relation $\omega = -\rho\frac{\partial h_s}{\partial \psi}$.

Further, if there is no back flow in the channel, equation (21) gives the resul that $\omega_0 < U$, from which it follows that $-\frac{\partial h_s}{\partial \psi} < U$ in the free stream. Using dimensional quantities,

$$N = \frac{q_{\text{central}}}{\omega_0 H} = q'_{\text{central}}\,\frac{c_0}{\omega_0 H} = \frac{q'_{\text{central}}}{\omega_0'}\,,$$

and so the condition becomes $N > \frac{q_{\text{central}}}{U}$ where q_{central} (the value of the undisturbed upstream velocity at the centre of the channel) and U are again in

non-dimensional form. On substitution for q central the condition reduces to the previous result namely $N > \frac{1}{2}$.

Finite Difference Approximations to the Fundamental Equations and Method of Solution.

Before obtaining finite difference approximations to equations (18) and (19), the equations are written in a form more amenable for replacement by finite difference approximations.

Introducing the non-dimensional quantity

$$\chi = \rho^{-\frac{1}{2}} \quad (\text{i.e. } \chi' = \chi/\chi_0 = \rho_0/\rho^{\frac{1}{2}}) ,$$

and substituting in equation (18), the latter becomes

$$\frac{\partial}{\partial x}\left(\chi^2 \frac{\partial \psi}{\partial x}\right) + \frac{\partial}{\partial y}\left(\chi^2 \frac{\partial \psi}{\partial y}\right) - \frac{1}{\chi^2}\frac{\partial h_0}{\partial \psi} = 0 .$$

A little manipulation now shows that this equation may be expressed as

$$\nabla^2 (\chi\psi) - \psi \nabla^2 \chi - \frac{1}{\chi^3}\frac{\partial h_0}{\partial \psi} = 0, \qquad (25)$$

where the non-dimensional Laplacian operator $\nabla^2 \equiv \frac{\partial^2}{\partial x^2} + \frac{\partial^2}{\partial y^2}$. Equation (19) can be written as

$$\tfrac{1}{2}\chi^4\left[\left(\frac{\partial \psi}{\partial x}\right)^2 + \left(\frac{\partial \psi}{\partial y}\right)^2\right] = h_0 - \frac{1}{\gamma - 1}\cdot\frac{1}{\chi^2(\gamma - 1)} ,$$

or in the form

$$\frac{\gamma - 1}{2}\left[\left(\frac{\partial \psi}{\partial x}\right)^2 + \left(\frac{\partial \psi}{\partial y}\right)^2\right] = \left[\frac{h_0(\gamma - 1)}{\chi^4} - \frac{1}{\chi^2(\gamma + 1)}\right]. \qquad (26)$$

Equations (25) and (26) are now replaced by finite difference approximations.

Since the flow is compressible, the corners must be treated separately, and in the calculation are excluded by the network chosen (Figure (5)). Although over most of the field, the net given in problem I is suitable, there are many irregular stars in the region near the corners of the constriction. Accordingly, a general net as shown in Figure (6) is used to establish

the finite difference approximations.

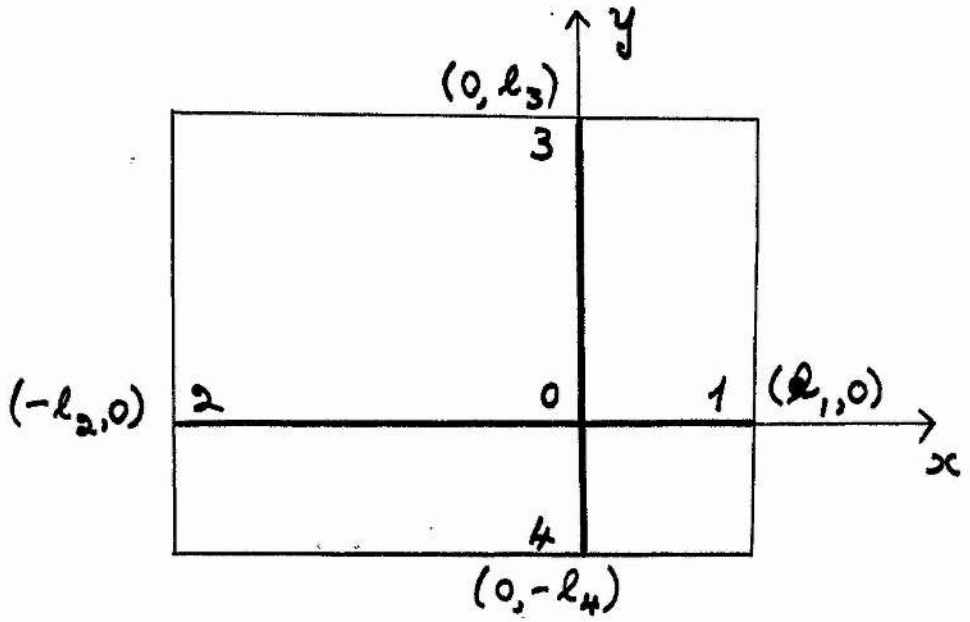

Figure (e)

In this five-point net, ℓ_1, ℓ_2, ℓ_3 and ℓ_4 are the non-dimensional increment in the x-and y- directions, the typical linear dimension being again H, the channel width.

Using Taylor's theorem in the case of the five-point net shown in Figure (the value of a function f, can be expanded at the several nodes as follows:

$$f_1 = f_o + \ell_1 \left(\frac{\partial f}{\partial x}\right)_o + \frac{\ell_1^2}{2!} \left(\frac{\partial^2 f}{\partial x^2}\right)_o + \cdots\cdots$$

$$f_2 = f_o - \ell_2 \left(\frac{\partial f}{\partial x}\right)_o + \frac{\ell_2^2}{2!} \left(\frac{\partial^2 f}{\partial x^2}\right)_o - \cdots\cdots$$

from which

$$(f_1 - f_o)\frac{1}{\ell_1} + (f_2 - f_o)\frac{1}{\ell_2} = \frac{(\ell_1 + \ell_2)}{2}\left(\frac{\partial^2 f}{\partial x^2}\right)_o$$

neglecting terms of the third order and higher in the lengths ℓ_1 and ℓ_2. Applying an exactly similar analysis to get $\left(\frac{\partial^2 f}{\partial y^2}\right)_o$, the following finite difference approximation is obtained:

$$\nabla^2 f = \frac{\partial^2 f}{\partial x^2} + \frac{\partial^2 f}{\partial y^2} = \frac{2}{\ell_1(\ell_1+\ell_2)}(f_1-f_o) + \frac{2}{\ell_2(\ell_1+\ell_2)}(f_2-f_o)$$

$$+ \frac{2}{\ell_3(\ell_3+\ell_4)}(f_3-f_o) + \frac{2}{\ell_4(\ell_3+\ell_4)}(f_4-f_o)$$

$$= \frac{2}{(\ell_1+\ell_2)} \sum_{r=1,2} \frac{1}{\ell_r}(f_r-f_o) + \frac{2}{(\ell_3+\ell_4)} \sum_{r=3,4} \frac{1}{\ell_r}(f_r-f_o) .$$

Using this last equation, first with $f = \chi\psi$, and then with $f = \chi$, and substituting in equation (25), the following finite difference equation, corresponding to equation (25) is obtained:

$$R_o \equiv \frac{2}{(\ell_1+\ell_2)} \sum_{r=1,2} \frac{\chi_r(\psi_r-\psi_o)}{\ell_r} + \frac{2}{(\ell_3+\ell_4)} \sum_{r=3,4} \frac{\chi_r(\psi_r-\psi_o)}{\ell_r}$$

$$- \chi_o^{-3}\left(\frac{\partial h_g}{\partial \psi}\right)_o = 0 , \qquad \text{----------(27)}$$

where R_o is the residual at the node O.

Similarly, choosing $f = \psi^2$ and $f = \psi$, it is seen that

$$\left(\frac{\partial \psi}{\partial x}\right)^2 + \left(\frac{\partial \psi}{\partial y}\right)^2 = \frac{1}{2}\nabla^2(\psi^2) - \psi\nabla^2\psi$$

$$= \frac{1}{(\ell_1+\ell_2)} \sum_{r=1,2} \frac{(\psi_r^2-\psi_o^2)}{\ell_r} + \frac{1}{(\ell_3+\ell_4)} \sum_{r=3,4} \frac{(\psi_r^2-\psi_o^2)}{\ell_r}$$

$$- \frac{2}{(\ell_1+\ell_2)}\psi_o \sum_{r=1,2} \frac{(\psi_r-\psi_o)}{\ell_r} - \frac{2}{(\ell_3+\ell_4)}\psi_o \sum_{r=3,4} \frac{(\psi_r-\psi_o)}{\ell_r}$$

$$= \frac{1}{(\ell_1+\ell_2)} \sum_{r=1,2} \frac{(\psi_r-\psi_o)^2}{\ell_r} + \frac{1}{(\ell_3+\ell_4)} \sum_{r=3,4} \frac{(\psi_r-\psi_o)^2}{\ell_r} .$$

Substituting in equation (26), and introducing D_o the result

$$D_o \equiv \frac{\gamma-1}{2}\left[\frac{1}{(l_1+l_2)}\sum_{r=1,2}\frac{(\psi_r-\psi_o)^2}{l_r}+\frac{1}{(l_3+l_4)}\sum_{r=3,4}\frac{(\psi_r-\psi_o)^2}{l_r}\right]$$

$$=\left[\frac{1+(\gamma-1)(\tfrac{1}{2}v^2-\omega_o\psi)}{\chi_o^4}-\frac{1}{\chi_o^{2(\gamma+1)}}\right], \qquad \text{----------(28)}$$

is obtained, which is the approximate finite difference equation corresponding to equation (26). On the channel walls, either $\frac{\partial\psi}{\partial x}$ or $\frac{\partial\psi}{\partial y}$ is zero, and one of the three-point figures shown in Figure (f) is used

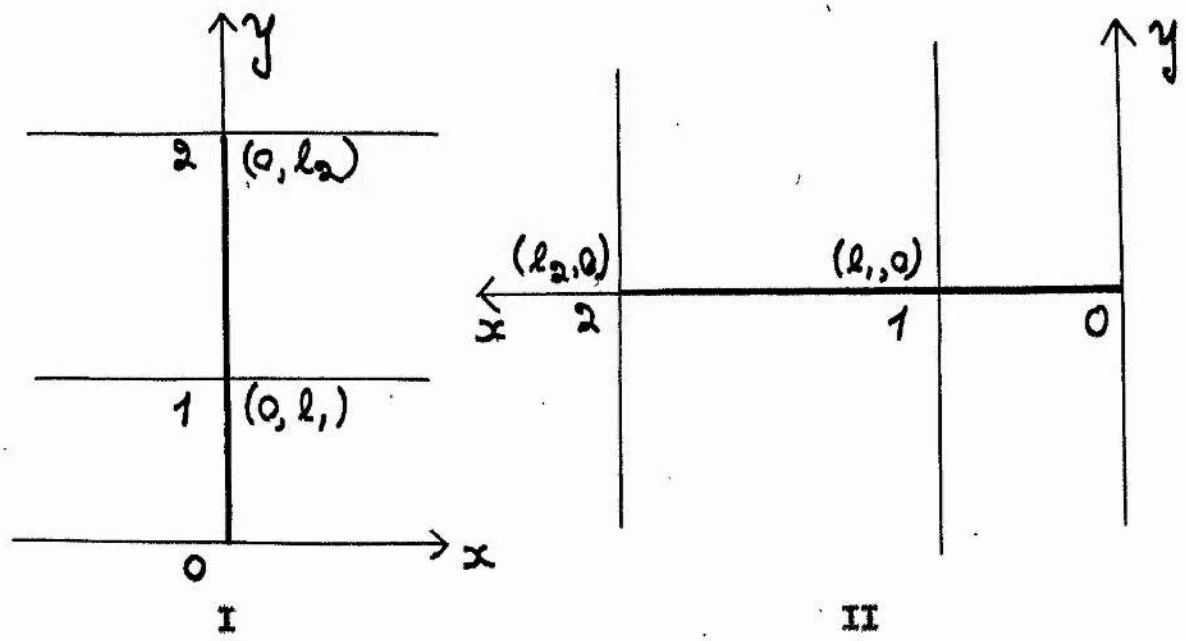

Figure (f)

Using Figure (f) I and expanding f at the nodes,

$$f_1 = f_o + l_1\left(\frac{\partial f}{\partial y}\right)_o + \frac{l_1^2}{2}\left(\frac{\partial^2 f}{\partial y^2}\right)_o + \cdots\cdots$$

$$f_2 = f_o + l_2\left(\frac{\partial f}{\partial y}\right)_o + \frac{l_2^2}{2}\left(\frac{\partial^2 f}{\partial y^2}\right)_o + \cdots\cdots ,$$

from which, neglecting terms of the third order and higher in the length l_1 and

$$\left(\frac{\partial f}{\partial y}\right)_o = \left[\frac{l_2}{l_1(l_2-l_1)}(f_1-f_o) - \frac{l_1}{l_2(l_2-l_1)}(f_2-f_o)\right],$$

and on substituting $f = \psi$, the required approximation to $\left(\frac{\partial \psi}{\partial y}\right)^2$ is obtained, namely

$$\left(\frac{\partial \psi}{\partial y}\right)^2 = \frac{1}{(l_2 - l_1)^2}\left[\frac{l_2}{l_1}(\psi_1 - \psi_0) - \frac{l_1}{l_2}(\psi_2 - \psi_0)\right]^2 \quad \text{.------(29)}$$

An exactly similar formula is obtained for $\left(\frac{\partial \psi}{\partial x}\right)^2$ using Figure (f) II.

Thus, the field is covered with a net (Figure (5)), values of ψ assigned to each internal node, equation (28) used to give D, and thus χ, and finally the residue R_0 is evaluated from equation (27). The initial ψ-distribution inside the boundary is altered until R_0 is approximately zero at every node. A relaxation pattern, which is a systematic means of eliminating the residuals at the node, can be derived, using the method described by Green and Southwell [45]. The pattern is similar in type to, but more difficult to use than, that obtained by Mitchell [28]. However, due to the complexity of the governing equations, judicious trial and error methods are quicker in this case, and in most problems of this type, where the stagnation enthalpy varies from stream line to stream line.

In calculating χ at a node in practice, several graphs of D against χ (dropping the 0 subscript) for various values of ψ are drawn. From equation (28),

$$D = \left[\frac{1 + (\gamma - 1)(\tfrac{1}{2}U^2 - \omega_0 \psi)}{\chi^4} - \frac{1}{\chi^{2(\gamma+1)}}\right], \quad \text{----------(30)}$$

the values of ψ being in the range, zero to the largest free stream value (the mass flow parameter) $U - \omega_0/2$, and χ for any D and ψ can be obtained by interpolation on the ψ curves. The shape of these curves is shown in Figure (6a), Figure (6b) being the full shape for $h_s = \frac{1}{\gamma - 1}$. The maximum is obtained from

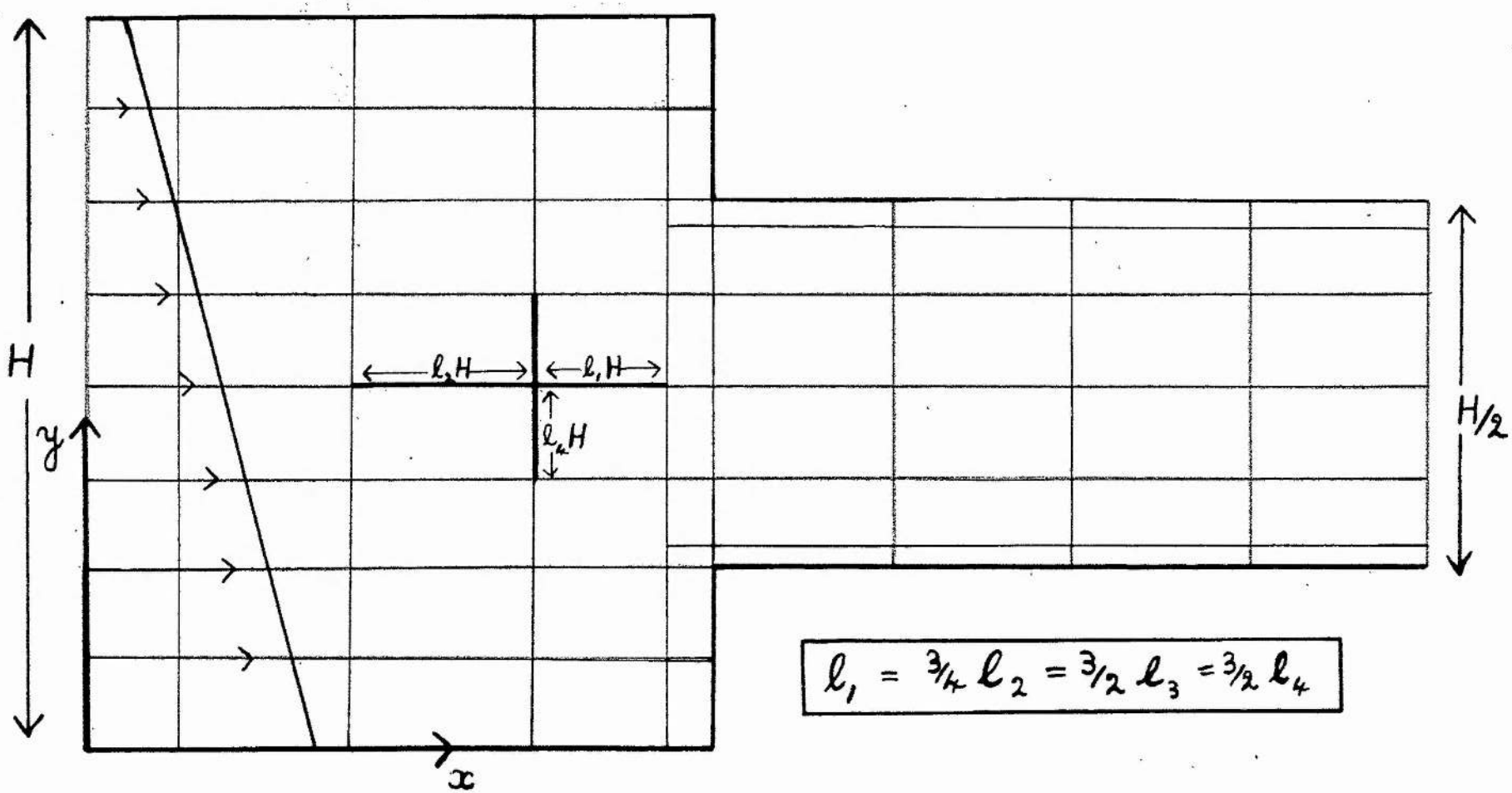

Figure (5) Illustration of the compressible shear flow problem.

$$\frac{\partial D}{\partial \chi} = 0 = -h_0 \, 4(\gamma-1)\chi^{-5} + 2(\gamma+1)\chi^{-2\gamma-3}$$

from which the maximum χ_m is given by

$$\chi_m = \left(\frac{\gamma+1}{\gamma-1} \cdot \frac{1}{h_0}\right)^{1/4(\gamma-1)} \quad \text{----------(31)}$$

If $\chi > \chi_m$, the flow is supersonic, $\chi < \chi_m$ corresponding to subsonic flow. In the simpler case of rotational flow behind a bow shock wave, h_0 is the same on every streamline and only one curve of $D \sim \chi$ is obtained for all ψ.

The sharp corners of the constriction are excluded from the region of calculation, since the velocity at the inner corners is theoretically infinite. This is done by choosing the original network as shown in Figure (5), with $\ell_1 = \ell_2$ and $\ell_3 = \ell_4$, where the density, but not the residue, is calculated for the nodes nearest the corners and walls upstream of the constriction. Equations (27) and (28) are used in their general form for the irregular stars, with $\ell_1 = \ell_2 = 2\ell_3 = 2\ell_4$ at the regular stars. On the upstream channel walls $\ell_2 = 2\ell_1$, but at other points the ratio varies.

When the residuals have been effectively reduced to zero, the original mes lengths are halved or quartered and the same procedure carried out. This procedure is repeated until the required degree of accuracy is obtained. In this problem, the x-increments are taken to be twice the corresponding y-increm this being more advantageous than taking equal increments.

The velocity at every point is evaluated from equation (28), since the velocity q, is given by

$$q^2 = \frac{1}{\rho^2}\left[\left(\frac{\partial \psi}{\partial x}\right)^2 + \left(\frac{\partial \psi}{\partial y}\right)^2\right],$$

which, written in its approximate finite difference form, is

$$q^2 = \frac{2}{\gamma-1}\,\chi_0^4\, D_0 \quad \text{----------(32)}$$

at the node 0. On the channel walls, the approximate finite difference

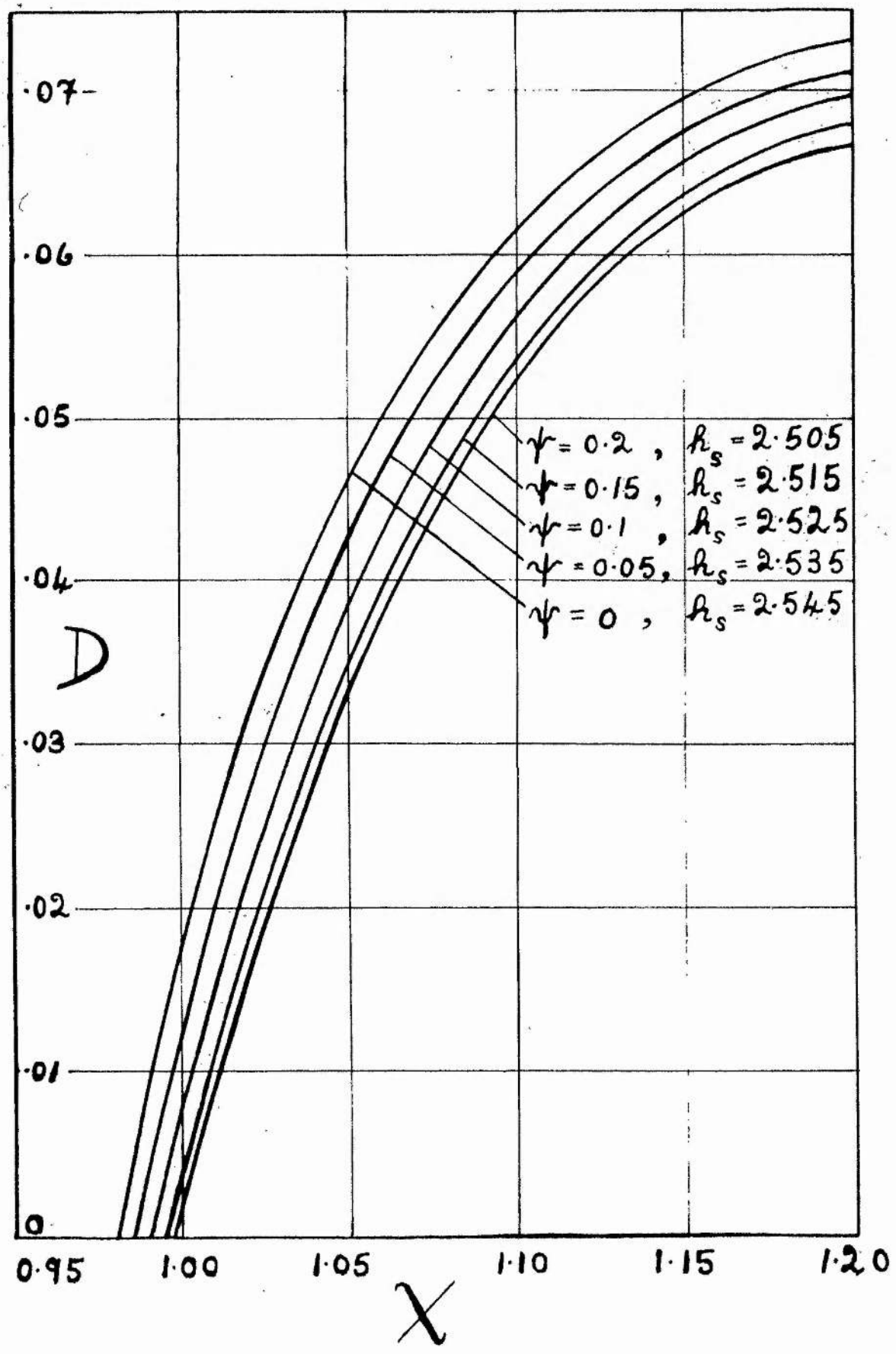
·07
·06
·05
·04
·03
·02
·01
0
D
0·95
1·00
1·05
1·10
1·15
1·20
χ
ψ = 0·2 , h_s = 2·505
ψ = 0·15 , h_s = 2·515
ψ = 0·1 , h_s = 2·525
ψ = 0·05, h_s = 2·535
ψ = 0 , h_s = 2·545

Figure (6a)

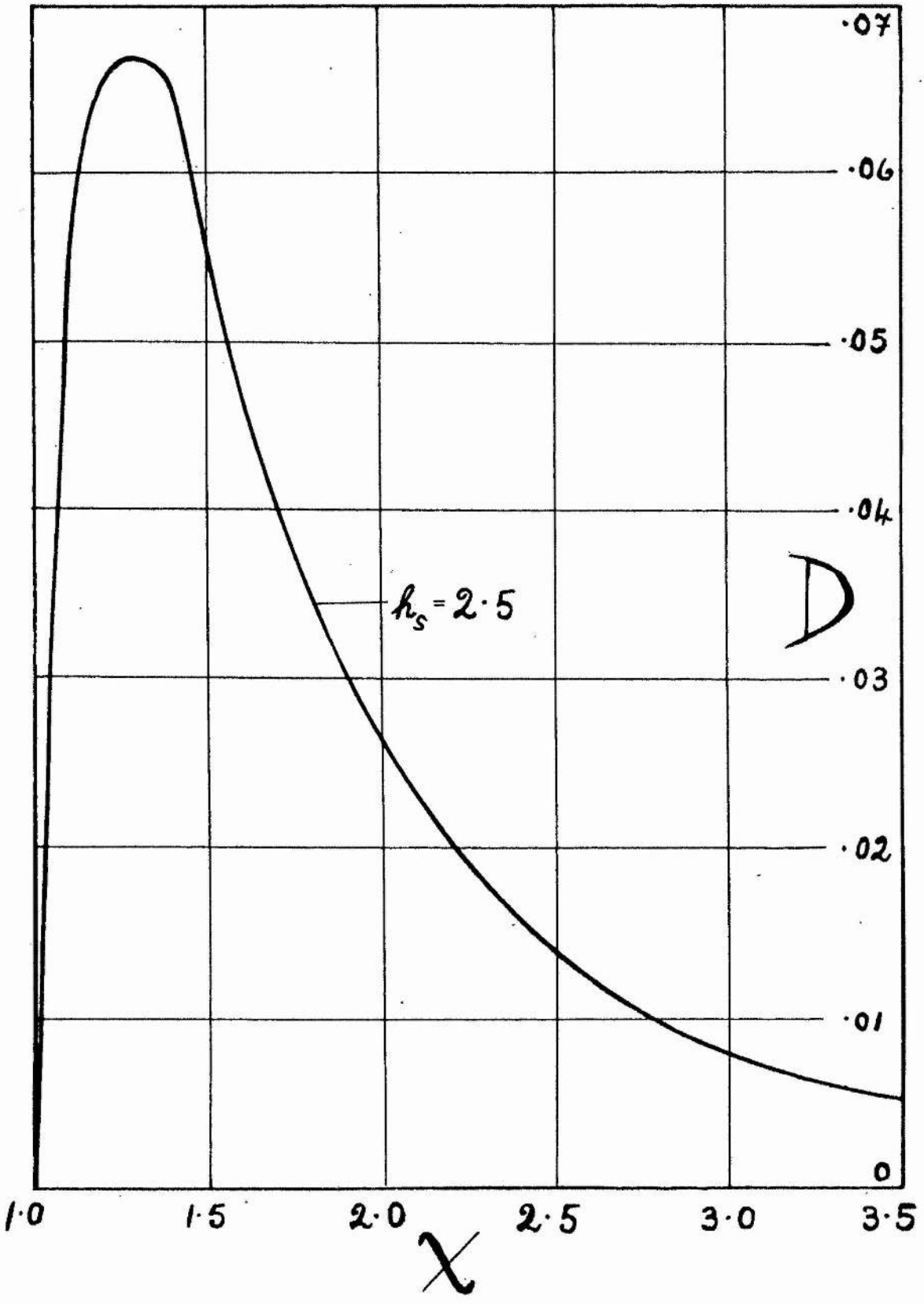

Figure (6b)

replacements from equation (29) for $(\frac{\partial \psi}{\partial x})^a$ or $(\frac{\partial \psi}{\partial y})^a$ are used for evaluating D_o. In practice, graphs of χ against the velocity q are drawn for various values of h_s (in effect, ψ) as shown in Figure (7a) and the density ρ against q in Figure (8a), the 'b' figures being the full curves for $h_s = \frac{1}{\gamma - 1}$.

As has been stated, the velocity at the corners is theoretically infinite and gives rise to a small supersonic region round the corners, shown schematica in Figure (g), where q = 1 is taken as sonic velocity.

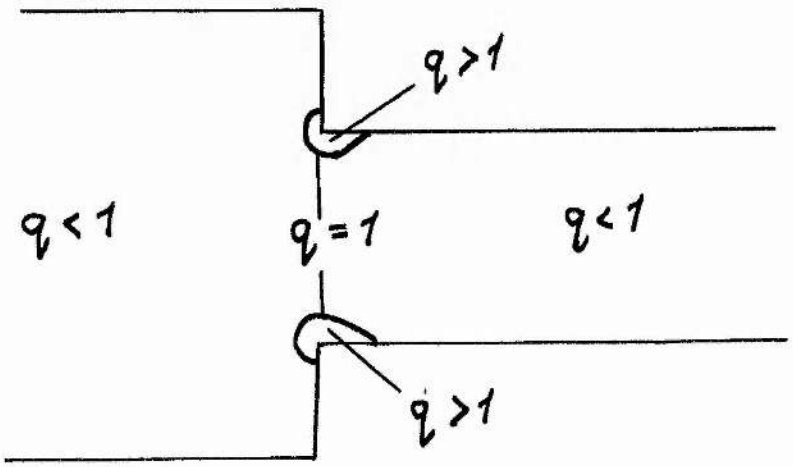

Figure (g).

Although a detailed examination of the corners is not the primary purpose of this problem, the network being chosen as in Figure (5), the supersonic 'bubble can be found from the point of view of position and size, using the method described by Mitchell and Rutherford [46]. However, the position and magnitude of the 'bubbles' is of no importance in practice, since every real fluid has viscosity and the presence of a boundary layer, however thin, smoothes out a sharp corner and prevents local supersonic regions in a flow of this type

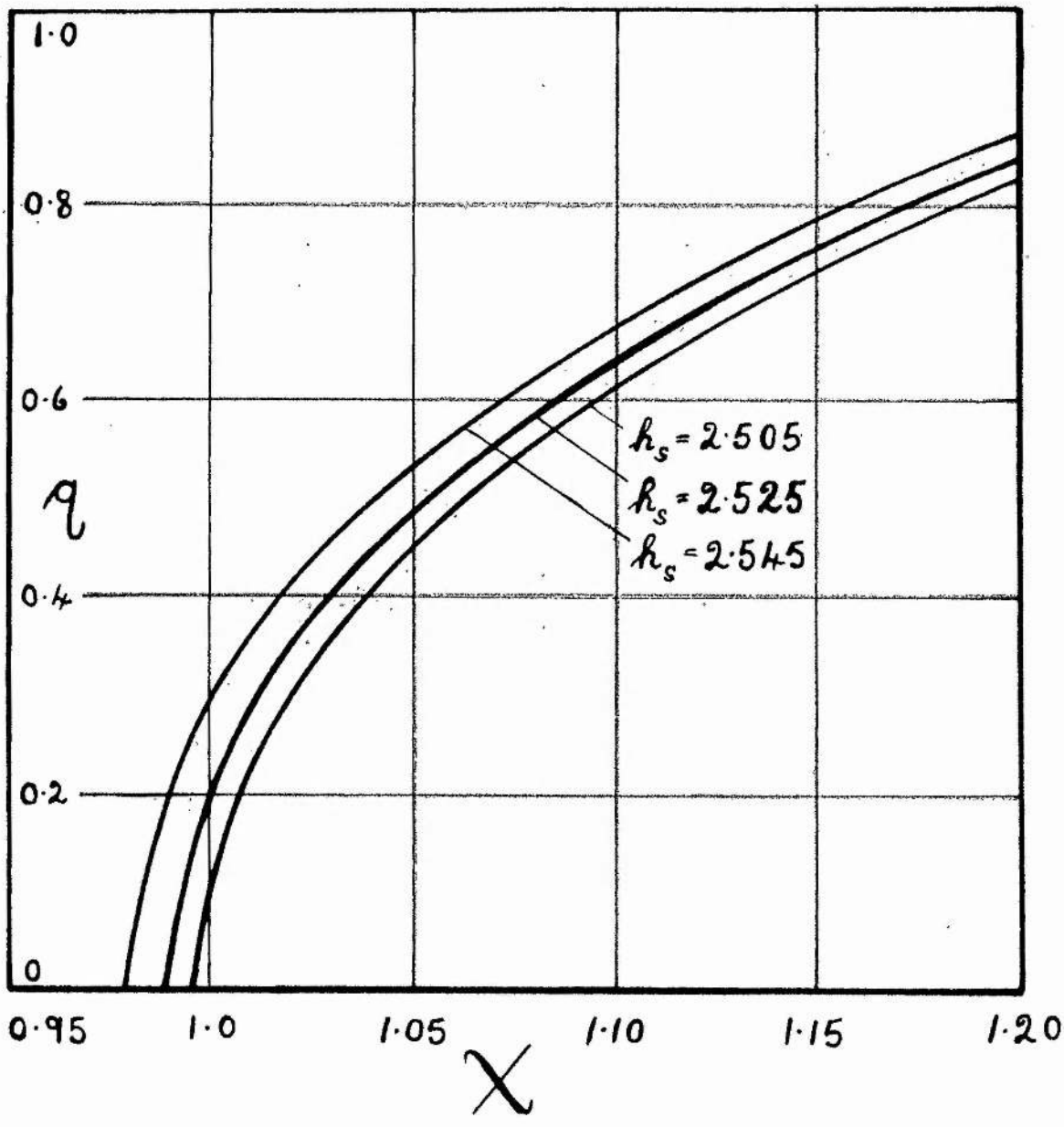

Figure (7a)

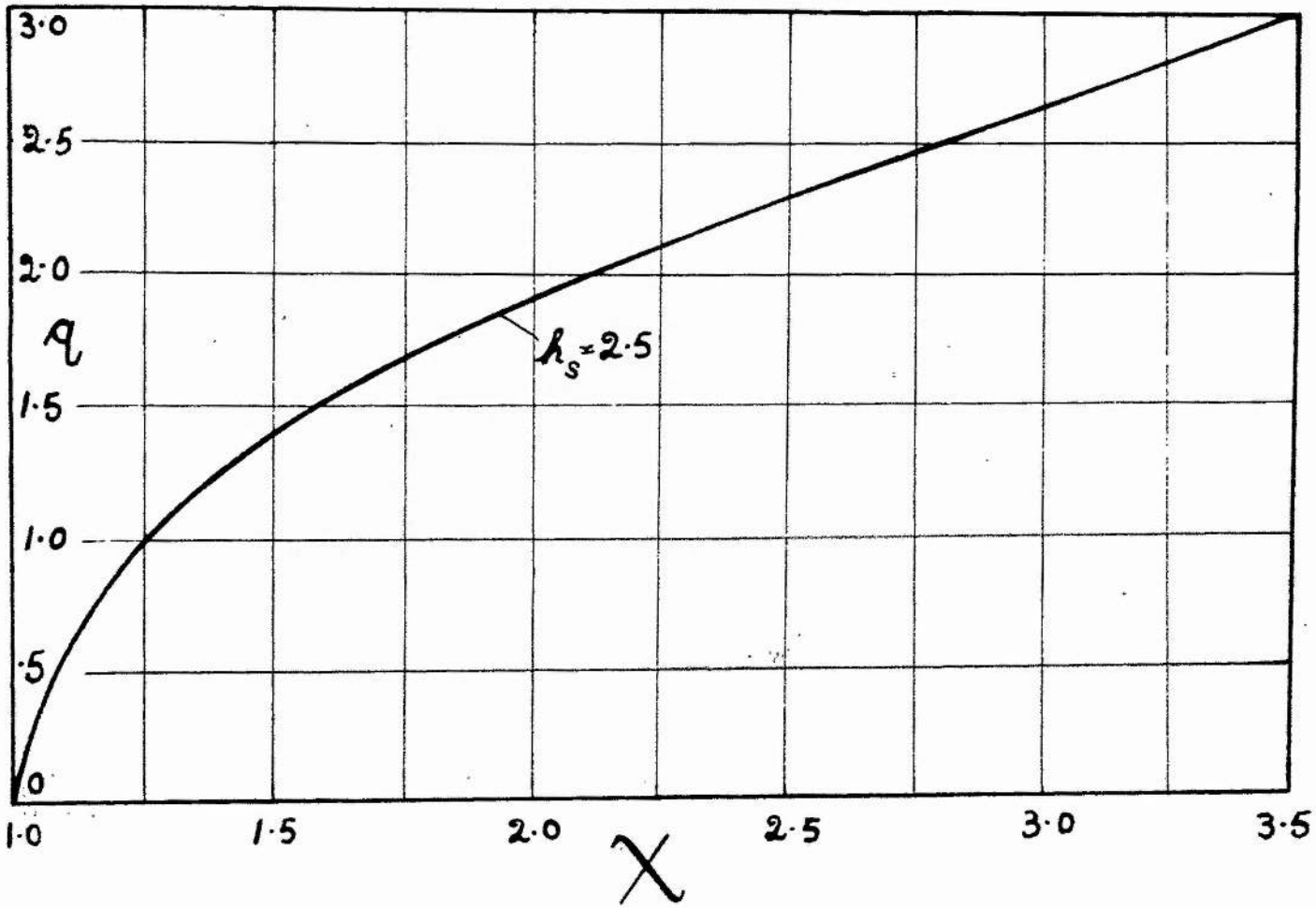

Figure (7b)

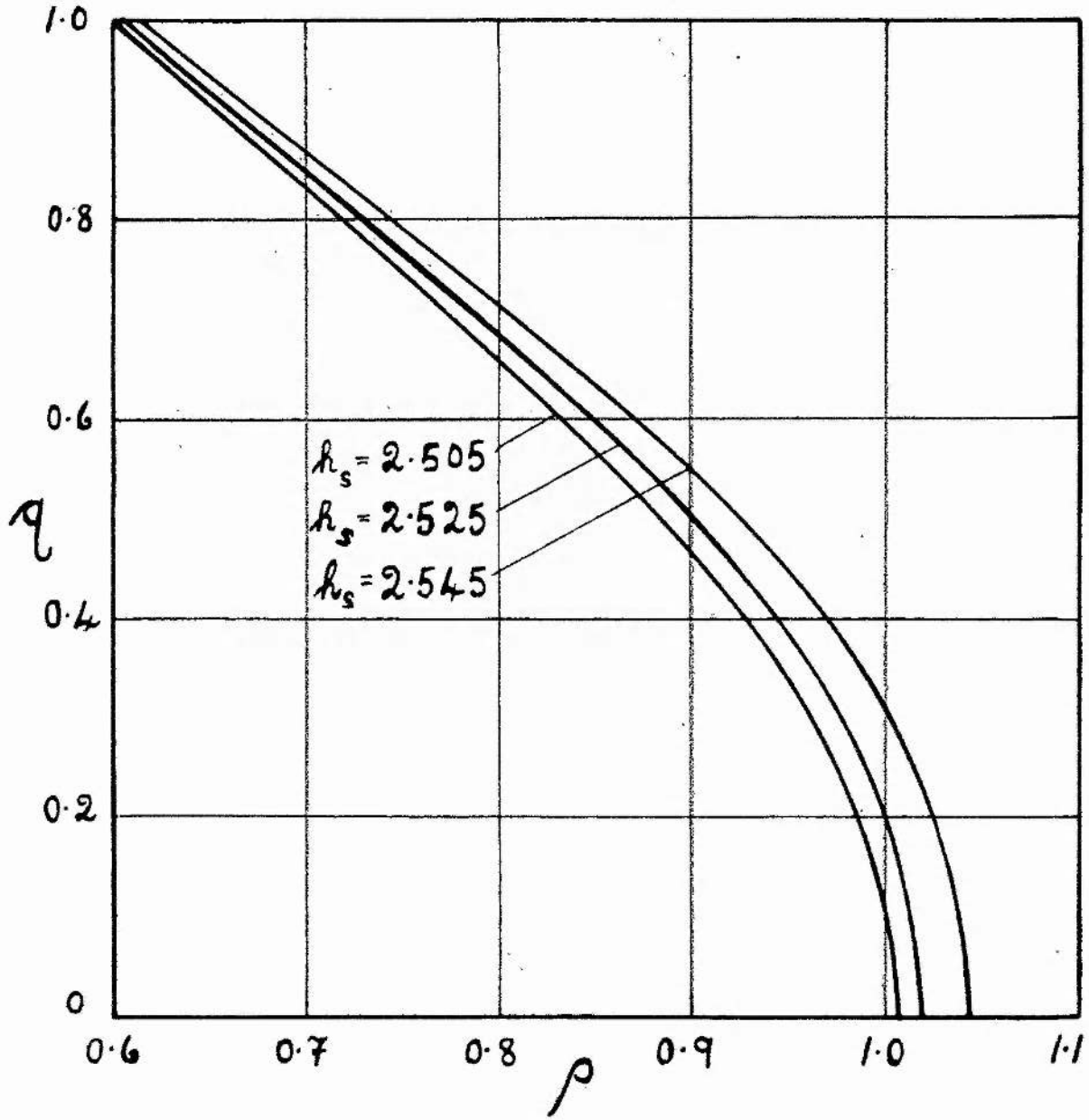

Figure (8a) Velocity against density.

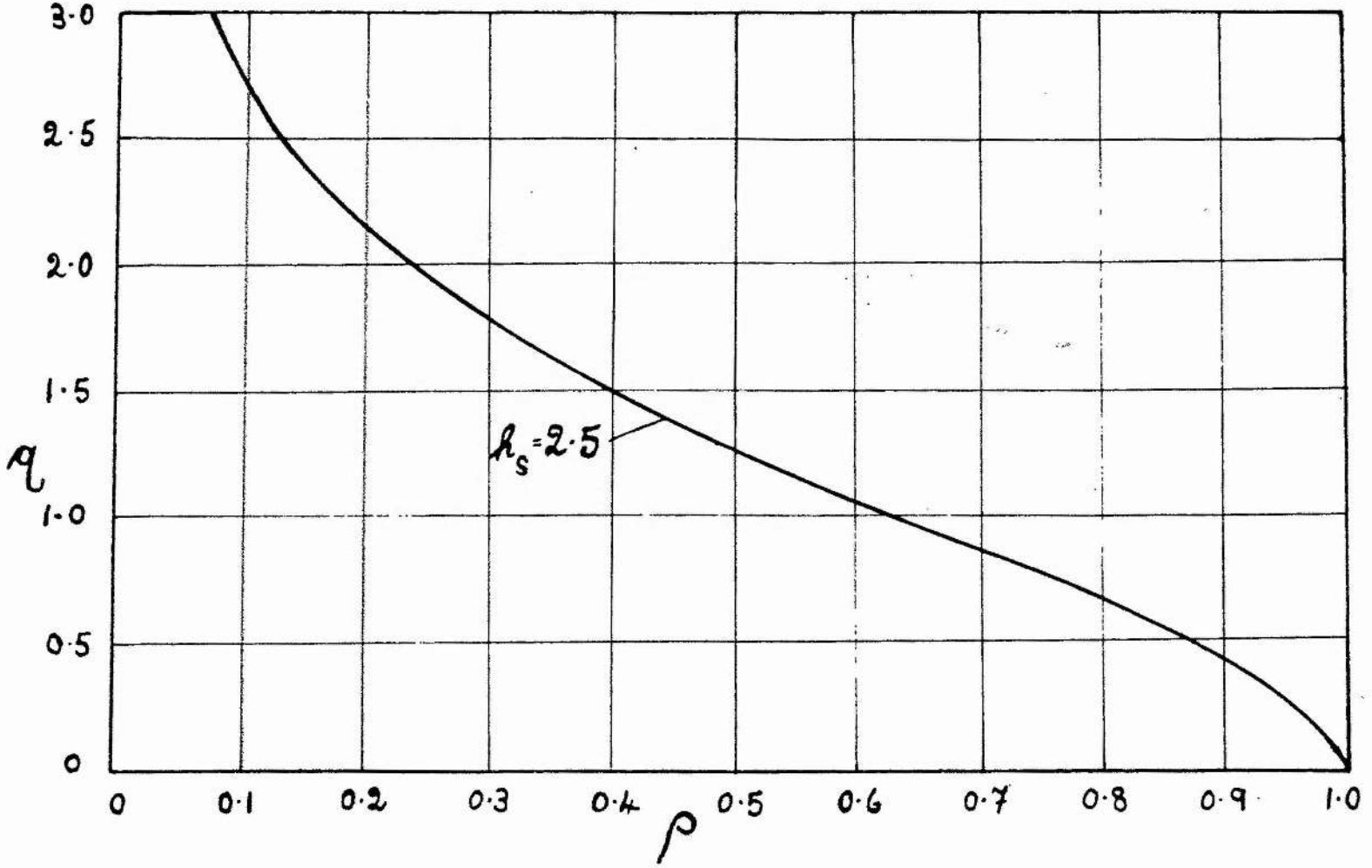

Figure (8b) Velocity against density.

From the nature of the finite difference relations used it is seen that the application of divided finite difference approximations is possible near the constriction. This method, as yet virtually unused, involves non-constant increments. These decrease in geometric progression towards the region where a more accurate picture is desired, in this case the region round the constriction. The success of such a method is assured, since the method described in this problem is virtually the same, the increments varying in the region of the constriction.

Throughout this work, no reference has been made to the stability and convergence of the difference equations as defined by O'Brien, Hyman and Kaplan [34].

Numerical Example.

The problem evaluated has $U = 0.3$, and $\omega_0 = 0.2$, giving $N = 1$. The initial and final boundary conditions are given by equations (20), (21), (22) a (23), the final density being obtained from equation (24) with $\gamma = 1.4$. The initial calculation is made with $\ell_1 = \ell_2 = \frac{1}{4}$ and $\ell_3 = \ell_4 = \frac{1}{8}$, except in the region of the constriction and near the walls downstream of the constrictio where the values are taken to be one quarter of those given above. Undisturbe flow conditions are assumed to exist at a distance 1.5H upstream, and downstrea of the constriction. The problem is illustrated in Figure (5).

A value of ψ is assigned to each internal node, with $\psi = 0$ and 0.2 on the lower and upper walls respectively. Intermediate nodes have values of in the range $0 < \psi < 0.2$. The free stream flow values of ψ are given by equations (20) and (22), and ρ_1 is obtained as the subsonic solution of equation (24). The stagnation enthalpy $h_s = 2.545 - 0.2\psi$, which lies between the limits 2.545 and 2.505. Graphs of D against χ for values of

ψ between 0 and 0.2 are shown in Figure (6a), the maxima, and thus points of sonic velocity, being obtained from equation (31).

The procedure is as follows:

1. Obtain the boundary conditions from the appropriate equations and as a check show that the residuals at all the points are zero,

2. evaluate the full equations (27), (28) and (29) for all internal nodes, regular and irregular,

3. assign values of ψ at each node 0,

4. calculate D_o from equation (28),

5. obtain χ_o from the appropriate graph (or by interpolation) in Figure (6a), and

6. obtain R_o from equation (27).

In general the first values of ψ at the various internal nodes result in non-zero values for the residuals R_o, and the original ψ values are altered and operations 1. to 6. repeated in order, until R_o is approximately zero everywhere. This simultaneous relaxation is carried out with values of ψ taken to the third decimal place until the residuals $R_o \leqslant 0.005$ at all points in the field.

The velocity at every node is obtained from equation (32) or from the graphs in Figure (7a), or by evaluating the density $\rho = {}^{1}/_{\chi^2}$ and using Figure (8a). The pressure at every point is obtained from Figure (9).

Diagrams of the stream lines, constant velocity lines and constant vorticity lines are shown in Figures (10), (11), and (12) respectively.

Again, since relaxation is a purely numerical procedure, no distinction is made between the flow into, and the flow out of the constriction. Thus, Figures (10), (11) and (12) are applicable to the flow out of the constriction, the arrows being merely reversed in the several profiles. When the flow is

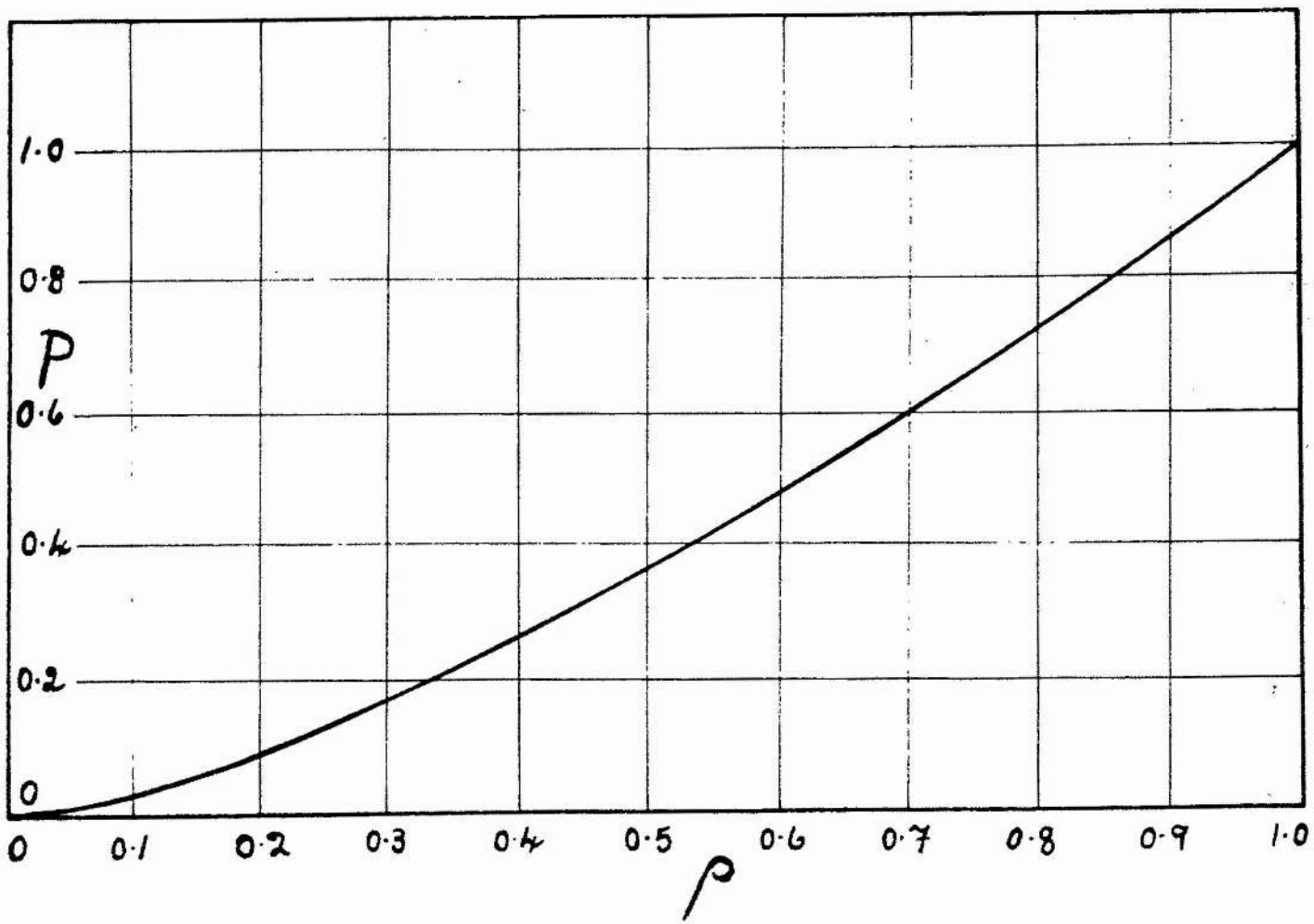

Figure (9) Pressure against density.

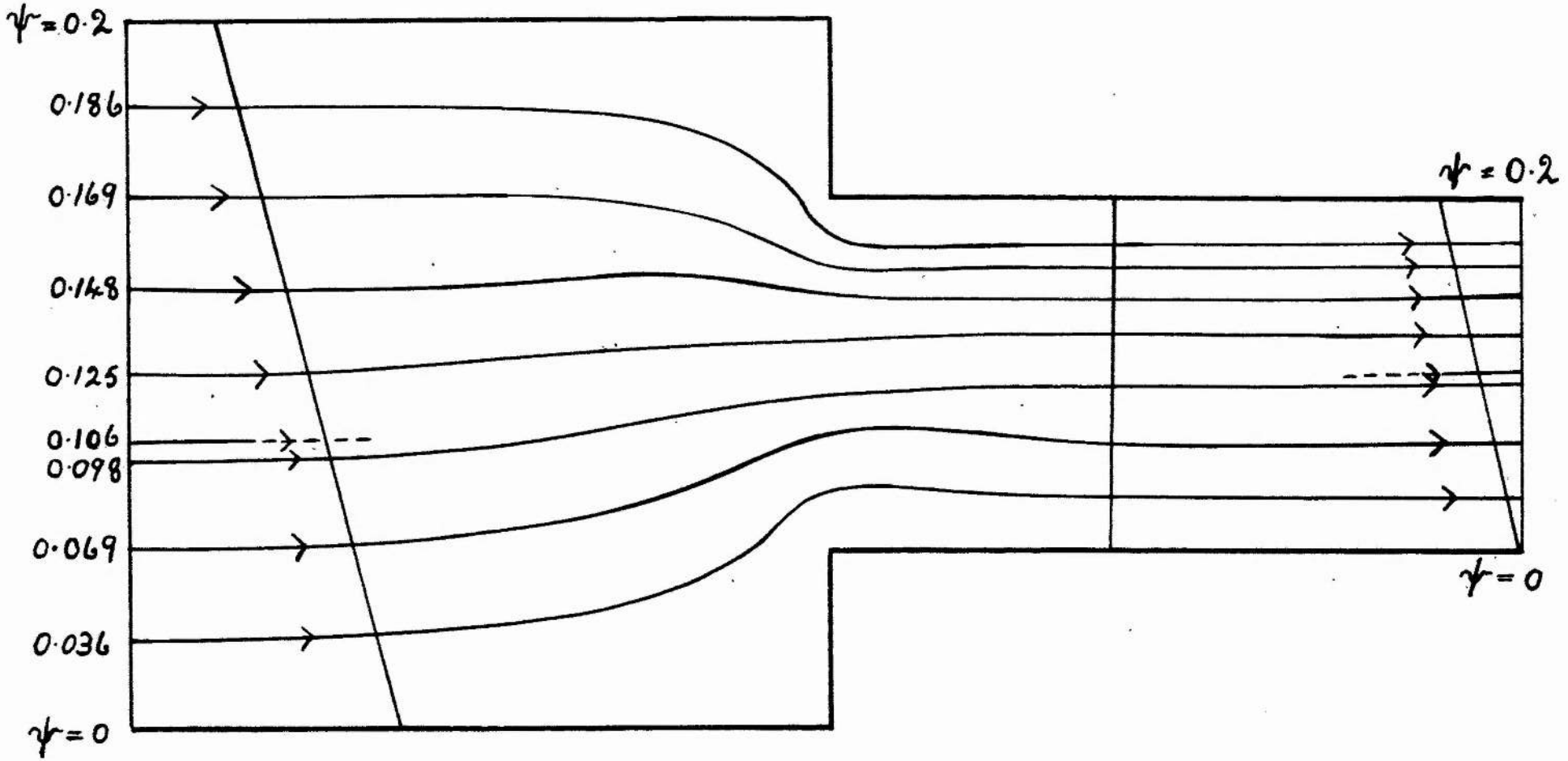

Figure (10) Illustration of the stream lines for the compressible shear flow.

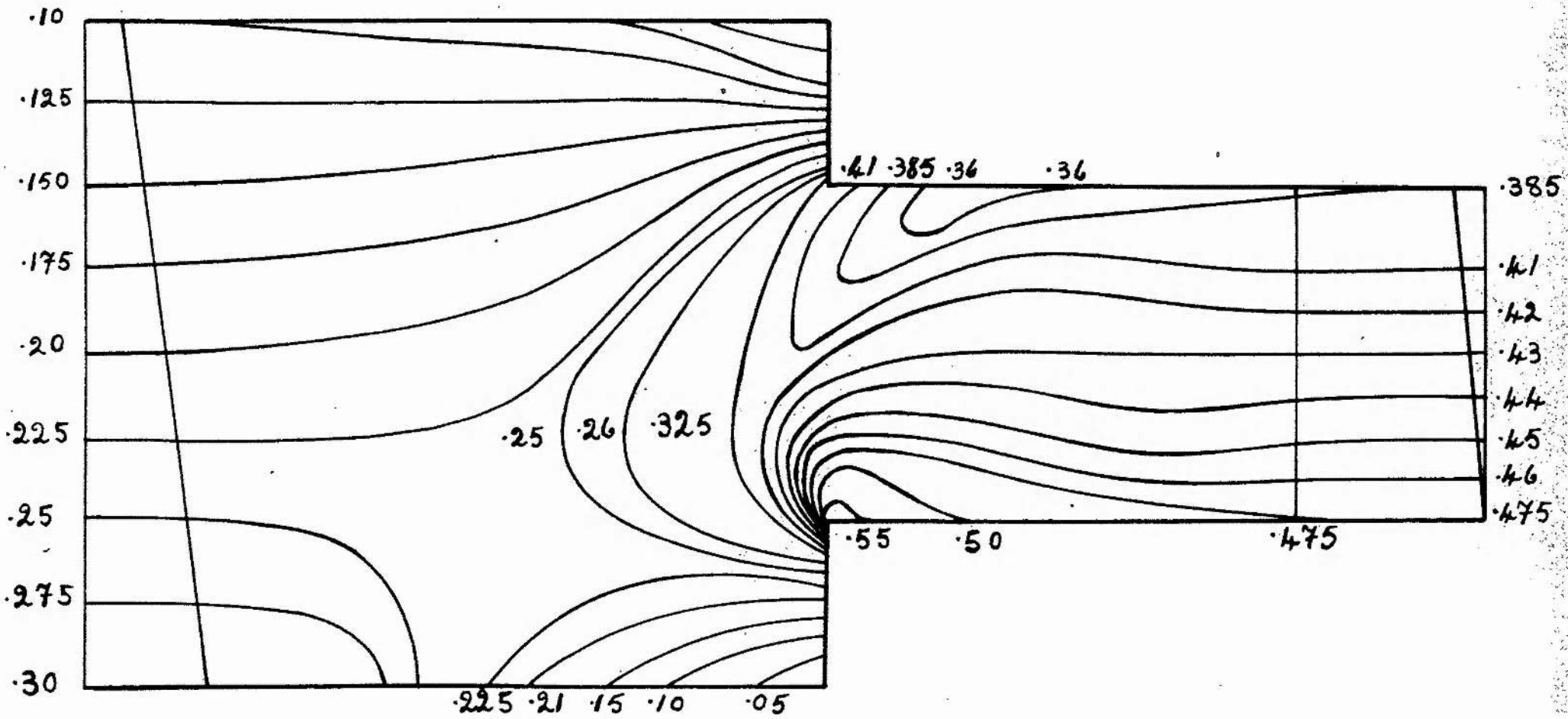

Figure (11) Lines of constant velocity for the compressible shear flow.

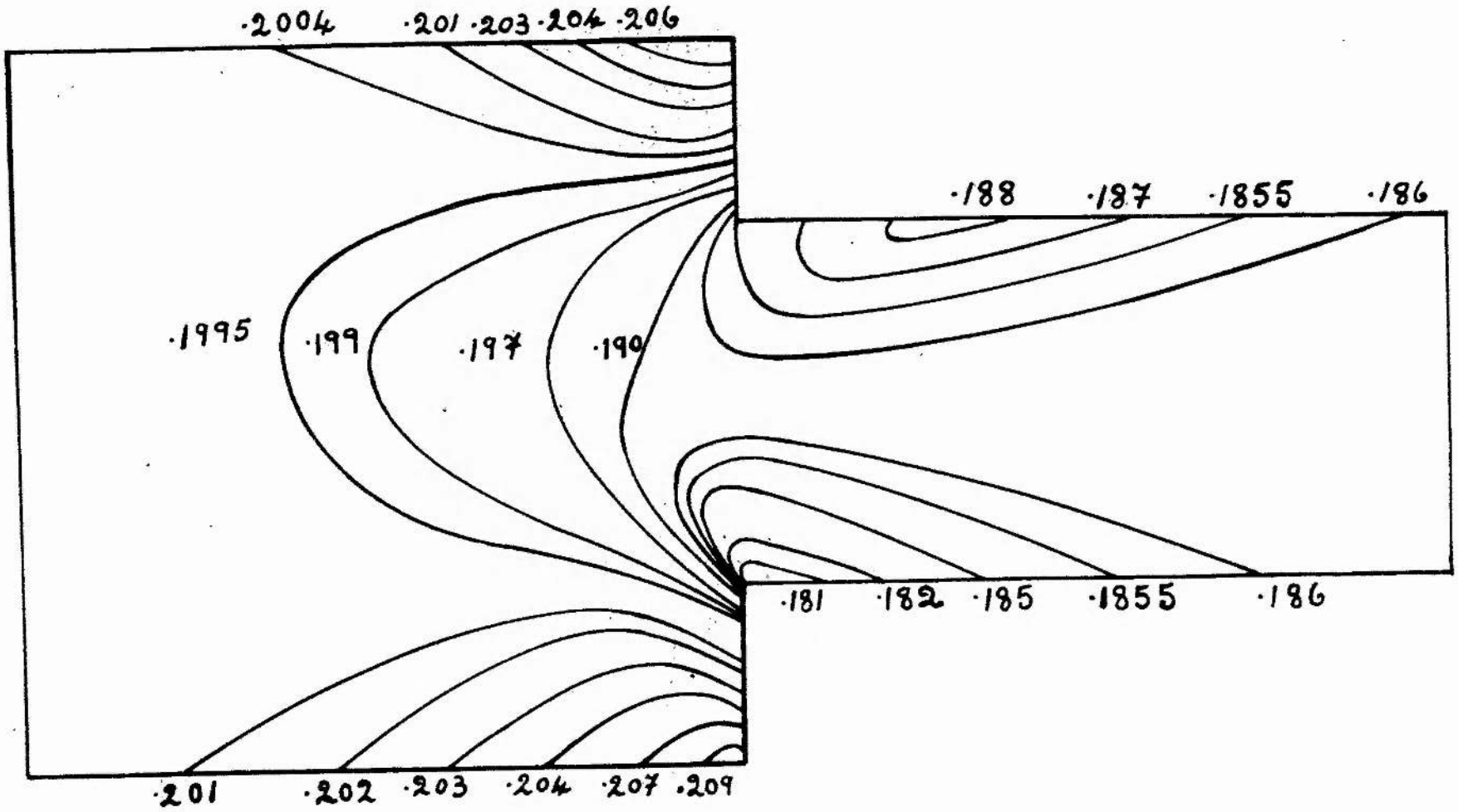

Figure (12) Lines of constant vorticity for the compressible shear flow.

into the constriction, the final central stream line comes from a region of higher velocity in the undisturbed flow upstream of the constriction than that on the central line at that station, the non-dimensional deflection δ, being -0.09. When the flow is from the constriction the central stream line in the downstream undisturbed flow comes from a region of lower velocity in the initial free stream, the deflection δ, being $+0.05$.

From Figures (11) and (12), it can be seen that there are regions of low velocity and high vorticity in the outer corners of the constriction. This tends to suggest that in a flow of a real fluid these regions would be excluded from the main stream by free stream lines, with perhaps small vortex regions between the free stream lines and the corners. These regions differ in size since the flow is not symmetrical. The non-symmetrical nature of the flow is perhaps shown most clearly at the inner corners, where the lower one displays a region of very high velocity, whilst the upper one does not. Of course, as stated previously, there are small localised supersonic regions at both corners, which have not been detected by the net used.

Summary and Conclusion.

The relaxation method described in this chapter is used to evaluate the inviscid two-dimensional rotational flow of both an incompressible and a compressible fluid through a channel with a sharp constriction present. In each case, the stream lines, lines of constant velocity and vorticity are indicated. It is to be expected, that an incompressible flow and a low speed compressible one will not differ markedly in their general features. This is backed up by the diagrams of the respective stream lines and constant velocity lines. The limits for ψ and free stream velocity values differ, however, and the incompressible values are five times those of the compressible case (for example, Figures (3) and (10

In the deflections of the central stream lines, there is no difference in the actual values, to the degree of accuracy used in the calculations. Thus, in view of the fact that solutions for the incompressible rotational flow past cylinders of various cross sections are known (chapters II and III), it may be deduced, that in the low speed compressible rotational flow past these cylinders, the general features, both quantitatively and qualitatively, will not differ markedly from those already obtained for the incompressible case.

The velocity diagrams, Figures (4) and (11), again display the same generc features, namely low velocities in the outside corners of the constriction, and large velocities at the inner corners, in both cases the region of highest velocity being on the lower of the two inner corners. The region of low velocity on the upper wall downstream of the constriction, although displayed by both flows, is much more marked in the compressible case. From Figure (12) this region is also seen to be a region of high vorticity, and in practice coul develop into a small dead air region bordered by a free stream line. This wil tend to 'soften' the sharpness of the upper corner. Thus, in practice, the flow in the compressible case may 'soften' the sharp constriction, making the change in cross section much more gradual.

Before the corners were excluded, in the preliminary calculation, very hig values of the velocity were obtained at the inner corners of the constriction. The supersonic regions which appear there are of small physical importance in the flow of a real fluid and are omitted in the calculations. They can be obtained, but there is some doubt as to the validity of the final result.

It should be noted, that lines of constant vorticity are also lines of constant density, and from Figures (8), lines of constant pressure can be obtained. The drop in pressure across the channel, at stations other than

in the free stream, can thus be obtained, if desired.

One important feature arising from the compressible case is the fact that the presence of a constriction tends to decrease the value of the vorticity, changing it in this case from 0.2 to 0.187 in the free stream. Initially the vorticity is constant across the channel, and finally the vorticity is constant, with a value which differs, of course, from the original value.

One further result of importance, is the fact that a large vorticity results in back flow, which in practice would possibly result in break away. Thus, there is a possibility that there can be breakaway in a flow, if high vorticity regions are present. The condition on the non-dimensional number N, for no obvious back flow in the channel, is that it must be numerically greater than $\frac{1}{2}$, in both the compressible and incompressible cases.

In conclusion, it must be remembered that relaxation is an approximate process, and no matter how fine a mesh is used, a discontinuity may be missed. Until, however, theoretical solutions are obtained, relaxation constitutes a ve powerful technique, since particular parts of a field can be examined in great detail, provided the stream function and, if necessary, its derivatives, are known with sufficient accuracy at the boundaries. The ability to treat parts of the field independently, makes it useful where wind tunnel evidence shows certain features of a flow. The more that is known about a particular problem the more accurate is the final relaxation solution.

One prohibitive feature of a relaxation technique is the fact that it involves much laborious calculation. It is neither possible nor profitable to reproduce the calculations in detail.

GENERAL CONCLUSIONS

Conclusions of a more specific nature are given at the end of each chapter Accordingly only a short summary of these will be given at this stage, particul attention being paid to results of a general nature.

(1). Throughout this thesis, there is the repeated appearance of the non-dimensional number $N = U/\ell\omega$, where U, ℓ and ω, are a typical velocity, length and vorticity respectively. In the constant shear flow past cylinders, this number is the principal parameter in the expressions for the deflections of the stagnation points and stagnation stream lines. Its importance, however, i not restricted to constant shear flow, as is evident from the study of cylinder in a flow with variable rotation. In this case, another parameter appears, which in particular instances is related directly to the number N. The number N also appears in such quantities as lift coefficients, in expressions for the circulation, and finally, in flow through a channel, it again plays an importan role. If the latter has straight parallel sides, for example, it has been sho that a necessary condition for no back flow in the channel, is $N \geq \frac{1}{2}$, where U is the undisturbed velocity along the centre line and ℓ is the breadth of the channel. In view of this fact, it is possible, that in the flow of a fluid through a channel of varying cross section, a large accumulation of vorticity might be the cause of breakaway from the channel sides. In fact, N appears to have an importance in rotational flow comparable to the Reynold's number in viscous flow.

(2). It seems quite likely that the large displacements in the stagnation stream lines obtained by Young and Maas [35] are due primarily to the three-dimensional nature of the flow. From the study in the third chapter of the approximation to the rotational flow in a boundary layer and the resulting

graphs of the magnitude of the displacement of the stagnation stream line, it is not surprising that in the two-dimensional work carried out with a pitot tube in a boundary layer by Davies [37], little or no displacement effect was found. Thus, in view of this experimental evidence, and the small displacements in both the constant and variable shear flows found in this thesis, it seems a reasonable explanation of the discrepancy between the theoretical values and those obtained by Young and Maas. The theoretical solution to any three-dimensional problem, however, would in all probability be sufficient to verify the fact. From the last chapter, the admission of compressibility does not appear to alter either the order or direction of the displacement, in the case of low speed flow. Thus, except for supersonic flow, where no evidence is yet available, there appears no doubt, that in a rotational flow past a body, there is always a displacement, of the stagnation stream line, and this displacement is in the direction of a region of higher velocity than that opposite the geometric centre of the body.

(3). The problems encountered in attempting to obtain analytical solutions of variable shear flows are considerable. Even in the comparatively simple case of a free stream linear shear flow past a cylinder whose cross section is not circular, serious analytical difficulties arise, as illustrated in chapter III. However, stream functions can be obtained in a closed form for some cylinders not circular in cross section, although the numerical calculations involved are considerable. In flows with variable shear one further boundary condition is required to give a unique solution. It is that the circulation round a path coinciding with the perimeter of the cylinder is unaltered when the cylinder is "inserted" into the flow. In view of complicated nature of the calculations necessary to obtain analytical solutions of the problems with

variable shear, numerical solutions by relaxation together with a study of the convergence of such solutions, are in need of considerations.

(4). The presence of compressibility in a two-dimensional rotational flow greatly increases the difficulty of obtaining analytical solutions, the equations in this case being non-linear. The hodograph plane can not be used as is shown fairly conclusively by Goldstein and Lighthill [24], and accordingly relaxation methods assume first order of importance. However, even in the comparatively simple problem of isentropic, compressible, rotational flow through a channel with straight parallel sides containing a constriction, the boundary conditions are difficult to define, and in any particular example they must be given careful consideration. The calculation in itself is fairly complicated, and in any example, will involve the simultaneous relaxation of the two governing equations. The important questions of round-off errors, since the problem is of elliptic type, and convergence offer some difficulty, because of the non-linear nature of the differential equations.

In the problem of a body in a channel, through which an incompressible constant shear flow is passing, relaxation solutions can be obtained, using trial and error methods for obtaining the stream line which moves on to the cylinder. Such a problem, is amenable to solution with an electronic computer. It is possible that this method of solution can be extended to include compressible flow problems, although the numerical calculations will be immense.

Until wind tunnel results giving the position of shock waves become available, nothing can be said concerning shear problems in supersonic flow, whilst the problem of mixed sub- and supersonic flow still gives rise to difficulty from the point of view of establishing the necessary boundary

conditions for a unique solution.

In conclusion, it can be stated that until the mathematical theory is sufficiently developed to solve the differential equations of rotational flow, relaxation methods despite their approximate nature, will provide useful information concerning shear flow problems. Thus, it is recommended that relaxation methods be employed in any problem on rotational flow, where the rotation is of a fairlycomplicated nature, or the boundary conditions are difficult to apply, whether the fluid is compressible or incompressible.

Acknowledgements.

I am indebted to Dr. A.R. Mitchell for his assistance, numerous suggestions, and constant encouragement during my period of research under his supervision. I am also grateful to Professor E.T. Copson and the staff of the Mathematics Department in St. Andrews for many helpful discussions. My thanks are also due to the Carnegie Trust for the Universities of Scotland for the Research Scholarship I held from October 1953 until September 1955. Finally, I wish to thank Mr. J. Gerrard of the Physics Department, St. Andrews, for the preparation of the photographs used in this thesis.

BIBLIOGRAPHY

1. H.von Helmholtz — Über Integrale der Hydrodynamischen Gleichungen welche den Wirbelbewegungen entsprechen
Crelle, (1858) Wiss. Abh. (i) 101.

2. H. Lamb — Hydrodynamics
6th edition 1932 (Dover publication)

3. L. Crocco — Una nuova funzione di corrente per lo studio del moto rotazionale dei gas
Rend. della R. Accad. dei Lincei
Vol. XXIII Ser. 6. fasc.2. 1936.

4. C. Ferrari — On Rotational Conical Flow
N.A.C.A. T.M. 1933. 1952 (translation)

5. G. Cotusso — A variational principle in plane hydrodynamics
Atti. Accad. Naz. Lincei. Rend. Cl. Sci. Fis. Mat. Nat. (8) 102. 1951.

6. G. Heinrich — On the Theory of Steady Frictionless Vortex Flow
Anz. Akad. Wiss. Wien. 87. 1950.

7. M.H. Martin — Steady, Rotational, Plane Flow of a Gas
Amer. J. Math. Vol. LXXII. 1950.

8. M.H. Martin — Plane Rotational Prandtl-Meyer Flows
J. Math. and Phys. Vol.XXIX.No.2. 1950.

9. M.H. Martin — Steady, Plane, Rotational Prandtl-Meyer Flow of a Polyotropic Gas
J. Math. and Phys. Vol. XXIX.No.4. 1950.

10. G.S.S. Ludford and M.H. Martin — One-Dimensional Anisentropic Flow
Comm. Pure and App. Math. Vol.VII.1.1954.

11. D Naylor — The Simple Wave in Rotational Gas Flows
J. Rat. Mech. Anal. Vol.3. 4. 1954.

12. R.C. Prim — Steady Rotational Flow of Ideal Gases
J. Rat. Mech. Anal. Vol.1. 3. 1952.

13. W.R. Sears — The Linear-Perturbation Theory for Rotational Flow
J. Math. and Phys. Vol.XXVIII. 1949.

14. C. Truesdell — Two Measures of Vorticity
J. Rat. Mech. Anal. Vol.2. 2. 1952.

15. A. Vazsonyi — On Rotational Gas Flows
Quart. App. Math. Vol.III. 1945.

16. H.S. Tsien — Symmetrical Joukowski Airfoils in Shear Flow
Quart. App. Math. Vol.1. 1943.

17. A. Coombs. — Notes on the Forces acting on a two-dimensional Aerofoil i Shear Flow in the Presence of a Plane Boundary
Proc. Camb. Phil. Soc. Vol. 45. 4. 1949.

18. D.G. James — Two-dimensional Airfoils in Shear Flow. I.
Quart. J. Mech. App. Math. Vol.IV. 4. 1951.

19. K.De. Kumar — On the extension to Blasius's Theorem
Bull. Calcutta Math. Soc. 45. 1953.

20. Y.H. Kuo — On the Force and Moment acting on a body in Shear Flow
Quart. J. App. Math. Vol.1. 1943.

21. M. Richardson — The Pressure Distribution on a body in Shear Flow.
Quart. J. App. Math. Vol.3. 1945.

22. P. Prakash — Two-dimensional Steady Flows Superposable on a Source, Sink or Doublet
Bull. Calcutta Math. Soc. Vol. 45. No.2. 1953.

23. A.R. Mitchell and J.D. Murray — Two-dimensional Flow with constant shear past Cylinders with various Cross Sections
Z.A.M.P. Vol.VI. Fasc. 3. 1955.

24. S. Goldstein and M.J. Lighthill — A note on the Hodograph Transformation for the two-dimensional Vortex Flow of an Incompressible Fluid
Quart. J. Mech. App. Math. Vol.III. 3. 1950.

25. J.J. Kramer and J.D. Stanitz — Two-dimensional Shear Flow in a 90° elbow
N.A.C.A. T.N. 2736. 1952.

26. A. Thom — The Flow at the mouth of a Stanton Pitot
A.R.C. T.M. 1796. No.15,288. 1952.

27. A.F. Cornock — The Numerical Solution of Poisson's and the Bi-Harmonic Equations
Proc. Camb. Phil. Soc. Vol.50. No.4. 1954.

28. A.R. Mitchell — Application of Relaxation to the Rotational Field of Flow behind a Bow Shock Wave
Quart. J. Mech. App. Math. Vol.IV.3. 1951.

29. H.W. Emmons — Shock Waves in Aerodynamics
A.R.C. Report 8130. 1944.

30. S.I. Pai — Supersonic Rotational Flow over Two-Dimensional Ogives. Proc. 3rd Midwest Conf. Fluid Mech. Univ. of Minnesotta. 1953.

31. J.G. Charney, R. Fjörtoft, and J. von Neumann — Numerical Integration of the Baratropic Vorticity Equation. Quart. J. Geoph. Tellus. Vol.2. 4. 1950.

32. G.W. Platzman — The computational stability of Boundary Conditions in Numerical Integration of the Vorticity Equation. Archiv. Meteor. Geoph. und Bioklimatologie. Ser. A. 7. 29. Wien. 1954.

33. A.R. Mitchell and F. McCall — The Rotational Field behind a Bow Shock Wave in Axially Symmetric Flow using Relaxation Methods. Proc. Roy. Soc. Edin. Ser. A. Vol. LXIII.4. 27. 1952.

34. G. O'Brien, M. Hyman, and S. Kaplan — A study of the Numerical Solution of Partial Differential Equations. J. Maths. Phys. Vol.XXIV. 1951.

35. A.D. Young, and J.N. Maas — The behaviour of a Pitot Tube in a Transverse Total-pressure Gradient. A.R.C. Report. R. and M. 1770. 1937.

36. N.H. Johannesen and W.A. Mair — Experiments with large Pitot Tubes in a Narrow Supersonic Wake. A.R.C. Report. F.M. 1755. No.15,067. 1952.

37. F.V. Davies — Some effects of Pitot Size on the Measurements of Boundary Layers in Supersonic Flow. R.A.E. T.N. Aero. 2179. F.M. 1824. 1952.

38. L.M. Milne-Thomson — Hydrodynamical Images. Proc. Camb. Phil. Soc. 36. 1940.

39. D.B. De Haan — Nouvelles Tables D'Intégrales Définies. 1939. (Stechert and Co., New York).

40. H. and B.S. Jeffries — Methods of Mathematical Physics. 1946. (Cambridge University Press).

41. G.N. Watson — A Treatise on the Theory of Bessel Functions. 1952. (Cambridge University Press).

42. W. Gröbner and N. Hofreiter — Integral Tafel. II. Bestimmte Integrale. 1950. (Springer-Verlag. Wien und Innsbruck).

43. - — British Association Mathematical Tables. Bessel Functions I and II. (Volumes VI and X). 1952. (Cambridge University Press).